h Schubert

Prof. Ulli Englert

TECHNISCHE
UNIVERSITÄT
WIEN
Vienna University of Technology

DISSERTATION

MIXED METAL OXO CLUSTERS

ausgeführt zum Zwecke der Erlangung des akademischen Grades
eines Doktors der technischen Wissenschaften

unter der Leitung von

O.Univ.Prof. Dr.rer.nat. Ulrich Schubert
E165 Institut für Materialchemie

eingereicht an der Technischen Universität Wien
Fakultät für Technische Chemie

von

Christine Artner
e0325882
Dr. Ponzaunerstraße 11
2263 Dürnkrut

Wien, am 5. März 2014

"Luminous beings are we ...

not this crude matter."

Yoda

in

The Empire Strikes Back

Acknowledgements

There are so many people I met during my life at the university. I shared so many good times, but also stressful and hard times with them. They all helped me to develop as a chemist and as a person. The people I want to express my special gratitude to:

Prof. Ulrich Schubert for giving me the opportunity to work in his group. I am thankful for the interesting topic, the professional and nice working atmosphere he provided and his support for all the additional training in X-ray diffraction. Most of all, I thank him for the scientific freedom and that I could develop my own ideas.

Matthias Czakler for the excellent cooperation in our cluster project, the fruitful discussions about chemistry and many other things.

Berthold Stöger for help and support in crystallographic hard times.

Marlene Kaposi (Möller), Martina Schroffenegger, Ayse Koyun and Stefan Kronister for the great job they did in the lab and the many experiments they performed.

Van An for being the best desk colleague and her curiosity for all the gossip. Elisabeth, her dignified successor, for being the other ”vegetarian”.

Christian and Martin for surviving the many hours in the lab courses, and the days after.

Jasmin for her enthusiasm in the evenings and the white wine sauces.

Werner Artner for keeping all the instruments in the X-ray centre in excellent shape. It was a pleasure working there. Thanks also to Matthias Weil, Erich Halwax and Klaudia Hradil for help with instruments and interpretation of data.

Anita for her help with all the administrative things and for providing me sweets, whenever I visited her.

All other former and current working colleagues for the nice atmosphere, the cakes, the chats and many more: Angelika, Anja, Aparna, Bernhard, Catarina, Christoph, Felix, Harald, Hongzhi, Jakob, Jingxia, Maia, Marco, Melitta, Michael, Miriam, Mohsin, Rupali, Rupert, Stefan, Stephan, Sarah, Sven, Valeria and Wenjing.

Our neighbouring working group for providing dinner after a long working day and ”lending” us dry solvents.

The people from the Fachschaft Doktorat. For the working weekends and the discussions beyond the scientific world. I learned so much and really enjoyed it.

Mathias Gartler for the nice lunches and matcha drinks, that I can tell him everything and that he brings me down to earth sometimes.

My parents for supporting me throughout my life, my father for delivering all the things I forgot at home and my mother for providing me with fresh vegetables and fruits from the garden.

Reinhard for calming me down and for beeing there.

Kurzfassung

Diese Arbeit beschäftigt sich mit der Synthese und Strukturbestimmung neuer gemischt-metallischer Oxo Cluster, wobei das Augenmerk auf gemischt-metallischen Oxo Clustern lag, welche Ti oder Zr bzw. ein weiteres Metall enthalten. Funktionelle Carboxylate wurden als Liganden eingesetzt, um die Möglichkeit zu schaffen diese Cluster später über kovalente Bindungen in Hybridmaterialien einbauen zu können. Das Ziel hierbei ist es geordnete Netzwerke zu erhalten, dazu ist es notwendig die geometrische Anordnung der Liganden zu kennen. Dies lässt sich idealerweise mit Einkristallröntgenbeugung überprüfen, NMR wiederum gibt Auskunft über die Stabilität der Cluster in Lösung.

Der Einfluss verschiedener Carbonsäuren auf die Bildung von Clustern wurde anhand von gemischten Ti/Zr Oxo Clustern untersucht. Einige der erhaltenen Cluster mit Benzoat, bzw. Benzoatderivaten als Liganden sind isostrukturell zu bekannten Ti/Zr Methacrylat Clustern.

Unterschiedliche Ti und Zr Alkoxide wurden verwendet, um den Einfluss der Alkoxo-Gruppen auf die Bildung von Pivalat-Clustern zu analysieren. Zwei pentanukleare Cluster sind ähnlich methacrylat-substituierten Oxo Clustern, jedoch wandelten sich beide nach einigen Wochen zu Clustern mit oktaedrischem Kern um. Die Struktur aller anderen Pivalat Cluster kann als Kombination der Struktur von reinen Ti und Zr Clustern angesehen werden, die meisten davon zeigten einen oktaedrischen Kern. In $Zr_6Ti_8O_{15}(OH)_4(O^{n}Bu)_2(OPiv)_{20}(HOPiv)_2$ (OPiv = Pivalat) sind zwei solcher Zr3Ti3 Einheiten durch weitere zwei Ti Atome verbunden. Das oktaedrische Strukturprinzip lässt sich auch in einem Adamantancarboxylat Cluster wiederfinden.

Der zweite Teil der Arbeit beschäftigt sich mit der Synthese gemischt-metallischer Oxo Cluster aus Ti oder Zr Alkoxiden und verschiedenen Metallacetaten durch Umsetzung mit Carbonsäuren, meist Methacrylsäure. So war es möglich einige gemischt-metallische Cluster mit Ti zu erhalten, mit Zr führte jedoch nur Silber zu einem gemischt-metallischen Oxo Cluster. Dieser Cluster erwieß sich auch unter einem anderen Gesichtpunkt als Besonderheit. Es war dies der einzige Cluster, bei welchem Hydrolyseprodukte von Methacrylsäure koordinierten.

Die Struktur von gemischten Zn/Ti und Cd/Ti Clustern lässt sich vom bekannten Ti6 Cluster mit flachem Clusterkern ableiten. Dies trifft auch auf einen Fe/Ti Cluster zu, allerdings teilen sich hier Fe und Ti dieselben Atompositionen. Ca und Ti bildeten endlose Ketten an kondensierten Ca2Ti4 Clustern, die wiederum ähnlich zu Ti6 Clustern sind. Die Reaktion von $Sr(OAc)_2$ (OAc = Acetat) mit unterschiedlichen Ti Alkoxiden resultierte in verschiedenen Clustern. Mit $Ti(O^nBu)_4$ wurde ein Cluster erhalten, welcher ähnlich dem der Ca2Ti4 Ketten ist, $Ti(O^iPr)_4$ jedoch führte zur Bildung eines Sr2Ti8 Clusters. Die beiden Sr Atome befinden sich hier in einem Ring, welcher aus acht Ti Atomen gebildet wird. Dieser Hohlraum kann auch durch Pb besetzt werden, jedoch nur wenn $Ti(O^nBu)_4$ als Ti Quelle verwendet wird. Die Verwendung von $Ti(O^iPr)_4$ führte zur Ausbildung eines ähnlichen Clusters, bei welchem zwei Ti Atome fehlen. Es ist möglich, die koordinierten Alkoholgruppen in Pb2Ti8 auszutauschen, indem ein Überschuss Allylalkohol bei der Synthese beigefügt wird, welche bei Raumtemperature durchgeführt wurde. Wird die Reaktionslösung allerdings erhitzt, erhält man $Pb_6Ti_6O_9(OAc)(OMc)_{17}$ (OMc = Methacrylat), wobei die Methacrylsäure nachträglich hinzugefügt wurde. Die Reaktion von $Pb(OAc)_2$ mit $Ti(O^iPr)_4$ in einer alkoholischen Lösung führte zu $Pb_4Ti_8O_{10}(O^{i}Pr)_{18}(OAc)_2$.

Die Struktur von Ln/Ti Clusters hängt stark von der Ionengröße des Lanthanoides ab. La, Ce, und Nd formen einen Ln2Ti6 Kern, Elemente ab Sm jedoch führen zu Ln2Ti4. Bei einem starken Überschuss von Ti Alkoxid, in Kombination mit La oder Ce Acetat, wurde wiederum ein LnTi4 Cluster erhalten.

Die Verwendung von Propionsäure führte nur im Fall von Cu und Ti zu einem gemischt-metallischen Cluster, wobei der selbe Cluster auch mit Methacrylsäure erhalten wurde.

Abstract

New mixed-metal oxo clusters were synthesised and characterised by single crystal X-ray diffraction. Functionalised carboxylate ligands were used for later incorporation in hybrid materials through covalent bonds. For ordered networks, the knowledge of the geometrical arrangement of the ligands is a prerequisite, which is best monitored by single X-ray diffraction, whereas NMR gives information about the stability of the clusters in solution. This work focuses on mixed-metal oxo clusters of Ti and Zr, as well as on mixed-metal oxo clusters containing either Ti or Zr and a second metal.

The influence of different carboxylic acids on the formation of mixed Ti/Zr oxo clusters was studied. Several clusters with benzoate and benzoate derivatives as ligands were obtained, which are all isostructural to known Ti/Zr methacrylate oxo clusters.

The influence of the kind of Ti or Zr alkoxide on the formation of oxo clusters was systematically studied for Ti/Zr pivalate clusters. Two pentanuclear clusters are also structurally related to methacrylate clusters, but they rearranged after weeks to clusters with an octahedral core. The structure of all other pivalate clusters can be seen as a combination of known Ti and Zr clusters, several of which showed an octahedral cluster core. Two Zr3Ti3 units are joined together through two additional Ti atoms in $Zr_6Ti_8O_{15}(OH)_4(O^nBu)_2(OPiv)_{20}(HOPiv)_2$ (HOPiv = pivalic acid). The octahedral structure motive is also observed for a cluster with adamantanecarboxylate ligands.

The second part of this work deals with oxo clusters synthesised from Ti or Zr alkoxides and different metal acetates, with mainly methacrylate ligands. It was possible to obtain oxo clusters of Ti with a number of different divalent and trivalent metals, whereas Zr resulted in a mixed metal oxo cluster only in combination with Ag. This cluster was also special in another way. It is the only cluster where the methacryate ligand was not stable and hydrolysed derivatives were coordinated.

The structure of mixed Zn/Ti and Cd/Ti clusters can be derived from Ti6 clusters with a flat cluster core. This was also observed in a Fe/Ti cluster, but here Fe and Ti share the same atom positions. Ca and Ti build endless chains of condensed M2Ti4 clusters units, which are again similar to Ti6 clusters. The reaction of $Sr(OAc)_2$ (OAc = acetate) with various Ti alkoxides resulted in different clusters. With $Ti(O^nBu)_4$ a cluster similar to the Ca2Ti4 cluster chains formed, but with $Ti(O^iPr)_4$ it resulted in a Sr2Ti8O8 cluster core. The two Sr atoms are located in a ring, formed by eight Ti atoms. The cavity of the Ti8 ring can also be accessed by Pb, when $Ti(O^nBu)_4$ was used as Ti source. Here the change of the alkoxide to $Ti(O^iPr)_4$ leads to the formation of a similar cluster core of Pb2Ti6O5. It is also possible to exchange the alcoholate groups in Pb2Ti8O8, by addition of allyl alcohol to the reaction mixture at room temperature. When the reaction mixture is heated and methacrylic acid is added afterwards $Pb_6Ti_6O_9(OAc)(OMc)_{17}$ (OMc = methacrylate) is formed. Reaction of $Pb(OAc)_2$ and $Ti(O^iPr)_4$ in an alcoholic solution, without addition of carboxylic acid leads to the formation of $Pb_4Ti_8O_{10}(O^iPr)_{18}(OAc)_2$.

The structure of Ln/Ti clusters depends strongly on the ionic size of the lanthanide. La, Ce and Nd resulted in a Ln2Ti6 core, whereas for the later lanthanides (starting from Sm) a Ln2Ti4 core was obtained. A cluster with LnTi4 core was formed with La or Ce acetate and a large excess of Ti alkoxide.

The use of propionic acid was only successful for the combination of Cu and Ti, an isostructural cluster were also synthesised with methacrylic acid.

Part of this work have been published

1. ”Conversion of methacrylate into 2-hydroxy-2-methylpropionate ligands in the coordination sphere of a Ag-Zr oxo cluster”. Artner, C.; Czakler, M.; Schubert, U. *Chem. Eur. J.* **2014**, *20*, 493-498.
2. ”Crown-ether-like structures derived from a $Ti_8O_8(carboxylate)_{16}$ metallacycle”. Artner, C.; Koyun, A.; Schubert, U. *Dalton Trans.* **2013**, *42*, 6694-6696.

Glossary

XRD	X-ray diffraction
NMR	Nuclear magnetic resonance
IR	Infrared spectroscopy
EDX	Energy-dispersive X-ray spectroscopy

E	Element
E(n)	Atom position of E
E(n)’	Symmetry equivalent atom position of E(n)
E(nA)	Disordered position of E(n)
μ_n	Ligand bridging n atoms
η_1	Hapticity

Chemicals

HOProp	Propionic acid	CH_3CH_2COOH
HOMc	Methacrylic acid	$CH_2=(CH_3)CCOOH$
HOPiv	Pivalic acid	$(CH_3)_3CCOOH$
HOAda	Adamantanecarboxylic acid	$C_{10}H_{15}COOH$
HOBenz	Benzoic acid	C_6H_5COOH
EtOH	Ethanol	CH_3CH_2OH
^{i}PrOH	1- Propanol	$CH_3(CH_2)_2OH$
^{n}PrOH	2- Propanol	$(CH_3)_2CHOH$
^{n}BuOH	1- Butanol	$CH_3(CH_2)_3OH$
AllylOH	Allylic alcohol	$CH_2=CH_2CH_2OH$

Crystallography

a, b, c	Unit cell lenghts
α, β, γ	Unit cell angles
V	Unit cell volume
λ	Wavelengths
M_r	Molecular mass
Z	Formula units
D_x	Calculated density
μ	Absorption coefficient
Θ	Diffraction angle

NMR

δ	Chemical shift
s	singlet
d	doublet
t	triplet
quart	quartet
quint	quintet
sept	septet
m	multiplet
br	broad

IR

s	strong
m	middle
w	weak
b	broad

Contents

Part I

General

Chapter 1

Introduction

1.1 Definition of Clusters

Clusters were defined by F.A. Cotton as compounds where metal atoms are connected mainly through metal-metal bonds [1]. In recent years the term 'cluster' is increasingly used for 'cage compounds' where the metal atoms are connected through ligands or non-metals, like oxygen or sulphur.

This works deals with metal oxo clusters. It such clusters the metals are connected through metal-oxygen-metal bonds rather than metal-metal bonds.

1.2 Hybrid Materials

Metal oxo cluster are exciting building blocks for inorganic organic hybrid materials. In such materials, inorganic components are embedded into or bonded to an organic matrix or vice versa, organic molecules into an inorganic matrix.

Two main classes of hybrid materials exist, which can be distinguished by the interaction between the inorganic and organic entities [2].

> **Class I** materials or nanocomposites are characterised by weak interaction between the inorganic and organic building blocks. These are typically hydrogen bonds, van der Waals interactions or other weak electrostatic interactions.
>
> **Class II** materials on the other hand are characterised by strong bonds between the inorganic and organic components. Reactive sites on the inorganic components are needed in order to form covalent or ionic bonds. To achieve highly ordered networks, the geometry and number of these functional ligands is crucial. Such stable and sterically well-defined tethering of the inorganic building blocks can overcome problems such as phase separation, aggregation or leaching [3].

Several classes of components can act as inorganic building blocks beside clusters, e.g. nanoparticles, fibre, whiskers and lamellae.

Clusters and nanoparticles of the same composition show similar particle coalescence and surface reactivity, but clusters have great advantages over nanoparticles [4]. Clusters can be analysed by standard techniques, used for molecular compounds. For example, NMR and IR, and when crystallised, their structure can be determined with single crystal X-ray diffraction [5, 6]. Hence they have a defined composition and structure. Furthermore these analytical tools allow control of the surface modification. [7]. Clusters are often soluble which allows better mixing of the precursors for the hybrid material. Their smaller size results in a higher surface/internal volume ratio. All these factors enhance the quality of the final material [8].

There is an increasing interest in functional hybrid materials. Clusters can add chemical or physical properties to the material like magnetic, electronic, optical properties, catalytic activity or piezoelectricity [3].

1.3 Sol-Gel Process

Oxo clusters are formed by the sol-gel process from metal salts or metal alkoxides, as shown in reactions (2.1)-(2.5) for metal alkoxides [9]. Although the precise dosage of water added to a solution of metal alkoxides is quite challenging, it is possible to form clusters [10].

Hydrolysis

$$\mathrm{M{-}OR + H_2O \longrightarrow M{-}OH + ROH} \tag{1.1}$$

The formed M-OH groups may undergo further condensation reactions:

Formation of oxo bridges

$$\mathrm{M{-}OH + RO{-}M \longrightarrow M{-}O{-}M + ROH} \tag{1.2}$$

$$\mathrm{M{-}OH + HO{-}M \longrightarrow M{-}O{-}M + H_2O} \tag{1.3}$$

(Oxolation)

Formation of hydroxo bridges

$$\mathrm{M{-}OH + ROH{-}M \longrightarrow M{-}OH{-}M + ROH} \tag{1.4}$$

$$\mathrm{M{-}OH + H_2O{-}M \longrightarrow M{-}OH{-}M + H_2O} \tag{1.5}$$

(Olation)

For large hydrolysis ratios (= H_2O/alkoxide) the oxolation is favoured against the elimination of alcohol (Eq.2.2 and 2.3). The formation of hydroxo bridges occurs mainly in solution, which are stabilising coordinated alcohols (Eq. 2.4 and 2.5).

This process was extensively studied for silicon alkoxides [11], but can be extended to metal alkoxides. Due to the higher Lewis acidity of metals compared to Si, the reactivity of metal alkoxides is much higher than that of Si. Hydrolysis of metal alkoxides does not require any catalysts, but rather moderators in order to obtain gels instead of precipitates [12].

The driving force behind the high reactivity of metal alkoxides is the high coordination number with respect to their charge. For example, Ti has a typical coordination number of 6 and a charge of 4+, therefore it binds convalently to four OR groups. Completion of the coordination sphere of Ti is achieved by coordination of a solvent or oligomerisation, where OR groups bridge two or three metal atoms.

The degree of oligomerisation is strongly dependent on the OR group and the solvent. Oligomerisation is lower for sterically demanding OR groups. $Ti(OMe)_4$ and $Ti(OEt)_4$ have a very low steric hindrance. They both form a tetramer in the solid state [13,14], $Ti(OCH_2^tBu)_4$, on the other hand, is a dimer [15]. Similar observations are made in benzene solution. While the tetramer is favoured for $Ti(OR)_4$ R = Me, Et, ^{n}Bu [16,17], monomeric species appear for R = ^{i}Pr or ^{t}Bu [15].

In alcoholic solution, an alcohol can coordinate to the metal centre to increase its coordination number and is stabilised by hydrogen bonds to neighbouring alkoxo groups. This coordination competes with the formation of oligomers. The stability of such alcohol adducts is strongly dependent on the Lewis basicity of the alcohol, the Lewis acidity of the metal and also the coordination number of the metal. Hence, alcohol adducts are more stable for Zr and Hf than for Ti. It is possible that the coordinated alcohols (HOR') are involved in an exchange process. The hydrogen of the alcohol is transferred to an alkoxo group (OR) and consequently the HOR group is eliminated. Such a reaction opens the possibility of substituting the OR groups of an alkoxide.

Oligomerisation greatly influences the reactivity of the metal alkoxide [18,19]. All Ti atoms in $Ti(OEt)_4$ have a coordination number of 6, in the monomeric structures only 4. Hence, the reactivity of metal alkoxides with sterically demanding OR groups is higher. The basicity of μ_3-OR and μ_2-OR is higher and therefore they are more easily substituted.

1.3.1 Sol-gel process involving carboxylic acids

The hydrolytic stability of oxo clusters with only alkoxo ligands is quite low. To enhance the stability towards water and moisture they can be modified with bidentate or tridentate ligands, like β- diketonates, phosphonates or carboxylates [20].

The sol-gel process involving carboxylic acids is described below leading to carboxylate substituted oxo clusters [21].

Substitution

$$\mathrm{M(OR)_n + mR'COOH \rightleftharpoons M(OR)_{n-m}(OOCR')_m + mROH} \tag{1.6}$$

Esterification

$$\mathrm{ROH + R'OOH \longrightarrow ROOCR' + H_2O} \tag{1.7}$$

Hydrolysis and Condensation

$$\mathrm{M(OR)_{n-m}(OOCR')_m + H_2O \longrightarrow\ \longrightarrow M_wO_x(OR)_y(OOCR')_m + ROH} \tag{1.8}$$

These reactions do not proceed consecutively, but simultaneously. The substitution and esterification are in fact competing reactions (Eq. 1.6 and 1.7). If a molar ratio of alkoxide/acid of 1 is applied, no esterification takes place and one alkoxide is substituted by an acetate. This was observed in the reaction of $Ti(O^{n}Bu)_4$ and an equimolar quantity of acetic acid resulting in $Ti(O^{n}Bu)_3(OOCMe)$. The acid was completely consumed and butanol was found in the reaction solution, but no ester. Spectroscopic investigations suggested that the acetate ligands in $Ti(O^{n}Bu)_3(OOCMe)$ are bridging and therefore a higher coordination for Ti is obtained [22]. With higher amounts of acid an oxo cluster is formed ($M_wO_x(OR)_y(OOCR_{'})_m$), rather than a carboxylate-substituted metal alkoxide ($M(OR)_{n-m}(OOCR_{'})_m$). Several examples for such reactions are found in literature (Tab. 1.1 and 1.2).

Esterification (Eq. 2.7) is favoured against coordination of the acid at temperatures above 60°C. When $Ti(O^{i}Pr)_4$ and acetic acid were reacted in the molar ratio 1/1.2 at room temperature, the cluster $Ti_6O_4(O^{i}Pr)_{12}(OAc)_4$ was formed [23], but above 80°C the more condensed structure of $Ti_{12}O_{16}(O^{i}Pr)_4$ was obtained [24].

The Lewis-acidity of the metal alkoxides catalyses the esterification. This very slow in situ production of water allows a very controlled hydrolysis of the intermediate substituted alkoxides.

An alternative mechanism is proposed [5], where no water is produced. Coordinating carboxylates and neighbouring OR groups are forming an ester, with simultaneous building of an oxygen bridge according to Eq. 1.9 and 1.10.

$$\mathrm{M{-}OR + M{-}OOCR' \longrightarrow M{-}O{-}M + R'COOR} \tag{1.9}$$

$$\mathrm{M{-}OR + M{-}OR \longrightarrow M{-}O{-}M + ROR} \tag{1.10}$$

An example for such an ester elimination was observed for $\mathrm{Ti_6O_4(OEt)_8(OOCMe)_8}$ which converted into $\mathrm{Ti_6O_6(OEt)_6(OOCMe)_6}$ [25]. The cluster $\mathrm{Ti_4O_2(O^iPr)_{10}(OOCH)_2}$ was monitored over a few weeks and degradated with the loss of $\mathrm{HCOO^iPr}$ [26].

The two mechanisms do not exclude each other, and both may happen.

Table 1.1: Titanium oxo clusters and alkoxides

	R^1	R^2	cif code	Ref.
$\mathrm{Ti_2(\mu_2\text{-}O)(\mu_2\text{-}OOCR^2)_2(OR^1)_2(OOCR^2)_2(HOR^2)_2}$	^{i}Pr	$\mathrm{CCl_3}$	MEKPUN	[27]
$\mathrm{Ti_3(\mu_3\text{-}O)(\mu_3\text{-}OR^1)(\mu_2OR^2)_3(OR^2)_6}$	H	^{i}Pr	FAMSAO	[28]
	Me	^{i}Pr	YUCPUH	[29]
$\mathrm{Ti_3(\mu_3\text{-}O)(\mu_2OR^1)_3(\mu_2\text{-}OOCR^3)_2(OR^1)_5}$	^{i}Pr	$\mathrm{CPh_3}$	FAMRUH	[28]
$\mathrm{Ti_3(\mu_3\text{-}O)(\mu_2OR^1)_2(\mu_2\text{-}OOCR^2)_2(OR^1)_6}$	$\mathrm{CH_2^tBu}$	H	GODJEO	[22]
	$\mathrm{CH_2^tBu}$	$\mathrm{CH_3}$	GODKUF	[22]
	$\mathrm{CH_2^tBu}$	$\mathrm{CH_2CMe_3}$	GOFWAZ	[22]
	^{i}Pr	$\mathrm{C_6H_5}$	LURGIO	[30]
$\mathrm{Ti_3(\mu_3\text{-}O)(\mu_2\text{-}OR^1)_2(\mu_2\text{-}OOCR^2)_3(OR^1)_5}$	^{i}Pr	$\mathrm{CCl_3}$		[27]
$\mathrm{[Ti_3(\mu_3\text{-}OR^1)_2(\mu_2\text{-}OR^1)_3(OR^1)_6][FeCl_4]}$	^{i}Pr		GAFHAX	[31]
$\mathrm{Ti_4(\mu_4\text{-}O)(\mu_2\text{-}OR^1)_6(OR^1)_8}$	furfuryloxo		BOHVAW	[32]
	$\mathrm{CH_2\text{-}_2\text{-}SC_4H_7}$		KEYKIK	[33]
$\mathrm{Ti_4(\mu_4\text{-}O)(\mu_2\text{-}OR^1)_5(OR^1)_{10}H}$	Et		DEJRAN	[34]
$\mathrm{Ti_4(\mu_4\text{-}O)(\mu_2\text{-}O)(\mu_2\text{-}OR^1)_4(\mu_2\text{-}OOCR^2)_2(OR^2)_6}$	^{i}Pr	H	GOMVIN	[26]
	^{i}Pr	$\mathrm{O^iPr}$	ALAQUZ	[35]
	Et	isonicotinato	LUVGUF	[36]
$\mathrm{Ti_4(\mu_3\text{-}O)_4(\mu_2\text{-}OOR^2)_4(OR^1)_4}$	^{i}Pr	$\mathrm{CCo_3(CO)_9}$	TOWXEI	[37]
	^{n}Bu	$\mathrm{CCo_3(CO)_9}$	PAGWAV	[38]
$\mathrm{Ti_4(\mu_3\text{-}O)_2(\mu_2\text{-}OOR^2)_6(OR^1)_6}$	^{i}Pr	C=CH2	XOSYOT	[39]
	^{i}Pr	C(Me)=CH2	XOSYIN	[39]
	^{i}Pr	4-Vinylbenzoato	UXODUH	[40]
$\mathrm{Ti_4(\mu_3\text{-}O)_2(\mu_2\text{-}OR^1)_2(acac)_2(OR^1)_8}$	^{i}Pr		NOCYOT	[41]
$\mathrm{Ti_4(\mu_3\text{-}OR^1)_4(\mu_2\text{-}OR^1)_4(OR^1)_{14}}$	Et		TIETOX	[13]
$\mathrm{Ti_4(\mu_3\text{-}OR^1)_2(\mu_2\text{-}OR^1)_4Cl_2(OR^2)_8}$	Me	^{i}Pr	UHUNUH	[42]
$\mathrm{Ti_4(\mu_3\text{-}OR^1)_2(\mu_2\text{-}OR^1)_4(OR^1)_{10}}$	Me		TIMEOX	[14]
	Et		REZMAK	[43]
$\mathrm{[Ti_4(\mu_2\text{-}O)_6(DMSO)_{12}]Cl_4}$			RUKDEG	[44]

Continued on next page

	R^1	R^2	cif code	Ref.
$Ti_6(\mu_3\text{-}O)_6(\mu_2\text{-}OOCR^2)_6(OR^1)_6$	Et	PhOPh	PAWHEA	[25]
	^iPr	H	GOMVOT	[26]
	^iPr	CH_3	TECPOH	[45]
	^iPr	^tBu	EBEHAV	[46]
	^iPr	$4\text{-}NC_5H_4$	LUVHAM	[36]
	^iPr	CH_2Ph	LUXDOX	[47]
	^iPr	$CHCl_2$	MEKQAU	[27]
	^iPr	Ph−COOiPr		[48]
	$CH_2{}^tBu$	C_6H_5	AJIMAH	[49]
	$CH_2{}^tBu$	^iPr	GODREW	[22]
	$CH_2{}^tBu$	CH_3	IZIHIJ	[50]
	^iBu	CMe_2Et	KAWZAL	[51]
	^nBu	C^tBu	QUJTOF	[52]
	$SiMe_3$	^tBu	KIVLEH	[53]
	$SiMe_3$	$CH_2{}^tBu$	KIVLIL	[53]
	$SiMe_3$	$C(Me)_2Et$	KIVLOR	[53]
$Ti_6(\mu_3\text{-}O)_6(\mu_2\text{-}OR^1)_6(\mu_2\text{-}OOCR^2)_6(\mu_2\text{-}H_2O)_2$	^iBu	^tBu	KAWZIT	[51]
$Ti_6(\mu_3\text{-}O)_4(\mu_2\text{-}OR^1)_4(OR^1)_8(\mu_2\text{-}OOCR^2)$	OEt	$CCo_3(CO)_9$	TOWXAE	[37]
$Ti_6(\mu_3\text{-}O)_2(\mu_2\text{-}O)_3(OR^1)_4(\mu_2\text{-}OR^1)_2(\mu_2\text{-}OOCR^2)_8$	^iBu	^tBu	KAWZEP	[51]
$Ti_6(\mu_3\text{-}O)_2(\mu_2\text{-}O)_2(\mu_2\text{-}OR^1)_6(\mu_2\text{-}OOCR^2)_4(OR^1)_6$	^iPr	Me	GEQLAP	[24]
	^iPr	$CCo_3(CO)_9$	TOWXIM	[37]
$Ti_6(\mu_3\text{-}O)_2(\mu_2\text{-}O)_2(\mu_2\text{-}OR^1)_2(\mu_2\text{-}OOCR^2)_8(OR^1)_6$	Et	Me	GAXXAE	[54]
	Et	$C(Me){=}CH_2$	XUWQIP	[55]
	^iPr	Me	KICSOE	[56]
	^nPr	Ph	AJIMEL	[49]
	^nPr	Norb	LELZIM	[57]
	^nPr	$CH{=}CH_2$	XOSYEJ	[39]
	^nPr	$C(Me){=}CH_2$	XOSYUZ	[39]
	^nPr	$C(Me)_2{\equiv}CH$	VAJZUD	[58]
	^nBu	Me	SEJYAH	[23]
$Ti_7(\mu_4\text{-}O)_2(\mu_3\text{-}O)_2(\mu_2\text{-}OR^1)_8(\mu_2\text{-}OR^2)(O^nPr)_{10}$	Et	PrO	EBOVOH	[59]
$Ti_7(\mu_4\text{-}O)_2(\mu_3\text{-}O)_2(\mu_2\text{-}OR^1)_8(OR^1)_{12}$	Et		SOFTOW	[60]
$Ti_8(\mu_3\text{-}O)_4(\mu_2\text{-}O)_6(\mu_2\text{-}OOCR^1)_{12}$	$CHMe_2$			[61]
	CCl_3			[61]
$Ti_8(\mu_2\text{-}O)_8(\mu_2\text{-}OOCR^1)_{16}$	NEt_2		POJQUB	[62]
	^tBu		RALZOU	[63]
	C_6F_5		YUZNAI	[64]
	Ph			[65]
	$CH_2{}^tBu$		HIJJAN	[66]
	$C(Me){=}CH_2$			[67]
$Ti_8(\mu_4\text{-}O)_4(\mu_2\text{-}O)_2(\mu_2\text{-}OR^1)_8(OR^1)_{12}$	CH_2Ph		KOGYAG	[68]
$Ti_9(\mu_3\text{-}O)_2(\mu_2\text{-}O)_6(\mu_2\text{-}OOCR^2)_{16}(OR^1)_4$	^nPr	$C(Me){=}CH_2$	SUPQOJ	[69]

Continued on next page

	R^1	R^2	cif code	Ref.
$Ti_{10}(\mu_4\text{-}O)_4(\mu_3\text{-}O)_2(\mu_2\text{-}O)_2(\mu_2\text{-}OR^1)_{10}(OR^1)_{14}$	Et		KOGYEK	[68]
$Ti_{11}(\mu_3\text{-}O)_{13}(\mu_2\text{-}OR^1)_{18}$	^{i}Pr		DIQYUX	[70]
$Ti_{11}(\mu_3\text{-}O)_{10}(\mu_2\text{-}O)_3(\mu_2\text{-}OR^1)_7(OR^1)_6(OR^2)_5$	^{i}Pr	Et	YAVYOJ	[71]
$Ti_{12}(\mu_3\text{-}O)_{14}(\mu_2\text{-}O)_2(\mu_2\text{-}OR^1)_4(OR^1)_{12}$	^{i}Pr		YAVYEZ	[71]
	^{i}Pr		GEQLET	[24]
	CH_2^tBu		AMADIC	[72]
$Ti_{12}(\mu_3\text{-}O)_{14}(\mu_2\text{-}O)_2(\mu_2\text{-}OR^1)_4(OR^2)_6(OR^1)_6$	^{i}Pr	Et	YAVYID	[71]
$Ti_{12}(\mu_4\text{-}O)_2(\mu_3\text{-}O)_{10}(\mu_2\text{-}OR^1)_4(\mu_2\text{-}OOCR^2)_6(OR^1)_{14}$	^{n}Pr	Me	IZIHOP	[50]
$Ti_{14}(\mu_3\text{-}O)_{12}(\mu_2\text{-}O)_6(\mu_2\text{-}OR^1)_2(\mu_2\text{-}OOCR^2)_{12}(OR^1)_8$	CH_2^iPr	$C(Me)_2Et$	KAWYUE	[51]
$Ti_{14}(\mu_3\text{-}O)_{17}(\mu_2\text{-}O)_2(\mu_2\text{-}OH)(\mu_2\text{-}OOCR^2)_4(OR^1)_{13}$	^{t}Bu	Me	OPUQEW	[73]
$Ti_{16}(\mu_4\text{-}O)_4(\mu_3\text{-}O)_8(\mu_2\text{-}O)_4(\mu_2\text{-}OR^1)_{16}(OR^1)_{16}$	Et		SEGVOP	[60]
$Ti_{16}(\mu_4\text{-}O)_4(\mu_3\text{-}O)_8(\mu_2\text{-}O)_4(\mu_2\text{-}OR^1)_{16}(OR^1)_{12}(OR^2)_4$	Et	^{n}Pr	MAKDIM	[74]
$Ti_{16}(\mu_4\text{-}O)_4(\mu_3\text{-}O)_8(\mu_2\text{-}O)_4(\mu_2\text{-}OR^1)_{16}(OR^1)_{10}(OR^2)_6$	Et	CH_2CCl_3	ONUTUN	[75]
$Ti_{16}(\mu_4\text{-}O)_4(\mu_3\text{-}O)_8(\mu_2\text{-}O)_4(\mu_2\text{-}OR^1)_{16}(OR^1)_8(OR^2)_8$	Et	^{n}Pr	MAKDOS	[74]
$Ti_{17}(\mu_3\text{-}O)_{20}(\mu_2\text{-}O)_4(OR^1)_{20}$	^{i}Pr		LIDJUD	[70]
$Ti_{17}(\mu_4\text{-}O)_4(\mu_3\text{-}O)_{16}(\mu_2\text{-}O)_4(\mu_2\text{-}OR^1)_4(OR^1)_{16}$	^{i}Pr		QAYCEA	[76]
$Ti_{17}(\mu_4\text{-}O)_4(\mu_3\text{-}O)_{16}(\mu_2\text{-}O)_4(\mu_2\text{-}O^iPr)_4(\mu_2\text{-}OOCR^2)_4(O^iPr)_{12}$		4-(NMe_2)Ph	QAYDAX	[76]
		CH=CH-(4-(NMe_2)Ph)	QAYDEB	[76]
		CH=CHPh	QAYDUR	[76]
$Ti_{18}O_{27}(OH)(OR^1)_{17}$	^{t}Bu		ZUCTIA	[77]
$Ti_{18}(\mu_4\text{-}O)(\mu_3\text{-}O)_{20}(\mu_2\text{-}O)_4(\mu_2\text{-}OR^1)(\mu_2\text{-}OOCR^2)_{10}(OR^1)_{10}$	^{n}Bu	Me	OPUQIA	[73]
	^{n}Bu	Et	QAYFAZ	[76]
$Ti_{28}(\mu_4\text{-}O)_2(\mu_3\text{-}O)_{32}(\mu_2\text{-}O)_6(\mu_2\text{-}OOCR^2)_{12}(OR^1)_{20}$	^{t}Bu	Me	OPUQOG	[73]
$Ti_{34}(\mu_4\text{-}O)_{10}(\mu_3\text{-}O)_{30}(\mu_2\text{-}O)_{10}(\mu_2\text{-}O^iPr)_8(\mu_2\text{-}OOCR^2)_6(O^iPr)_{22}$		4-(NMe_2)Ph	QAYFED	[76]

1.3.2 Parameters influencing cluster formation

The composition and size of the cluster formed during the sol-gel reaction depends on several parameters:

- Type of Alkoxide
- Type of Carboxylic Acid
- Ratio Carboxylic Acid/Alkoxide
- Conditions

Type of Alkoxide As mentioned before, the degree of oligomerisation of the alkoxide influences its reactivity. When, for example, $Ti(O^nPr)_4$ was reacted with 2 equivalents of acrylic acid (HOAcr) the cluster $Ti_6O_4(O^nPr)_8(OAcr)_8$ was formed. The same reaction with $Ti(O^iPr)_4$ leads to $Ti_4O_2(O^iPr)_6(OAcr)_6$ under the same conditions and with the same acid/alkoxide ratio [39].

Type of Carboxylic Acid The carboxylic acid may influence the formed cluster due to steric hindrance, but also carboxylate bond strengths can play a role. The reaction of $Ti(O^nPr)_4$ with 4 equivalents of carboxylic acid lead in the case of $HOOC(CH_2)_2C{\equiv}CH$ to $Ti_6O_4(O^{n}Pr)_8(OOCR)_8$ [58], but with methacrylic acid (HOMc) a more condensed structure was obtained ($Ti_9O_8(O^{n}Pr)_4(OMc)_{16}$) [69].

Ratio Carboxylic Acid/Alkoxide When the carboxylic acid ratio is low, most of it is consumed for substitution rather than esterification. This leads to a low O/M ratio and to clusters with a large number of OR groups. High amounts of carboxylic acid lead to a large amount of produced water and more condensed clusters are formed. This is well illustrated by the reaction of $HOOCCCl_3$ with $Ti(O^iPr)_4$ in molar ratios 1:2 and 2:1. For a Ti:acid ratio of 1:2 the cluster $Ti_3O(O^{i}Pr)_7(OOCCCl_3)_3$ was obtained, whereas with higher amounts of acid $Ti_2O(O^{i}Pr)_2(HO^{i}Pr)_2(OOCCCl_3)_4$ was formed [27].

But the most condensed structures were obtained with medium alkoxide/acid ratios. When methacrylic acid was reacted with $Zr(O^nBu)_4$ in molar ratios 1.6, 4 and 7 the clusters $Zr_6O_2(O^{n}Bu)_{10}(OMc)_{10}$ [78], $Zr_6O_4(OH)_4(OMc)_{12}$ and $Zr_4O_2(OMc)_{12}$ [79] were obtained. $Zr_6O_4(OH)_4(OMc)_{12}$ has the most condensed structure. With very high ratios of carboxylic acid, many coordination sites are occupied by carboxylate ligands, leaving only few coordination sites for condensation reactions.

Conditions Higher temperatures support the esterification process, as reported earlier. Solvents influence the oligomerisation of the alkoxides. Furthermore, carboxylate groups are very dynamic in solution [80] and can undergo exchange processes [7,81,82], which can also lead to a rearangement of the clusters [83–85].

1.3.2.1 Key figures

Degree of Condensation

The ratio of metal atoms to oxo bridges in a cluster is called the degree of condensation. For Ti clusters they range between 0.33 and 1, for carboxylate substituted clusters below 2. The degree of condensation for Zr clusters is generally higher, due to the higher coordination number.

The degree of condensation depends highly on the complexation ratio c and the hydrolysis ratio h. More condensed structures are obtained as c decreases and h increases.

Complexation Ratio c

$c = L/M$ The ratio of organic ligands to metal atoms. The reactivity of an alkoxide depends on the electronegativity and size of the metal.

Hydrolysis Ratio h

$\mathbf{h=H_2O/M}$ The ratio of water to metal atoms.

Poisoning Ratio

The proportion of coordination sites which are occupied by poison ligands is called poisoning ratio. These poison ligands are stable towards hydrolysis or condensation reaction. All non-bridging ligands have to be considered as poison [86].

Table 1.2: Zirconium oxo clusters and alkoxides

Formula	R^1	R^2	cif code	Ref.
$\mathrm{Zr_3(\mu_3\text{-}O)(\mu_3\text{-}OR^1)(\mu_2\text{-}OR^1)_3(OR^1)_6}$	$^{\mathrm{t}}$Bu		DANSAM	[87]
	CH$_2^{\mathrm{t}}$Bu		KAWLUQ	[88]
$\mathrm{Zr_3(\mu_3\text{-}O)(\mu_3\text{-}OR^1)(\mu_2\text{-}OR^2)_3(OR^2)_6}$	$^{\mathrm{t}}$Bu	CH$_2^{\mathrm{t}}$Bu	AMADUO	[72]
	Cl	$^{\mathrm{t}}$Bu	GISPED	[89]
$\mathrm{Zr_3(\mu_3\text{-}O)(\mu_3\text{-}OR^1)(\mu_2\text{-}OH)(\mu_2\text{-}OR^1)_2(OR^1)_6}$	$^{\mathrm{t}}$Bu		GISPIH	[89]
$\mathrm{[Zr_3(\mu_3\text{-}OR^1)(\mu_3\text{-}OR^2)(\mu_2\text{-}OR^1)_3(OR^1)_6][B(C_6F_5)_4]}$	$^{\mathrm{t}}$Bu	$^{\mathrm{n}}$Bu	SOKDOM	[90]
$\mathrm{Zr_3(\mu_3\text{-}O)(\mu_2\text{-}OR^1)_2(\mu_2\text{-}OOCR^2)_3(OR^1)_3(OOCR^2)_2}$	$^{\mathrm{i}}$Pr	Me	KAWLAW	[88]
	CCHCl$_2$		RENWUD	[91]
$\mathrm{Zr_3(\mu_3\text{-}O)(\mu_2\text{-}OR^1)(\mu_2\text{-}OOCR^2)_3(OR^1)_5}$	CH$_2^{\mathrm{t}}$Bu	Me	KAWMAX	[88]
$\mathrm{Zr_3(\mu_3\text{-}O)(\mu_2\text{-}OR^1)_2(\mu_2\text{-}OOCR^2)_2(OR^1)_6}$	$^{\mathrm{t}}$Bu	Ph	XIBMAW	[92]
$\mathrm{Zr_4(\mu_4\text{-}OR^1)_4(\mu_3\text{-}OR^1)_2(\text{-}OR^1)_{10}}$	$^{\mathrm{n}}$Pr		ECIXET	[93]
$\mathrm{Zr_4(\mu_3\text{-}OH)_4(OR^1)_{12}}$	6-bromo-2-naphthoxy		XENPEM	[94]
$\mathrm{Zr_4(\mu_4\text{-}O)(\mu_2\text{-}O)(\mu_2\text{-}O\,^iPr)_4(\mu_2\text{-}OOCH)_2(O\,^iPr)_6}$	$^{\mathrm{i}}$Pr	H	KAWKUP	[88]
$\mathrm{Zr_4(\mu_4\text{-}O)(\mu_2\text{-}OR^1)_6Cl_8}$	Me		MOTUBS	[95]
$\mathrm{Zr_4(\mu_3\text{-}O)_2(\mu_2\text{-}OOCR^1)_{10}(OOCR^1)_2}$	C(Me)=CH$_2$		REBPAP	[79]
			MINFAQ	[96]
			SUSFIW	[7]
$\mathrm{Zr_5(\mu_3\text{-}O)_4(\mu_2\text{-}OOCR^2)_6(OR^1)_2(OOCR^2)_4(HOR^1)_4}$	$^{\mathrm{n}}$Pr	CMe$_2$Br	LUNCIG	[97]
$\mathrm{Zr_5(\mu_3\text{-}O)_3(\mu_2\text{-}ONep)_2(\mu_2\text{-}OOCR^1)_6(ONep)_6}$	$^{\mathrm{i}}$Pr	CH$_2^{\mathrm{t}}$Bu	KAWMEB	[88]
	C$\,^{\mathrm{t}}$Bu	CH$_2^{\mathrm{t}}$Bu	KAWMOL	[88]
$\mathrm{Zr_6(\mu_3\text{-}O)_4(\mu_3\text{-}OH)_4(\mu_2\text{-}OOCR^1)_9(OOCR^1)_3}$	C(Me)=CH$_2$		REBNUH	[79]
$\mathrm{Zr_6(\mu_3\text{-}O)_4(\mu_3\text{-}OH)_4(\mu_2\text{-}OOCR^1)_{12}}$	C$\,^{\mathrm{t}}$Bu		LEXTAK	[98]
	CH$_2^{\mathrm{t}}$Bu		LELZOS	[57]
	C(CH$_3$)$_2$Et		LEXTEO	[98]
$\mathrm{Zr_6(\mu_3\text{-}O)_4(\mu_3\text{-}OH)_4(\mu_2\text{-}OOCR^1)_9(OOCR^1)_3}$	$^{\mathrm{i}}$Pr		FAPNEQ	[84]
	C(Me)=CH$_2$		GOCXEB	[99]
	C$_6$H$_5$		GOCXIF	[99]
	exo-Norb		LELZUY	[57]
$\mathrm{Zr_6(\mu_3\text{-}O)_4((\mu_3\text{-}OH)_4(\mu_2\text{-}R^1)_8(H_2O)_8}$	glycine		CUNTUB	[100]
$\mathrm{Zr_6(\mu_3\text{-}O)_4(\mu_3\text{-}OH)_4(\mu_2\text{-}OOCR^1)_6(\mu_2\text{-}OOCR^2)_2(OOCR^1)_2(OOCR^2)(\eta_1\text{-}OOCR^2)(BuOH)}$				
	C(Me)=CH$_2$	CH=CH$_2$	FAPNIU	[84]
$\mathrm{Zr_6(\mu_3\text{-}OH)_8(\mu_2\text{-}OH)_8(\mu_2\text{-}OOCR^1)_8}$	bis(3,5-dimethylpyrazol-1-yl)		ISEDOZ	[101]
$\mathrm{Zr_6(\mu_3\text{-}OH)_8(\mu_2\text{-}HR^1)_4(\mu_2\text{-}R^1)_4(H_2O)_8}$	glycine		LODTII	[102]
$\mathrm{Zr_6(\mu_3\text{-}OH)_8(\mu_2\text{-}OOCR^2)_8(OOCR^2)_4(OR^1)_4]}$	Me	CHPh$_2$	POQPEQ	[103]
$\mathrm{Zr_6(\mu_3\text{-}O)_6(\mu_2\text{-}OH)_2(\mu_2\text{-}OOCR^1)_6(OOCR^1)_2(\eta_1\text{-}OOCR^1)_2(R^2)_2}$				
	CHPh$_2$	1,10-phenantholine	LOKRUY	[104]
$\mathrm{[Zr_6(\mu_3\text{-}O)_4(\mu_3\text{-}O)_4(\mu_2\text{-}OOCR^1)_9(OOCR^1)_3]_2}$	CH=CH$_2$		GOCXAX	[99]
	CH$_2$CH$_2$−SH		NIHNOI	[105]
	EtC≡CH		VAKBAM	[58]
	Me		YEMVES	[85]

Continued on next page

Formula	R^1	R^2	cif code	Ref.
	Me		YEMVIW	[85]
	Et		YEMVOC	[85]
	$C{=}CMe_2$		YEMVUI	[85]
$[\mathrm{Zr}_6(\mu_3\text{-O})_4(\mu_3\text{-O})_4(\mu_2\text{-OOCR}^1)_9(\mu_2\text{-OH})_3]_2$	CH_2^tBu		MOMYUJ	[106]
$[\mathrm{Zr}_6(\mu_3\text{-O})_4(\mu_3\text{-O})_4(\mu_2\text{-OOCR}^1)_6(\mu_2\text{-OOCR}^2)_3(\mathrm{OOCR}^1)_3]_2$				
	Et	$C(Me){=}CH_2$	YEMWAP	[85]
$[\mathrm{Zr}_6(\mu_3\text{-O})_4(\mu_3\text{-O})_4(\mu_2\text{-OOCR}^2)_2(\mu_2\text{-OOCR}^1)_2(\mathrm{OOCR}^1)_3$				
		Me	YEMWET	[85]
$[\mathrm{Zr}_6(\mu_3\text{-O})_8(\mu_2\text{-OOCR}^1)(\mu_2\text{-OOCR}^2)_8(\mathrm{OOCR}^1)_3]_2$	Me	Et	OMUSAR	[107]
$\mathrm{Zr}_6(\mu_3\text{-O})_2(\mu_2\text{-OR}^1)_6(\mathrm{OOCR}^2)_2(\mathrm{OR}^1)_{10}(\mathrm{HOR}^1)_2$	^nPr	$C_{10}H_6O$	FESQOJ	[108]
$\mathrm{Zr}_6(\mu_3\text{-O})_2(\mu_2\text{-OR}^1)_6(\mu_2\text{-OOCR}^2)_6(\mathrm{OR}^1)_2(\mathrm{OOCR}^2)_4$	^nBu	$C(Me){=}CH_2$	XORPID	[109]
$\mathrm{Zr}_6(\mu_3\text{-O})_2(\mu_2\text{-OR}^1)_8(\mu_2\text{-OOCR}^2)_6(\mathrm{OOCR}^2)_4$	4Me, 4^nBu	$C(Me){=}CH_2$	XORPOJ	[109]
$\mathrm{Zr}_6(\mu_2\text{-O}^n\mathrm{Bu})_4(\mu_2\text{-OR}^1)_6(\mathrm{OR}^2)_{14}$	$EtNH_2$	^nBu	TIYGEO	[42]
$\mathrm{Zr}_{10}(\mu_3\text{-O})_6(\mu_3\text{-OH})_4(\mu_3\text{-OOCR}^2)_8(\mu_2\text{-OOCR}^2)$	C_6H_4OH		FESQUP	[99]
$\mathrm{Zr}_{13}(\mu_4\text{-O})_8(\mu_2\text{-OR}^1)_{24}(\mathrm{OR}^1)_{12}$	Me		JIDNIT	[110]
	Me		TAWWUK	[111]

1.3.2.2 Mixed-Metal Oxo Clusters

Mixed-metal oxo clusters contain at least two different metals, linked through oxygen. The introduction of oxo clusters containing two different metals opens the field to an even larger variety of building blocks with different physical and chemical properties. Through strong anchoring of these clusters to the organic matrix these properties may also be established in the hybrid material [3].

The purpose of preparing most mixed-metal alkoxides and clusters was their use as precursors for functional oxides, for example lead-zirconate-titanate (PZT) or strontium- and barium-titanate [112]. Many of them were investigated in the group of Liliane Hubert-Pfalzgraf [113]. Only very few examples of mixed-metal oxo clusters with carboxylate ligands are known. These are Ti/Zr [78, 114], Ti/Zr/Hf [115] and Ti/Y [116] clusters with methacrylate ligands as well as Ti/Pb [117, 118], Ti/Cu [119] and Ti/Cd [120] clusters with acetates. Whereas the latter were obtained starting from metal acetates and Ti alkoxides, Ti/Zr and Ti/Zr/Hf clusters were synthesised from a mixture of alkoxides, similar to the synthesis of mono-metallic clusters. This approach is quite limited, due to the instability of most other metal alkoxides. When synthesising mixed-metal oxo clusters and alkoxides with Ti, the Ti source was mainly a Ti alkoxide. The second metal was introduced by several sources.

Alkaline earth/Ti clusters are feasible through in situ synthesis of the alkaline earth alkoxide. The pure metal (Sr or Ba) was heated to reflux in the corresponding alcohol to give the alkoxide. The cluster was then synthesised by adding a Ti alkoxide to the cooled solution. Al/Ti alkoxides were also synthesised from Al. Here the Al was heated in a solution of ^iPrOH in the presence of $Ti(O^iPr)_4$ and $HgCl_2$ [121].

Metal acetyl acetonates were used to synthesise mixed-metal alkoxides and clusters of Mg [122], Co [50] and Ni [112] with Ti. Due to the strong binding of the acac ligand, it cannot be removed. This is also the case when metal halides are used as source. The halides can only be substituted if potassium salts of Ti alkoxides are used, or pure potassium was added to the reaction mixture.

A list of several mixed-metal oxo clusters and alkoxides containing Ti is given in Tab. 1.3.

Table 1.3: Mixed-metal alkoxides and clusters containing Ti

Formula	Metal source	cif code	Ref.
$\mathrm{Mg_2Ti_2(OMe)_8(acac)_4}$	$\mathrm{Mg(acac)_2}$, $\mathrm{Ti(OMe)_4}$	ERIKAR	[122]
$\mathrm{[Ti_2(OC_2H_5)_8Cl]_2Mg_2Cl_2}$	$\mathrm{MgCl_2}$, $\mathrm{Ti(OEt)_4}$	VISFAE	[123]
$\mathrm{CaTi_2(OCH_2^tBu)_{10}(NC_5H_5)_2}$	$\mathrm{Ca(N(SiMe_3)_2)_2}$, $\mathrm{Ti_2(OCH_2^tBu)_8}$	VUTFAS	[124]
$\mathrm{CaTi_4(OEt)_{18}}$		POMBIC	[125]
$\mathrm{CaTi_4(OEt)_{18}}$	$\mathrm{Ca(OEt)_2}$, $\mathrm{Ti(OEt)_4}$		[126]
$\mathrm{Sr_4Ti_2O(thd)_4(OEt)_{19}(EtOH)_2}$	Sr in EtOH, $\mathrm{Ti(OEt)_4}$	UMINOU	[127]
$\mathrm{Sr_4Ti_2O(thd)_4(O^nPr)_{10}(^nPrOH)_2}$	$\mathrm{Sr_2Ti_2(thd)_4(O^iPr)_8}$	WOBXIV	[128]
$\mathrm{Sr_4Ti_2OL_{10}(LH)_2Cl_4}$	Sr, $\mathrm{SrL_2}$, $\mathrm{Cp_2TiCl_2}$,	YUBXUP	[129]
	LH= $\mathrm{CH_3OCH_2CH_2OH}$		
$\mathrm{Sr_2Ti(O^iPr)_8(^iPrOH)_3}$	$\mathrm{Sr(OEt)_2}$ from Sr, $\mathrm{Ti(O^{\mathit{i}}Pr)_4}$	GENSOH	[130]
$\mathrm{[Sr_2Ti(OEt)_8(EtOH)_5]n}$	$\mathrm{Sr(OEt)_2}$ from Sr, $\mathrm{Ti(OEt)_4}$		[130]
$\mathrm{Sr_2Ti_2(thd)_4(OEt)_8(EtOH)_2}$	Sr in EtOH, $\mathrm{Ti(OEt)_4}$	UMINIO	[127]
$\mathrm{Sr_2Ti_2(thd)_4(O^iBu)_8}$	Sr in $\mathrm{^iBuOH}$, $\mathrm{Ti(O^iBu)_4}$, thd	UMINUA	[127]
$\mathrm{Sr_2Ti_2O_2(p\text{-}^tBu{-}calix[4]arene)_2}$	Sr, $\mathrm{Ti(O^{\mathit{i}}Pr)_4}$	UNEMEF	[131]
$\mathrm{Sr_6Ti_4O_4(O^iPr)_{20}}$	$\mathrm{Sr(O^iPr)_2}$, $\mathrm{Ti(O^{\mathit{i}}Pr)_4}$	IWULER	[132]
$\mathrm{Sr_3Ti_2O_2(thd)_6(OOC^tBu)_2L_2(Hpz)_2}$	$\mathrm{Sr(thd)_2(Hpz)_3}$, $\mathrm{Ti(O^iPr)_2(thd)_2}$	IPEJUI	[133]
Hpz = Pyrazole, Hthd=Tetramethylheptanedion, L= $\mathrm{^tBuC(O)CH_2CH_2O}$			
$\mathrm{(py)_2Sr[Ti(ONep)_5]_2}$	$\mathrm{Sr_5O(ONep)_9(py)_4}$, $\mathrm{[Ti(ONep)_4]_2}$	VUTFEW	[124]
$\mathrm{[SrTi_2(OEt)_{10}(EtOH)_5]n}$	$\mathrm{Sr(OEt)_2}$ from Sr, $\mathrm{Ti(OEt)_4}$		[130]
$\mathrm{SrTi_4O_2(O^iPr)_{14}(HO^iPr)_2}$	$\mathrm{Sr(O^iPr)_2}$, $\mathrm{Ti(O^{\mathit{i}}Pr)_4}$	IWULIV	[132]
$\mathrm{SrTi_4(OEt)_{18}}$	$\mathrm{Sr(OEt)_2}$ from Sr, $\mathrm{Ti(OEt)_4}$	GENSIB	[130]
$\mathrm{[Ba_2Ti(OEt)_8(EtOH)_5]_n}$	$\mathrm{Ba(OEt)_2}$, $\mathrm{Ti(OEt)_4}$		[130]
$\mathrm{Ba_4Ti_4O_4(O^iPr)_{16}(^iPrOH)_3}$	Ba, $\mathrm{Ti(O^{\mathit{i}}Pr)_4}$	KOKREH	[134]
	$\mathrm{Ba(O^iPr)_2}$, $\mathrm{Ti(O^{\mathit{i}}Pr)_4}$	WIBLOI	[135]
$\mathrm{Ba_2Ti_2O_2(HOMe)_{12}(p\text{-}^tBu{-}calix[4]arene)_2)_2}$	Ba, $\mathrm{Ti(O^{\mathit{i}}Pr)_4}$	UNENAC	[131]
$\mathrm{Ba_2Ti_2(thd)_4(OEt)_8(EtOH)_2}$	$\mathrm{Ba(thd)_2}$, $\mathrm{Ti(OEt)_4}$	ZESCIJ	[136]
thdH = 2,2,6,6-tetramethylheptane-3,5-dione			
$\mathrm{Ba_2Ti_2(thd)_4(O^nPr)_8(HO^nPr)_2}$	Ba, $\mathrm{Ti(O^{\mathit{n}}Pr)_4}$	YOGGIL	[137]
$\mathrm{BaTi(OPh)_6}$	Ba, $\mathrm{Ti(O^{\mathit{i}}Pr)_4}$	ZERLOX	[29]
$\mathrm{Ba_2Ti_{40}(OMe)18\,(MeOH)_7}$	$\mathrm{Ba(OMe)_2}$, $\mathrm{Ti(OMe)_4}$	NUKLOU	[138]
$\mathrm{(py)_2BaTi_2(ONep)_{10}}$	Ba, $\mathrm{Ti_2(ONep)_8}$	VUTFIA	[124]
$\mathrm{[BaTi_2(OEt)_9(EtOH)_4][OEt]}$	$\mathrm{Ba(OEt)_2}$, $\mathrm{Ti(OEt)_4}$	ZASVEU	[126]
$\mathrm{Ba_4Ti_{13}O_{18}(OEtOMe)_{24}}$	$\mathrm{Ba(OEtOMe)_2}$, $\mathrm{Ti(OEtOMe)_4}$	TAMPEC	[139]
$\mathrm{BaTi_3O_2(O^iPr)_{12}}$	$\mathrm{Ba(O^iPr)_2}$, $\mathrm{Ti(O^{\mathit{i}}Pr)_4}$	RATJOL	[140]

Hthd = tetramethylheptanedion, Hpz = pyrazole, Nep = $\mathrm{C^tBu}$, pin = pinacolate
dmae = $\mathrm{OEtNMe_2}$, THME = $\mathrm{(OMe)_3Et}$

Continued on next page

Formula	Metal source	cif code	Ref.
$\mathrm{BaTi_4(OEt)_{18}}$	$\mathrm{Ba, Ti(OEt)_4}$	POMBOI	[125]
$\mathrm{Ba_2Ti_{10}O_8(OH)_5(OMc)_{20}(O^iPrOMe)_2}$	$\mathrm{BaTi(O^iPrOMe)_6}$	EDEXAN	[141]
$\mathrm{Y_2Ti_4O_4(OMc)_{14}(HOEtOMe)_2}$	$\mathrm{Y(OEtOMe)_3, Ti(O^{\mathit{n}}Pr)_4}$	IXIJII	[116]
$\mathrm{Y_2Ti_4O_4(OMc)_{12}(OEtOMe)_2(HOMc)_2}$	$\mathrm{Y(OEtOMe)_3, Ti(O^{\mathit{n}}Pr)_4}$	IXIJAA	[116]
$\mathrm{Y_2Ti_4O_4(OMc)_{12}(OEtOMe)_2}$	$\mathrm{Y(OEtOMe)_3, Ti(O^{\mathit{n}}Pr)_4}$		[116]
$\mathrm{Cl_2YTi_2(O^iPr)_9}$	$\mathrm{YCl_3, KTi_2(O^iPr)_9}$		[140]
$\mathrm{Ce_2Ti_2O_2(pin)_4(O^iPr)_4(^iPrOH)_2}$	$\mathrm{[Ce_2O(pin)_2(pinH)]_m, Ti(O^{\mathit{i}}Pr)_4}$	CURQEL	[142]
$\mathrm{Sm_4TiO(O^iPr)_{14}}$	$\mathrm{SmI_2, [NaTi(OCHMe_2)_5]n}$	WICZUD	[143]
$\mathrm{(Tb_{0.9}Er_{0.1})_4TiO(O^iPr)_{14}}$	$\mathrm{TbCl_3, ErCl_3, Ti(O^{\mathit{i}}Pr)_4}$	NAQNUO	[144]
$\mathrm{Er_2Ti_4O_2(OEt)_{18}(HOEt)_2}$	$\mathrm{ErCl_3,Ti(OEt)_4}$	PUPYEE	[145]
$\mathrm{Eu_3TiK_3O_2(O^tBu)_{11}(OMe/OH)(HO^tBu)}$	$\mathrm{EuCl_3, Ti(O^tBu)_4, K}$	KAFXUM	[146]
$\mathrm{SmTi_2Cl_7O(THF)_6}$	$\mathrm{Sm, TiCl_4}$	QANBEN	[147]
$\mathrm{[Ti_2O(OEt)_8(EtOH \cdot NdCl)]_2}$	$\mathrm{NdCl_3,Ti(OEt)_4}$,	DEJRIV	[34]
$\mathrm{LnTi_{28}O_{38}(OEt)_{40}H_2Cl}$	$\mathrm{LnCl_3, Ti(OEt)_4}$ Ln = La, Ce	DEJQUG	[34]
$\mathrm{CrTi_3O(OEt)_{14}Cl}$	$\mathrm{CrCl_2, Ti(OEt)_4}$	IBANEG	[148]
$\mathrm{Ti_4O(OEt)_{15}(Mn_2Cl_3)}$	$\mathrm{MnCl_2, Ti_7O_4(OEt)_{20}}$	EWONOU	[149]
$\mathrm{FeTi_2(O^iPr)_9Cl}$	$\mathrm{FeCl_2, Ti(O^{\mathit{i}}Pr)_4}$	XIZJAR	[150]
$\mathrm{[Ti_3(OMe)_2(O^iPr)_9][Fe_4TiCl_4O(O^iPr)_9]}$	$\mathrm{FeCl_2, Ti(O^{\mathit{i}}Pr)_4}$	XIZJEV	[150]
$\mathrm{Co_4Ti_2O(O^nPr)_{10}(acac)_4}$	$\mathrm{Co(acac)_2, Ti(O^{\mathit{n}}Pr)_4}$	VAGHAO	[50]
$\mathrm{Co_2Ti_2(OEt)_8(acac)_4}$	$\mathrm{Co(acac)_2, Ti(OEt)_4}$	VAGGIV	[50]
$\mathrm{Co_2Ti_2(OMe)_8(acac)_4}$	$\mathrm{Co(acac)_2, Ti(OMe)_4}$	ERIJUK	[151]
$\mathrm{Co_2Ti_2(O^iPr)_{10}(acac)_2}$	$\mathrm{Co(acac)_2, Ti(O^{\mathit{i}}Pr)_4}$	GUVGAF	[152]
$\mathrm{CoTi_7O_5(OEt)_{19}Cl}$	$\mathrm{CoCl_2(EtOH)_x, KTi_2(OEt)_9}$	QUQLAQ	[149]
$\mathrm{CoTi_7O_5(OEt)_{18}Cl_2}$	$\mathrm{CoCl_2, Ti_7O_4(OEt)_{20}}$	IBAMUV	[148]
$\mathrm{Co_2Ti_2((OMe)_3Et)_2(O^iPr)_2((OOCCCo_3(CO)_9)}$	$\mathrm{Co(CO)_6, Ti(O^{\mathit{i}}Pr)_4}$	PAHBAB	[38]
$\mathrm{ICoTi_{11}O_{14}(O^iPr)_{27}}$	$\mathrm{CoI_2, Ti(O^{\mathit{i}}Pr)_4}$	QICGAT	[153]
$\mathrm{[(BrCo)_6Ti_{15}O_{24}(O^iPr)_{18}Br][Ti_{12}O_{15}(O^iPr)_{17}]}$	$\mathrm{CoBr_2, Ti(O^{\mathit{i}}Pr)_4}$	FEBVAL	[154]
$\mathrm{Ni_2Ti_2(acac)_4(OEt)_8}$	$\mathrm{Ni(acac)_2, Ti(OEt)_4}$	MIWTAO	[112]
$\mathrm{[Ti_2O(OEt)_9(NiCl)]_2}$	$\mathrm{NiCl_2, Ti_7O_4(OEt)_{20}}$	EWONUA	[149]
$\mathrm{Cu_6Ti_4O_6(OH)(OEtNMe_2)_6(OBenz)_9}$	$\mathrm{Cu(OBenz)_2 \cdot 2\,H_2O}$, $\mathrm{Ti(dmae)_4}$	LIYXEX	[155]
$\mathrm{Cu_6Ti_4O_6(OH)(OEtNMe_2)_6(OMetBenz)_9}$	$\mathrm{Cu(2{-}MeBenz) \cdot H_2O, Ti(dmae)_4}$	LIYXIB	[155]
$\mathrm{CuTi_2(O^iPr)_5Cl}$	$\mathrm{CuCl_2, KTi_2(O^iPr)_9}$	RATJIF	[140]
$\mathrm{Cu_6Ti_4(dmae)_6(OH)O_6(OAc)_9}$	$\mathrm{Cu(OAc)_2 \cdot H_2O, Ti(dmae)_4}$	WIDLAX	[119]
$\mathrm{Ti_4O(OEt)_{15}(CuCl)}$	$\mathrm{CuCl_2}$, $\mathrm{Ti_7O_4(OEt)_{20}}$	EWONIO	[149]
$\mathrm{Ti_4O(OEt)_{15}(ZnCl)}$	$\mathrm{ZnCl_2, Ti_7O_4(OEt)_{20}}$	EWONAG	[149]
$\mathrm{CdTi_2(O^iPr)_9I}$	$\mathrm{CdI_2, KTi_2(O^iPr)_9}$	TOCNII	[156]

Hthd = tetramethylheptanedion, Hpz = pyrazole, Nep = $\mathrm{C^tBu}$, pin = pinacolate
dmae = $\mathrm{OEtNMe_2}$, THME = $\mathrm{(OMe)_3Et}$

Continued on next page

Formula	Metal source	cif code	Ref.
$(CdBaTi_2(O^iPr)_{12})_2$	$CdCl_2$, $KBa(O^iPr)_3$	TOCNUU	[156]
$Cd_4Ti_4O_6(OR)_4(OCCF_3)_4(OAc)_4(HOAc)_4$	$Cd(OAc)_2 \cdot 2\,H_2O$, $Ti(OEt)_4$ $R{=}CHCH_2NMe_2$	WEBWIL	[120]
$Al_2Ti(O^iPr)_{10}$	Al, $Ti(O^iPr)_4$	REGYOR	[121]
$AlTi(O^iPr)_4(C_6F_5)_3$	$Al(C_6F_5)_3$, $Ti(O^iPr)_4$	QOMXUM	[157]
$SnTi(OEt)_4Cl_4(HOEt)_2$	$SnCl_4$, $Ti(OEt)_4$	AMUPAA	[158]
$SnTi(OEt)_4Cl_4(HOEt)_2 \cdot EtOH$	$SnCl_4$, $Ti(OEt)_4$	AMUNUS	[158]
$[SnTi_2(O^iPr)_9][SnCl_3]$	$[ClSn(Ti_2(O^iPr)_9]_2$, $SnCl_2$	NOYMAP	[159]
$I_2SnTi_2(O^iPr)_{10}$	SnI_4, $KTi(O^iPr)_5$	RUMZOM	[160]
$Sn_3Ti(ONep)_4(THME)_2$	$Sn_3(THME)_2$, $Ti(ONep)_4$	OFIZUY	[161]
$[Ti_3(O^iPr)_{11}][Sn_2I_6(O^iPr)_3]$	SnI_4, $KTi(O^iPr)_5$, $KTi_2(O^iPr)_9$	NOYLUI	[159]
$Pb_4Ti_4O_6(OAc)_4(O^iPr)_8$	$Pb_2Ti_2O(OAc)_2(O^iPr)_8$		[117]
$Pb_2Ti_2O(OAc)_2(O^iPr)_8$	$Pb(OAc)_2$, $Ti(O^iPr)_4$	NAYPUY	[117]
$Pb_2Ti_4O_2(OAc)_2(OEt)_{14}$	$Pb(OAc)_2$, $Ti(OEt)_4$		[117]
$[PbTi_2O(OAc)(OEt)_7]_2$	$Pb(OAc)_2$, $Ti(O^iPr)_4$	YEVWIF	[118]
$Pb_2Ti_3O_2(OOCC(Et)Bu)_2(O^iPr)_{10}$	$Pb(OCC(Et)Bu)_2$, $Ti(O^iPr)_4$	JEBSIT	[162]
$Pb_2Ti_4(OOCC(Et)Bu)_4(O^iPr)_{16}$	$Pb(OOCC(Et)Bu)_2$, $Ti(O^iPr)_4$,	JEBSOZ	[162]
$Pb_2Ti_4(OOCC(Et)Bu)_4(O^nBu)_{16}$	$Pb(OCC(Et)Bu)_2$,$Ti(O^nBu)_4$		[163]
$[PbTi_2O(OEt)_8]n$	$Pb_4O(OEt)_6$, $Ti(OEt)_4$		[117]
$Pb_4TiO(O^iPr)_4(NH_2C_4H_9)_3$	$Pb(N^tBu)_2SiMe_2$, $Ti(O^iPr)_4$	RODMAY	[164]
$Pb_2Ti_2O(O^iPr)_{10}$	$[Pb(O^iPr)_2]n$, $Ti(O^iPr)_4$, reflux	YIYKUM	[165]
	$[Pb_4O(O^iPr)_6]$, $Ti(O^iPr)_4$		[165]
	room temperature		
$BiTi_2O(O^iPr)_9$	$Bi(O^tBu)_3$, $Ti(O^iPr)_4$	PAWZIW	[166]

1.4 General Structure of Metal Oxo Clusters

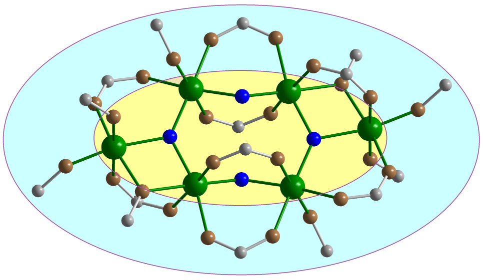

Figure 1.1: Core-shell structure of a metal oxo cluster. Core oxygen atoms are drawn in blue. The yellow area marks the cluster core and the blue area the cluster shell or ligand sphere.

Metal oxo clusters generally posses a core-shell structure as shown in Fig. 1.1. A cluster can be divided into two parts: The cluster core and the ligand sphere or cluster shell. The cluster core is built by the metals and oxygen bridging these metals. Oxygen bridge either two metals

(μ_2-O) or three metals (μ_3-O). In rare cases they can also bridge four of five metals (μ_4-O, μ_5-O). Sometimes these oxygen atoms are protonated, mainly due to charge balance. Although hydrogen are often not found in the electron density map, the existence of those is evidenced in the elongated M-O bond lengths.

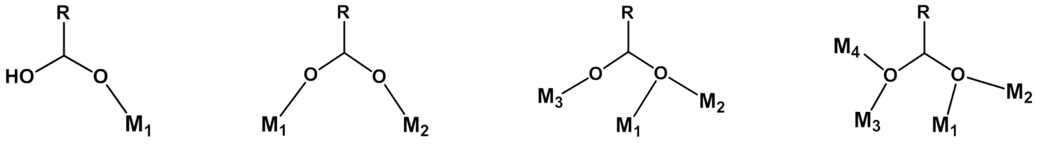

(a) η_1- Terminal (b) μ_2- Bridging (c) μ_3- Bridging (d) μ_4- Bridging

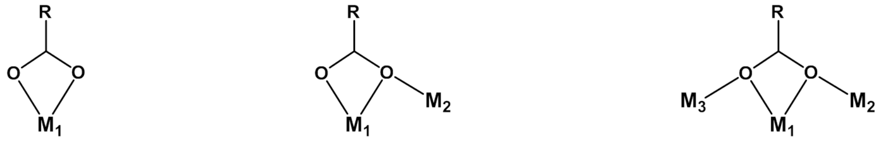

(e) Chelating (f) Chelating/μ_2- Bridging (g) Chelating/μ_3- Bridging

Figure 1.2: Compendium of common coordination motives of carboxylic acids and carboxylate ligands in oxo-carboxo-clusters.

The ligand sphere stabilises the cluster core. In the case of carboxylate-substituted oxo clusters, the sphere contains mainly carboxylate and alkoxy ligands. A compendium of possible coordination modes is drawn in Figs. 1.2-1.3. Carboxylates can bridge or chelate metals. The most common coordination for carboxylates is bridging two metals (Fig. 1.2(b)), but also bridging three or four metals is possible (Fig. 1.2(c)-(d)). A combination of chelating and bridging also exists. Here one oxygen of a chelating ligands is additionally coordinating to a second metal or even a third metal (Fig. 1.2(f)-(g)). Terminal carboxylates (Fig. 1.2(a)) are often stabilised by hydrogen bridges to neighbouring alkoxy ligands or core oxygen. The distinction between a carboxylate and a carboxylic acid coordinating is often ambiguous, as the location of the hydrogen atom is often challenging.

Alkoxo ligands are either bridging (Fig. 1.3(b)) or terminal (Fig. 1.3(a)). The latter is often found in exposed positions on the cluster. Bridging of more than two metals is also possible (Fig. 1.3(c)).

1.4.1 Differences between Ti and Zr

The most stable oxidation state for both metals is +IV. The Zr^{4+} ion is larger than the Ti^{4+} ion, therefore it favours higher coordination numbers. Most common coordination numbers for Zr are 7 and 8, compared to 6 for Ti. The coordination sphere of Ti^{4+} is an octahedron, often distorted. The shape of the Zr coordination sphere is strongly dependent on the environment.

The ionic radius of Ti^{4+} in a sixfold-coordination is 0.605 Å, [167], the $Ti^{4+}-O^{2-}$ bond lengths are typically between 1.8 and 2 Å. The ion size of the Zr^{4+} is 0.78 Å in a 7-fold coordination and 0.84 Å for 8-fold coordination. The $Zr^{4+}-O^{2-}$ bonds are typically between 2.0 and 2.2 Å.

These two factors explain the differences in the structure of Ti and Zr clusters. Zr clusters are generally more condensed than Ti clusters, expressed by the degree of condensation. This is calculated by the ratio core-oxygen/metal-ion. The maximum degree of condensation found for Ti clusters is 1, in Zr clusters it can reach 1.33.

Titanium is often coordinated to terminal alkoxy groups, which can also be protonated. Coordinated alkoxy groups and alcohol molecules differ greatly in the Ti-O distance. Those of alkoxy ligands are often below 1.8 Å, whereas Ti- alcohol bond lengths are above 2.1 Å. Terminal alkoxy ligands are less often observed for Zr. Zr favours chelating carboxylates, which provide the same charge. The Zr−O bonds of chelating carboxylates are longer than Zr−O bonds of bridging ligands, and the O-C-O angle of the carboxylate groups are smaller than in the bridging ligand. Ti atoms chelated by a carboxylate ligand are very rare, because this would lead to a highly distorted $[TiO_6]$ octahedron.

1.4.2 Remarks on further reading

Oxo clusters will be called just 'cluster' in the remainder of this thesis, as this work deals exclusively with oxo clusters. Abbreviations of clusters are used instead of their full formula, a list for all cluster abbreviations is given in Tab.1.4.

1.5 Structures in the Literature

Coordination compounds with oxygen atoms bridging metal atoms appear with various ligands. Apart from alkoxo and carboxylate ligands, they are known for dialkoholates, oximates, amines and ligands where more than two alkoholate or amino groups are present. There are also a lot of structures which originate from metal-Cp and Cp derivatives. Similarities can be drawn between these ligands and oxo-alkoxo clusters or oxo-carboxylate clusters.

The most common structures of Zr and Ti oxo clusters are described below. They are restrained to oxo-alkoxo and oxo-carboxylate clusters, as these are the most relevant for the present work. A list of all Ti and Zr oxo clusters is given in Tabs. 1.1 - 1.2 -.

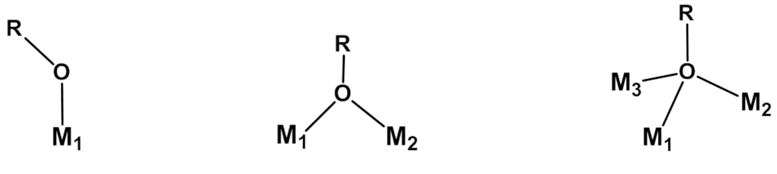

(a) Terminal (b) μ_2- Bridging (c) μ_3- Bridging

Figure 1.3: Compendium of common coordination motives of alkoxo and alkoxy ligands.

Table 1.4: List of used abbreviations for known Zr/Ti clusters.

Zr3	Clusters with Zr_3O cluster core
Zr4	Clusters with Zr_4O_2 cluster core
Zr6Oct	Zr6 clusters with octahedral cluster core
Zr6flat	Zr6 clusters with a flat cluster core
Ti3	Clusters with Ti_3O cluster core
Ti4	Clusters with Ti_4O_2 cluster core
Ti6Prism	Ti6 clusters with prismatic cluster core
Ti6flat	Ti6 clusters with a flat cluster core
Ti8ring	Clusters formed by eight edge sharing $[TiO_6]$ octahedra
Zr2Ti4met	$Zr_2Ti_4O_4(O^nBu)_6(OMc)_{10}$ (OMc=methacrylate)
Zr4Ti4met	$Zr_4Ti_4O_6(O^nBu)_4(OMc)_{16}$
Zr4Ti2met	$Zr_4Ti_2O_4(O^nBu)_2(OMc)_{14}$
Zr6Ti2met	$Zr_6Ti_2O_6(OMc)_{20}$

1.6 Zirconium Clusters

1.6.1 Structure of Zr3 clusters

Clusters with three Zr atoms usually have a Zr_3O cluster core. Two different structure motives are known depending on the ligand sphere. In the first structure only alkoxo ligands are coordinated and the general formual is $Zr_3(\mu_3\text{-O})(\mu_3\text{-OR})(\mu_2\text{-OR})_3(OR)_6$. This structure is only known for bulky groups, like O^tBu and OCH_2^tBu, Zr has here only a coordination number of 6. In the second structure the coordination number is increased by partial substitution of the alkoxo groups with carboxylates. Instead of the μ_3-OR and one terminal alkoxy group there are two μ_2- carboxylates. One of the μ_2-OR groups can be subsituted with a bridging carboxylate. Some of the terminal alkoxy groups can be substituted by chelating carboxylates, resulting in the general formula $Zr_3(\mu_3\text{-O})(\mu_2\text{-OR})_2(OR)_{5+x-y}(\mu_2\text{-OOCR})_{3-x}(\eta_1\text{-OOCR})_y$. An example of an oxo-carboxo Zr3 cluster is given in Fig 1.4(a).

1.6.2 Structure of Zr4 clusters

In the clusters with general formula $Zr_4O_2(OOCR)_{12}$ two Zr coordination polyhedra are corner sharing, with bridging μ_3-O. The other two Zr atoms are joined on both sides, coordinating to the μ_3-O. These outer Zr atoms are chelated by a carboxylate. The remaining carboxylates bridge two Zr atoms, resulting in coordination numbers of 7 for inner Zr and 8 for the outer Zr atoms, as shown in Fig.1.4(b). In a modifiaction of this cluster type, one carboxylate is chelating/bridging one inner Zr atom resulting also in an 8-fold coordination sphere.

One cluster, containing four Zr is known where all Zr atoms are linked through a μ_4-O and are arranged to a distorted tetrahedron.

1.6.3 Structure of Zr6 clusters

Three different structures for Zr6 clusters are known in literature. The most common is a cluster where the six Zr atoms are arranged to an octahedron (see Fig. 1.4(d)). Two of these clusters are connected by four ligands in the second cluster type (Zr12). With large ligands it is possible to form a flat cluster core (Fig. 1.4(c)).

1.6.3.1 Zr6 Octahedron

In the basic structure first described by Kickelbick *et al.* [69] the six Zr atoms are arranged in a regular octahedron. The general formula is $Zr_6O_4(OH)_4(OOCR)_{12}$.

Every face of the octahedron is capped by a core-oxygen. Hence every core oxygen is coordinating to three Zr atoms. The Zr-O bonds of four of these core oxygen are significantly longer than those of the other four core oxygen. Therefore, these four oxygen are protonated. Core oxygen with long bonds are adjacent to core oxygen with short bonds, hence every Zr atom has two short Zr-O bonds and two long Zr-O bonds to the core oxygen.

Three of the twelve carboxylates are chelating, the corresponding Zr atoms are at one face of the octahedron. The core oxygen of this face is strongly bonding. All other carboxylates bridge two Zr atoms. In a modification of this cluster type, all carboxylates are bridging Zr atoms.

1.6.3.2 Zr12

In the closely related structure with the general formula $[Zr_6O_4(OH)_4(OOCR)_{12}]_2$ two Zr6 octahedra are connected by four carboxylates. These four carboxylates are located opposite to the chelating carboxylates and are singly bonded to the three non-chelated Zr atoms. These carboxylates bridge to three Zr atoms of the next Zr6 unit.

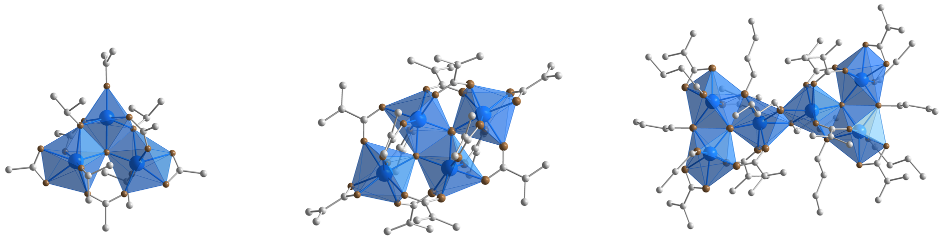

(a) **Zr3** $Zr_3O(OR)_5(OOCR^1)_5$

(b) **Zr4** $Zr_4O_2(OOCR^1)_{12}$

(c) **Zr6 with flat core** $Zr_6O_2(OR)_{10}(OOCR^1)_{10}$

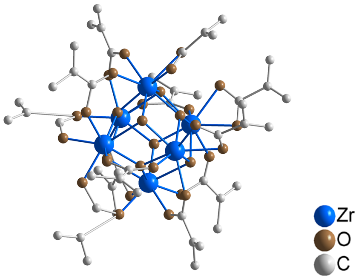

(d) **Zr6 octahedron** $Zr_6O_4(OH)_4(OOR^1)_{12}$

Figure 1.4: Molecular structure of Zr oxo clusters.

It was shown by Puchberger and co-workers, that the Zr12 cluster cannot be converted into the Zr6 cluster [85].

1.6.3.3 Zr6 clusters with flat core

In $Zr_6O_2(O^nBu)_{10}(OMc)_{10}$ and $Zr_6O_2(O^nBu)_2(OMe)_4(OMc)_{14}$ [94] two equivalent $[Zr_3O]$ units are connected by two bridging alkoxo groups (Fig1.4(c)). These $[Zr_3O]$ units are closely related to the Zr_3O clusters, as the coordination within the $[Zr_3O]$ units is very similar to that of Zr3 clusters.

There are also two core oxygen atoms in $Zr_6O_2(O^nPr)_{16}(HO^nPr)_2(OOC{-}C_{10}H_6O)_2$ [93], but the cluster core is actually a $[Zr_4O_2]$ unit with two additional Zr atoms on the edge. These two Zr atoms are not coordinated to the core oxygen atoms and link only through bridging carboxylates. The two 1-oxo-β-naphthylate units are tridentate. The carboxylate group is chelating a Zr atom of the Zr_4O_2 unit and the third oxygen is coordinated to the additional Zr atom.

1.7 Titanium Clusters

Similar clusters are also found for titanium. In general, the chelating carboxylates are substituted by terminal alkoxy groups, compared with the Zr clusters.

1.7.1 Structure of Ti3 clusters

An isostructural cluster to $Zr_3(\mu_3\text{-}O)(\mu_3\text{-}OR)(\mu_2\text{-}OR)_3(OR)_6$ exists also for Ti, but in this case it is also obtained with less bulky groups. In oxo-carboxylate Ti3 clusters with the general formula $Ti_3O(OR)_8(OOCR^1)_2$ the three titanium atoms are connected through one core oxygen as shown in Fig.1.5(a). The carboxylates are all bridging, as well as two or three alkoxo ligands. The remaining alkoxy ligands are all terminal. In clusters with only two bridging alkoxo groups, one Ti has only a coordination number of 5.

1.7.2 Structure of Ti4 clusters

The structure of Ti4 clusters is also very similar to those of Zr4 clusters according to Fig.1.5(b). The chelating carboxylates are here substituted by terminal alkoxy groups. Bridging carboxylates can also be exchanged with bridging alkoxo groups.

1.7.3 Structure of Ti6 clusters

A flat and a more condensed cluster type is also known for Ti6 clusters.

1.7.3.1 Ti6 prism

A similar structure to the Zr6 octahedron is also known for Ti. Due to the lower coordination number, there are only six core oxygen atoms. The structure of the cluster core is also not a regular octahedron, but is better descripted as a hexagonal prism, where Ti and O alternate within the hexagon (Fig.1.6). The general formula for this cluster is $Ti_6O_6(OR)_6(OOCR_1)_6$.

Every Ti atoms is coordinating to an alkoxy group, each of which is located on the top and bottom of the layer. The angle between the Ti-OR bond and the base is almost 90°. The carboxylates are bridging two Ti atoms of different layers, forming a ring around the lateral surface of the prism.

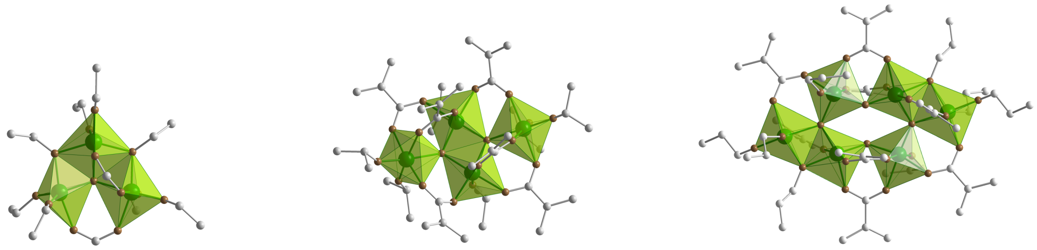

(a) **Ti3**
$Ti_3O(OR)_9(OOCR^1)$

(b) **Ti4**
$Ti_4O_2(OR)_6(OOCR^1)_6$

(c) **Ti6 with flat core**
$Ti_6O_4(OR)_8(OOCR^1)_8$

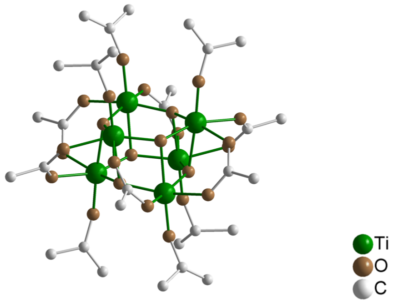

(d) **Ti6 prism**
$Ti_6O_6(OR)_6(OOCR^1)_6$

Figure 1.5: Molecular structure of Ti oxo clusters.

(a) Core of the Ti6 Prism

(b) Core of the Zr6 Octahedron

Figure 1.6: Comparison of the cores of octahedral Ti6 and Zr6 clusters.

1.7.3.2 Ti6 cluster with a flat core

The basic formula for the Ti6 cluster with a flat cluster core is $Ti_6O_4(OR)_8(OOCR_1)_8$. The core consists of two $Ti_3(\mu_3\text{-O})$ units joined by two μ_2-O according to Fig. 1.5(c). All ligands coordinate the cluster core. The outer Ti atom is linked to one neighbouring Ti atom through a bridging alkoxo group and one bridging carboxylate. It is connected to the second Ti atom through a bridging carboxylate. This Ti atom further coordinates to a terminal alkoxy group. The outer Ti atom is coordinated to two terminal alkoxy groups. The two inner Ti atoms are further connected through one bridging carboxylate.

Two structures of this cluster are known. One where twelve alkoxo ligands are coordinating, instead of eight, resulting in a formula $Ti_6O_4(OR)_{12}(OOCR^1)_4$. The outer Ti is connected to both neighbouring Ti through one bridging alkoxo group and one bridging carboxylate. Additionally two alkoxo ligands are bridging 'over' the cluster core. There are also two bridging alkoxo grpups in $Ti_6O_4(O^iPr)_4(HO^iPr)_4(ONp)_6$ (ONp= Naphthalene-2,3-diolate), but only four ONp ligands are bridging Ti atoms. Two ONp are chelating the outer Ti atoms, and the remaining alkoxy ligands are all terminal.

1.7.4 Ti8 ring

In clusters with the general structure $Ti_8O_8(OOCR)_{16}$ eight corner sharing $[TiO_6]$ octahedra are forming a Ti_8O_8 ring. The eight Ti atoms are approximately coplanar. The eight μ_2-core oxygen atoms point to the centre of the ring and are located slightly off the Ti ring plane. The void can be accessed by small molecules, for example solvent molecules or a diethylammonium cation. One of the two bridging carboxylate ligands per unit is approximately located in the plane of the Ti8 ring. The other eight carboxylate ligands are almost perpendicular to the ring, alternating above and below it.

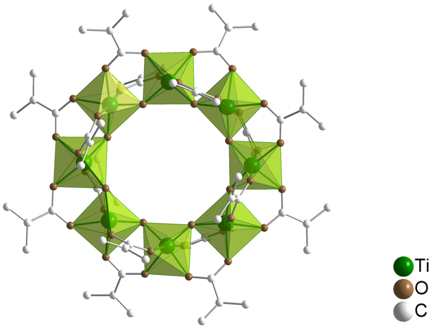

Figure 1.7: Molecular structure of $Ti_8O_8(OMc)_{16}$ [67].

1.8 Mixed Zirconium/Titanium Clusters

Moraru and co-workers synthesised four mixed Zr/Ti oxo cluster with methacrylate ligands and different Zr:Ti ratios [78]. Those were $Zr_2Ti_4O_4(O^nBu)_6(OMc)_{10}$ [Zr2Ti4met], $Zr_4Ti_2O_4(O^nBu)_2(OMc)_{14}$ [Zr4Ti2met], $Zr_4Ti_4O_6(O^nBu)_4(OMc)_{16}$ [Zr4Ti4met] and $Zr_6Ti_2O_6(OMc)_{20}$ [Zr6Ti2met]. A comparison of these four cluster cores is illustrated in Fig. 1.8. The cluster cores are zig-zag chains of ZrO_7 and ZrO_8 polyhedra, the $[TiO_6]$ octahedra are coordinated on the side of these chains.

With increasing the Zr content, the number of coordinating alkoxo ligands is decreasing. In Ti4Zr2met every Ti is coordinated to one O^nBu ligand. The remaining two are bridging a Ti and a Zr atom. All methacrylates are bridging. In Zr4Ti4met two methacrylates are chelating the two inner Zr atoms. The four OBu groups in Zr4Ti4 are all terminally coordinated to the two Ti atoms on the edge of the cluster core.

These two Ti atoms are missing in Zr4Ti2met. Hence there are no terminal alkoxy groups. The two O^nBu groups are bridging two Zr atoms. The inner Zr atoms are not chelated by methacrylates, but the Zr atoms at the end of the zig-zag chain are coordinated to two chelating

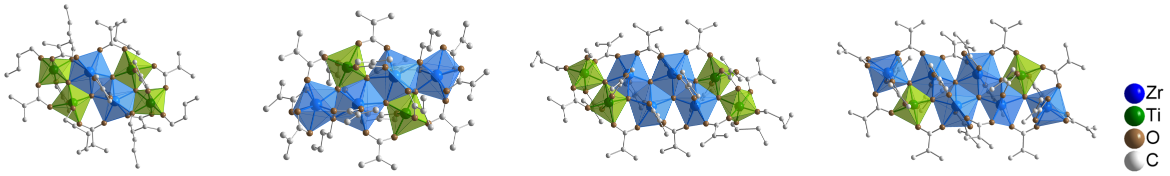

(a) Zr2Ti4met (b) Zr4Ti2met (c) Zr4Ti4met (d) Zr6Ti2met

Figure 1.8: Molecular structure of mixed Zr/Ti methacrylate clusters.

methacrylates each. Chelating ligands appear also in Zr6Ti2met, as well as the two methacrylates chelating the two innermost Zr atoms. But there are no longer alkoxo ligands.

An isostructural cluster to Zr4Ti2met has been obtained with acetic acid [114]. In $Zr_5HfTi_2O_6(OMc)_{20}$ [115] two Zr sites are partly substituted by Hf atoms compared to Zr6Ti2met.

Table 1.5: Mixed-metal clusters of Zr, Ti and Hf

	R^1	R^2	cif code	Ref.
$Zr_2Ti_4O_4(OR^1)_6(OOCR^2)_{10}$	^{n}Bu	$C(Me)=CH_2$	QOWJAN	[78]
	^{i}Pr	Me	DILFAG	[114]
$Zr_4Ti_4O_6(OR^1)_4(OOCR^2)_{14}$	^{n}Bu	$C(Me)=CH_2$	QOWHUF	[78]
$Zr_4Ti_2O_4(OR^1)_2(OOCR^2)_{16}$	^{n}Bu	$C(Me)=CH_2$	QOWJER	[78]
$Zr_6Ti_2O_6(OOCR^2)_{20}$		$C(Me)=CH_2$	QOWJIV	[78]
$Zr_5HfTi_2O_6(OOCR^2)_{20}$		$C(Me)=CH_2$	KAGBUQ	[115]

Chapter 2

Aim of this work

The aim of this work was to synthesise new mixed-metal oxo clusters and structurally characterise them by single crystal X-ray diffraction. The focus will be on mixed-metal oxo clusters of Ti and Zr, as well as on mixed-metal oxo clusters containing either Ti or Zr.

Metal oxo clusters were previously studied for their application in inorganic-organic hybrid materials. For this purpose the clusters need to be functionalised, which can for example be achieved by organofunctional carboxylates, for example methacrylic acid. It has the advantage that it has a polymerisable group, which allows incorporation in class II hybrid materials.

The key to ordered networks is the control of the geometry of the ligands on the surface of the cluster, which is best monitored by single crystal X-ray diffraction. A desirable option is to have an anisotropic functionalization of the cluster surface, which implies a mixed ligand sphere of non-functional and functional ligands. A possibility to obtain such cluster is ligand exchange, but often the structure of the cluster changes during such a reaction. Therefore, it is important to find clusters having the same structure and coordination, but different ligands. Part of this work focuses on the influence of different carboxylic acids on the formation of mixed-metal oxo clusters.

One approach to control the structure of the clusters and the arrangement of the ligands is to use oxo clusters containing two different metals. Ideally, due to the different bonding characteristics of the used metals, an anisotropic functionalization could be obtained. Hence, several combinations of Ti and Zr with a second metal will be examined.

Until now only few carboxylate substituted clusters of group IV elements containing two different metals are known. The first group are methacrylate clusters of Ti with Zr, Zr and Hf or Y, which were all synthesised from a mixture of metal alkoxides and reacted with methacrylic acid. The second group are mixed-metal oxo clusters of Ti with Pb, Cu or Cd with acetate ligands. These ligands originate from the reaction of metal acetates with Ti alkoxides.

Metal acetates are promising starting compunds for mixed-metal oxo clusters containing Ti. The question is, whether it is possible to synthesise these clusters also with functionalised carboxylic acids, like methacrylic acid. Furthermore, the variety of metals can be expanded to other Ti-metal combinations and even mixed metal/Zr clusters. This might also give rise to clusters with new chemical and physical properties, which can be incorporated to the hybrid material.

The various Ti and Zr alkoxides often show different reactivities. Part of this work was to study the influence of the type of metal alkoxide on the formation of mixed Ti/Zr oxo clusters and other mixed-metal oxo clusters.

Part II

Results and Discussion

Details of the synthesis and experimental procedures are found in chapter 8. Tables of bond distances and angles listed in Appendix A. Crystal data, data collection parameters and refinement details of all measured crystals are found in Appendix B.

A list of all obtained new clusters and their abbreviations is given in Tab. 2.1.

Table 2.1: List of all obtained clusters and their abbreviation

Abbreviation	**Formula**	Descriped in
Mixed Zr/Ti cluster		
Zr4Ti2benz	$Zr_4Ti_2O_4(O^nBu)_2(OBenz)_{14} \cdot 2\,THF$	Sec.3.1.1
Zr4Ti2tBubenz	$Zr_4Ti_2O_4(OR)_{0.8}(OOCC_6H_4{-}^tBu)_{15.2}(HOOCC_6H_4{-}^tBu)$	Sec.3.1.2
Zr4Ti2ClMebenz	$Zr_2Ti_4O_4(O^nBu)_6(OOC{-}C_6H_4{-}CH_2Cl)_{10}$	Sec.3.1.1
ZrTi2piv	$ZrTi_2O(O^iPr)_4(OMc)_6$	Sec.3.2.1
Zr3Ti2piv	$Zr_3Ti_2O_3(O^nBu)_3(OPiv)_{11}$	Sec.3.2.2.1
Zr2Ti3piv	$Zr_2Ti_3O_3(O^nPr)_4(O^iPr)(OPiv)_9$	Sec.3.2.2.2
Zr4Ti2piviPr	$Zr_4Ti_2O_5(OH)_2(O^iPr)(OPiv)_{11} \cdot 2\,HOPiv$	Sec.3.2.3.2
Zr4Ti2pivnPr	$Zr_4Ti_2O_5(OH)_2(O^nPr)(OPiv)_{11}$	Sec.3.2.3.1
Zr4Ti2pivAc	$Zr_4Ti_2O_5(OH)_2(O^iPr)(OPiv)_{11}(HOPiv) \cdot 2\,HOPiv \cdot H_2O$	Sec.3.2.3.4
Zr3Ti3piv	$Zr_3Ti_3O_4(OH)_3(O^nBu)_3(OPiv)_{10}$	Sec.3.2.3.5
Zr6Ti8piv	$Zr_6Ti_8O_{15}(OH)_4(O^nBu)_2(OPiv)_{20}(HOPiv)_2 \cdot 2\,HOPiv$	Sec.3.2.4
Zr4Ti3ada	$Zr_4Ti_3O_7(O^nBu)_2(OOCAda)_{12}$	Sec.3.3
	HOOCAda = 1-Adamantanecarboxylic acid	
Mixed Ti clusters		
Zn2Ti4	$Zn_2Ti_4O_4(O^iPr)_2(OMc)_{10}$	Sec.4.1.1
Cd4Ti2	$Cd_4Ti_2O_2(OAc)_2(OMc)_{10}(HO^iPr)_2$	Sec.4.1.2
Ca2Ti4	$[Ca_2Ti_4O_4(OAc)_2(OMc)_{10}]_n$	Sec.4.2.1.1
Ca2Ti4a	$[Ca_2Ti_4O_4(OAc)(OMc)_{11}(HOMc) \cdot {}^nBuOH]_n$	Sec.4.2.1.2
Sr2Ti4	$[Sr_2Ti_4O_4(OMc)_{12}(HOMc)_2]_n$	Sec.4.2.2
Sr2Ti8	$Sr_2Ti_8O_8(O^iPr)_{1.73}(OAc)_{2.27}(OMc)_{16}$	Sec.4.3.1
Pb2Ti8	$Pb_2Ti_8O_8(O^nBu)_2(OAc)_{0.656}(OMc)_{17.354}({}^nBuOH)_2$	Sec.4.3.2
Pb2Ti8allyl	$Pb_2Ti_8O_8(O^nBu)_2(OMc)_{18}(AllylOH)_2$	Sec.4.3.2.1
Pb2Ti8nPr	$Pb_2Ti_8O_8(O^nPr)_2(OAc)_{0.484}(OMc)_{17.516}({}^nPrOH)_2$	Sec.4.3.2.2
Pb2Ti6	$Pb_2Ti_6O_5(O^iPr)_{2.76}(OMc)_{15.24}$	Sec.4.3.3

Continued on next page

Abbreviation	**Formula**	Descriped in
Pb2Ti6nPr	$Pb_2Ti_6O_5(O^{n}Pr)_3(OMc)_{15}$	Sec.4.3.3.1
Pb4Ti8Ac	$Pb_4Ti_8O_{10}(O^{i}Pr)_{18}(OAc)_2$	Sec.4.4.1
Pb6Ti6	$Pb_6Ti_6O_9(OAc)(OMc)_{17}$	Sec.4.4.2
Cu4Ti5met	$Cu_4Ti_5O_6(OMc)_{16}$	Sec.4.5.1
Cu4Ti5metS	$Cu_4Ti_5O_6(OMc)_{16} \cdot 2\,CH_2Cl_2$	Sec.4.5.1
Cu4Ti5prop	$Cu_4Ti_5O_6(OProp)_{16}$	Sec.4.5.2
FeTi5	$FeTi_5O_4(O^{i}Pr)_4(OMc)_{10}$	Sec.4.6
LnTi4	$LnTi_4O_3(O^{i}Pr)_2(OMc)_{11}$	Sec.4.7.1
	Ln = La, Ce	
Ln2Ti6	$Ln_2Ti_6O_6(HO^{i}Pr)_2(OMc)_{18}$	Sec.4.7.2
	Ln = La, Ce, Nd	
Ln2Ti4	$Ln_2Ti_4O_4(OAc)_2(OMc)_{12}(OHMc)_2$	Sec.4.7.3
	Ln = Sm, Eu, Gd, Ho	
Mixed Zr clusters		
Ag2Zr8	$Ag_2Zr_8O_6(hmp{-}H)_2(hmp)_2(OMc)_{16}(HOMc)_2$	Sec.5.1
	hmp = 2-(hydr)oxo-2-methylpropionate	
Monometallic		
Ti6prop	$Ti_6O_6(O^{i}Pr)_2(OProp)_{10}$	Sec.6.1.1
Ti6pivPB	$Ti_6O_4(O^{n}Pr)_2(O^{n}Bu)_6(OPiv)_8$	Sec.6.1.2
Ti6pivBB	$Ti_6O_4(O^{n}Bu)_8(OPiv)_8$	Sec.6.1.3
Ti8prop	$Ti_8O_8(OProp)_{16}$	Sec.6.1.4
Zr4benz	$Zr_4O_2(OBenz)_{12}$	Sec.6.2.1
Zr4piv	$Zr_4O_2(OPiv)_{12}$	Sec.6.2.2
Zr6piv	$Zr_4O_2(OBenz)_{12}$	Sec.6.2.3

Chapter 3

Structure of Mixed Titanium/Zirconium Clusters

3.1 Benzoic Acid Derivatives

All below described clusters were synthesised from a mixture of Ti and Zr alkoxides and different carboxylic acids. THF was mainly used as solvent.

Mixed-metal oxo clusters of Zr and Ti were obtained with benzoic acid (C_6H_5COOH), 4-tert−butyl benzoic acid ($^{t}Bu{-}C_6H_4COOH$) and 4-chlor−methyl benzoic acid ($ClCH_2{-}C_6H_4COOH$) (Fig. 3.1). The clusters with benzoate and 4-tert−butyl benzoate are isostructural to Zr4Ti2met decribed in Sec. 1.8. $Zr_2Ti_4O_4(O^{n}Bu)_6(OOC{-}C_6H_4{-}CH_2Cl)_{10}$ is isostructural to Ti4Zr2met.

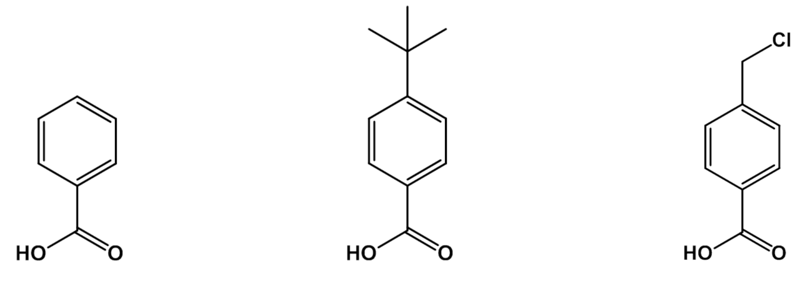

(a) Benzoic acid (b) ^{t}Bu-Benzoic acid (c) Cl-Me-Benzoic acid

Figure 3.1: Benzoic acid derivatives

3.1.1 Benzoic acid

In $Zr_4Ti_2(\mu_3\text{-}O)_4(\mu_2\text{-}O^{n}Bu)_2(\mu_2\text{-}OBenz)_{10}(OBenz)_4 \cdot 2\,THF$ (HOBenz= benzoic acid) (Fig. 3.2) the outer Zr atoms Zr(2) are disordered over two sites, as well as one oxygen atom of the chelating carboxylate (O(16)) according to Fig. 3.3. An effect on the other light atoms of this group was not observed. The distance between Zr(2) and Zr(2A) on the second site is only 0.214(18)

Å. Small shifts in the Zr-O bond lengths are observed (Tab. A.1). Zr(2A) binds stronger to the bridging O^{n}Bu group than Zr(2). On the other hand the Zr(2A) bond of the benzoate bridging the two Zr atoms is weakened (Zr(2)-O(3) 2.149(2), Zr(2A)-O(3) 2.056(10); Zr(2)-O(5) 2.144(2), Zr(2A)-O(5) 2.327(18) Å). Due to the shift of the Zr(2A) position, the bond lengths of the second chelating benzoate decrease (Zr(2)-O(14) 2.219(2), Zr(2)-O(15) 2.333(3); Zr(2A)-O(14) 2.100(13), Zr(2A)-O(15) 2.140(19) Å). All other bonds of Zr(2A) do not differ much from those of Zr(2).

Two THF molecules cocrystalised with the cluster, both show no coordination to the cluster. An electron density of 44 electrons was still present in the unit cell, the nature of these molecules could not be elucidated, but are probably disordered solvent molecules.

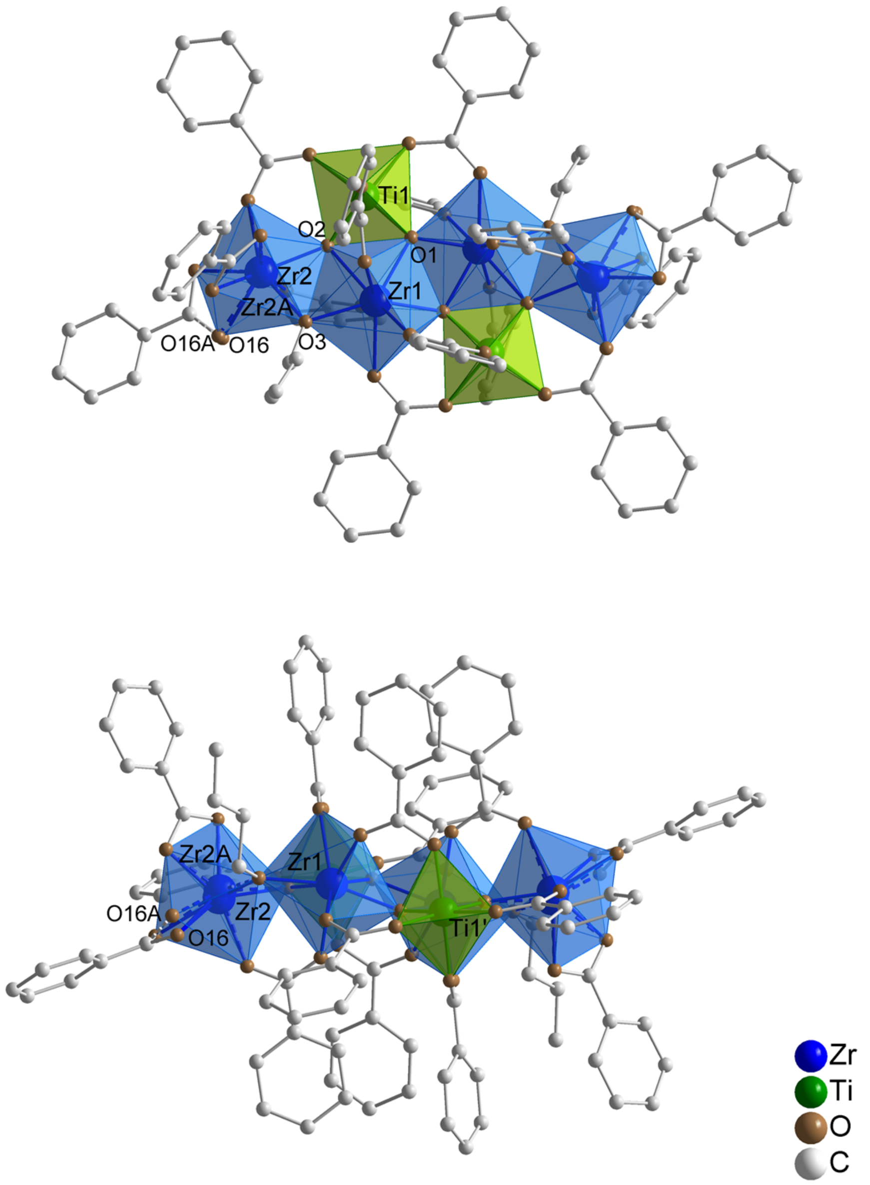

Figure 3.2: Molecular structure of $Zr_4Ti_2(\mu_3\text{-}O)_4(\mu_2\text{-}O^nBu)_2(\mu_2\text{-}OBenz)_{10}(OBenz)_4 \cdot 2\,THF$. Hydrogen atoms are omitted for clarity.

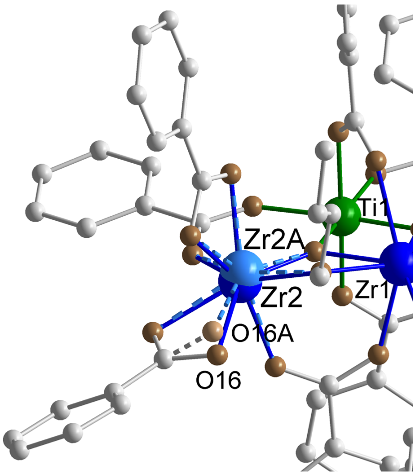

Figure 3.3: Details of $Zr_4Ti_2(\mu_3\text{-O})_4(\mu_2\text{-O}^n\text{Bu})_2(\mu_2\text{-OBenz})_{10}(\text{OBenz})_4 \cdot 2\,\text{THF}$

3.1.2 4-^{t}Butyl–benzoic acid

The crystal quality of the tert-butyl benzoate cluster was quite poor. Nevertheless a disorder of the ligand sphere compared to Zr4Ti2met was observed. This originates from the cocrystalisation of very similar clusters, viz. $Zr_4Ti_2O_4(OOCC_6H_5-{}^t\text{Bu})_{16}$ with an occupancy of 60% and $Zr_4Ti_2O_4(OR)_2(OOCC_6H_5-{}^t\text{Bu})_{14}$ with an occupancy of 40%, resulting in a formula of $Zr_4Ti_2(\mu_3\text{-O})_4(\mu_2\text{-OR})_{0.8}(\mu_2\text{-OOCC}_6H_5-{}^t\text{Bu})_{11.2}(\text{OOCC}_6H_5-{}^t\text{Bu})_4$ (Fig. 3.4).

The second cluster is isostructural with Zr4Ti2met. In the first cluster, Zr(1) and Zr(2) are not connected by one bridging alkoxo ligand and one bridging carboxylate, but instead two carboxylates. This affects also one of the chelating carboxylates on Zr(2). The new position of this carboxylate is further apart from the new bridging carboxylate. An effect on the position of the Zr atoms was not observed, but the distance between the two Zr atoms is larger than in the benzoate cluster (Zr(1)-Zr(2) 3.7276(14) instead of 3.4935(13) Å). The Ti(1)-Zr(2) distance on the other hand is slightly shorter (3.6808(19) instead of 3.7515(14) Å). The remaining bond lengths are not affected by this disorder. For a comparison of the bond lengths with those of Zr4Ti2met see Tab. A.1)

The exact nature of the OR group could not be resolved, as only the position of the oxygen atom could be determined. To obtain a neutral cluster this group needs to provide a charge of -1. Therefore it is not possible that this oxygen is a core oxygen. Due to the composition of the mother liquid, there are three possibilities for this group: O^{n}Bu, O^{i}Pr or OH.

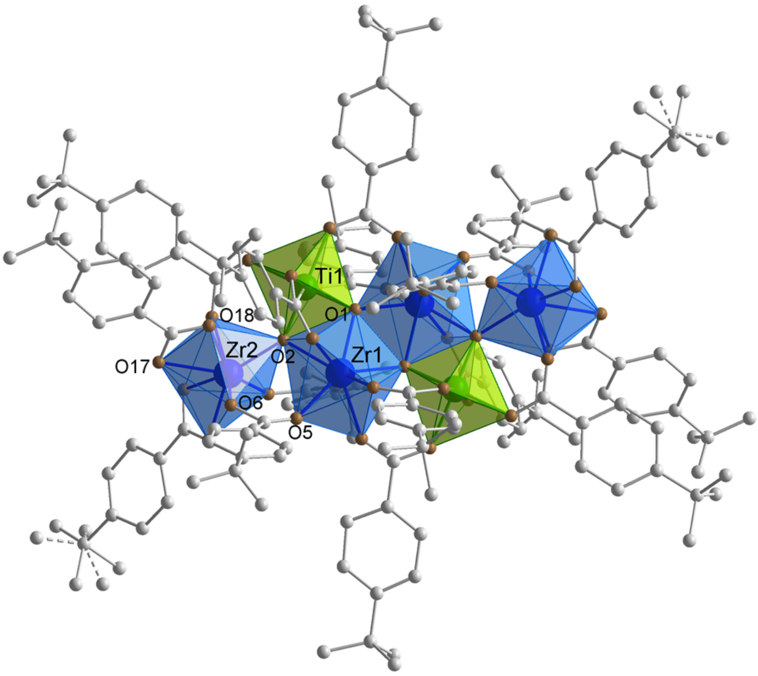

(a) Cluster 1: $Zr_4Ti_2O_4(OOCC_6H_5-{}^tBu)_{16}$

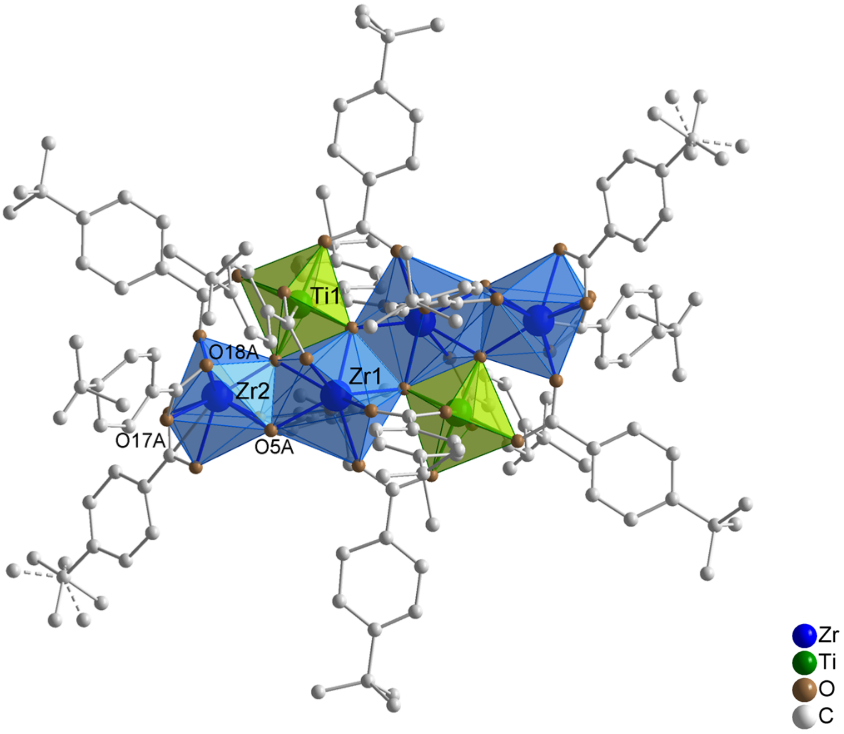

(b) Cluster 2: $Zr_4Ti_2O_4(OR)_2(OOCC_6H_5-{}^tBu)_{14}$

Figure 3.4: Molecular structure of the two clusters of $Zr_4Ti_2(\mu_3\text{-}O)_4(\mu_2\text{-}OR)_{0.8}(\mu_2\text{-}OOCC_6H_5-{}^tBu)_{11.2}(OOCC_6H_5-{}^tBu)_4$. Hydrogen atoms are omitted for clarity.

3.1.3 4-Cl–Methyl–benzoic acid

The molecular structure of $\mathrm{Zr_2Ti_4(\mu_3\text{-}O)_4(\mu_2\text{-}O^nBu)_4(O^nBu)_2(\mu_2\text{-}OOCC_6H_4{-}CH_2Cl)_{10}}$ (Fig. 3.5) is isostructural to that of Zr2Ti4met. But the crystal structure differs. Even though the Cl-methyl benzoate cluster crystallises in the higher space group $P2_1/c$ the molecular structure is of lower symmetry than that of the Ti4Zr2met cluster. Due to the missing inversion centre in the centre of the cluster, the asymetric unit is doubled and all atoms of the cluster are symmetrically independent. This is probably caused by the disorder of the Cl atoms.

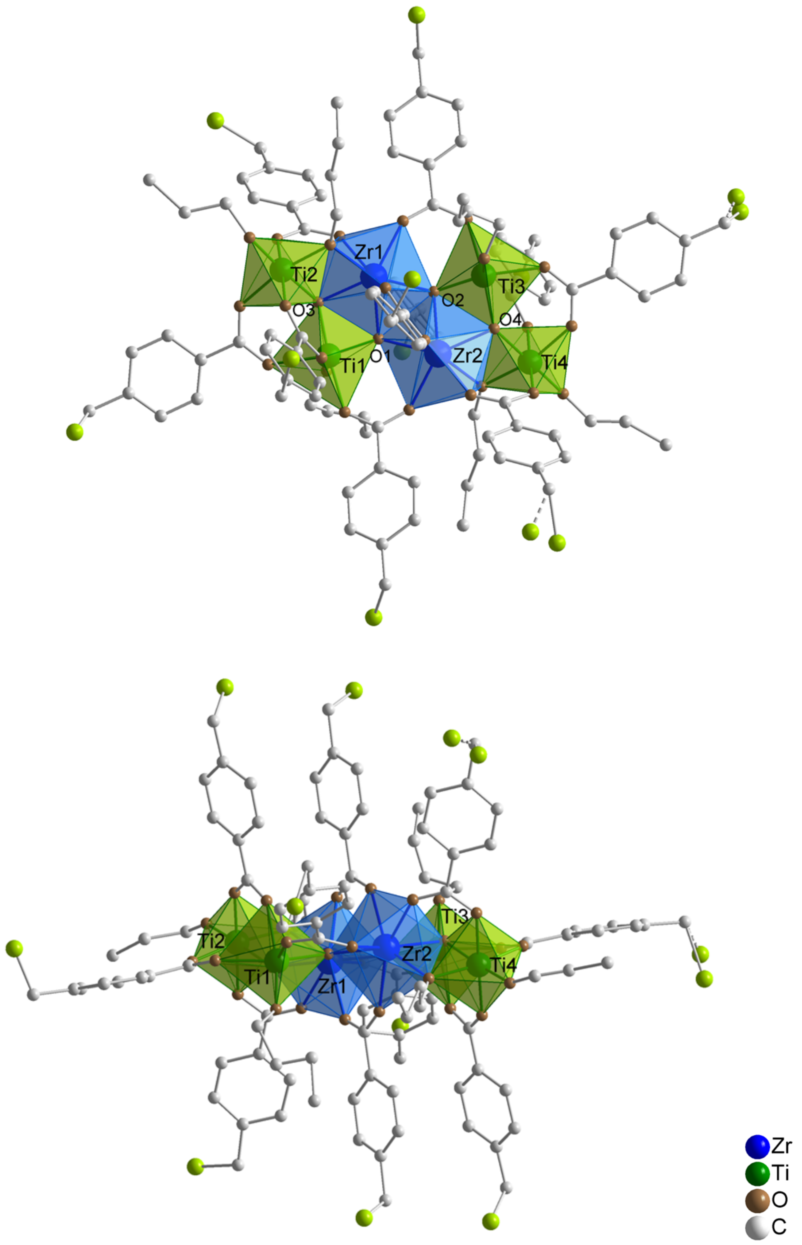

Figure 3.5: Molecular structure of $\mathrm{Zr_2Ti_4(\mu_3\text{-}O)_4(\mu_2\text{-}O^nBu)_4(O^nBu)_2(\mu_2\text{-}OOCC_6H_4{-}CH_2Cl)_{10}}$. Hydrogen atoms are omitted for clarity. Disordered parts are drawn with dashed bonds.

3.2 Pivalic Acid

Clusters with pivalate were synthesised from a mixture of Ti and Zr alkoxides and pivalic acid at room temperature. Details are described in the experimental section on page 99.

3.2.1 ZrTi2piv

In ZrTi$_2$(μ_3-O)(μ_2-O^{i}Pr)$_2$(O^{i}Pr)$_2$(μ_2-OPiv)$_5$(η_1-OPiv) (Fig. 3.6) two Ti atoms and one Zr atom are connected by one core μ_3-O. The core oxygen atom is located slightly above the plane spanned by the three metal atoms. The sum of M-O(1)-M angles is 349.14(18)° (Tab. A.4). The Ti-O(1) distances are almost identical (Ti(1)-O(1) 1.9365(12), Ti(2)-O(1) 1.9381(12) Å) and the Zr-O bond is the shortest in the structure (Zr(1)-O(1) 2.0533(12) Å) (Tab. A.3).

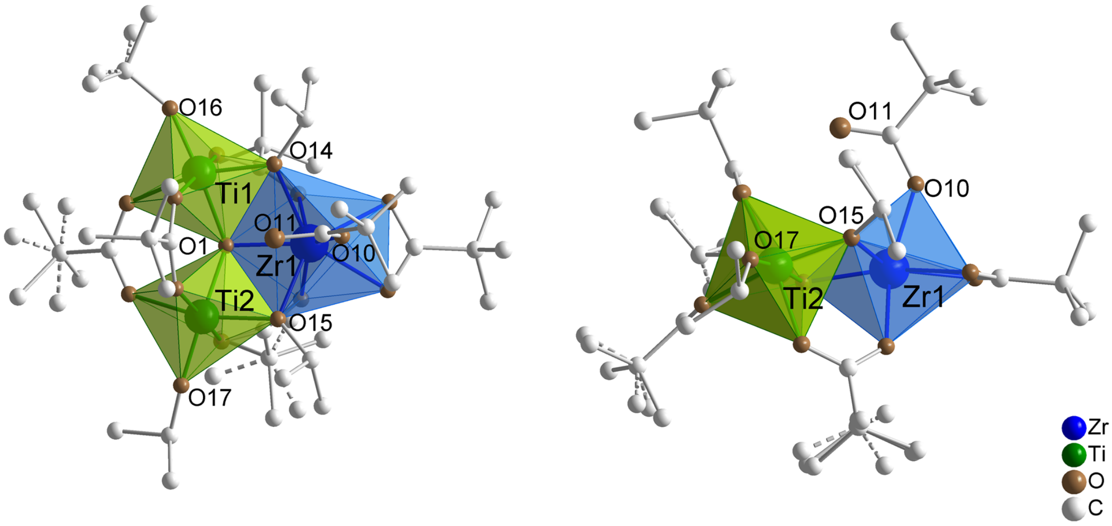

Figure 3.6: Different views of the molecular structure of ZrTi$_2$(μ_3-O)(μ_2-O^{i}Pr)$_2$(O^{i}Pr)$_2$(μ_2-OPiv)$_5$(η_1-OPiv). Disordered parts are drawn with broken bonds. Hydrogen atoms are omitted for clarity

Besides the core oxygen atom, the Zr atoms are coordinated to each Ti atom through one bridging pivalate and one O^{i}Pr group. The Zr coordination polyhedron is edge sharing with the [TiO$_6$] octahedra. The Zr-O bond lengths to each of the ligands is comparable, as well as those of Ti(1) and Ti(2). The Ti-O^{i}Pr bond lengths are slightly shorter than the Ti-OPiv bond lengths (Ti(1)-O(3) 2.0040(13), Ti(1)-O(14) 1.9252(13); Ti(2)-O(5) 2.0358(13), Ti(2)-O(15) 1.9365(12) Å). The Zr-O distances of these two ligands do not differ (Zr(1)-O(2) 2.2524(12), (Zr(1)-O(4) 2.2312(12); Zr(1)-O(14) 2.2471(12), Zr(1)-O(15) 2.2227(12) Å).

One pivalate is chelating the Zr atom, the two Zr-O bond lengths being the longest in the structure (Zr(1)-O(12) 2.2602(13), Zr(1)-O(13) 2.2540(13) Å). The eighth coordination site is occupied by a η_1-pivalate. The second oxygen atom of the pivalate which is not bonded to a metal atom points in direction of the core oxygen atom. Although the geometry would anticipate hydrogen bonds to the core oxygen, the distance between the two oxygen is too large (O(1)$\cdots$O(11) 3.7505(18) Å). Furthermore, the pivalate ligand has to be deprotonated for charge balance.

The last pivalate is bridging the Ti atoms, where the carboxylate group in located in the same plane as the cluster core. The Ti-O bond lengths differ only slightly (Ti(1)-O(8) 2.0550(14), Ti(2)-O(9) 2.0436(13) Å) and are in both cases the longest in this structure. A terminal O^iPr group coordinating to each of the Ti atoms is completing their coordination sphere. Their Ti-O bond lengths are very short with Ti(1)-O(16) 1.7682(13) and Ti(2)-O(17) 1.7852(13) Å.

The [TiO_6] octahedra are strongly distorted. The largest angle is between the bridging and the terminal alkoxy group (O(14)-Ti(1)-O(16) 104.41(6)°; O(15)-Ti(2)-O(17)102.05(6)°), while the angle between the core oxygen atom and the bridging alkoxo group is decreased (O(1)-Ti(1)-O(14) 79.48(5)°; O(1)-Ti(2)-O(15) 78.50(5)°). The remaining angles are in the normal range around 90° (84.48(5)-95.96(6)°).

The cluster has a pseudo mirror plane through Zr(1) and O(1), perpendicular to the metal layer. The reason for the resulting low symmetry of the unit cell is most probably the thermal motion if the ^{t}butyl group and consequently the need to refine some of the ^{t}butyl groups on two ideal positions (indicated by dashed bonds in Fig. 3.6).

The molecular structure of the cluster is closely related to monometallic Zr3 or Ti3 clusters (Sec. 1.6.1), i.e. the Ti atoms shows similar coordination as in the Ti3 cluster and Zr coordinates as in the Zr3 cluster.

3.2.2 Clusters with M5O3 cluster core

3.2.2.1 Zr3Ti2piv

$Zr_3Ti_2(\mu_3\text{-}O)_3(\mu_2\text{-}O^nBu)(O^nBu)_2(\mu_2\text{-}OPiv)_7(OPiv)_4$ (Fig. 3.7) represents an intermediate product to a cluster with [M_6O_7] core. The cluster rearranged after about three weeks to Zr_4Ti_2 (see Sec. 1.8). This explains also the bad crystal quality and their poor resolution. The two terminal alkoxy groups and the pivalate chelating Ti(1) makes this cluster quite unstable.

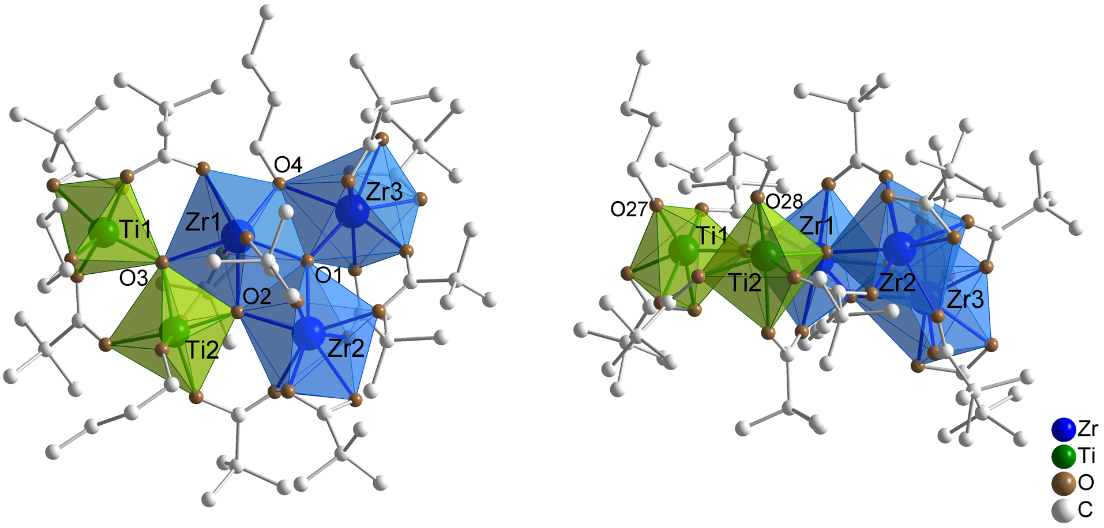

Figure 3.7: Different views of the molecular structure of $Zr_3Ti_2(\mu_3\text{-}O)_3(\mu_2\text{-}O^nBu)(O^nBu)_2(\mu_2\text{-}OPiv)_7(OPiv)_4$. Hydrogen atoms are omitted for clarity

There are several unusual issues about this cluster. There are three clusters crystallising in the unit cell (Fig. 3.8(a)). The three clusters are not symmetry related, as they crystallise in the triclinic space group $P\bar{1}$. Their molecular structures do not differ from each other and there are only small variations in the bond lengths. Only bond lengths of one cluster are discussed. A full list of bond lengths ang angles of all three clusters is given in Tabs. A.5 and A.6.

The cluster core can be described as three triangular [$M_3(\mu_3\text{-}O)$] units, arranged to a flat cluster core (Fig. 3.7). The first unit consists of three Zr atoms coordinating to O(1), the second of two Zr atoms and one Ti atom (Zr(2), Zr(3), Ti(2), O(2)) and the last unit is build by the two Ti atoms and one Zr atom (Ti(1), Ti(2) and Zr(3), O(3)). Each M_3O unit is an isosceles triangle with two shorter (3.207(3) - 3.4085(16) Å) and one longer M···M distances (3.744(3) - 3.8844(18) Å). Two M-O bonds of O(3) are considerably larger than those of the other core oxygen atoms (Ti(2)-O(3) 1.917(10), Zr(1)-O(3) 2.238(8) Å compared to 1.836(9)-1.861(7) Å for the other Ti-O bonds and 2.046(8)-2.118(8)Å for the other Zr-O bonds). The sum of bond angles for the core oxygen atoms are close to 360° (358.8 - 359.1°).

O^nBu groups and pivalates act as ligands. Zr(1) coordinates to all of the other metal atoms through one bridging ligand. A O^nBu group bridges Zr(1) and Zr(3), pivalates are bridging Zr(1) with all other metals. The bond lengths of the alkoxo ligand are in the same range as those of the pivalates (2.123(8)- 2.169(9) Å compared to 2.112(10) - 2.221(10) Å). Zr(2) is connected to Zr(3) through two pivalates (bond lenghts between 2.102(9) and 2.194(10) Å) and to Ti(2) through one pivalate (Zr(2)-O(15) 2.251(9), Ti(2)-O(16) 1.976(11) Å). One pivalate bridges the two Ti atoms with equal M-O lengths (Ti(1)-O(17) 2.034(10), Ti(2)-O(18) 2.035(9) Å). The remaining four pivalates are all chelating. One is chelating Ti(1) and Zr(2) each, and two bond to Zr(3). The bond lengths here are larger than those of the bridging pivalates (Ti(1)-O 2.141(8) - 2.045(10), Zr-O 2.203(9) - 2.328(9) Å). Two terminal O^nBu groups are completing the coordination sphere of the two Ti atoms.

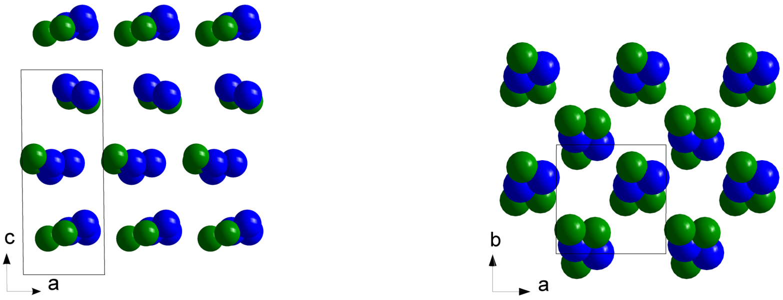

(a) Zr3Ti2piv (b) Zr2Ti3piv

Figure 3.8: Comparison of the crystal structures of M5piv clusters. For clarity only Zr and Ti are displayed in a space filling model.

Ti atoms with chelating carboxylate ligands are not very common. The rigid octahedral coordination sphere of Ti makes it very difficult for a carboxylate ligand chelating a Ti atom. The O-Ti(1)-O angle of the chelating ligand is only 60.849(40)° and thus far from the ideal rectangular angle. But also the coordination sphere of the non-chelated Ti(2) is strongly distorted, with O-M-O angles of *cis*-oxygen atoms between 78.5(3)-102.2(4) Å. The sevenfold coordination sphere of Zr(1) has the form of a pentagonal bipyramid. Zr(2) and Zr(3) have a coordination number of 8.

3.2.2.2 Zr2Ti3piv

The core of $Zr_2Ti_3(\mu_3\text{-}O)_3(\mu_2\text{-}O^nPr)_2(O^iPr)(O^nPr)_2(\mu_2\text{-}OPiv)_7(OPiv)_2$ is also constructed of five metal atoms and three oxygen atoms, in the same way as in the previous cluster (Fig. 3.9). Compared to the previous cluster, one Zr polyhedron is substituted by a Ti octahedron, i.e. the position of Zr(3) is substituted by Ti(3). The cell parameters change dramatically, from a clearly triclinic cell with a very large *c* axis to an almost monoclinic cell with half the volume, with only two clusters crystallising in the unit cell (Fig. 3.8(b)).

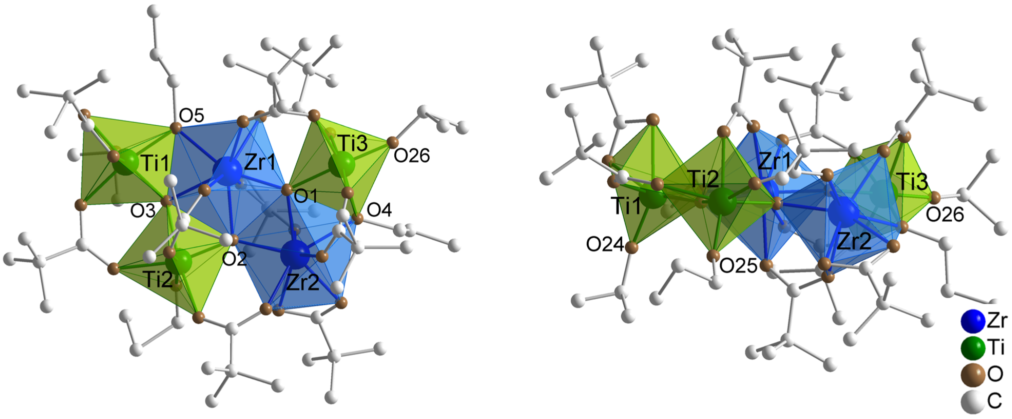

Figure 3.9: Different views of the molecular structure of $Zr_2Ti_3(\mu_3\text{-}O)_3(\mu_2\text{-}O^nPr)_2(O^iPr)(O^nPr)_2(\mu_2\text{-}OPiv)_7(OPiv)_2$. Hydrogen atoms are omitted for clarity

The substitution of a Zr atom with a Ti atom also effects the ligand sphere, as Ti has only six coordination sites instead of 8 for Zr(3). Zr(1) and Ti(2) were connected through one bridging pivalate in Zr3Ti2, but here they are linked by one bridging O^nPr group. Furthermore, Zr(1) and Zr(3) were coordinated through a bridging O^nBu, but in this cluster Ti(3) and Zr(1) are joined by two bridging pivalates. Two pivalates were bridging Zr(3) and Zr(2), whereas Ti(3) and Zr(2) in Zr2Ti3piv are connected by one μ_2-OPiv and one μ_2-O^nPr. The last coordination site on Ti(3) is occupied by a terminal O^iPr group. The rest of the ligand sphere is equivalent to $Zr_3Ti_2O_3(O^nBu)_3(OPiv)_{11}$, with the exception that O^nPr groups are coordinating to the Ti atoms instead of O^nBu. As a consequence of the modifications in the ligand sphere, both $[TiO_6]$ octahedra are corner sharing with the $[Zr(1)O_7]$ pentagonal bipyramid.

Attention should be drawn to the OR groups on the cluster. This cluster was synthesised from a mixture of metal alkoxides with different ligands, $Ti(O^iPr)_4$ and $Zr(O^nPr)_4$. Only O^nPr groups bridge two metals, but the terminal alkoxy groups are both O^iPr and O^nPr. This shows that the OR groups can be exchanged between the different metals. A comparison of bond lenghts of Zr3Ti2piv and Zr2Ti3piv is given in Tab. A.5, angles are listed in and A.7.

3.2.2.3 Comparison with other clusters

Similar structure motives are known for the mixed Ti/Zr methacrylate clusters (Sec. 1.8). Zr_2Ti_3 can be derived from the Zr2Ti4met cluster. Compared to that structure one Ti is missing in Zr2Ti3piv. The core of Zr3Ti2 can be identified in Zr4Ti4met. The cluster core of $ZrTi_2$piv is also a structure element in Zr2Ti3piv, but in Zr3Ti2piv only one $[TiO_6]$ octahedron is corner sharing with the coordination polyhedron of the central Zr atom.

3.2.3 Clusters with octahedral cluster core

3.2.3.1 Zr4Ti2 with O^{n}Pr group

The cluster $Zr_4Ti_2O_5(OH)_2(O^nPr)(OPiv)_{11}$ was formed in various reaction mixtures, containing different Ti and Zr alkoxides. Only the solvent molecules co-crystalising with the cluster were different, but included at least two pivalic acids. The cluster described below was the result of the rearangement of Zr2Ti3piv in the mother liquid after several months.

In $Zr_4Ti_2(\mu_3\text{-}O)_5(\mu_3\text{-}OH)_2(O^nPr)(\mu_2\text{-}OPiv)_7(OPiv)_4 \cdot 2.5HOPiv \cdot 0.5^nPrOH$ (Fig. 3.10) the six metal atoms are arranged in an octahedron, with vicinal Ti atoms (Fig. 3.13(a)). All faces of the octahedron except one are capped with a core oxygen atom. The triangle not capped by an oxygen atom is that of the two Ti atoms and Zr(4). The distance of the Zr(4) to the two Ti atoms is almost 0.5 Å greater than those between the Ti atoms and any of the other Zr atoms. (Ti(1)-Zr(4) 3.6849(9), Ti(2)-Zr(4) 3.7714(10) Å against 3.0423(8) - 3.2790(8) Å) All Zr-Zr distances are around 3.5 Å. A list of all bond lengths and agnles is given in Tabs. A.8 and A.10.

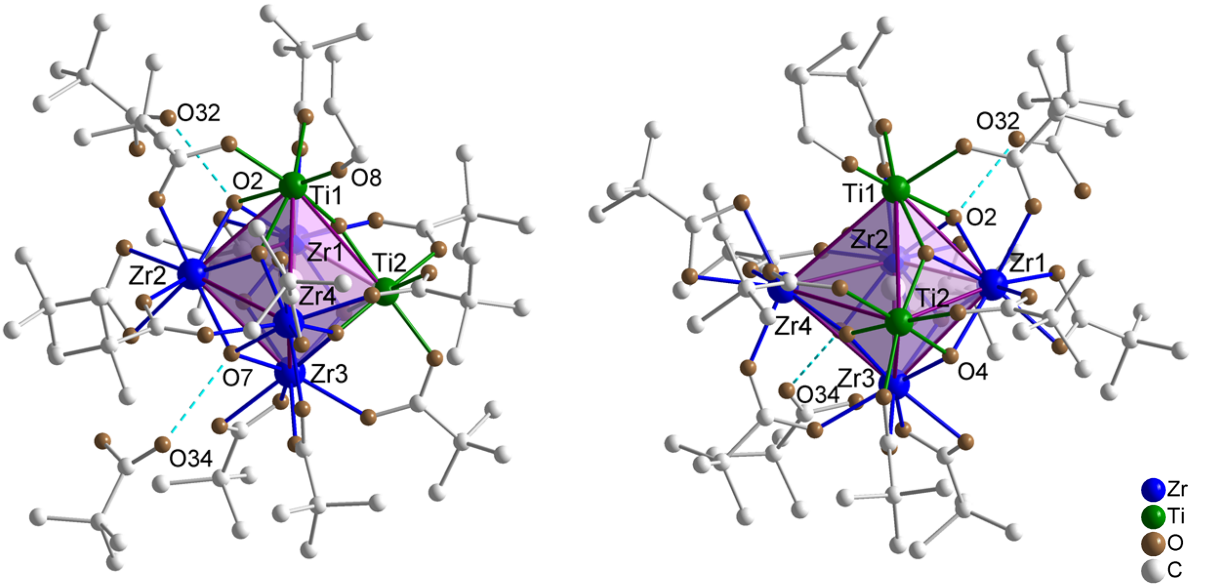

Figure 3.10: Different views of the molecular structure of $Zr_4Ti_2(\mu_3\text{-}O)_5(\mu_3\text{-}OH)_2(O^nPr)(\mu_2\text{-}OPiv)_7(OPiv)_4 \cdot 2.5HOPiv \cdot 0.5^nPrOH$. Solvent molecules and hydrogen atoms are omitted for clarity. Blue dashed lines indicate hydrogen bonds.

Two core oxygen atoms, O(2) and O(7), showed longer M-O bonds compared to the other five core oxygen atoms. O(2) binds to Ti(1), Zr(1) and Zr(2) and O(7) bridges Zr(2), Zr(3) and Zr(4). Especially the Ti(1)-O(2) distance is much larger than the other Ti-O distances (2.155(3) Å compared to 1.818(3) - 1.940(3) Å). The effect on the Zr–O bond lengths is little weaker (Zr-O(2), O(7) 2.206(3) - 2.290(3) Å compared to 2.082(3) - 2.166(3) Å). The elongation of the bond length is due to a shift of the oxygen atoms out of the M_3 plane, visible also in the sum of the M-O-M angles. For O(2) and O(7) this sum is about 299° and 307°, for the other core oxygen atoms this sum is close to the ideal of 360° (339 - 356°), except for O(4). The Zr-O(4) bond lengths are also quite long (Zr(1)-O(4) 2.144(3), Zr(3)-O(4) 2.184(3) Å) and the sum of the angles is 306°, but the Ti(2)-O(4) bond length is normal with 1.818(3) Å. To obtain a neutral cluster, it was assumed that O(2) and O(7) are in fact OH groups. This would explain the elongation of the M-O bonds of O(2) and O(7). Another reason for this elongation are strong hydrogen bonds to two free pivalic acids, which also crystallised with the cluster (O(2)$\cdots$ O(31) 2.785(5) Å, O(7)$\cdots$O(33) 2.758(4) Å). The C-O bonds of O(31) and O(33) are double bonds, because the bond lengths are smaller than those of the second oxygen of the pivalic acid. The hydrogen atoms could be identified in the difference electron density map and are closer to the oxygen atom of the free acid. Nevertheless the exact position of the hydrogen atoms is ambiguous.

The $\mathrm{O}^{\mathrm{n}}\mathrm{Pr}$ group is coordinated to one Ti atom, with a very short Ti-O bond length of Ti(1)-O(8) 1.747(3) Å. The coordination sphere of Ti(1) is much more distorted than that of Ti(2). The angles between oxygen atoms in *trans* position are between 159.39(13) and 176.51(14)°, where they are much closer to 180° for Ti(2) with 171.79(12) - 177.31(14)°. The same applies for oxygen atoms in *cis* position (O-Ti(1)-O 78.86(12)-102.78(14)°, O-Ti(2)-O 85.52(12)-91.80(13)°).

Most pivalates in the structure are bridging two Zr atoms or Ti and Zr. Ti(2) and Zr(4) coordinate to three bridging pivalates, all others bond to two pivalates. The remaining four pivalates are chelating one Zr atom each. All Ti-O bonds of the bridging pivalates are above 2 Å, and those of the Zr between 2.171(3) - 2.234(3) Å. The chelating pivalates have Zr-O bond lengths from 2.219(3) to 2.301(3) Å.

Besides the two pivalic acids also one 1-propanol and another pivalic acid co-crystallised, both solvent molecules have an occupancy of about 50%. They show no interaction with the cluster. Zr4Ti2pivnPr was also obtained with a butanol co-crystallising with the cluster, besides two pivalic acids. The pivalic acid molecules showed hydrogen bonds as described above, but the butanol showed no interaction.

3.2.3.2 Zr4Ti2 with $\mathrm{O}^{i}\mathrm{Pr}$ group

In $\mathrm{Zr_4Ti_2(\mu_3\text{-}O)_5(\mu_3\text{-}OH)_2(O^iPr)(\mu_2\text{-}OPiv)_7(OPiv)_4 \cdot 2\,HOPiv}$ the $\mathrm{O}^{\mathrm{n}}\mathrm{Pr}$ ligand on Ti(1) is substituted by a $\mathrm{O}^{\mathrm{i}}\mathrm{Pr}$ ligand as shown in Fig. 3.11. Apart from this the cluster core and the coordination sphere are equal to Zr4Ti2pivnPr described before. It showed hydrogen bonds to free pivalic acids as well. All differences in bond lengths and atom distances are within 0.02 Å. Tabs. A.8 and A.10 give a comparison of all bond lengths and angles in the two variations of the $\mathrm{Zr_4Ti_2O_7}$ cluster cores.

3.2.3.3 Comparison with the octahedral Zr6 cluster

The structure of Zr4Ti2pivnPr and Zr4Ti2piviPr can be easily derived from the known Zr6 octahedral cluster (Sec. 1.6.3.1). Compared to this cluster, two Zr atoms in Zr4Ti2piv are substituted by Ti atoms. There are only seven core oxygen, one less than in the monometallic Zr cluster. This is also observed in the structure of prismatic Ti6 clusters (Sec. 1.7.3.1), which has only six core oxygen atoms . The reason is the lower coordination number of Ti, which needs to bind to ligands with higher charges.

3.2.3.4 Zr4Ti2 with coordinated acid

In $\mathrm{Zr_4Ti_2(\mu_3\text{-}O)_5(\mu_3\text{-}OH)_2(O^iPr)(\mu_2\text{-}OPiv)_8(\eta_1\text{-}OPiv)(\eta_1\text{-}HOPiv)(OPiv)_2 \cdot 2\,HOPiv \cdot H_2O}$ (Fig. 3.12) the two chelating pivalates on Zr(1) and Zr(3) are substituted by a η_1-pivalic acid on Zr(1) and a η_1-pivalate on Zr(3) compared to Zr4Ti2piv. The two remaining coordination sites on Zr(1) and Zr(3) are occupied by a pivalate bridging these two Zr atoms. Due to the poor quality of the crystal, the hydrogen atom possitions were calculated. Hydrogen bonds could still be

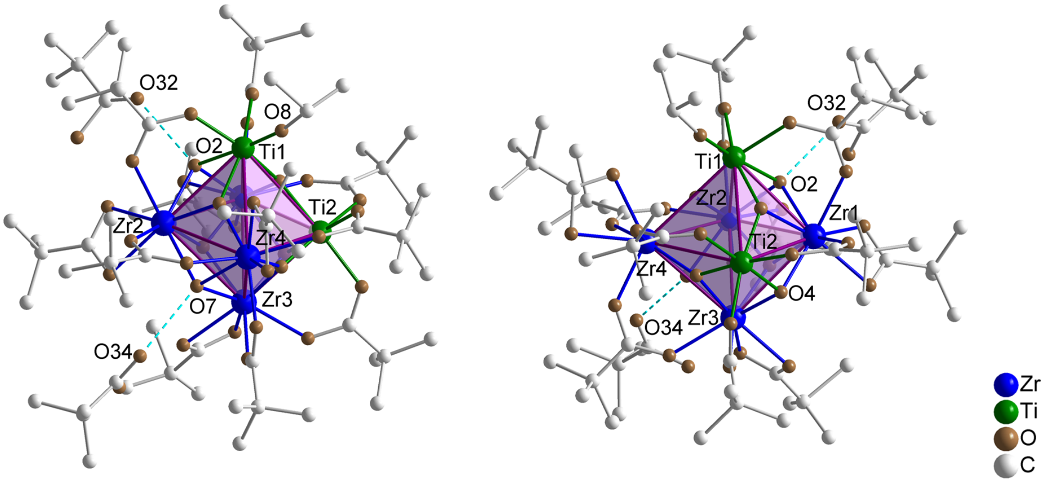

Figure 3.11: Different views of the molecular structure of $Zr_4Ti_2(\mu_3\text{-}O)_5(\mu_3\text{-}OH)_2(O^iPr)(\mu_2\text{-}OPiv)_7(OPiv)_4 \cdot 2\,HOPiv$. Blue dashed lines indicate hydrogen bonds.

observed, on the basis of $O_{Acceptor} \cdots O_{Donator}$ distances. Bond distances and angles are listed in Tabs. A.8 and A.10.

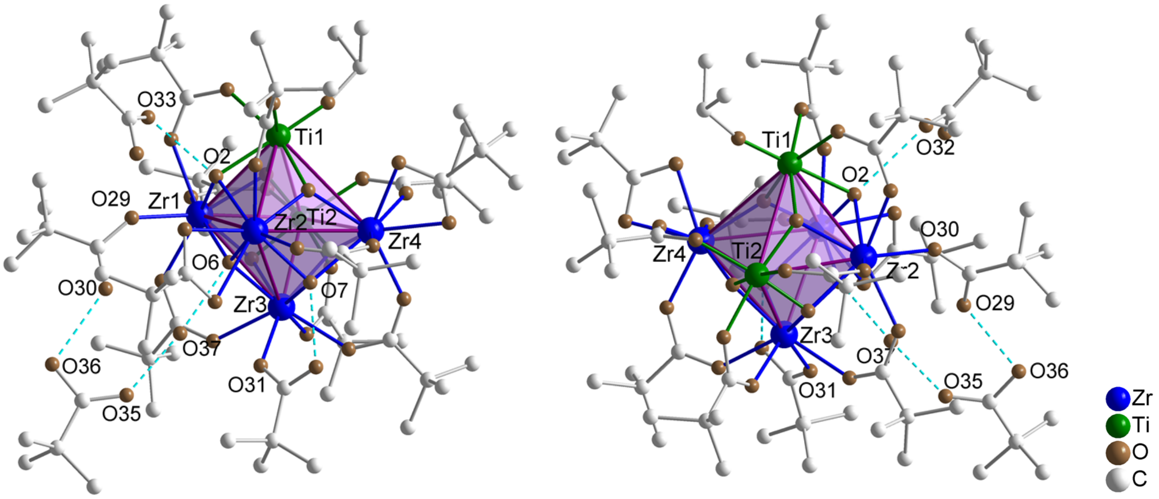

Figure 3.12: Different views of the molecular structure of $Zr_4Ti_2(\mu_3\text{-}O)_5(\mu_3\text{-}OH)_2(O^iPr)(\mu_2\text{-}OPiv)_8(\eta_1\text{-}OPiv)(\eta_1\text{-}HOPiv)(OPiv)_2 \cdot 2\,HOPiv \cdot H_2O$. Blue dashed lines indicate hydrogen bonds.

The core oxygen O(2) and O(7) show larger bonds to the metals than the other core oxygen atoms, as in the other octahedral pivalate clusters. O(7) shows hydrogen bonds to the acid coordinated to Zr(3) (O(7)$\cdots$O(34) 2.575(9)Å) and O(2) to a free pivalic acid (O(2)$\cdots$O(32) 2.777(10)Å). The pivalic acid coordinating to Zr(1) shows hydrogen bonds to a non-coordinated water molecule. The cluster needs one additional hydrogen atom for charge balance. An elongation of the Zr-O(4) bonds was observed, as in the cluster before. But there are no oxygen atoms within 3Å, suitable for H bonds. Another possible site for a hydrogen would be the η_1-pivalate, but the C-O bonds are almost equal (C(54)-O(29) 1.285(16), C(54)-O(30) 1.274(15) Å). Furthermore, the non-bonded oxygen O(30) shows hydrogen bonds to a free pivalic acid (O(30)$\cdots$O(36) 2.5905(11) Å). The C(69)-O(36) bond length is larger than the C(69)-O(35) bond length (C(69)-O(36) 1.320(17), C(69)-O(35) 1.239(16) Å), hence the hydrogen atom bonds to O(36). O(35) is close to a non-coordinated water molecule (O(35)$\cdots$O(37) 2.280(9) Å) and this water molecule shows also hydrogen bonds to the core oxygen O(6) (O(6)$\cdots$O(37) 2.475(7)Å). The Zr-O(6) bonds are in the normal range between 2.082(6) - 2.126(7) Å, hence O(6) is not hydrated.

Despite the modification in the ligand sphere, the bond lengths and metal distances do not change much from the above described Zr4Ti2 clusters, a comparison is given in Tab. A.8.

(a) Zr4Ti2 core (b) Zr3Ti3 core

Figure 3.13: Cluster cores of M6O7 pivalate clusters.

3.2.3.5 Zr3Ti3piv

In $Zr_3Ti_3(\mu_3\text{-O})_4(\mu_3\text{-OH})_3(O^nBu)_3(\eta_1\text{-OPiv})_2(\mu_2\text{-OPiv})_6(OPiv)_2$ (Fig. 3.14) one Zr atom is substituted by a Ti atom compared to the former clusters (Fig. 3.13(b)). This affects also the shape of the cluster core. It is best described as a hexagonal prism, with the metal and core oxygen atoms alternating within the hexagon, as in Ti6 clusters with a prismatic core (Sec. 1.7.3.1). Compared to these Ti6 clusters, the top face, which is built by the three Zr atoms, is additionally capped by a core oxygen atom, resulting in seven core oxygen atoms, one more than in the Ti6 clusters.

As in the Ti6 clusters, the Ti are coordinating to terminal O^{n}Bu groups with very short Ti-O distances between 1.751(2) and 1.765(2) Å, and the angle between the Ti-O^{n}Bu bond and the Ti3 face is about perpendicular. All three Ti are also coordinating to the two neighbouring Zr atoms through bridging pivalates.

Two η_1-pivalates are also found in this cluster, but in contrast to Zr4Ti2Ac they bind to the same Zr(1). These two ligands show strong hydrogen bonds to neighbouring OH groups (Fig 3.14). The hydrogen atoms could be identified in the difference electron map and were found close to O(2) and O(4) (O(2)$\cdots$O(28) 2.556(3), O(4)$\cdots$O(30) 2.484(3) Å). The third OH group of O(7) shows also hydrogen bonds, but to a free pivalic acid. This hydrogen atom was also found in the difference electron density map (O(7)$\cdots$O(31) 2.801(3) Å). Another evidence for the OH groups are the M-O bond distances of these three oxygen atoms, which are elongated and the sum of angles is much below 360° (299.4 - 304.9°). The Ti-O bonds for O(2), O(4) and O(7) are between 2.038(2) and 2.136(2) Å compared to 1.898(2)-1.947(2) Å. The effect on the Zr-O bonds is smaller, for those of O(2), O(4) and O(7) they are between 2.178(2) - 2.233(2) Å compared to 2.038(2) - 2.181(2) Å for the others. Two chelating pivalates on Zr(2) and Zr(3) are completing the ligand sphere of this cluster, the Zr-O bond lengths being typical quite long (2.228(2) - 2.254(2) Å).

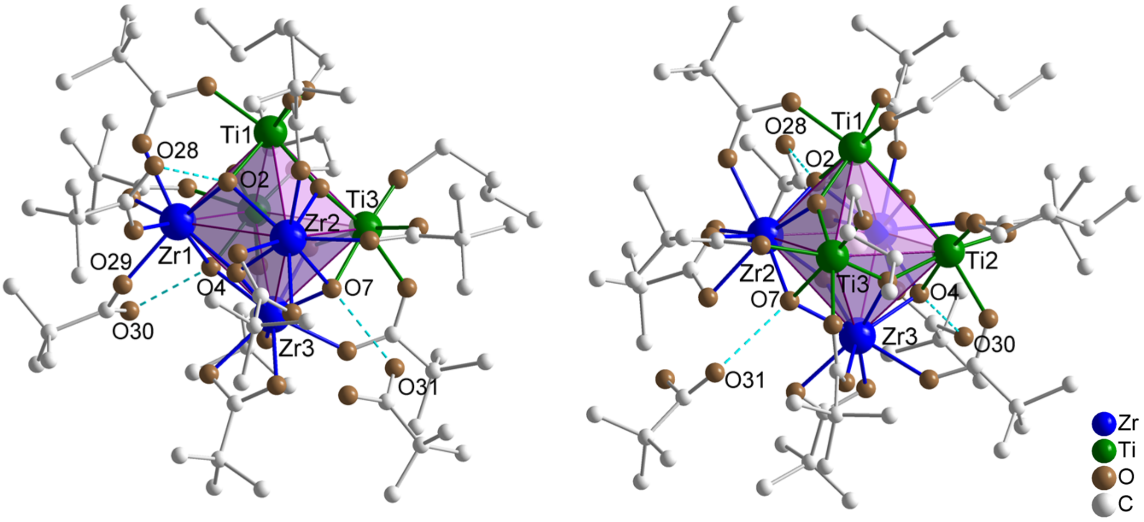

Figure 3.14: Different views of the molecular structure of $Zr_3Ti_3O_4(OH)_3(O^nBu)_3(OPiv)_{10} \cdot HOPiv \cdot H_2O$. Blue dashed lines indicate hydrogen bonds.

This cluster can be seen as a combination of the Ti6 cluster and the octahedral Zr6 cluster. Except for the coordinating pivalic acids, the Zr atoms show the same coordination sphere as in the Zr6O8 cluster and the Ti atoms have the same environment as in the Ti6O6 cluster. Also the bond lengths and angles are comparable according to Tab. A.9 and A.11.

3.2.4 Zr6Ti8piv

In $Zr_6Ti_8(\mu_3\text{-O})_{10}(\mu_3\text{-OH})_4(\mu_2\text{-O})_5(\mu_2\text{-O}^n\text{Bu})_2(\mu_2\text{-OPiv})_{15}(\eta_1\text{-HOPiv})_2(\text{OPiv})_4 \cdot 2\,\text{HOPiv}$ two Zr_3Ti_3 octahedra are connected through two additional Ti atoms (Fig. 3.15). But the cluster is not symmetrical, due to differences in the ligand sphere of the two Zr_3Ti_3 fragments. The shape of the fragments is comparable to the above described Zr3Ti3 cluster, but the coordination mode is again different (Fig. 3.16). The distances between Ti and Zr are about 3.3Å and those of metal of the same type around 3.5Å. The two bridging Ti(4) and Ti(8) are closer to each other with a distance of 3.150(7) Å (Tab.A.12).

Instead of coordinating to terminal alkoxy groups the three Ti atoms in fragment 1 (Ti(1), Ti(2) and Ti(3)) are coordinating to the neighbouring Ti(4) atom through μ_2-oxygen atoms (Fig. 3.17). Whereas in the second fragment only Ti(6) and Ti(7) are coordinating through μ_2-O to the bridging Ti(8), the third Ti(5) is connected by a bridging pivalate to Ti(8). As a consequence, the distance between Ti(5) and Ti(8) is much larger than those of the μ_2-O connected Ti atoms (Ti(5)-Ti(8) 4.534(4); Ti-Ti(4) 3.372(7)-3.395(7)Å, Ti-Ti(8) 3.385(7)-3.399(6) Å). The Ti- μ_2-O bonds for Ti(1) to Ti(3) are exceptionally short and in the range of terminal alkoxy groups (Ti(1)-O(8) 1.672(15), Ti(2)-O(9) 1.710(15), Ti(3)-O(10) 1.700(15) Å). In contrast, the Ti(4)-O distances are 0.25 Å longer and hence in the range of core oxygen atoms (1.936(15)- 1.959(15) Å). In the second fragment all Ti-O distances are between 1.799(15)- 1.825(15) Å.

In both fragments the Ti atoms connect to two neighbouring Zr atoms through bridging pivalates, as it was the case for the Zr3Ti3 cluster. Differences are again in the coordination of the Zr atoms. In fragment 1 pivalates are chelating all three Zr atoms, whereas in fragment 2 only Zr(6) is chelated. The other two Zr atoms Zr(4) and Zr(5) are coordinating to a pivalic acid, and an additional pivalate is bridging these two Zr atoms. The pivalic acids show hydrogen bonds

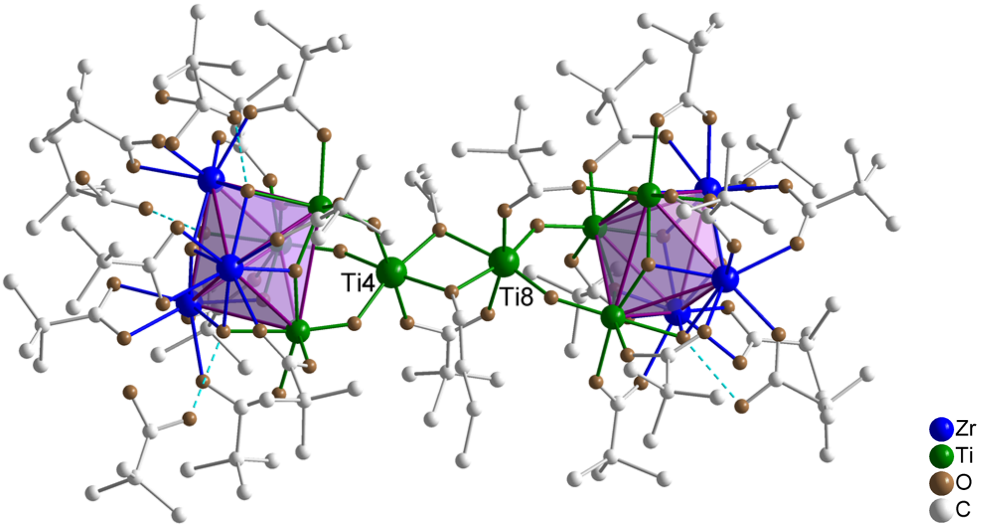

Figure 3.15: Molecular structure of $Zr_6Ti_8O_{15}(OH)_4(O^nBu)_2(OPiv)_{20}(HOPiv)_2$. Blue dashed lines indicate hydrogen bonds.

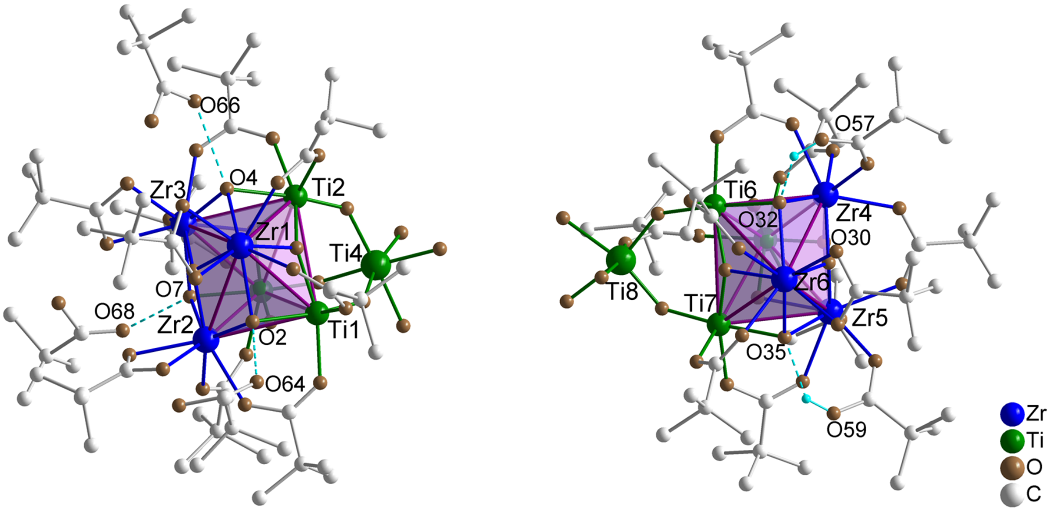

(a) Fragment 1 (b) Fragment 2

Figure 3.16: The two fragments of $Zr_6Ti_8O_{15}(OH)_4(O^nBu)_2(OPiv)_{20}(HOPiv)_2$ in different views. Blue dashed lines indicate hydrogen bonds.

to core oxygen atoms (O(32)···O(57) 2.593(14), O(35)···O(59) 2.630(14)Å). The hydrogen atom was identified in the electron density map and are coordinated to the η_1-pivalic acid. The M−(μ_3-O) bonds of the core oxygen O(32) and O(35) are again elongated. As a consequence the $[M_3O]$ fragment is pyramidal, notable in the sum of M-O-M angles (Tab. A.13). They are around 300° for O(32) and O(35), compared to 342.3(19) - 350.8(19)°. O(30) shows also a small angle sum of 309.6(20)°. The Zr-O(30) are also longer, but the Ti(5)-O(30) bond is exceptionally short (1.777(16)Å). Hydrogen bridges to this oxygen atom were observed. Nevertheless, one additional hydrogen atom is required for charge ballance. It is most likely that this hydrogen atom is bonded to O(30), because the M-O-M angles of the other oxygen atoms are much closer to 360°.

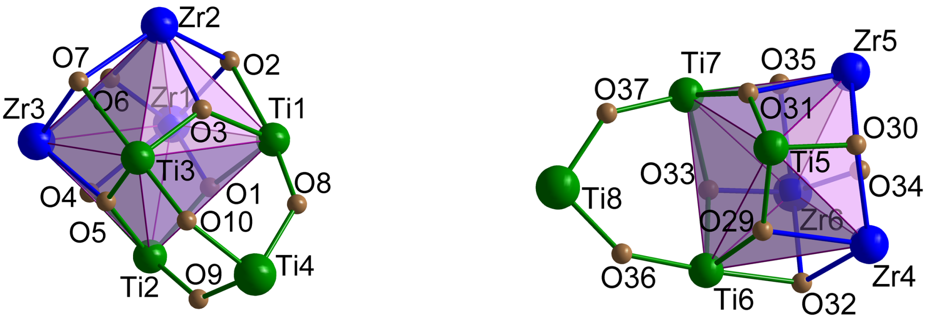

(a) Fragment 1 (b) Fragment 2

Figure 3.17: Cluster core of $Zr_6Ti_8O_{15}(OH)_4(O^nBu)_2(OPiv)_{20}(HOPiv)_2$

In fragment 1 there are also core oxygen atoms with elongated M-O bonds, but here they show hydrogen bonds to free pivalic acids (O(2)$\cdots$ O(64) 2.815(13); O(4)$\cdots$ O(66) 2.794(18), O(7)$\cdots$O(68) 2.790(17)Å). Similar to the Zr4Ti2 clusters, O(64), O(66) and O(68) are double bonded to the carbon atom. The hydrogen atoms could again be determined from the difference electron map, and were also close to the acid. Again the exact of the hydrogen atom is not clear, but for charge balance it was assumed that O(2), O(4) and O(7) are OH group.

The coordination of the bridging Ti atoms, Ti(4) and Ti(8), is completed by two bridging O^nBu groups and one bridging pivalate.

Beside this cluster another cluster co-crystallised. The structure of this Zr5 cluster could not be completely elucitated, because of the bad scattering of the crystal and the low occupancy of this cluster below 50 %. Only the position of the Zr and some of the oxygen and carbon atoms could be determined. A fragment of this Zr5 cluster is shown in Fig. 3.18(a). The structure is very similar to $Zr_5O_4(O^nPr)_2(OOCC(Me)_2Br)_{10}(HO^nPr)_4$ [97] (Fig. 3.18(b)). Compared to this cluster there are still some ligands missing in the Zr5 cluster here reported.

This Zr5 cluster is also the reason for the low symmetry. The Zr6Ti8 cluster can be solved in the rhombohedral space group $\overline{R}$, but due to the Zr5 cluster the symmetry needed to be reduced to $P\bar{1}$.

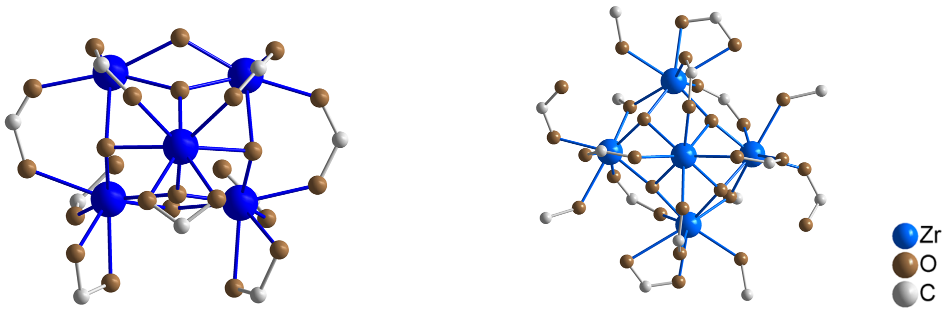

(a) Fragment of the Zr5 cluster co-crystallising with Zr6Ti8piv

(b) $Zr_5O_4(O^nPr)_2(OOCC(Me)_2Br)_{10}(HO^nPr)_4$

Figure 3.18: Comparison of the Zr5 cluster fragment, with the molecular structure of $Zr_5O_4(O^nPr)_2(OOCC(Me)_2Br)_{10}(HO^nPr)_4$. The ^tBu group of the Zr5 fragment and the $C(Me)_2Br$ as well as the CH_2CH_3 group have been omitted for clarity.

3.3 1-Adamantanecarboxylic Acid

The Zr3Ti3 structure motive is also found in $Zr_4Ti_3O_7(O^{n}Bu)_2(OOCAda)_{12}$ (HOOCAda = 1-adamantanecarboxylic acid) (Fig. 3.19). Here an additional Zr atom is connected to two Ti (Ti(2) and Ti(2)') atoms through a μ_3-oxygen. On the other hand, two faces of the Zr3Ti3 octahedron are not capped by oxygen atoms. These are the faces built by Ti(1), Ti(2), Zr(2) and the three Ti atoms, respectively (Fig.3.20).

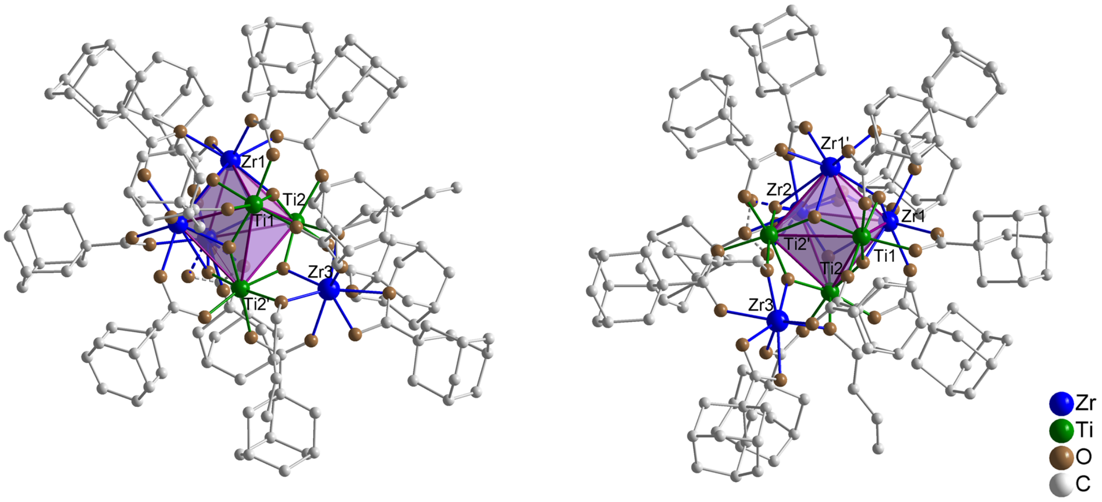

Figure 3.19: Different views of the molecular structure of $Zr_4Ti_3O_7(\mu_2\text{-}O^{n}Bu)_2(\mu_2\text{-}OOCAda)_{10}(OOCAda)_2$. Disordered parts are drawn with broken bonds. Hydrogen atoms are omitted for clarity.

The outer Zr(3) atom coordinates additionally to Ti(2) and Ti(2)' through a bridging $O^{n}Bu$ and a bridging carboxylate group. In contrast, Zr(4) and Ti(1) are only connected by a pivalate. Two carboxylates are bridging Ti(1) and both its neighbouring Zr(1) and Zr(1)', which show also bridges to Ti(2) and Ti(2)'. Zr(2) is only coordinated to Zr(1) and Zr(1)' through one bridging carboxylate group. Zr(2) and Zr(3) are chelated by a carboxylate group. Both ligands showed disorder over two sites, i.e. the O-C-O plane was turned by about 90°. A list of all bond lenghts and angles is given in Tabs. A.14 and A.15

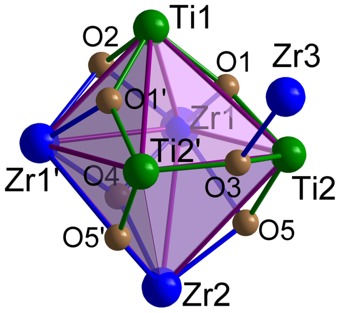

Figure 3.20: $Zr_4Ti_3O_7$ cluster core of $Zr_4Ti_3O_7(O^{n}Bu)_2(OOCAda)_{12}$.

The core has a mirror plane, spanned by Ti(1), Zr(3) and Zr(4). Many of the adamantyl groups showed strong thermal motions and needed to be refined on two ideal positions. This disorder could not be resolved if the symmetry was reduced, hence the final refinement was in the orthorhombic space group *Pnma*. Their extensive movement was also the reason for the poor crystal quality and the resulting poor refinement.

3.3.1 Comparison with pivalate clusters

The octahedral cluster core, observed for the pivalate clusters, is also a structure motive in the cluster with adamantanecarboxylic acid. In contrast to the pivalate clusters this cluster has no coordinated OH groups and there are also no free carboxylic acids present in the structure to stabilise these groups. A reason might be the space required by the adamantanyl group. Such a large group does not fit in the space between the bonded carboxylates. The charge of the M_6 core was therefore balanced by an additional coordinating Zr atom, and not hydrogens. Whereas several different coordination modes were observed for the pivalate, adamantane carboxylate is similar sterically demanding as pivalate.

3.3.2 Comparison of the acids

The cluster cores of Zr/Ti cluster with benzoic acid derivatives are all almost flat. Clusters with pivalic acid on the other hand prefer more condensed structures. The reason is that pivalic acid is sterically more demanding than the other acids. The ^{t}butylic group close to the carboxylate group requires much more space than for example methacrylate or benzoate.

Chapter 4

Structure of Mixed Metal Clusters with Titanium

4.1 Zinc and Cadmium

4.1.1 Zinc

The reaction of $Zn(OAc)_2$ with $Ti(O^iPr)_4$and methacrylic acid in different molar ratios efforded clusters $Zn_2Ti_4(\mu_3\text{-}O)_2(\mu_2\text{-}O)_2(O^iPr)_2(\mu_2\text{-}OMc)_{10}$ (Fig. 4.1). The flat cluster core consists of two triangular $ZnTi_2O$ units, with a μ_3-O bridge between the three metal atoms. The angle between M$-$(μ_3-O) bonds is 360° within the standard deviation (359.9(2)°).

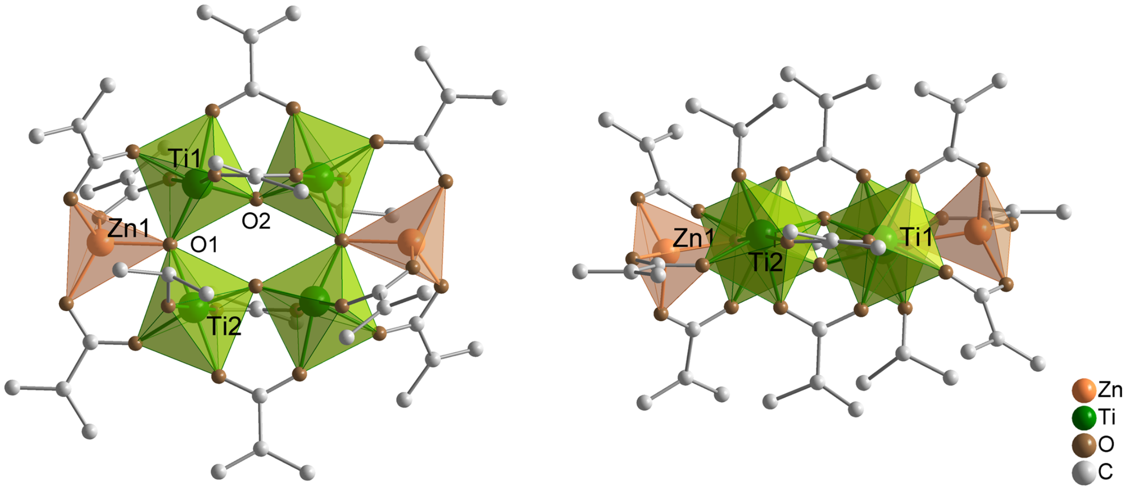

Figure 4.1: Molecular structure of $Zn_2Ti_4(\mu_3\text{-}O)_2(\mu_2\text{-}O)_2(O^iPr)_2(\mu_2\text{-}OMc)_{10}$. Hydrogen atoms are omitted for clarity

Due to an inversion centre the [$ZnTi_2O$] unit is equivalent to the asymmetric unit. Two [$ZnTi_2O$] units are connected through two μ_2-oxygen. In this way a Ti_4O_4 ring is formed, where Ti atoms and core oxygen atoms are alternating. The distance between adjacent Ti atoms is 3.3758(8) and 3.4587(8) Å, those of opposite Ti between 4.6966(8) and 4.9659(8) Å. The Zn-Ti distances are shorter with Zn(1)-Ti(1) 3.1470(4) and Zn(1)-Ti(2) 3.2701(4) Å. The Zn-(μ_3-O) distance is 1.9747(13) Å whereas the Ti-(μ_3-O) bond lengths are between 1.8712(13) Å and 1.9231(14) Å. Ti-(μ_2-O) distances are shorter with Ti(1)-O(2) 1.7550(13) Å and Ti(2)-O(2)

1.8784(13) Å.

The Zn atom additionally coordinates to both neighbouring Ti through methacrylates. Two are bridging to Ti(1) and one to Ti(2). These three methacrylates, together with the core oxygen atom form a tetrahedral coordination sphere around Zn. This tetrahedron is almost regular, as the Zn-O distances of the methacrylates vary only slightly between 1.9399(16) Å and 1.9568(16) Å and are not much shorter than the Zn-(μ_3-O) distance of 1.9747(13) Å. The O-Zn-O angles are between 103.24(6) and 116.79(6)°. The Ti-O bong lengths are somewhat longer (Ti(1)-O(4) 2.1057(15), Ti(1)-O(6) 2.0123(14), Ti(2)-O(8) 2.0435(14) Å).

Two methacrylates are bridging the two Ti atoms on the outer rim of the cluster core. One is equatorial to the ring, the other axial, where the symmetrically related axial methacrylates are on opposite sides of the cluster core. The axial methacrylate binds stronger to Ti(1) and the equatorial one stronger to Ti(2) (Ti(1)-O(9) 2.0752(14), Ti(2)-O(10) 2.0383(15); Ti(1)-O(11) 1.9994(14), Ti(2)-O(12) 2.0936(14) Å). The Ti(2) coordination sphere is completed by a terminal O^{i}Pr ligand, with very short Ti-O bonds (Ti(2)-O(13) 1.7821(14) Å).

4.1.2 Cadmium

Reaction of 1 mmol of $Cd(OAc)_2$ and 1 mmol of $Ti(O^iPr)_4$with 10 mmol of methacrylic acid resulted in crystals of $Cd_4Ti_2(\mu_3\text{-}O)_2(\mu_3\text{-}OAc)_2(\mu_3\text{-}OMc)_2(\mu_2\text{-}OMc)_8(HO^iPr)_2$ (Fig. 4.2).

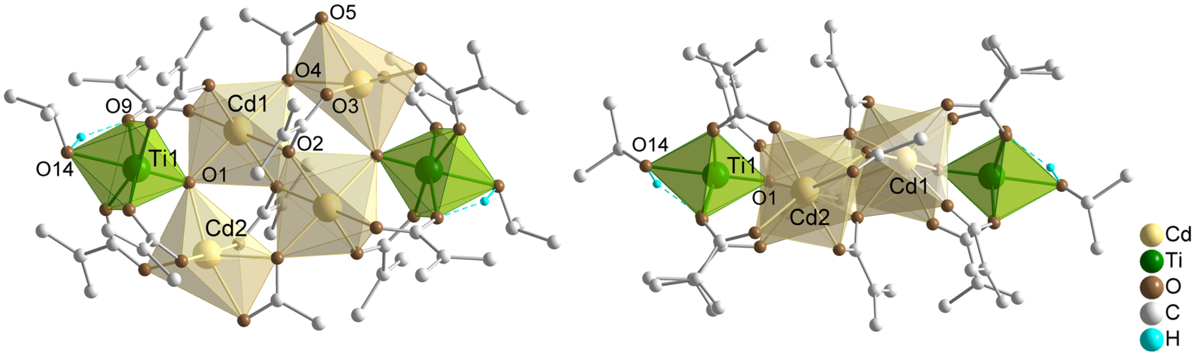

Figure 4.2: Molecular structure of $Cd_4Ti_2(\mu_3\text{-}O)_2(\mu_3\text{-}OAc)_2(\mu_3\text{-}OMc)_2(\mu_2\text{-}OMc)_8(HO^iPr)_2$. Only hydrogen of OH groups are drawn.

This cluster is similar to the Zn2Ti4 cluster, but here the four Ti atoms in the centre are substituted by Cd atoms and the outer atoms are Ti. The μ_3-O lies in the plane of the three metal atoms, the sum of O-M-O bond angles being again close to 360° (359.31(31)°). The two $[Cd_2TiO]$ units are connected through two acetates and two methacrylates, but no core oxygen. The acetate is chelating Cd(2) and bridges to Cd(1)'. The methacrylate bridges three Cd atoms, one oxygen atom bonds to Cd(1) and its symmetry equivalent Cd(1)', the second oxygen atom of the carboxylate group coordinates to Cd(2). Hence the two $[Cd(1)O_6]$ coordination polyhedra are edge sharing and the $[Cd(2)O_6]$ octahedra are corner sharing with each of the Cd(1) polyhedron. Both Cd atoms are octahedrally coordinated by oxygen atoms, but the $[Cd(2)O_6]$ octahedron is much more distorted than that of Cd(1). Where the O-Cd(1)-O angles of oxygen atoms in *cis* position are between 75.00(10) and 97.85(10)°, those of Cd(2) are between 55.50(8) and 109.49(9)° (see also Tab. A.16). The Cd-O bond distances of the μ_3-methacrylate and the chelating/μ_2-bridging acetate are all in the narrow range between 2.232(2) and 2.368(2) Å.

The μ_3-methacrylate and the chelating/bridging acetate cause the symmetry related Cd(1) atoms being closer to each other than the equivalent Ti atoms in the Zn2Ti4 cluster. The distance between Cd(1) and Cd(1)' is comparable with that of Cd(1) to Cd(2) (Cd(1)-Cd(2) 3.8904(8), Cd(1)-Cd(1)' 3.6618(8), Cd(1)-Cd(2)' 3.9525(8)). On the other hand, the symmetry related Cd(2) atoms are moved further apart (Cd(2)-Cd(2)' 6.9358(14) Å). The Ti atom is about equidistant to both Cd (Ti(1)-Cd(1) 3.4499(9), Ti(1)-Cd(2) 3.4521(9)Å).

Where the Cd-core oxygen bond lengths are in the typical range of Cd(1)-O(1) 2.262(2) and Cd(2)-O(1) 2.267(2) Å, the Ti(1)-O(1) distance of 1.698(2) Å is quite small. This is caused by an terminal alcohol coordinating to the Ti atom in *trans* position. The long Ti-O distance of the O^{i}Pr group (Ti(1)-O(14) 2.2186(3) Å) and the fact that the Ti(1)-O(14)-C(29) angle of the alcohol is 124.414(6)°) are indicators that O(14) is protonated. The proton was identified in the electron density map.

The remaining methacrylates are bridging the outer Ti atom and both neighbouring Cd atoms. Two methacrylates bridging the same Cd and Ti are located on opposite sides of the cluster core. The Cd-O bond lengths of these ligands differ only slightly between 2.228(3) and 2.279(3) Å, as well as the Ti-O bond lengths which vary only between 1.977(2) and 2.012(2)Å.

The exceptionally small Ti-core oxygen bond length below 1.7 Å is very rare. In $Ba_2Ti_4O(OMe)_{18}(MeOH)_7 \cdot MeOH$ [138], the core oxygen atom is bridging two Ba atoms and one Ti atom, with a Ti-O bond length of 1.695(6) Å. There a μ_3-OR group is in trans position to the short Ti-O bond.

A flat M_6 cluster core was also found for the only other known Cd/Ti carboxylate cluster. In $Cd_4Ti_4O_6(\mu_2\text{-OCHCH}_2NMe_2)_4(OCCF_3)_4(\mu_3\text{-OAc})_2(OAc)_2(HOAc)_4$ [120] the four Ti atoms are in the centre and the Cd atoms are coordinating on the side. Two Cd atoms are additionally coordinated to the Ti atoms above and below the $[Ti_4O_4]$ ring.

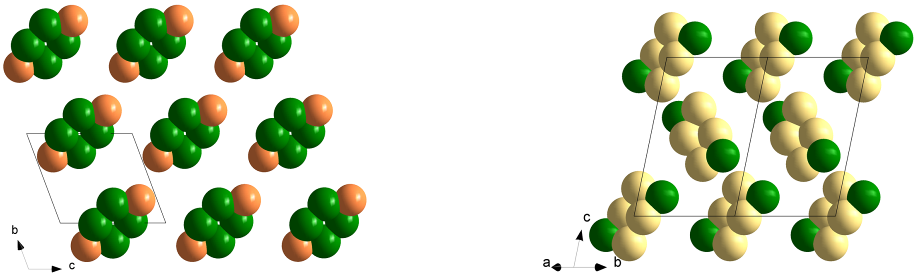

(a) Zn2Ti4 (b) Cd4Ti2

Figure 4.3: Crystal structures of Zn2Ti4 and Cd4Ti2.

4.1.3 Comparison with flat Ti6 clusters

Both clusters are comparable with Ti6 clusters having a flat cluster core (Sec. 1.7.3.2). In the Zn2Ti4 cluster the two outer Ti atoms are replaced by Zn atoms. But in Cd4Ti2 it is completely the opposite, where the four inner Ti atoms are replaced by Cd atoms. The lower charge of the Zn and Cd ions renders modification of the ligand sphere necessary. For the Zn cluster the substitution is possible because the radius of Zn^{2+} ions is 0.610 Å [167] and therefore only 0.05 Å larger than that of the Ti^{4+} ions. Zn is four-coordinated and therefore has two coordination sites less than Ti, which perfectly matches the lower charge. The tetrahedral coordination would not allow a replacement of the inner Ti atoms.

The Cd^{2+} ion is with 0.95 Å much bigger than the Ti^{4+} ion with 0.605 Å. They both are six-coordinated. Whereas the Ti coordination is octahedral, that of Cd is more flexible. Hence it coordinates to a chelating carboxylate group, which rarely occurs for Ti. The longer Cd-O distance rendes an additionally link the Cd atoms possible. This was necessary to balance the lower charge of the cluster core. A substitution of the outer Ti with Cd would not have been possible due to the much higher Cd-O bond length and the lower charge of Cd. But it is possible when coordinating additional Ti atoms, as was shown in $Cd_4Ti_4O_6(\mu_2^-OCHCH_2NMe_2)_4(OCCF_3)_4(\mu_3{-}OAc)_2(OAc)_2(HOAc)_4$ [120].

The ligand sphere of Zn2Ti4 differs only slightly from that of the flat Ti6 clusters. There are no bridging alkoxo group in Zn2Ti4 and no terminal alkoxy groups coordinating to the outer Zn atoms. The coordination motive of Cd4Ti2 is better compared with the second variation of the flat Ti6 cluster, as in $Ti_6O_4(OR)_{12}(OOCR,)_4$. Instead of the bridging alkoxo groups between the outer Ti and the inner Ti atoms there are only methacrylates bridges in Cd4Ti2. Instead of the bridging alkoxo group over the cluster core, the Cd4Ti2 has a μ_3-methacrylate bridging two Cd. The core oxygen atom in the Ti6 cluster is then replaced by the oxygen atom of an acetate in the Cd compound. The second oxygen atom replaces then one terminal alkoxy ligand of the inner Ti atom in the Ti6 cluster.

Due to the similar ion radii of Zn^{2+} and Ti^{4+}, the M-O distances are very close to those of the monometallic Ti clusters. Tabs. A.16 and A.17 compare the bond lengths and angles of Zn2Ti4 and Cd4Ti2 with those of $Ti_6O_4(O^nPr)_8(OMc)_8$ [39].

4.2 Chain-like Clusters of Calcium and Strontium

Most clusters are isolated molecules, evenly distributed in the crystal. This is not the case in the following Ca/Sr - Ti clusters. These clusters build endless parallel chains of condensed [M_2Ti_4] units (Fig. 4.4).

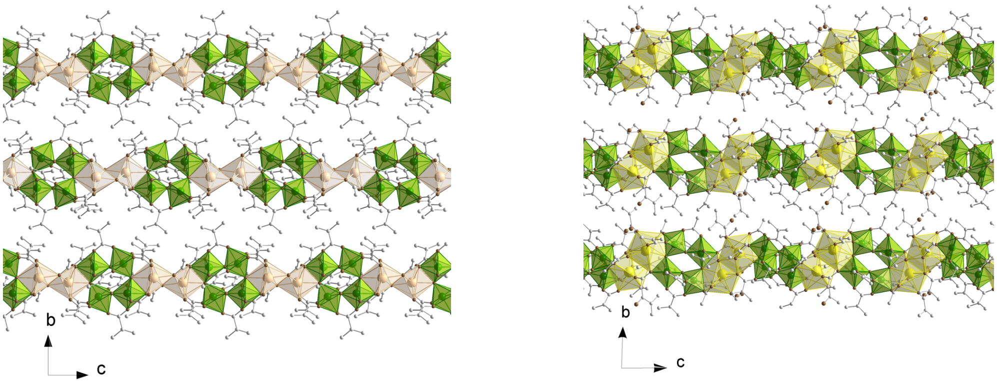

(a) Ca2Ti4 (b) Sr2Ti4

Figure 4.4: Distribution of the chains in the unit cell.

4.2.1 Calcium

Two similar structures of the Ca2Ti4 cluster were obtained. They differ in the ligand coordination and the crystal structure.

4.2.1.1 Ca2Ti4 (Structure 1)

The equimolar reaction of $Ca(OAc)_2$ and $Ti(O^iPr)_4$ or $Ti(O^nBu)_4$ with 4.5 mmol of methacrylic acids per mmol metal resulted in crystals of $[Ca_2Ti_4(\mu_3\text{-}O)_2(\mu_2\text{-}O)_2(\mu_3\text{-}OAc)_2(OMc)_{10}]_n$. One repeating unit of the cluster chain contains four titanium and two calcium atoms as shown in Fig. 4.5. This unit can be divided in two asymmetric units of $CaTi_2O$, where the metal atoms are connected through a μ_3-O. These two units are joined together by two μ_2-O. The distance between neighbouring Ti atoms and between Ca and Ti are all in the range between 3.3719(5) and 3.6524(6) Å, details are listed in Tab. A.18. While the core oxygen atom O(1) binds stronger to Ti(2) than to Ti(1), the opposite is true with O(2) (Ti(1)-O(1) 1.9645(16), Ti(1)-O(2) 1.7297(16), Ti(2)-O(1) 1.7600(16), Ti(2)-O(2) 1.9124(16) Å). The Ca- core oxygen atom distance is in the typical range of Ca-O bonds (Ca(1)-O(1) 2.4549(16) Å).

All metal atoms and the core oxygen atom of a cluster unit are arranged in a plane. The next cluster unit is shifted parallel to this plane according to Fig.4.5. The [Ca_2Ti_4] repeating units are connected through an acetate. One oxygen atom of the acetate is bridging Ca(1) and Ti(1), the other oxygen atom is bridging Ca(1) and Ca(1)'. Thus, the acetate is also chelating Ca(1). The distance between Ca(1) and Ca(1)' is 4.0045(9) Å. The Ca(1)-O(4) bond length is much longer than the Ca(1)'-O(4) distance (Ca(1)-O(4) 2.6593(19), Ca(1)'-O(4) 2.2916(18) Å). The Ti(3)-O(3) distance is the longest in the cluster with 2.1116(18) Å. Ca(1)-O(3) lies in between with 2.4276(17) Å.

Beside the acetate, Ca(1) and Ti(1) are additionally connected through one bridging methacrylate. Two methacryates are bridging Cu(1) and Ti(2), one above and one below the cluster core

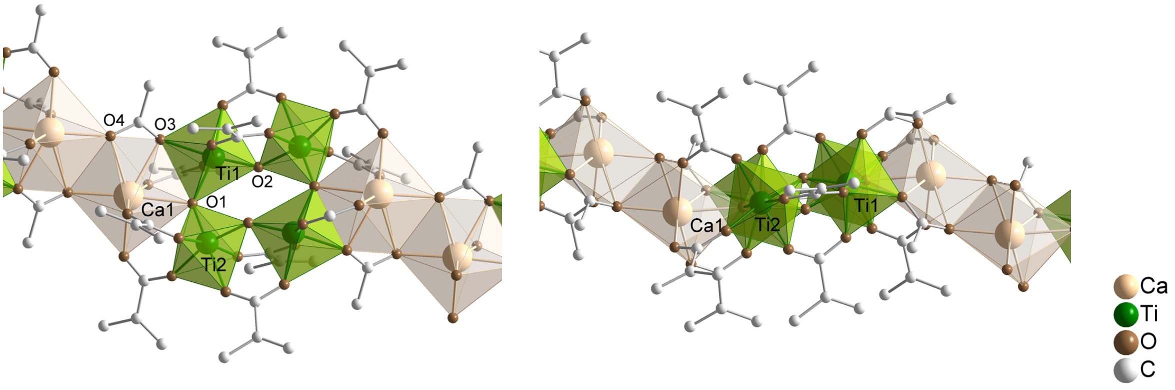

Figure 4.5: Structure of $[Ca_2Ti_4(\mu_3\text{-}O)_2(\mu_2\text{-}O)_2(\mu_3\text{-}OAc)_2(\mu_2\text{-}OMc)_{10}]_n$. Hydrogen atoms are omitted for clarity

plane. The Ca-O bond lengths of the methacrylates differ only slightly between 2.317(2) and 2.361(2) Å, as well as the Ti-O bond lengths of these ligands (Ti(1)-O(6) 1.9633(18), Ti(2)-O(8) 1.950(2), Ti(2)-O(10) 1.9575(19) Å). Two Ti atoms are linked through two methacrylates, additionally connecting the two asymmetric $[CaTi_2O]$ units. One ligand lies in the cluster core plane, while the other is axial to it. The equatorial methacrylate shows weaker bonds to Ti(2), whereas the Ti-O bonds in the axial methacrylate are equal (Ti(1)-O(13) 2.0044(17), Ti(2)-O(14) 2.1585(18); Ti(1)-O(11) 2.0205(18), Ti(2)-O(12) 2.0256(18) Å).

4.2.1.2 Ca2Ti4a (Structure 2)

Changes in the molar ratio of Ca:Ti to higher Ti contents during the synthesis led to variations in the structure of the above described cluster. Differences are observed in the ligand sphere and the linkage of the cluster units. This results also in a symmetry reduction from *Pccn* to $P\bar{1}$. The repeating cluster unit is doubled compared to the one described above and consists of four Ca and eight Ti. The asymmetric unit is Ca_2Ti_4, with connected Ca atoms. Reasons for this doubling are differences in the occupancy of the ligands. The acetate which links the cluster units is partly substituted by a methacrylate. The occupancy of the acetate on one site is 25%, while it has an occupancy of 75% on the second site (Fig. 4.6).

The Ca atoms in this cluster are additionally linked through one oxygen atom of a methacrylic acid ligand. This increases the coordination number of Ca to 8, instead of 7 before. The proton of the methacrylic acid shows hydrogen bonds to a non-coordinated butanol, which co-crystallised with the cluster. The Ca-O bond length to this bridging oxygen atom differ significantly, Ca(2)-O(15) 2.812(2) Å is much longer than Ca(1)-O(15) 2.489(2) Å. This bridging methacrylic acid ligand moves the Ca atoms closer to each other, the distance between Ca(1) and Ca(2) is smaller than the Ca distances in Ca2Ti4 (Ca(1)-Ca(2) 3.7089(8) compared to about 4 Åin structure 1). This affects also the linking carboxylate group. The Ca-O bond lengths of the chelated Ca(1) are now equal (Ca(1)-O(3) 2.560(2), Ca(1)-O(4) 2.5101(19) Å), the Ca(2)-O(4) is slightly lengthened (2.3604(19) Å). The bond lengths of the carboxylate group chelating Ca(2) are not equal, but still shorter than in the structure before (Ca(2)-O(19) 2.432(2), Ca(2)-O(20) 2.546(2) Å). All other bond lengths are comparable to the first cluster (Tab. A.18).

The crystal structure also changes due to the symmetry reduction according to Fig. 4.7. In structure 1 the parallel chains are arranged along *c*. Now they are arranged along [-111] and the distribution is also different.

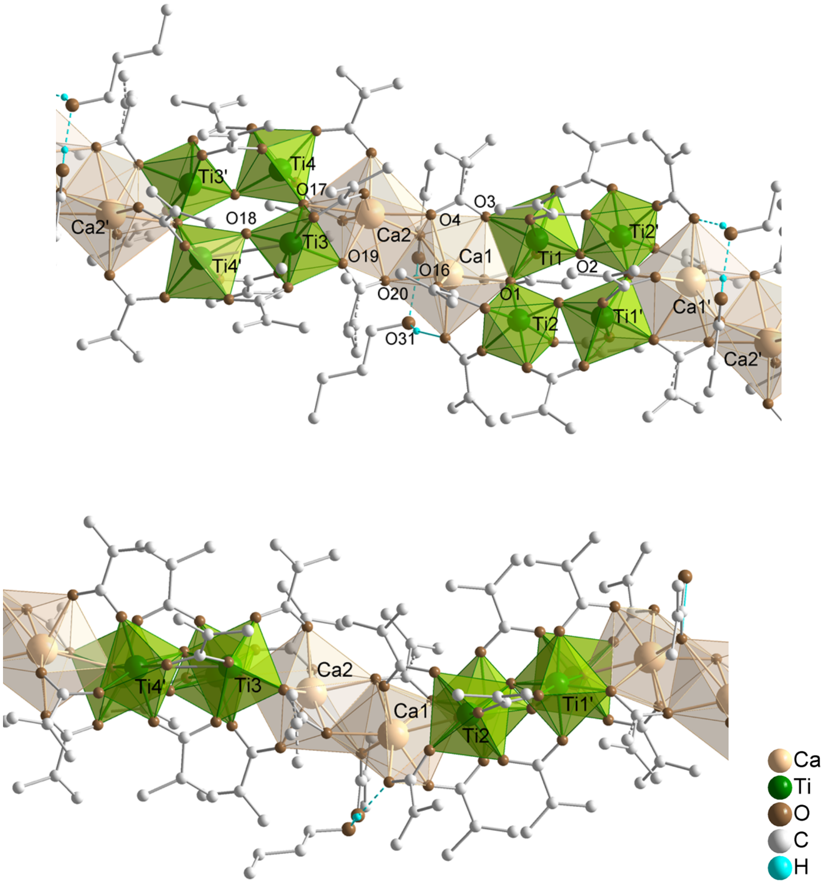

Figure 4.6: Structure of $[Ca_2Ti_4(\mu_3\text{-O})_2(\mu_2\text{-O})_2(\mu_3\text{-OAc})(\mu_3\text{-OMc})(\mu_2\text{-OMc})_{10}(\mu_2\text{-HOMc}) \cdot \text{BuOH}]_n$. Only hydrogen atoms coordinated to oxygen atoms are displayed.

4.2.2 Strontium

This cluster type was only obtained when $Sr(OAc)_2$ was reacted with $Ti(O^nBu)_4$. When $Ti(O^iPr)_4$ was used instead, a cluster with Sr2Ti8 cluster core was obtained (Sec. 4.3.1)

The cluster core of $[Sr_2Ti_4O_4(OMc)_{12}(HOMc)_2]_n$ (Fig. 4.8) is isostructural to the core of $Ca_2Ti_4O_4$. The ligand sphere differs from that of the Ca cluster, especially in the coordination of Sr as shown in Fig. 4.9. The Sr-O bond lengths are in general more than 0.1 Å larger than those of Ca-O, in respect to the larger Sr^{2+} ion (Tab. A.18).

The cluster units are now connected through four μ_3-OMc ligands, more than in the Ca clusters. These ligands show two different coordination motives. In the first methacrylate one oxygen atom bridges Sr(1) and Ti(1), where the other oxygen atom coordinates to Sr(2). In the second methacrylate one oxygen atom bridges the two Sr and the other oxygen atom binds to Ti(1). None of the methacrylates is chelating the Sr atoms, like in the Ca compounds. The corresponding Sr-O distances are too large to be considered a bond (Sr(1)$\cdots$O(4) 3.972(3) Å, Sr(2)$\cdots$O(16) 3.456(2) Å). The Sr(1)-O(3) bond is very long compared to Sr(2)-O(4), whereas it is the opposite in the second ligand (Sr(1)-O(3) 2.8769(17), Sr(2)-O(4) 2.598(4); Sr(1)-O(5) 2.5947(16), Sr(2)-O(5) 2.7048(16)). The Ti-O distance for the bridging oxygen atom is also somewhat larger than for the single bonded oxygen atom in the second methacrylate (Ti(1)-O(3) 2.0165(16), Ti(1)-O(6) 1.9623(16) Å).

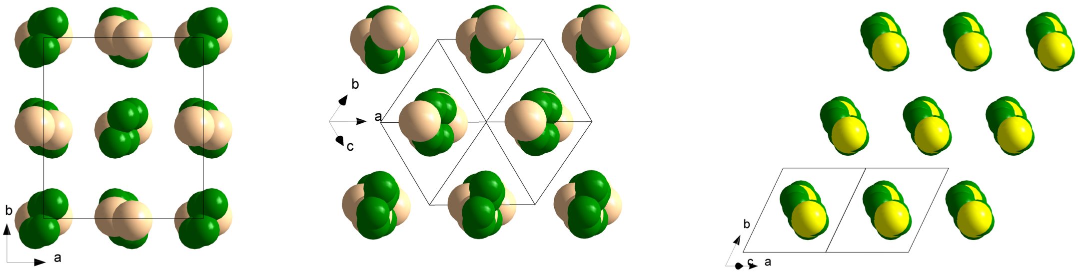

(a) Crystal structure of Ca2Ti4

(b) Crystal structure of Ca2Ti4a

(c) Crystal structure of Sr2Ti4

Figure 4.7: Comparison of the crystal structure. For clarity only metal atoms in space-filling model are displayed.

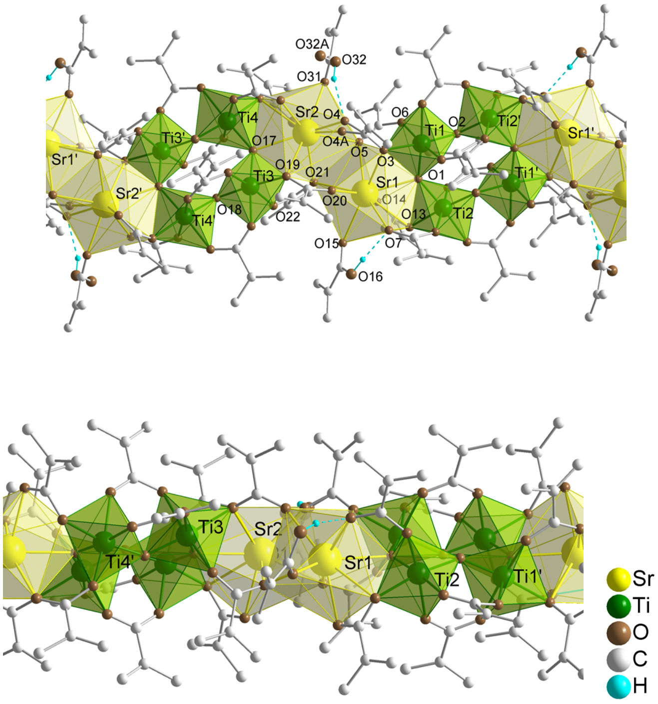

Figure 4.8: Structure of $[Sr_2Ti_4(\mu_3\text{-O})_2(\mu_2\text{-O})_2(\mu_3\text{-OMc})_6(\mu_2\text{-OMc})_6(\mu_2\text{-HOMc})_2]_n$. Only hydrogen atoms coordinated to oxygen atoms are displayed.

As in the Ca cluster two methacrylates bridge Sr(1) and Ti(2). One of the methacrylates is also chelating the Sr(1) atom, where the second Sr-O bond is very weak (Sr(1)-O(7) 2.6322(16); Sr(1)-O(13) 2.9464(17), Sr(1)-O(14) 2.5585(18) Å). The Ti-O bond lengths are somewhat longer in the chelating/bridging methacrylate (Ti(1)-O(3) 2.0165(16), Ti(1)-O(6) 1.9623(16) Å). All these ligands exist also in the second Sr_2Ti_4 unit, build by Sr(2), Ti(3) and Ti(4). Where Ti(3) is equivalent to Ti(1) and Ti(4) to Ti(2), the bond lengths and distances are comparable, details can be found in Tab. A.18.

The coordination spheres of the Sr atoms are completed by a η_1-—methacrylic acid. The orientation of these two ligands bonded to either Sr(1) or Sr(2) is not equal. The methacrylic

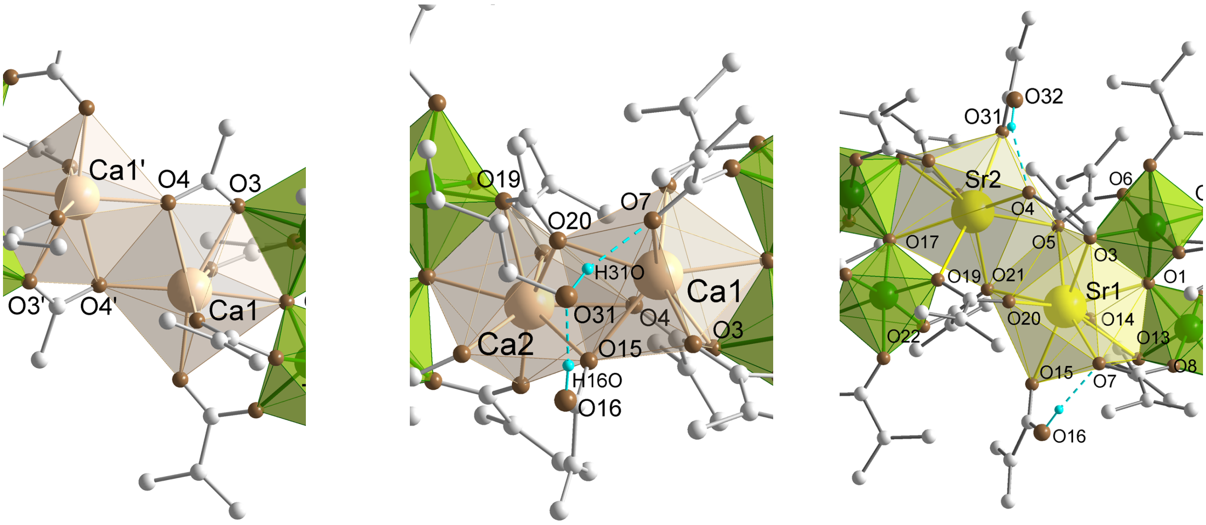

(a) Close up of Ca2Ti4 (b) Close up of Ca2Ti4a (c) Close up of Sr2Ti4

Figure 4.9: Comparison of the coordination around Ca and Sr. Only hydrogen atoms coordinated to oxygen atoms are displayed.

acid bonded to Sr(1) shows hydrogen bonds to the methacrylate bridging Sr(1) and Ti(2) (Sr(1)-O(15) 2.5577(17) Å; O(16)$\cdots$O(7) 2.728(2) Å). The acid bonded to Sr(2) on the other hand shows hydrogen bonds to O(4), which is of a μ_3-OMc (Sr(2)-O(31) 2.5559(17), O(32)$\cdots$O(4) 2.804(5) Å). The acid as well as O(4) are slightly disordered. The prime position is occupied by 75% and the second 25%. The second position shows no hydrogen bonds, due to the greater distance of O(32A) to O(4A) (O(32A)$\cdots$O(4A) 3.664(15) Å). The coordination number for Sr is 9 with two very long Sr-O bonds greater than 2.8 Å.

As Sr2Ti4 crystallised in the same space group as the second structure of the Ca2Ti4 cluster, the distribution in the crystal latice is equivalent to Ca2Ti4a (Fig.4.7), but the chains are oriented along [-101] (Fig.4.4).

4.2.3 Comparison with other clusters

These structures can again be derived from the Ti6 cluster with a flat cluster core. The outer two Ti atoms are here replaced by Ca or Sr, respectively. The Ti_4O_4 cluster unit stays intact. Due to the lower charge of the Ca^{2+} and Sr^{2+} ions and higher coordination numbers, the cluster are condensed to endless chains. In the previous Zn/Cd-Ti clusters this was not possible due to the lower coordination numbers of these ions.

4.3 Clusters based on the Ti8 Ring

The Ti8 ring structure was described in detail in Sec. 1.7.4. As mentioned there, guest molecules can be incorporated in the ring cavity. Sr and Pb are accessing this ring cavity in the structures decribed here.

4.3.1 Strontium

The reaction of $Sr(OAc)_2$ with $Ti(O^iPr)_4$ and methacrylic acid in different molar ratios resulted in a cluster with average composition $Sr_2Ti_8O_8(O^iPr)_{1.73}(OAc)_{2.27}(OMc)_{16}$. This structure actually results from the crystallisation of two centrosymmetric clusters with very similar structures on the same site, viz. $Sr_2Ti_8O_8(O^iPr)_2(OAc)_2(OMc)_{16}$ (a) with an occupancy of 86.5% (Fig. 4.10) and $Sr_2Ti_8O_8(OAc)_4(OMc)_{16}$ (b) with an occupancy of 13.5% (Fig. 4.11).

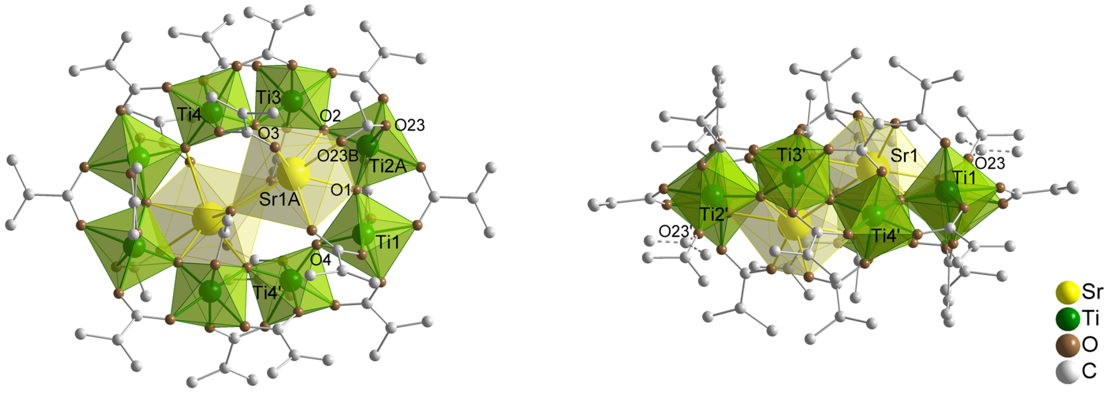

Figure 4.10: Molecular structure of $Sr_2Ti_8O_8(O^iPr)_2(OAc)_2(OMc)_{16}$ (a) with an occupancy of 86.5%. Hydrogen atoms are omitted for clarity. Disordered parts are drawn with broken bonds.

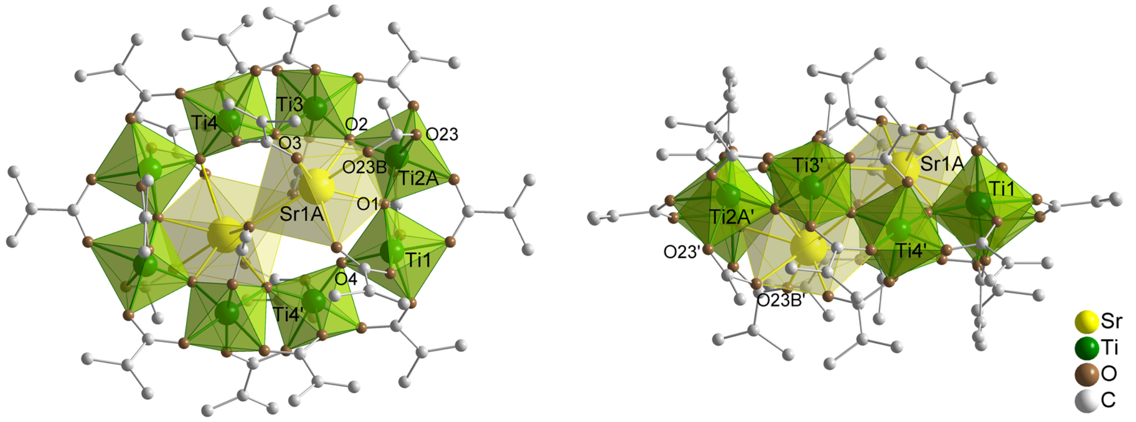

Figure 4.11: Molecular structure of $Sr_2Ti_8O_8(OAc)_4(OMc)_{16}$ (b) with an occupancy of 13.5%. Hydrogen atoms are omitted for clarity.

Common to both clusters is that the void of the Ti_8O_8 ring is occupied by two Sr atoms (see Fig. 4.10) with a Sr-Sr distance of 4.062(2) Å. Each Sr atom binds to four of the core μ_2-oxygen atoms of the Ti_8O_8 ring, each oxygen atom therefore bridges two Ti and one Sr. This causes the Ti_8O_8 ring to buckle; the shortest Ti-Ti distance thus becomes 7.879 Å and the longest 9.983 Å. The four crystallographic independent Ti atoms are approximately coplanar (Ti(4)-Ti(1)-Ti(2)-Ti(3) torsion angle 9.9(1)°), while the torsion angle Ti(2)-Ti(3)-Ti(4)'-Ti(1)' is 99.19(8)°. The Sr atoms are located above and below the distorted ring (see Fig. 4.11). The Sr- core oxygen distances to O(1) and O(2) are almost equal (Sr(1)-O(1) 2.535(3), Sr(1)-O(2) 2.554(3)), while the others are larger with Sr(1)-O(3) 2.699(3) and Sr(1)-O(4) 2.863(3) Å. The Ti(2) - core oxygen are the largest with Ti(2)-O(1) 1.886(4) and Ti(2)-O(2) 1.904(4) Å, where those of the other Ti atoms vary between 1.776(3) and 1.849(3) Å.

The Sr atoms are not only held in place by interaction with the core oxygen atoms of the ring system, but additionally interact with other ligands of the Ti_8O_8 ring. As a consequence, the ligand sphere around the $Ti_8O_8(OOCR)_{16}$ ring unit is partially rearranged compared to pure Ti8 clusters. Twelve of the sixteen methacrylate ligands still bridge two Ti atoms, i.e. around the ring two neighbouring Ti atoms are alternately bridged by two or one methacrylate ligand. The bond lengths vary between 1.988(3) and 2.153(3) Å.

The other four OMc ligands bridge one Sr and one Ti atom each (Sr(1)-O(7) 2.527(3), Ti(1)-O(8) 1.948(3); Sr(1)-O(9) 2.582(4), Ti(4)-O(10) 1.931(3) Å). One acetate ligand bridges the two Sr atoms through O(5) (Sr(1)-O(5) 2.491(3), Sr(1)'-O(5) 2.601(3) Å) and additionally Ti(3) (Ti(3)-O(6) 1.998(3) Å). The coordination of Ti(2) in (a) is completed by a terminal O^iPr ligand.

In the second cluster (b), these O^iPr ligands are substituted by acetate ligands, bridging Sr and Ti(2) (Fig. 4.11). The substitutional disorder affects the position of the Sr atoms and Ti(2). The influence of the additional acetate is also evidenced in the metal-oxygen distances. While the Ti-O distance of the alkoxy ligand in (a) is in the typical range (Ti(2)-O(23) 1.723(5) Å), that of the acetate ligand is unusually long (Ti(2A)-O(23B) 2.195(19) Å), indicating a rather weak coordination. The Sr(1A)-O distances in (b) spread over a wider range (2.149(12)-2.976(11) Å) than that of (a) (2.491(3)-2.601(3) Å). The largest distance of 2.976(11)Å is that of the other bridging acetate ligand (Sr(1A)'-O(5)), i.e. due to the new bridging acetate ligand the Sr-O distance of the other acetate bridge is lengthened. The short distance (2.149(12) Å) of one of the bridging methacrylate ligand (Sr(1A)-O(9)) may be a refinement artefact due to two disordered Sr positions. A full list of all bond lengths and angles is given in Tabs. A.21 and A.22.

4.3.2 Lead

Similar clusters to ones described above were obtained from the reaction of $Pb(OAc)_2$ with $Ti(O^nBu)_4$ and methacrylic acid. Here also two clusters co-crystallised viz. $Pb_2Ti_8O_8(O^nBu)_2(OMc)_{18}(^nBuOH)_2$ (a) (Fig. 4.12) with an occupancy of 65% and $Pb_2Ti_8O_8(O^nBu)_2(OAc)_2(OMc)_{16}(^nBuOH)_2$ (b) (Fig. 4.13) with occupancy of 35% resulting in an average composition $Pb_2Ti_8O_8(O^nBu)_2(OAc)_{0.66}(OMc)_{17.35}(^nBuOH)_2$.

The Pb atoms are also located above and below of the buckled Ti_8O_8 ring (Pb-Pb distance 4.515(4) Å) (Fig. 4.12). The Ti_8O_8 ring, however, is even more distorted, with the shortest Ti-Ti distance being 6.485 and the longest 9.742 Å(For a comparison of all bond lenghts and angles see Tabs. A.21 and A.22.) The four crystallographic independent Ti atoms are again approximately coplanar (Ti(4)-Ti(3)-Ti(2)-Ti(1) torsion angle 6.23(6)°), and the torsion angle Ti(2)-Ti(1)-Ti(4)'-Ti(3)' is increased to 135.54(6)°. Due to the shortening of the short ring axis, only three μ_2-oxygen atoms of the Ti_8O_8 ring coordinate to each Pb atom, while the other two (the oxygen atoms between Ti(1) and Ti(4) interact with both Pb atoms and thus become μ_4-O groups. The very large Pb-O(4) distances (2.931(4)-3.171(6) Å), however, indicate that this interaction is relatively weak. Among the Pb-(μ_3-O) distances that of Pb-O(3) is around 2.9 Å, while the others are between 2.572(5) and 2.717(9) Å.

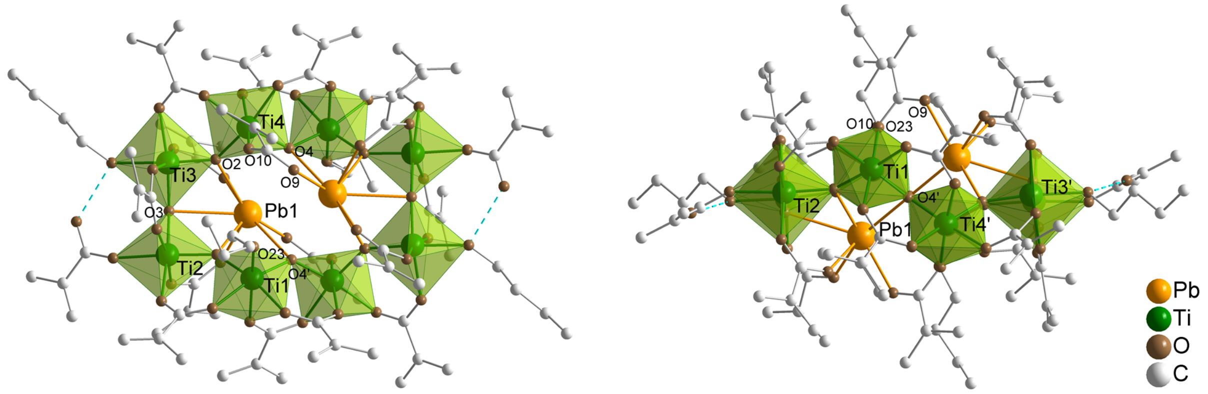

Figure 4.12: Molecular structure of $Pb_2Ti_8O_8(O^nBu)_2(OMc)_{18}(BuOH)_2$ (a) with an occupancy factor of 65%. Hydrogen bonds are drawn wish dashed bonds.

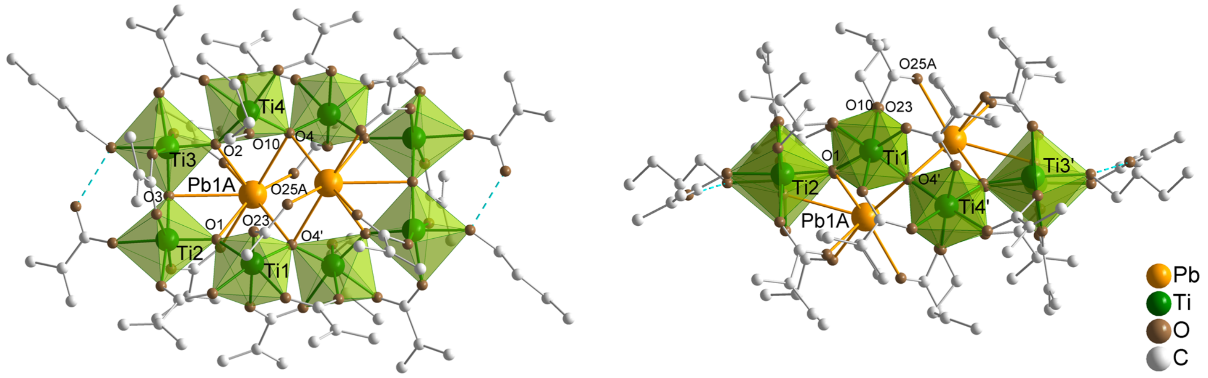

Figure 4.13: Molecular structure of $Pb_2Ti_8O_8(O^nBu)_2(OAc)_2(OMc)_{16}(BuOH)_2$ (b) with an occupancy of 35%. Only hydrogen atoms of OH groups are drawn.

In contrast to Sr2Ti8 only ten methacrylate ligands bridge the Ti atoms of the Ti_8O_8 ring. Ti(1) and Ti(4) are bridged by two methacrylate ligands, the others by only one. The Ti-O bond lengths of these ligands vary only between 2.033(5) and 2.073(5) Å. As in the structure of the Sr cluster, four OMc ligands bridge one Pb and one Ti atom each. The Pb-O bond lengths of the OMc ligands are the shortest and vary between 2.388(6) and 2.391(7) Å (Ti(2)-O(6) 1.940(6)Å, Ti(3)-O(8) 1.955(5) Å).

The main structural difference between the Sr and Pb cluster is that one (anionic) OMc ligand is substituted by the combination of an (anionic) O^nBu on Ti(3) (Ti(3)-O(24) 2.078(5)Å) and a (neutral) methacrylate ligand on Ti(2) (Ti(2)-O(21) 1.999(5)Å) which are connected through a hydrogen bond (O(22)$\cdots$O(24) 2.541(8)Å). The stronger distortion of the ring in the Pb cluster apparently does not allow another bridging OMc ligand between Ti(2) and Ti(3) on the most distant end of the distorted ring. There are several examples in literature, where the hydrogen-bridged combination of a coordinated alcohol molecule and a carboxylate ligand acts as a kind of bridging 'ligand' between two metal atoms [48, 99]. Comparison with the bond distances of $Ti_2(O^iPr)_6(\mu_2\text{-OOC}-C_6H_4-COO^iPr)(\eta_1\text{-OOC}-C_6H_4-COO^iPr)(^iPrOH)$ (Ti-O_{ROH} 2.072(1), Ti-OOCR 1.981(1) Å) [141] where the hydrogen atom of the hydrogen bridge was clearly located, indicates that the bonding situation in the Pb cluster is the same. The reverse situation (i.e. the combination of an O^nBu ligand and a neutral McOH), cannot be ruled out because the hydrogen could not be identified in the difference electron density map.

4.3.2.1 Allylic alcohol

A similar cluster was obtained, when an excess of allylic alcohol was added to the reaction mixture of Pb(OAc)$_2$,Ti(O^{n}Bu)$_4$ and methacrylic acid. Here only one structure type crystallised, which is isostructural to structure (a) of Pb2Ti8 (Fig 4.12). All the alkoxy ligands are substituted by OAllyl (HOAllyl= allylic alcohol), which show positional disorder over two sites. Hence this cluster has a composition of $Pb_2Ti_8O_8(O^nBu)_2(OMc)_{18}(AllylOH)_2$.

In this structure, the hydrogen atoms on the OAllyl groups coordinating to Ti(3) were identified in the difference electron density map. The Ti(3)-OAllyl bond was again long with 2.137(3)Å, and the distances between the oxygen atom of the allylic alcohol O(24) and the non-coordinated oxygen atom of the neighbouring methacrylate O(22) was 2.581(5) Å. This also proves the assumptions made for the structure before. All other distances are comparable with the cluster before.

4.3.2.2 O^{n}Pr derivative

A similar structure of the Pb2Ti8 cluster was obtained with Ti(O^{n}Pr)$_4$. The structure is again isostructural to Pb2Ti8, except for the alkoxy ligands which are now O^{n}Pr groups. Here again two similar clusters co-crystallised. Both are isostructural to structures (a) and (b) of Pb2Ti8, with the exception of a O^{n}Pr group coordinating instead of O^{n}Bu group. Structure (a) has an occupancy of 75.8% and structure (b) 24.2%, this results in an overall composition of $Pb_2Ti_8O_8(O^nPr)_2(OAc)_{0.48}(OMc)_{17.52}(^nPrOH)_2$.

4.3.3 Pb in the void of a fragment of the Ti8 ring

Another cluster was obtained, when Pb(OAc)$_2$ was reacted with Ti(O^{i}Pr)$_4$ instead of Ti(O^{n}Bu)$_4$ and methacrylic acid. The average composition of the cluster is $Pb_2Ti_6O_5(O^iPr)_{2.76}(OMc)_{15.24}$ (Fig. 4.14), again resulting from the crystallisation of two clusters with very similar structures on the same site, viz. $Pb_2Ti_6O_5(O^iPr)_3(OMc)_{15}$ (a) with an occupancy of 76% and $Pb_2Ti_6O_5(O^iPr)_4(OMc)_{14}$ (b) with an occupancy of 24% (Fig. 4.15).

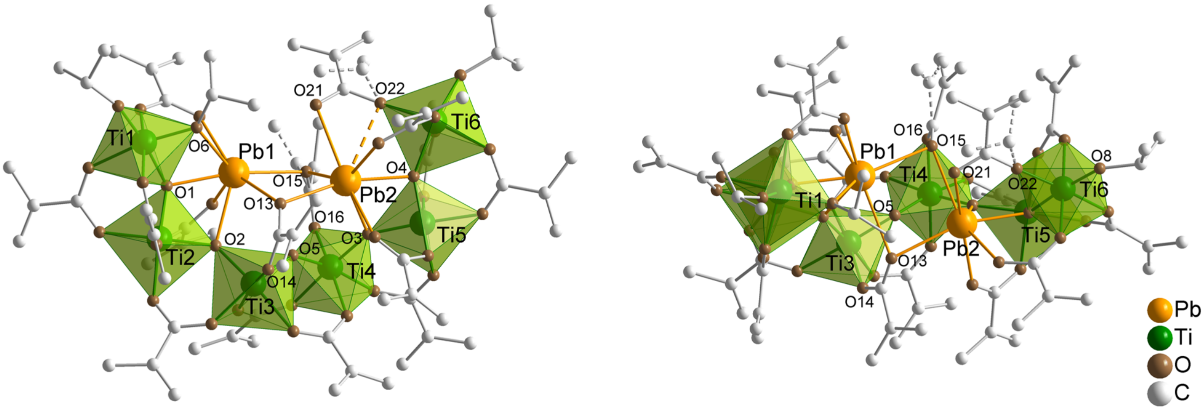

Figure 4.14: Molecular structure of $Pb_2Ti_6O_5(O^iPr)_{2.76}(OMc)_{15.24}$. Disordered parts are drawn with broken bonds.

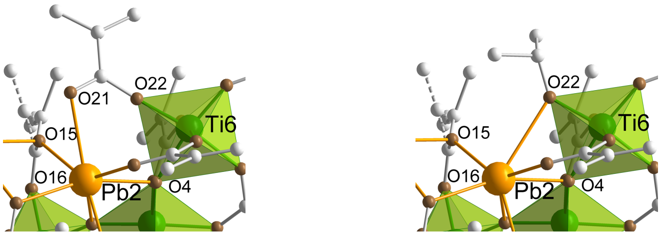

(a) $Pb_2Ti_6O_5(O^iPr)_3(OMc)_{15}$ (b) $Pb_2Ti_6O_5(O^iPr)_4(OMc)_{14}$

Figure 4.15: Details of the molecular structure of the two clusters of $Pb_2Ti_6O_5(O^iPr)_{2.76}(OMc)_{15.24}$. Disordered parts are drawn with broken bonds.

Compared to Pb2Ti8, two [TiO_6] octahedra are missing, i.e. the Ti_6O_5 unit is a fragment of the Ti_8O_8 reference structure. Otherwise the structures are rather similar, including the puckering of the ring (the torsion angle Ti(2)-Ti(3)-Ti(4)-Ti(5) is lowered to 115.49(3)° compared with the corresponding angle of 135.54(6)° in Pb2Ti8). The two lead atoms are much closer to each other (3.8448(3) Å) and to the ring plane than in Pb2Ti8. A full comparison of all bond lengths and angles with those of Pb2Ti8 is given in Tabs. A.21 and A.22.

Four core oxygen atoms are μ_3-bridging two Ti and one Pb atom (Pb-O 2.344(2)-2.558(2) Å). The fifth (bridging Ti(3) and Ti(4)) is μ_2, the distance to the Pb atoms being too large to be considered μ_4 as in Pb2Ti8 (Pb-O(5) 3.250(2) and 3.375(2) Å). The Ti-(μ_3-O) bond lengths of the terminal Ti atoms (Ti(1)-O(1) 1.978(2) and (Ti(6)-O(4) 1.972(2) Å) are significantly larger than those of the central Ti atoms (1.780(2)-1.881(2) Å for Ti(2)-Ti(5)).

Eight methacrylate ligands bridge Ti atoms, alternating two and one methacrylate between two neighbouring Ti atoms as in Sr2Ti8 (Ti-O 2.004(2)-2.120(3) Å). The other OMc ligands connect the Pb atoms to the Ti atoms of the ring fragment. Each titanium atom is connected to the central lead atoms by a bridging OMc ligand (Ti-O 1.94.3(3)-1.97.9(2) Å). While four of these ligands are clearly μ_2 with Pb-O distances between 2.41.5(2) and 2.49.1(3) Å, the other two, originating from Ti(3) and Ti(4) are μ_3, with a short and a longer Pb-O distance (Pb(1)-O(13) 2.995(3), Pb(2)-O(13) 2.699(2) and Pb(1)-O(15) 2.884(3) / Pb(2)-O(15) 2.8710(3) Å).

The two remaining coordination sites on the terminal Ti atoms of (b) are filled with one terminal (Ti(1)-O(7) 1.765(2) and Ti(6)-O(8) 1.763(3) Å) and one weakly bridging O^iPr. This group bridges to one central Pb atom (Ti(1)-O(6) 1.842(2) / Pb(1)-O(6) 2.798(2) and Ti(6)-O(22) 1.891(3) / Pb(2)-O(22) 3.027(3) Å) group each. In the first cluster the bridging O^iPr group on Ti(6) is substituted by a bridging OMc ligand, where the bond to Ti (Ti(6)-O(22) 1.891(3)) is also stronger than that to Pb (Pb(2)-O(21) 2.761(4) Å).

4.3.3.1 O^nPr derivative

A cluster similar to Pb2Ti6 was obtained, when $Ti(O^nPr)_4$ was used instead of $Ti(O^iPr)_4$. Here only cluster (a) of Pb2Ti6 was found, but due to the poor quality and the bad resolution it cannot be ruled out, that cluster (b) was also formed. Hence the formula is $Pb_2Ti_6O_5(O^nPr)_3(OMc)_{15}$. Except for the alkoxy ligands the cluster is isostructural to Pb2Ti6iPr(a). All the bond lengths are equivalent to the one previously decribed.

4.3.4 Comparison of the clusters

The structure of the Pb/Ti clusters depend strongly on the used Ti alkoxide. $Ti(O^nBu)_4$ gives only Pb2Ti8, $Ti(O^iPr)_4$ results only in Pb2Ti6 and $Ti(O^nPr)_4$ gives both clusters. Whereas the two Pb/Ti clusters are similar, the clusters obtained for Sr with different Ti alkoxides are structurally unrelated (see Sr2Ti4 in Sec.4.2.2).

4.4 Large Titanium/Lead Clusters

4.4.1 Pb4Ti8Ac

In an attemp to synthesise $Pb_2Ti_2O(OAc)_2(O^iPr)_8$ according to literature [117] crystals of $Pb_4Ti_8(\mu_4\text{-}O)_4(\mu_3\text{-}O)_4(\mu_2\text{-}O)_2(\mu_3\text{-}O^iPr)_2(\mu_2\text{-}O^iPr)_{11}(O^iPr)_5(\mu_2\text{-}OAc)_2$ (Fig. 4.16) were obtained after one year. Its cluster core can be divided into three layers of metals joined through core oxygen atoms within the layer, which are also connecting to metals of adjacent layer (Fig. 4.17).

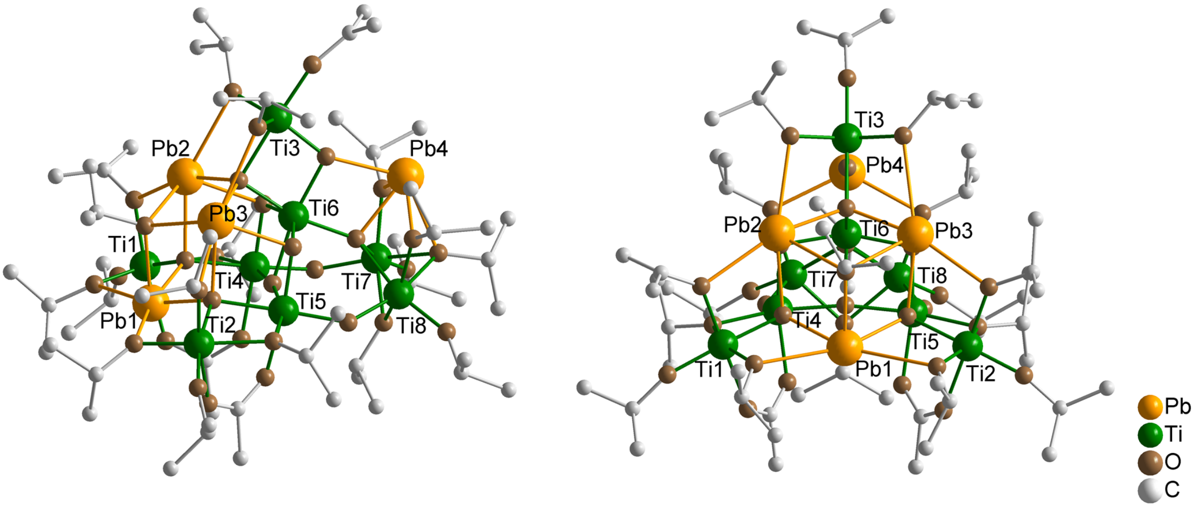

Figure 4.16: Molecular structure of $Pb_4Ti_8O_{10}(O^iPr)_{18}(OAc)_2$. Hydrogen atoms are omitted for clarity.

The bottom layer is built from three Ti and three Pb arranged in a triangle (Fig. 4.18(c)). The Ti atoms are located on the corner of this triangle and between lay the Pb atoms on the edge of the triangle. The distance between Pb atoms in this layer is about 3.8 Å and between Ti and Pb about 3.5 Å(Tab. A.23). Every Ti is linked to two Pb through a core oxygen atom. The Ti atoms are slightly above the Pb atoms, shifted towards the next layer. The bottom layer can also be seen as three condensed $[Pb_2Ti(\mu_4\text{-}O)]$ triangles, connected through a $\mu_3\text{-}O^iPr$. This alkoxo group bonds to Pb(1) much stronger than to Pb(2) and Pb(3), with bond lengths Pb(1)-O(11) 2.295(4), Pb(2)-O(11) 2.622(4) and Pb(3)-O(11) 2.620(4) Å.

The $[Pb_2TiO(1)]$ and $[Pb_2TiO(2)]$ unit have one Pb-O bond of about 2.3 Å and the other is about 2.4 Å (Pb(1)-O(1) 2.306(4), Pb(2)-O(1) 2.398(4); Pb(1)-O(2) 2.299(4), Pb(3)-O(2) 2.396(4) Å). The Ti-O distances are in both cases below 2 Å (Ti(1)-O(1) 1.978(4), Ti(2)-O(2) 1.986(4) Å). In the third $[Pb_2TiO(_3)]$ unit the Pb-O distances are equal, whereas the Ti-O is larger with Ti(3)-O(3) 2.064(4) Å (Pb(2)-O(3) 2.295(3) Pb(3)-O(3) 2.293(3) Å). All three core oxygen atoms O(1), O(2) and O(3) bond to a Ti of the next layer. This next layer contains three Ti atoms (Ti(4), Ti(5), Ti(6)). Here the Ti(4)-O(1) and Ti(5)-O(2) bonds are about 0.1 Å longer than the Ti(6)-O(3) bond (Ti(4)-O(1) 2.050(4), Ti(5)-O(2) 2.053(4), Ti(6)-O(3) 1.950(4) Å).

The core oxygen atom O(6) connects Ti(4), Ti(5) and Ti(6) and is not coordinating to any other metal (Fig. 4.18(b)). The distance of O(6) to the closest Pb(3) is above 3.4Å. Here the Ti-O(6) bonds of Ti(4) and Ti(5) are about 0.1 Å shorter than the Ti(6)-O(6) bond (Ti(4)-O(6) 1.921(4),Ti(5)-O(6) 1.917(4), Ti(6)-O(6) 2.027(4) Å). Additionally two μ_3-O between Ti(4) and

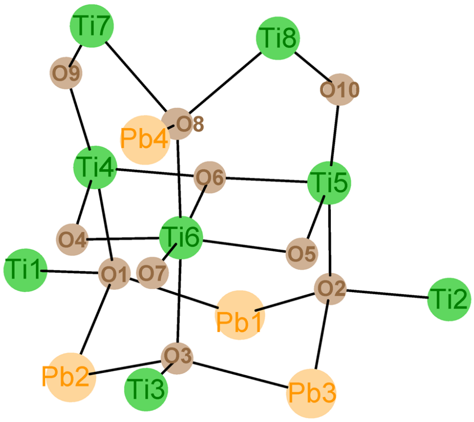

Figure 4.17: Cluster core of $Pb_4Ti_8O_{10}(O^iPr)_{18}(OAc)_2$.

Ti(6) and between Ti(4) and Ti(5) are coordinating to a Pb atom of the bottom layer (Pb(2) and Pb(3), respectively). There is again a difference in the Ti-O bond of Ti(4) and Ti(5) to the Ti(6)-O bonds (Ti(4)-O(4) 1.862(4), Ti(5)-O(5) 1.866(4); Ti(6)-O(4) 1.949(3), Ti(6)-O(5) 1.938(4) Å). The reason for the differences in the bond lengths of Ti(6) compared to Ti(4) and Ti(5) is a bridging oxygen atom between Ti(3), Ti(6) and Pb(4). This oxygen atom connects all three layers, but the Ti(6)-O(7) distance is again larger than the Ti(3)-O(7) bond (Ti(3)-O(7) 1.867(4), Ti(6)-O(7) 1.932(4) Å). The Pb-O bond lengths of these μ_3-O are all in the range between 2.387(4) and 2.402(4) Å.

The top layer (Fig. 4.18(a)) is formed from two Ti and one Pb atom, connected through μ_4-O(8), which also bonds to Ti(6). Ti(7) and Ti(8) are only weakly coordinating to O(8), with bond lengths Ti(7)-O(8) 2.118(4) Å and Ti(8)-O(8) 2.112(3) Å, whereas Ti(6)-O(8) is much shorter with 1.955(4) Å. Beside the above mentioned O(7), which links all three layers, there are two μ_2- oxygen atoms coordinating Ti of the top layer and Ti of the central layer. O(9) bridges Ti(4) and Ti(7), O(10) connects Ti(5) with Ti(8).

A mirror plane can be drawn through Pb(1), Ti(3), Ti(6) and Pb(4). This plane is perpendicular to the three planes described above. The oxygen atoms are also mirrored on this plane, but due to the orientation of the carbon atoms, the cluster is of lower symmetry than the cluster core.

The ligand sphere is quite diverse. The only two carboxylates are bridging Ti(1) and Ti(4) as well as Ti(2) and Ti(5). These two pairs of Ti atoms are also connected through a bridging O^iPr group. Both ligands bind stronger to the Ti of the central layer, Ti(4) and Ti(5). For the acetates the difference is about 0.1 Å (Ti(1)-O(13) 2.165(5), Ti(4)-O(14) 2.062(4); Ti(2)-O(15) 2.152(4), Ti(5)-O(16) 2.081(4) Å). The same differences in Ti-O bond lengths are found for the μ_2-O^iPr (Ti(1)-O(23) 2.086(4) Ti(4)-O(23) 1.989(4); Ti(2)-O(24) 2.084(4), Ti(5)-O(24) 1.995(4) Å).

All three Ti atoms of the bottom layer are coordinated to the two neighbouring Pb atoms of the layer through one μ_2-O^iPr. The Pb-O bonds are all long, between 2.634(4) and 2.870(4)Å. The Ti-O distances are almost equal between 1.860(4) and 1.872(5) Å. Three terminal alkoxy groups are completing the ligand sphere of the three Ti of the bottom layer. The Ti-O^iPr bonds are typically the smallest in the structure (Ti(1)-O(28) 1.804(4), Ti(2)-O(29) 1.807(4), Ti(3)-O(30) 1.802(4) Å).

There are no bridging ligands within the central layer, and between the central and the top layer. In the top layer, the three metals are connected through a μ_3-O^iPr. This O^iPr is perpendicular to the plane formed by the three metals, and oriented in the same direction as the μ_3-O^{i}Pr of the bottom layer. Every metal of the top layer is coordinated to both neighbouring metals through a μ_2-O^{i}Pr. The Ti-O bonds of Pb-Ti bridging alkoxo groups are equal and about 0.1 Å shorter than those of Ti-Ti bridging O^{i}Pr groups. (Ti(7)-O(25) 1.946(4), Ti(8)-O(26) 1.944(4); Ti(7)-O(27) 2.045(4), Ti(8)-O(27) 2.037(4) Å). The bond lengths of the μ_3-O^{i}Pr are even larger (Ti(7)-O(12) 2.176(4), Ti(8)-O(12) 2.175(4) Å). The same applies for the Pb-O bonds, those of μ_2-O^{i}Pr are 0.1 Å shorter than of the μ_3-O^{i}Pr (Pb(4)-O(25) 2.402(4),

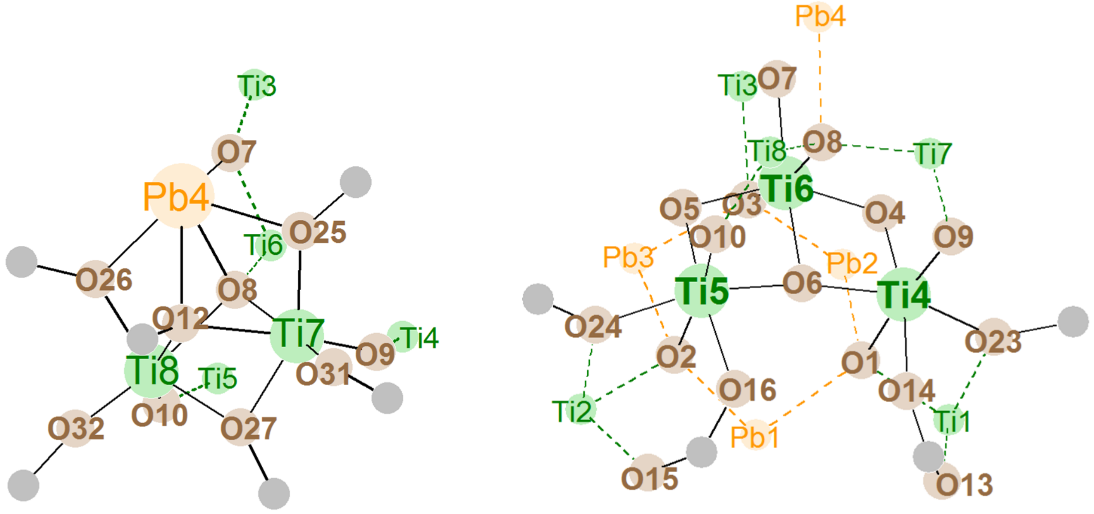

(a) Top layer (b) Central layer

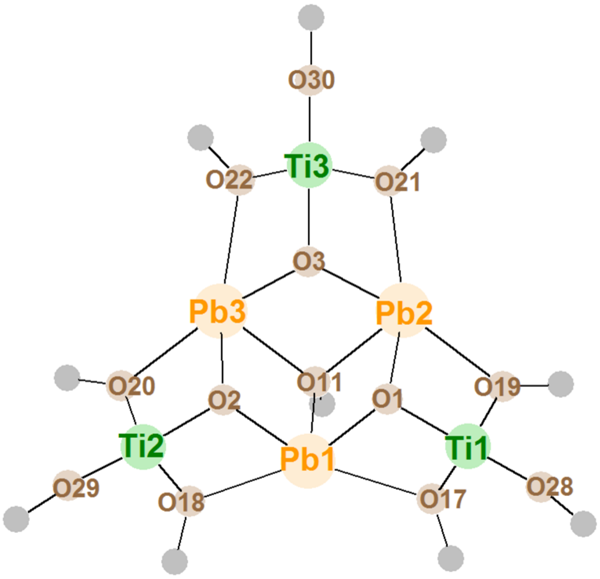

(c) Bottom layer

Figure 4.18: Schematic drawing of the layers in $Pb_4Ti_8O_{10}(O^iPr)_{18}(OAc)_2$. Dashed lines indicate bonds to metals of adjacent layers.

Pb(4)-O(26) 2.419(4); Pb(4)-O(12) 2.508(4) Å). Two terminal alkoxy groups are completing the coordination sphere of Ti(7) and Ti(8), with short Ti-O bonds (Ti(7)-O(31) 1.788(4), Ti(8)-O(32) 1.798(4) Å).

Ti(3) has only a coordination number of 5, arranged in a trigonal bipyramid. This is quite unusual for Ti, as it prefers an octahedral coordination.

4.4.2 Pb6Ti6

2 mmol (0.651 g) of $Pb(OAc)_2$, 2 mmol (0.568 g) of $Ti(O^iPr)_4$ and 4 mmol (0.278 g) of dry allylic alcohol were heated for 2h at 70°C and after cooling 18.9 mmol (1.62 g) of methacrylic acid were added. Crystals of $Pb_6Ti_6O_9(OAc)(OMc)_{17}$ (Fig. 4.19) were obtained after four months, whereas the sample synthesised at room temperature resulted in a Pb2Ti8 cluster core. The cluster core of $Pb_6Ti_6O_9(OAc)(OMc)_{17}$ can be separated in three layers of almost parallel metal planes (Fig. 4.20(a)). The central layer is a six-membered Ti ring according to Fig 4.20(b). The other two layers contain three Pb atoms each. One Pb atom of each layer is located right above the centre of the Ti6 ring as shown in Fig. 4.20(a). The others are outside the ring. Viewed from the top, these outer Pb atoms are arranged in a regular triangle, where two Pb atoms are lying above each other (Pb(3) and Pb(6)). All Pb atoms connect to the Ti atoms through core oxygen atoms, but only the outer Pb atoms are additionally coordinating through ligands to the Ti layer. The three lead atoms Pb(3), Pb(4) and Pb(6) show positional disorder, but no effect on the ligands was observed. The Pb distances within a layer are around 4 Å (3.9100(6) - 4.062(10) Å), those of different layers between 6.619(3) and 7.078(9) Å, except the two central Pb atoms, which are much closer (Pb(2)-Pb(5) 4.5535(7) Å).

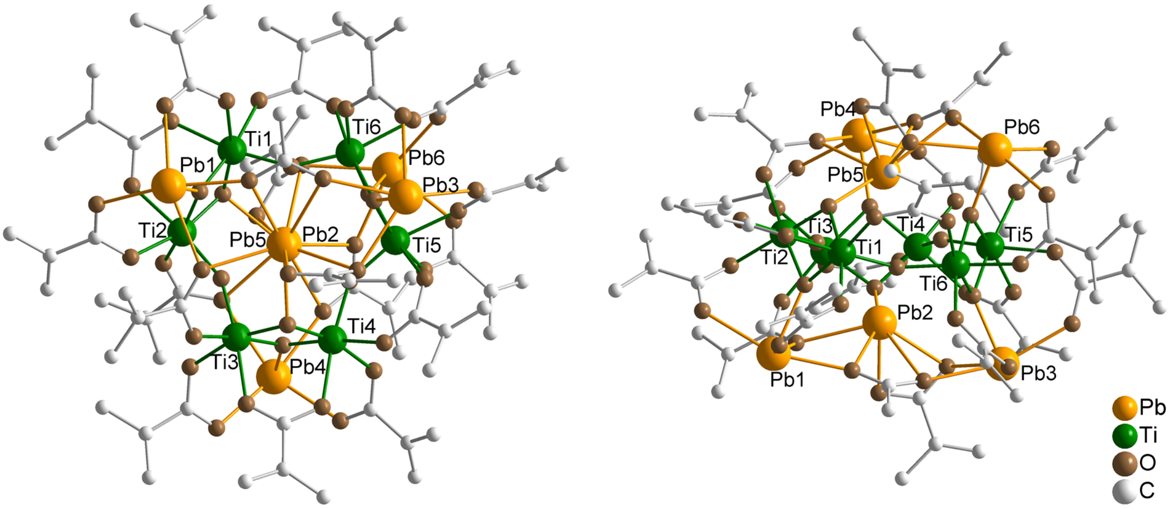

Figure 4.19: Molecular structure of $Pb_6Ti_6O_9(OAc)(OMc)_{17}$. Hydrogen atoms are omitted for clarity

In the central layer, the Ti atoms are connected alternating by two μ_3- or μ_2-oxygen atoms (Fig. 4.21(b)), where the μ_2-O lie within the Ti6 plane. The third atom coordinating to the μ_3-oxygen atom is a Pb atom. Hence the two μ_3-O connecting a pair of Ti atoms are linking to both of the two Pb layers. In this way every Pb atom is coordinated to one μ_3-O. Pb(3) and Pb(6) are linked to the same pair of Ti atoms (Ti(5) and Ti(6)). The two other Ti pairs are linked to one central and one outer Pb atom. Every μ_2-oxygen atom shows also long bonds to each of the two central Pb atoms with Pb-O bond lengths above 3 Å. The Ti-Ti distance

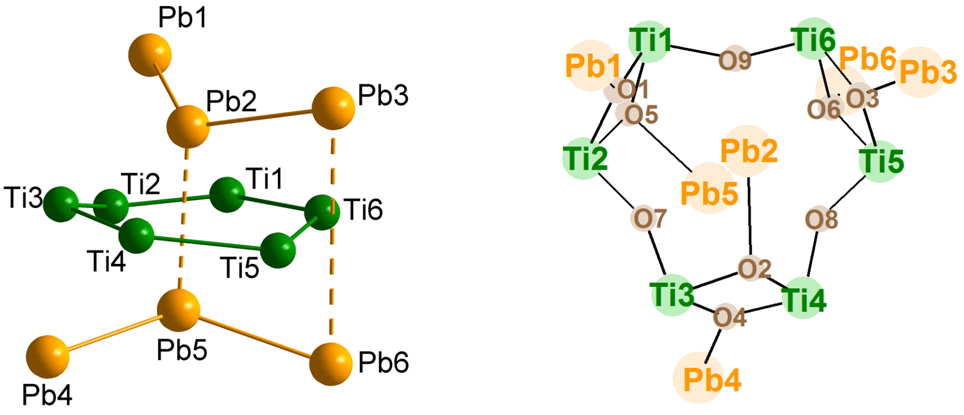

(a) Arrangement of the metal atoms

(b) Cluster core of Pb6Ti6

Figure 4.20: Structural details of $Pb_6Ti_6O_9(OAc)(OMc)_{17}$

between μ_3-O linked Ti is much shorter than those connected by μ_2-O (for μ_3-O 2.8398(8) - 2.9370(9) Å compared to 3.4930(10)-3.5914(10) Å μ_2-O), but the Ti-(μ_3-O) bonds are generally longer than the Ti-(μ_2-O) bonds (Ti-μ_3-O 1.831(2)-1.936(2) Å, Ti-μ_2-O 1.799(2)-1.868(2) Å). The Pb-O bonds of the central Pb(2) and Pb(5) are significantly longer than those of the outer Pb atoms (Pb(2)-O(2) 2.509(2), Pb(5)-O(5) 2.519(2) Å compared to 2.244(3)-2.284(2) Å for the others).

Within the central layer, the Ti atoms are not only connected through core oxygen atoms, but also μ_2- methacrylates. Only Ti(1) and Ti(4) are coordinated to both neighbouring Ti atoms according to Fig. 4.21(b)), but there is no methacrylate bridging Ti(2) and Ti(3), or Ti(5) and Ti(6). Explanations for the missing methacrylates are found in the adjacent Pb layers. One μ_3-methacrylate bridges Ti(3) with Pb(1) and Pb(2) and another one Ti(2) with Pb(4) and Pb(5) (Fig. 4.21(a) and Fig. 4.21(c)). The reason for the missing methacrylate between Ti(5) and Ti(6) are the two neighbouring Pb atoms Pb(3) and Pb(6). Ti(5) and Ti(6) link not only through μ_3-O to these Pb atoms, but also by four μ_2- methacrylates. These bridge both Ti(5) and Ti(6) with both Pb(3) and Pb(6). Bridging methacrylates appear also between the other outer Pb atoms (Pb(1) and Pb(4)) and their neighbouring Ti atoms. As Pb(1) and Pb(4) are not coordinating to the same pair of Ti atoms, Ti(1)-Ti(4) are only coordinating with one methacrylate to Pb(1) or Pb(4).

In the Pb layers, the Pb atoms are connected through two carboxylates. One carboxylate group bridges all three Pb atoms. It is chelating the central Pb atom and bridging to both other Pb atoms of the layer. In layer 1 this carboxylate ligand is an acetate group, but it is a methacrylate in layer 3. The Pb-O bonds are in both cases quite long, between 2.426(2) and 2.756(2) Å for the acetate and 2.496(3) - 2.674(3) Å for the methacrylate. The second carboxylate group stabilising the Pb layer is again chelating the central Pb atom, but bridges only to one other Pb atom. This outer Pb atom is not connected to a Ti atom through a μ_3-methacrylate. Here the Pb-O distance of the non-bridging oxygen atoms is much shorter (Pb(2)-O(17) 2.370(2); Pb(5)-O(21) 2.382(3)Å) and the other are between 2.610(4) and 2.674(2) Å.

Pb^{2+} has a free electron pair, which often requires space. It is also the reason for a distinction of short and long bonds, where short bond are located in one hemisphere of the coordination sphere of Pb. Voids around the Pb atoms in the structure are indicators for the location of the electron pair. In this cluster the free electron pair of the central Pb atom is pointing to the

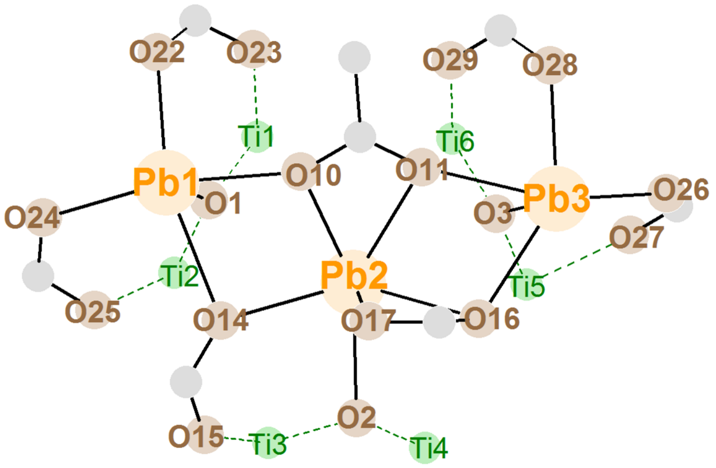

(a) Layer 1

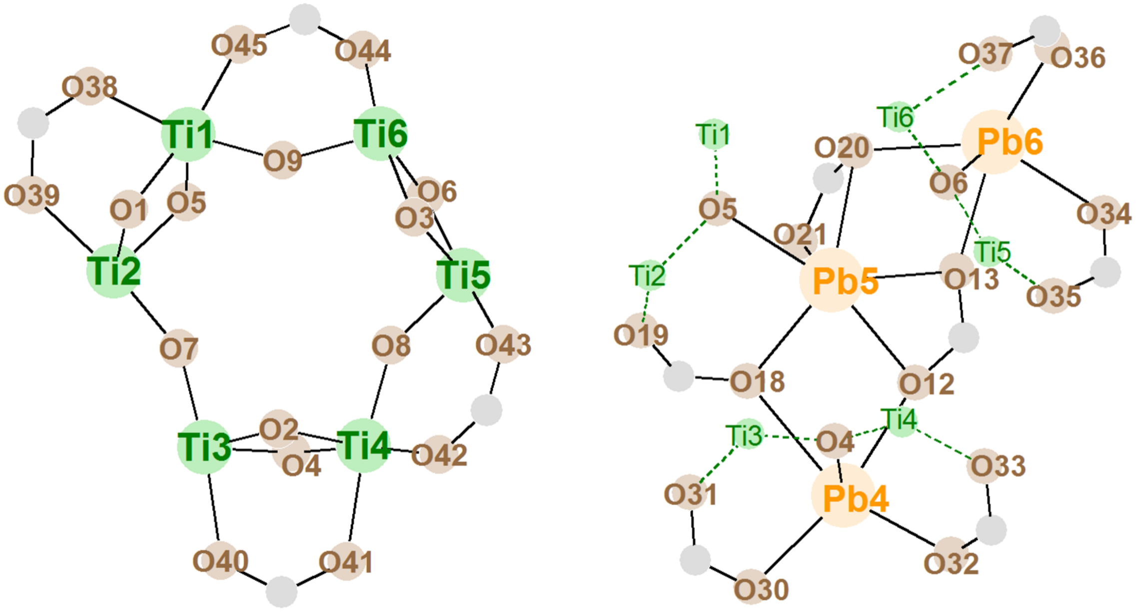

(b) Layer 2 (Central layer)

(c) Layer 3

Figure 4.21: Schematic drawing of the coordination in the three layers of $Pb_6Ti_6O_9(OAc)(OMc)_{17}$. Dashed lines indicate bonds to metals of adjacent layers.

centre of the Ti6 ring. Those of the outer Pb are outside the cluster. The central Pb atoms have 6 short bonds and three long ones, the outer Pb atoms show only 5 short bonds, but no long interaction.

The cluster packing in the crystal was quite dense, as shown in Fig. 4.22. The distance between Pb(1) atoms of different clusters is only 4.3999(7) Å and hence shorter than the intramolecular Pb(2)-Pb(5) distance of 4.5535(7) Å. An allylic alcohol molecule also crystallised with the cluster. It showed weak interaction to Pb(6), with a Pb-O distance of 3.12(2) Å. But there is no connection of the solvent to other clusters.

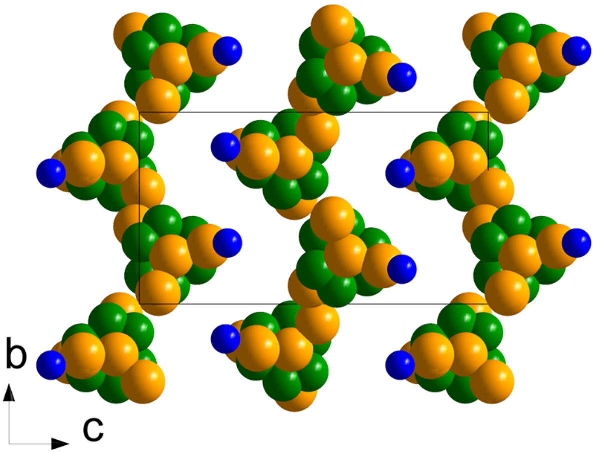

Figure 4.22: Crystal structure of $Pb_6Ti_6O_9(OAc)(OMc)_{17}$.

4.5 Copper

4.5.1 Methacrylic acid

This clusters can be synthesised from various Ti alkoxides, $Cu(OAc)_2$ and methacrylic acid applying different molar ratios. In $Cu_4Ti_5(\mu_3\text{-O})_6(\mu_2\text{-OMc})_{16}$ the Ti atoms are in their usual octahedral coordination with oxygen, while the copper atoms form a square pyramidal coordination sphere with oxygen. All five Ti atoms and the core oxygen atoms are arranged in a plane. Four Ti atom are connected to the central Ti(1) atom through one oxygen atoms each according to Fig. 4.23. The central Ti atom lies on an inversion centre, hence there are two pairs of symmetry equivalent Ti atoms.

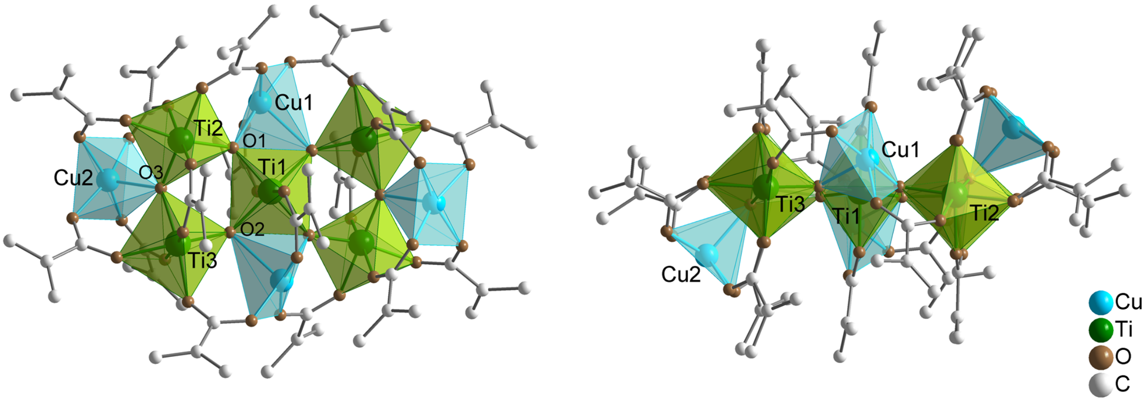

Figure 4.23: Molecular structure of $Cu_4Ti_5(\mu_3\text{-O})_6(\mu_2\text{-OMc})_{16}$. Hydrogen atoms are omitted for clarity

The four core oxygen atoms are also connecting two copper atoms with the central titanium atom. Hence these two $[CuO_5]$ pyramids are corner sharing with the TiO_6 octahedron. One of these Cu-core oxygen bond lengths is long, while the other is in the normal range (Cu(1)-O(1) 1.9585(9), Cu(1)-O(2) 2.3432(9) Å). Two other core oxygen atoms are connecting two titanium and one copper atom each, with a long Cu-O bond (Cu(2)-O(3) 2.1982(9) Å). The copper atoms are located above and below the Ti-core oxygen plane.

While the Ti(1)-O bond lengths are almost equal (Ti(1)-O(1) 1.9176(10) Å, Ti(1)-O(2) 1.9183(9) Å), that of Ti(2)-O(1) is with 1.8508(9) Å significantly longer than that of Ti(3)-O(2) 1.7684(10) Å. On the other hand, the Ti(2) distance to O(3) is shorter than that of Ti(3) (Ti(2)-O(3) 1.7985(9), Ti(3)-O(3) 1.9075 Å).

All methacrylates are bridging either two Ti atoms, or one Ti and one Cu atom. Two methacrylates coordinate in *trans* position to the central Ti atom. They bridge neighbouring Cu(1) atoms on opposite sides of the Ti-O plane. Two methacylates bridge Cu(1) and Ti(2) or Ti(3), respectively. Cu(2) on the edge of the cluster coordinates through four methacrylates to the neighbouring two Ti atoms. These two Ti atoms are also connected by one methacrylate. Considering their symmetry equivalents, there are sixteen methacrylate ligands in this cluster.

This cluster is also obtained with co-crystallised CH_2Cl_2, originating from the synthesis of $Cu(OMc)_2$, which was used instead of $Cu(OAc)_2$. The molecular structure is equivalent to the above described cluster (Fig.4.24). The cell is doubled compared to Cu_4Ti_5met. Therefore there are two clusters which are not symmetry related. But these two cluster do not differ in their structure and coordination mode. One of the CH_2Cl_2 molecules is slightly disordered. There are no indications of a coordination of these solvent molecules to the cluster. The bond distances

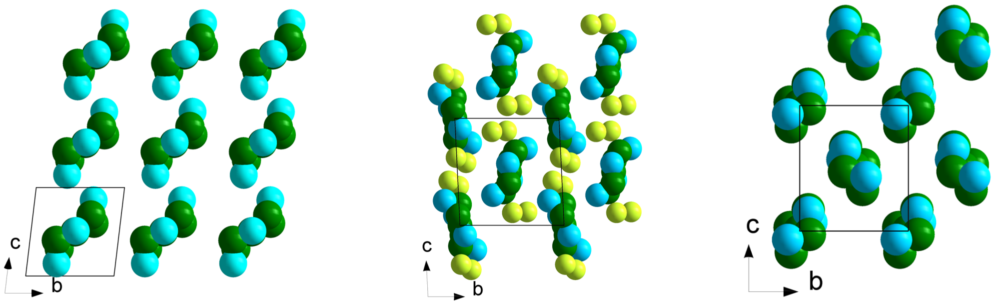

(a) Crystal structure of Cu4Ti5met

(b) Crystal structure of Cu4Ti5metS

(c) Crystal structure of Cu4Ti5prop

Figure 4.24: Comparison of the crystal structures of the three Cu/Ti clusters. Only metal atoms and solvent molecules in space filling mode are drawn.

are almost equal to that of the cluster without the methylene chloride, and differ only in the 0.01 Å range, as it is shown in Tab.A.27.

4.5.2 Propionic acid

The molecular structure of $Cu_4Ti_5O_6(OProp)_{16}$ (Fig. 4.25) is isostructural to the previous described Cu/Ti methacrylate cluster, apart of propionates coordinating instead of methacrylates. This does not affect the metal-metal distances and the metal-oxygen bond lengths according to Tab. A.27.

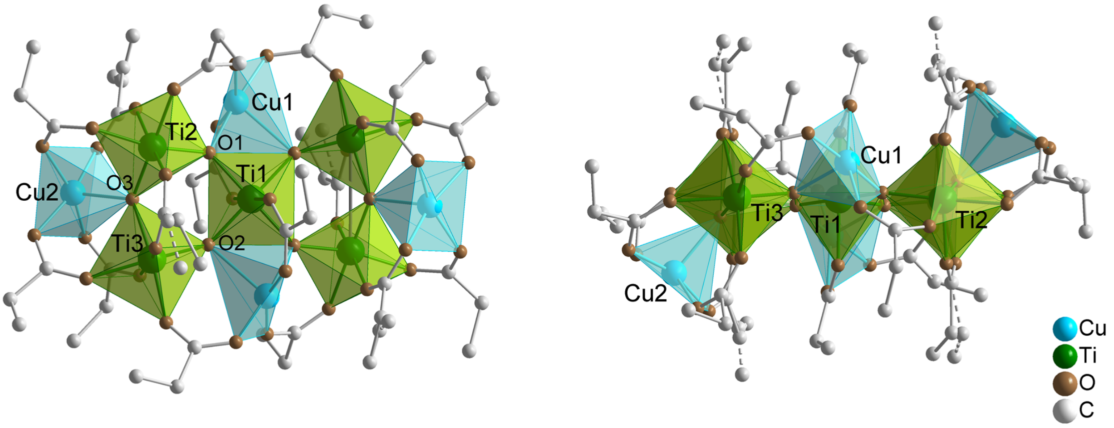

Figure 4.25: Molecular structure of $Cu_4Ti_5(\mu_3\text{-}O)_6(\mu_2\text{-}OProp)_{16}$. Hydrogen atoms are omitted for clarity. Disordered parts are drawn with dashed bonds.

Two molecular units are crystallising in the unit cell, as shown in Fig. 4.24. But due to the higher symmetry of the unit cell, these two clusters are symmetrically equivalent. The orientation of these two clusters is related to the 2_1 axis of the monoclinic space group $P2_1/c$.

4.6 Iron and Titanium

The reaction of 1 mmol of Fe(OAc)$_2$ and 2 mmol of Ti(O^{i}Pr)$_4$ with 17 mmol of methacrylic acid resulted after two weeks in redish-brown crystals of FeTi$_5$O$_4$(O$^{\mathrm{i}}$Pr)$_4$(OMc)$_{10}$. Fe^{2+} and Ti^{4+} have similar bonding characteristics with oxygen. Therefore the distinction between these two elements in the crystal structure is ambiguous. To have a proof for the incorporation of both metals, the crystals were washed with dry n-heptane and their metal content was checked with EDX. Both, Fe and Ti were found in the crystals.

The Ti^{4+} ion radius is 0.605 Å [167]. Fe^{2+} in octahedral coordination can be in high spin state or in the low spin state. The ion radius in the high spin state is 0.78 Å and that in low spin state is 0.61 Å. It can be assumed that iron is in the low spin state as it coordinates to oxygen in the cluster and O^{2-} is only a weak ligand.

The cluster core of FeTi$_5$(μ_3-O)$_2$(μ_2-O)$_2$(μ_2-O$^{\mathrm{i}}$Pr)$_2$(O$^{\mathrm{i}}$Pr)$_2$(μ_2-OMc)$_{10}$ is nearly isostructural to that of flat Ti6 clusters (Sec. 1.7.3.2). The four inner Ti sites are partly substituted by Fe atoms. The Ti/Fe(1) site has an occupancy for Fe of 34% and Ti/Fe(2) 16% (Fig. 4.26).

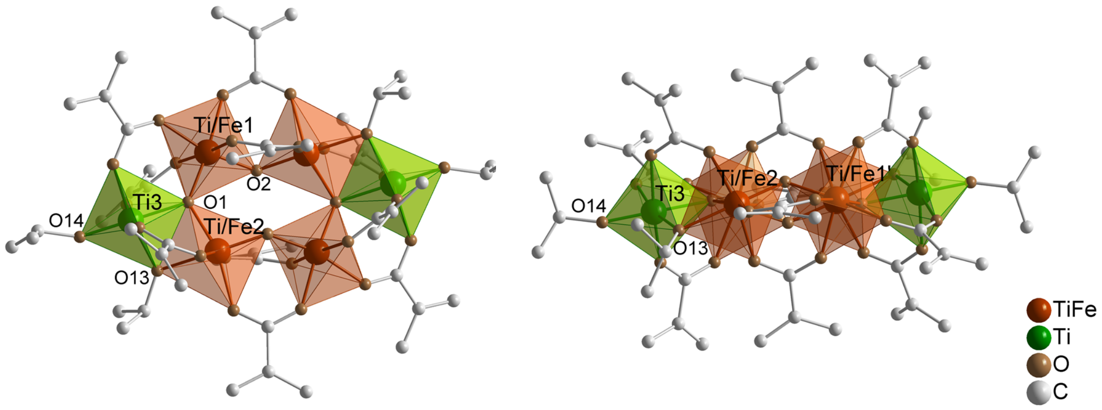

Figure 4.26: Molecular structure of FeTi$_5$(μ_3-O)$_2$(μ_2-O)$_2$(μ_2-O$^{\mathrm{i}}$Pr)$_2$(O$^{\mathrm{i}}$Pr)$_2$(μ_2-OMc)$_{10}$. Hydrogen atoms are omitted for clarity.

Due to the lower charge of the Fe^{+2} some modifications have to be made in the composition and coordination of the ligands. In the Ti6 cluster there were six terminal alkoxy groups, two on the outer Ti and one on one inner Ti. In FeTi5 one O^{i}Pr group is still coordinating to the outer Ti atom, but instead of the other two alkoxy groups, there is one methacrylate bridging the outer Ti and the mixed Fe/Ti(1) site. Hence every metal is now coordinated to each of the two neighbouring metal through two bridging ligands.

Tab.A.29 and Tab.A.30 show a comparison of the bond lengths and angles with Ti$_6$O$_4$(O$^{\mathrm{n}}$Pr)$_8$(OMc)$_8$ [78]. The M-O bonds and M-M distances are generally shorter in FeTi5 than in the Ti6 cluster. An exception are the distances to the bridging alkoxo group, the Fe/Ti(2)-O(13) bond is 0.5 Å longer than the according bond in Ti6, on the other hand the Ti(3)-O(13) bond is 1.902(3) Å and hence 0.6 Å shorter than in the Ti6 cluster.

4.7 Lanthanides

All clusters have been synthesised from $Ln(OAc)_3$, $Ti(O^iPr)_4$ and methacrylic acid.

4.7.1 LnTi4

This structure was obtained with La and Ce. The unit cell parameters, as well as the atom distances are almost equal for the La and the Ce structure. Bond lengths and angles will be discussed for the La compound (Tab. A.31).

Two clusters of $LnTi_4O_3(O^iPr)_2(OMc)_{11}$ crystallized in the unit cell, with space group $P\overline{1}$. One of the clusters showed disorder of the central Ln atom and one Ti atom, which also affected some of the ligands. Apart from this disorder the two clusters are equivalent in composition and coordination (Fig. 4.27 and Fig. 4.28). The crystallisation of two symmetrically non-related clusters resulted in an interesting crystal structure. According to Fig. 4.30 there are four different orientations of the cluster.

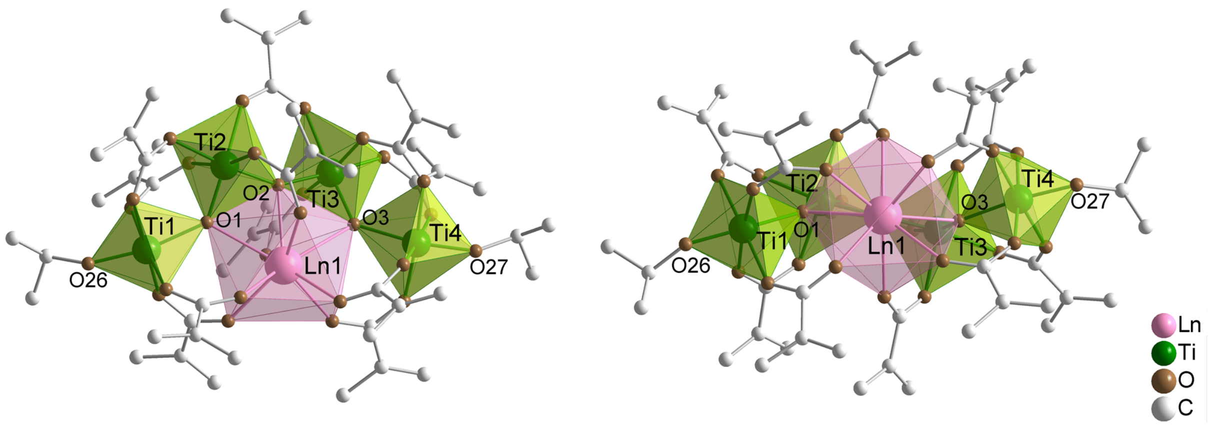

Figure 4.27: Molecular structure of $LnTi_4(\mu_3\text{-}O)_3(O^iPr)_2(\mu_2\text{-}OMc)_{11}$. Hydrogen atoms are omitted for clarity.

The cluster core consists of one lanthanide atom, surrounded by a semi-circle of four edge-sharing $[TiO_6]$ octahedra according to Fig. 4.27. The La distance to the two terminal Ti atoms Ti(1) and Ti(4) is much bigger than those of the centre Ti atoms (La(1)-Ti(1) 4.1282(6), La(1)-Ti(4) 4.0530(6), La(1)-Ti(2) 3.4489(5), La(1)-Ti(3) 3.4571(7) Å). The three μ_3-O linking the $[TiO_6]$ octahedra are also coordinating to the central lanthanide atom. Hence the two centre Ti atoms are corner-sharing with the $[LnO_9]$ coordination polyhedron, whereas the outer Ti atoms are only edge-sharing. All metal atoms and the core oxygen atoms are arranged almost in a plane. The torsional angle Ti(1)-Ti(2)-Ti(3)-Ti(4) is 60.25(3)°. While the Ti-O bond distance of the two centre Ti atoms Ti(2) and Ti(3) is of the shortest in the structure (Ti(2)-O(1) 1.790(2), Ti(2)-O(2) 1.825(2), Ti(3)-O(2) 1.841(2), Ti(3)-O(3) 1.779(2) Å) those of Ti(1) and Ti(4) are significantly larger (Ti(1)-O(1) 1.969(2), Ti(4)-O(3) 1.970(2) Å). The same applies for La, where La(1)-O(2) with 2.479(2) Å is about 0.2 Å shorter than La(1)-O(1) 2.641(2) and La(1)-O(3) 2.623(2) Å.

The lanthanide atom is not only held in place by the bridging core oxygen, but is additionally stabilised by ligands bridging to the Ti atoms. This results in an overall coordination number of 9 for Ln. The coordination polyhedron can be described as a square faced monocapped antiprism (SAPRS-9). [168]. Two methacrylates bridge Ln and each of the two terminal Ti atoms Ti(1) and Ti(4). They are arranged on both sides of the cluster core, the angle between the ligands and the plane being about 30°. The bond lengths of the metals to the oxygen atoms differ only slightly between 2.447(2) and 2.548(2) Å for La and between 1.925(2) and 1.977(2) Å for the two Ti atoms. La and the centre Ti(2) and Ti(3) are connected through one bridging methacrylate each. These two ligands are arranged on opposite sides of the cluster core, almost perpendicular to the plane. The bond distances are in the same range as before (La(1)-O(8) 2.545(2), La(1)-O(10) 2.558(2) Å; Ti(2)-O(9) 1.981(2), Ti(3)-O(11) 1.975(2) Å).

The cluster core is further stabilised by bridging methacrylates between Ti atoms. Two are coordinating Ti(1) and Ti(2) (Ti(3) and Ti(4) respectively), on both sides of the metal plane. One is almost perpendicular to the cluster core, the second is arranged in a much smaller angle. Only one methacrylate bridges between Ti(2) and Ti(3) is almost in the plane. The coordination sphere of Ti(1) and Ti(4) is completed by a O^{i}Pr ligand each. The Ti-O distances of these groups are the shortest in the structure, as it is typical for terminate alkoxy groups (Ti(1)-O(26) 1.782(2), Ti(4)-O(27) 1.774(2) Å).

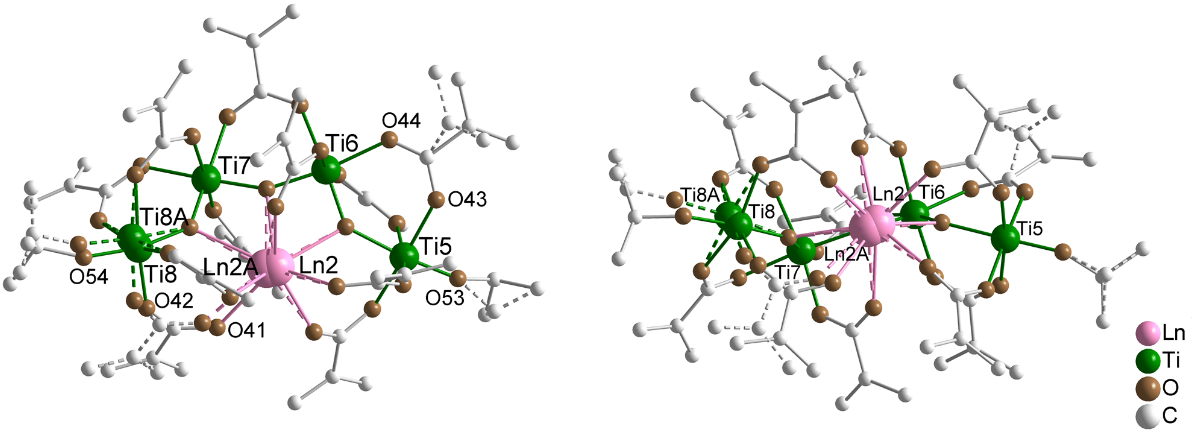

Figure 4.28: Molecular structure of the disordered second cluster in LnTi$_4$(μ_3-O)$_3$(O^{i}Pr)$_2$(μ_2-OMc)$_{11}$. Disordered parts are drawn with dashed bonds. Hydrogen atoms are omitted for clarity

In the second cluster the central Ln atom shows positional disorder according to Fig. 4.28. La(2A) is shifted from the original La(2) position 0.262(5) Å towards Ti(8), which is also disordered, the distance between Ti(8) and Ti(8A) is 0.412(8) Å. This also affects the methacrylate bridging La(2) and Ti(8), as well as the terminal alkoxy group on Ti(8). The occupancy of the main part is about 70%, and that of the second part 30%. Furthermore the ^{i}Pr group of the second alkoxy group on Ti(5) is disordered, as well as the C=CH$_2$(Me) group of the methacrylate bridging Ti(5) and Ti(6).

The structure can also be derived from previously described Sr2Ti8 and Pb2Ti8 clusters. In Sr$_2$Ti$_8$O$_8$(O^{i}Pr)$_2$(OAc)$_2$(OMc)$_{16}$ and Pb$_2$Ti$_8$O$_8$(O^{n}Bu)$_2$(OMc)$_{18}$(^{n}BuOH)$_2$, respectively, the two centre Sr/Pb atoms are surrounded by eight Ti atoms, arranged in a ring (Sec. 4.3.2). The Ln/Ti cluster described here can be seen as half of the Sr/Ti or Pb/Ti cluster.

4.7.2 Ln2Ti6

When the ratio of Ti:La is changed to higher proportions of La in the reaction mixture, a cluster with the composition La$_2$Ti$_6$O$_{62}$(OMc)$_{18}$(HO^{i}Pr) was obtained. This cluster was also synthesised with Ce and Nd. The bond lengths and cell parameters are again almost equal and will only be discussed for the La compound (Tab. A.32). The Ln atoms also showed positional disorder. The occupancy of the main part is 85% and the distance between La(1) and La(1A) is 0.27(3) Å.

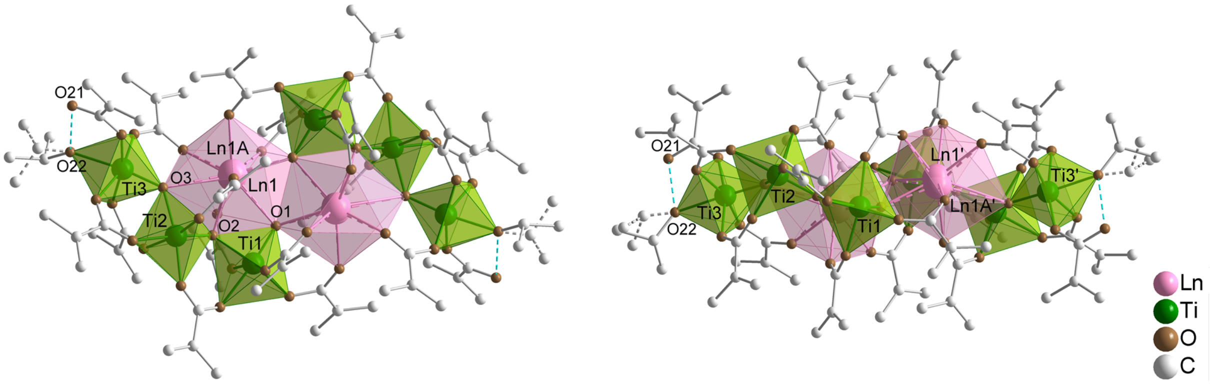

Figure 4.29: Molecular structure of Ln$_2$Ti$_6$(μ_3-O)$_6$(μ_2-OMc)$_{18}$(HO^{i}Pr)$_2$. Hydrogen atoms are omitted for clarity. Blue dashed lines indicate hydrogen bonds.

In Ln$_2$Ti$_6$O$_6$(μ_2-OMc)$_{18}$(HO^{i}Pr)$_2$ two [LnTi$_3$O$_2$] units are connected through two μ_3-O. The [LnTi$_3$O$_2$] units are equivalent, due to an inversion centre. Within this unit each Ln is surrounded by a chain of three edge-sharing [TiO$_6$] octahedra (Fig. 4.29). The core oxygen atoms linking the Ti are also coordinating to the Ln atom. The Ln-Ti distance is increasing from Ti(1) to Ti(2) and Ti(3). Whereas the Ln-Ti(1) distance is 3.4567(15)Å, that of Ti(3) is almost 1 Å larger (La(1)-Ti(3) 4.3801(19), La(1)-Ti(2) 3.6557(18)Å). The Ti(1) and Ti(2) coordination octahedra are edge-sharing with the Ln coordination polyhedra. Ti(2) is connected to the Ln atom by two μ_3-O (O(2) and O(3)) and Ti(1) is connected by O(2) and O(1). O(1) coordinates also to Ln(1)' and therefore links the two [LnTi$_3$O$_2$] units. Ti(3) connects only through O(3) to the Ln atom, but the La(1)-O(3) distances is already very long with 3.0454(34) Å (La(1)-O(1) 2.538(3), La(1)-O(1)' 2.552(3), La(1)-O(2) 2.526(3) Å). The Ti-O bond lengths also differ widely. Each Ti has one very short bond to a core oxygen atom (Ti(1)-O(1) 1.705(3), Ti(2)-O(2) 1.743(3), Ti(3)-O(3) 1.742(3)), but the Ti(1)-O(2) and Ti(2)-O(3) bonds are more than 0.2 Å longer (Ti(1)-O(2) 1.987(3), Ti(2)-O(3) 1.976(3)Å). All metal atoms and the core oxygen atom lie on a slightly corrugated plane.

The cluster core is stabilised by several ligands. One methacrylate bridges the lanthanide atom and each Ti of the asymmetric unit. The lanthanide is additionally connected through two bridging methacrylates to Ti(1)' of the other asymmetric unit. The methacrylates bridging Ln(1)-Ti(1) and Ln(1)-Ti(2) are perpendicular to the cluster core plane and on opposite sides of it, while the one bridging Ln(1) and Ti(3) is coplanar (La(1)-O(4) , La(1)-O(10) 2.545(4), La(1)-O(12) 2.458(4) , Ti(1)-O(5) 2.004(3) , Ti(2)-O(11) 1.954(3), Ti(3)-O(13) 1.944(4) Å). The two methacrylate ligands linking Ln(1) and Ti(1)' are also arranged on opposite sides of the cluster core plane (La(1)-O(6) 2.482(4), La(1)-O(8) 2.496(4), Ti(1)'-O(7) 1.977(3), Ti(1)'-O(9) 1.990(3) Å). One coplanar methacrylate bridges Ti(1) and Ti(2), while two are bridging Ti(2) and Ti(3), one axial and the other coplanar to the cluster core plane. The Ti(1)-O(14) bond length is quite long with 2.185(3) Å, but all the other Ti-O bonds are in the expected range between 1.974(4) and 2.101(3) Å.

The two remaining coordination sites on Ti(3) are occupied with an alcohol ligand and a methacrylate. Due to the strict octahedral coordination of Ti it is almost impossible for the methacrylate to chelate the Ti. Such coordination would cause too much stress on the bonds in the carbonyl group. Questions always arise on the localisation of the hydrogen, and whether it is an alcohol and a methacrylate coordinating, or the opposite. Sometimes the hydrogen atom can be identified in the electron density map, but often this is not possible especially in large structures. This was also the case in this structure but the large Ti(3)-O(22) distance of 2.158(4) Å indicates that the hydrogen atom is closer to the alkoxy group than the methacrylate group. Hydrogen bonds are then stabilising the η_1-methacrylate (O(22)$\cdots$O(21) 2.653(7) Å).

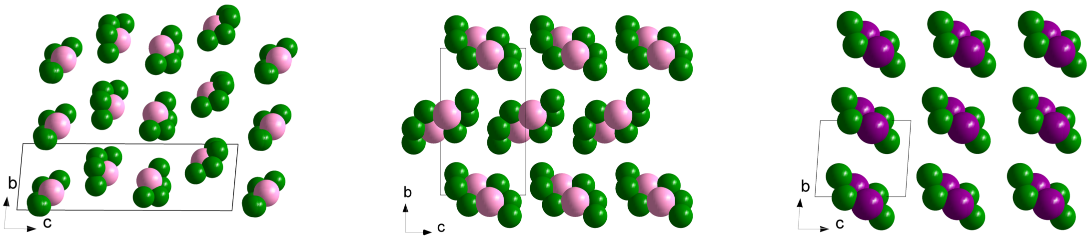

(a) LnTi4 (b) Ln2Ti6 (c) Ln2Ti4

Figure 4.30: Comparison of the crystal structure of the three different Ln/Ti clusters

4.7.3 Ln2Ti4

Continuing the lanthanide series, another cluster type was obtained. $Ln_2Ti_4O_4(OMc)_{14}(HOMc)_2$ is isostructural to the reported Y/Ti cluster obtained by Jupa et al. $Y_2Ti_4O_4(OMc)_{14}(HOMc)_2$ [116]. The cluster was obtained with Sm, Eu, Gd and Ho. Their bond lengths and angles are almost equivalent, therefore only those of the Eu compound are discussed. The lanthanide atom is again disordered, with occupancy of 66% for the main part. The distance between Eu(1) and Eu(1A) is 0.247(7) Å.

The structure resembles that of the previous described Ln2Ti6 cluster. When two outer Ti atoms are removed, the core of the Ln2Ti4 cluster is obtained. Compared to Ln2Ti6, the cluster core in less buckled (Fig. 4.31). This cluster has as well an inversion centre, the asymmetric unit contains one Ln and two Ti atoms. The two [TiO_6] octahedra are corner-sharing, with Ti(1)-O(2) 2.022(2) being almost 0.3 Å greater than Ti(2)-O(2) 1.733(3) Å. This oxygen atom bonds also to the central Ln(1) (Eu(1)-O(2) 2.491(3) Å). The other core oxygen atom bridges Ti(1), Ln(1) and Ln(1)' (Ti(1)-O(1) 1.718(2), Eu(1)-O(1) 2.319(3), Eu(1)'-O(1) 2.457(4) Å). Hence, only the Ti(1) coordination octahedron is edge-sharing with the Ln coordination polyhedron. The Ln(1)-Ti(2) distance is also much longer than the Ln(1)-Ti(1) distance and even larger than in the Ln2Ti6 cluster (Eu(1)-Ti(1) 3.302(2) Å, Eu(1)-Ti(2) 3.780(3) Å).

The removal of one Ti affects also the ligand sphere. There is still one methacrylate bridging Ln(1) and Ti(1) (Eu(1)-O(7) 2.343(2), Ti(1)-O(8) 1.992(2) Å), but two between Ln(1) and Ti(2). One of them is perpendicular to the cluster core plane (Eu(1)-O(9) 2.341(4), Ti(2)-O(10) 1.987(3) Å), the other coplanar (Eu(1)-O(11) 2.282(4), Ti(2)-O(12) 1.981(3) Å). Two methacrylates are bridging Ln(1) and Ti(1)', one lying in the cluster core plane (Eu(1)-O(3) 2.368(3), Ti(1)'-O(4) 1.958(2) Å), the other almost perpendicular (Eu(1)-O(5) 2.464(3), Ti(1)'-O(6) 2.019(2) Å). One methacrylate bridges the two Ti atoms (Ti(1)-O(13) 2.128(2), Ti(2)-O(14) 1.991(3) Å).

The coordination sphere of Ti(2) is completed by two η_1-methacrylates. One of the methacrylates is protonated at the non-coordinated oxygen, showing strong hydrogen bonds to the neighbouring methacrylate (Ti(2)-O(15) 2.140(2), Ti(2)-O(17) 1.974(3)Å) The position of the hydrogen atom was calculated. Because the Ti(2)-O(15) distance is about 0.15 Å longer than that

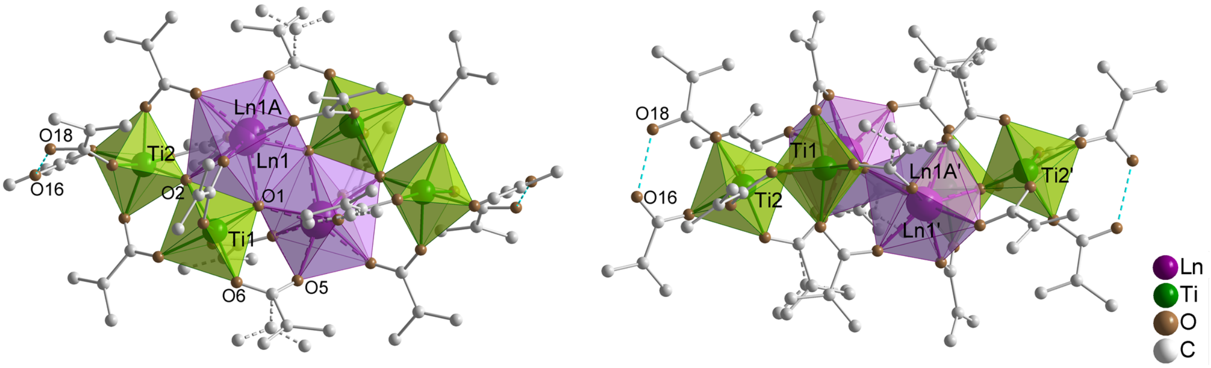

Figure 4.31: Molecular structure of $Ln_2Ti_4(\mu_3\text{-}O)_4(\mu_2\text{-}OMc)_{12}(\eta_1\text{-}OMc)_2(\eta_1\text{-}HOMc)_2$. Hydrogen atoms are omitted for clarity. Blue dashed lines indicate hydrogen bonds.

of Ti(2)-O(17) and therefore weaker, it is more likely that the hydrogen atom is close to O(16) (O(16)$\cdots$O(18) 2.454(8) Å).

4.7.4 Comparison of the lanthanide clusters

The structure of the Ln-Ti clusters depends strongly on the ionic size of the lanthanide. Tab 4.1 compares the ionic size with the obtained cluster core.

Table 4.1: Comparison of the cluster type depending on coordination characteristics. CN = Coordination number.

Metal ion	CN	Ionic radius [Å]	M-O distance [Å]	Cluster core
La^{3+}	9	1.216	2.45 - 2.61	$LaTi_4O_3$
Ce^{3+}	9	1.196	2.42 - 2.62	$CeTi_4O_3$
La^{3+}	8	1.160	2.46 - 2.55	$La_2Ti_6O_6$
Ce^{3+}	8	1.143	2.41 - 2.53	$Ce_2Ti_6O_6$
Nd^{3+}	8	1.109	2.38 - 2.51	$Nd_2Ti_6O_6$
Sm^{3+}	8	1.079	2.32 - 2.51	$Sm_2Ti_4O_4$
Eu^{3+}	8	1.066	2.32 - 2.49	$Eu_2Ti_4O_4$
Gd^{3+}	8	1.053	2.27 - 2.51	$Gd_2Ti_4O_4$
Ho^{3+}	8	1.015	2.28 - 2.52	$Ho_2Ti_4O_4$
Y^{3+}	8	1.019	2.28 - 2.55	$Y_2Ti_4O_4$

Chapter 5

Structures of Mixed Metal Clusters with Zirconium

5.1 Zirconium and Silver

Reaction of Ag(OAc) with $Zr(O^nBu)_4$and methacrylic acid at room temperature lead to colourless crystals of $Ag_2Zr_8O_6(hmp{-}H)_2(hmp)_2(OMc)_{16}(HOMc)_2$ ($hmpH_2$ = 2-hydroxy-2-methylpropionic acid). In all clusters described above the methacrylate units were incorporated unchanged in the clusters. This was not the case in this Zr/Ag cluster.

The centrosymmetric cluster $Ag_2Zr_8O_6(hmp{-}H)_2(hmp)_2(OMc)_{16}(HOMc)_2$ crystallised with one hydrogen-bonded butanol and methacrylic acid molecule in each asymmetric unit (see Fig. 5.1). This methacrylic acid is disordered over two sites.

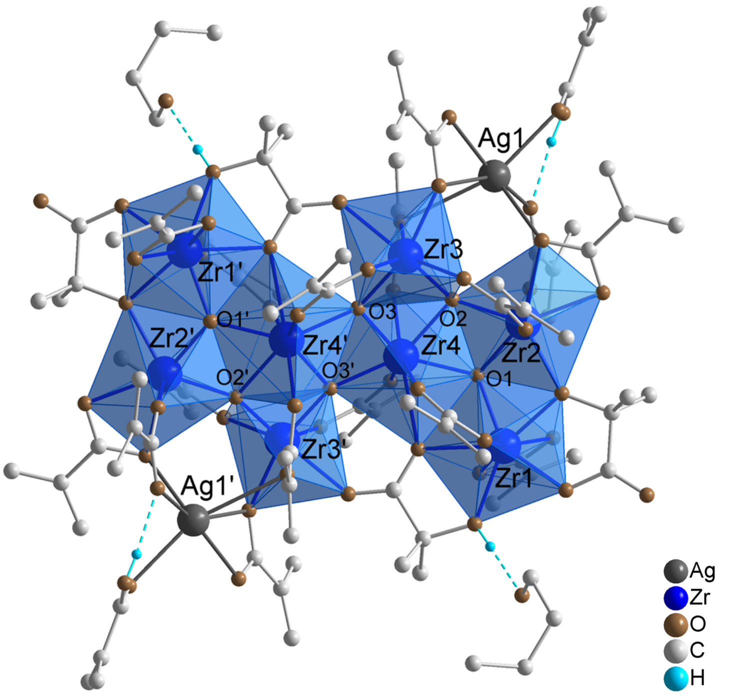

Figure 5.1: $Ag_2Zr_8(\mu_3\text{-}O)_6(\mu_3\text{-hmp}{-}H)_2(\mu_2\text{-hmp})_2(\mu_2\text{-OMc})_{16}(\eta_1\text{-HOMc})_2 \cdot 2\,BuOH \cdot 2\,HOMc$ (hmpH2 = 2-hydroxy-2-methyl- propionic acid). Only hydrogen atoms of OH groups are drawn.

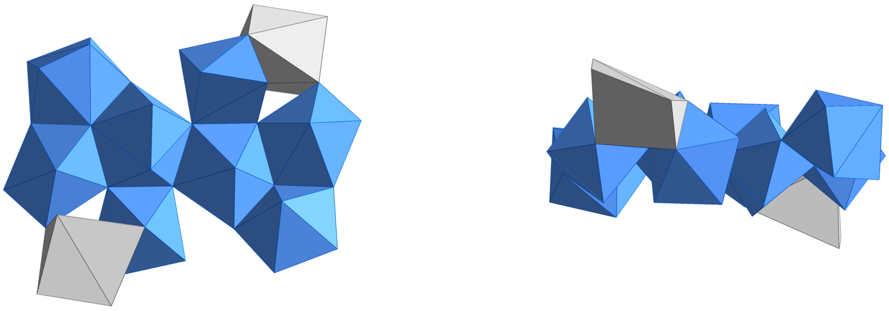

Figure 5.2: Metal coordination spheres in $Ag_2Zr_8O_6(hmp{-}H)_2(hmp)_2(OMc)_{16}(HOMc)_2$.

The Zr_8O_6 cluster core represents a new structural motif and can be described as a nearly planar arrangement of six condensed $[Zr_3(\mu_3\text{-}O)]$ units (Fig. 5.2). Two of the Zr_3O triangles are nearly planar (sum of O-Zr-O angles around O(2): 357.8°, around O(3): 359.0°) while the third is slightly pyramidal (sum of O-Zr-O angles around O(1) 341.2°). Each Zr3O unit is an isosceles triangle with two shorter (3.3361(6) - 3.4051(8) Å) and one longer $Zr\cdots Zr$ distances (3.6019(7) - 3.8859(6)Å). As a consequence, the Zr-O distances within the triangles range between 2.009(3) and 2.210(3) Å. The coordination numbers are 7 for Zr(3) and 8 for Zr(1), Zr(2) and Zr(4). Two OMc ligands are chelating Zr(1) (Zr(1)-O(24) 2.227(3), Zr(1)-O(25) 2.274(3) Å), six bridge two Zr atoms with bond lengths between 2.144(3) and 2.207(3) Å. The remaining methacrylates are all coordinating to silver.

Silver is located on the edge of the cluster, connected to the cluster core only through methacrylate ligands (see Fig. 5.3(a)). Ag and Zr(2) are connected through a bridging OMc ligand (Zr(2)-O(13) 2.076(3), Ag-O(12) 2.346(3) Å) and a chelating-bridging OMc ligand (Zr(2)-O(11) 2.254(3), Zr(2)-O(10) 2.324(3), Ag-O(10) 2.440(3) Å). Ag and Zr(3) are connected through a bridging OMc ligand (Zr(3)-O(15) 2.101(3), Ag-O(14) 2.289(3)Å) which exhibits an additional weak interaction between O(15) and the Ag ion (Ag-O(15) 2.839(3) Å). Another OMc ligand bridges Zr(3) and Zr(4) (Zr(3)-O(22) 2.230(3), Zr(4)-O(23) 2.186(3) Å) and additionally coordinates weakly to Ag through O(22) (Ag-O(22) 2.760(3) Å). The very distorted octahedral coordination of Ag is completed by coordination of an η_1-coordinated methacrylic acid molecule which is stabilized by a hydrogen bond between the OH group of the acid and an oxygen atom of the adjacent OMc group, which bridges Zr and Ag ($O(27)\cdots O(12)$ 2.722(4) Å). The hydrogen atom was located from a difference Fourier map.

The most remarkable feature of this cluster is the presence of 2-oxy- and 2-hydroxy-2-methylpropionate ligands (hmpH and hmp). The dianion of 2-hydroxy-2-methylpropionic acid (hmp) connects Zr(1) and Zr(2) as a bridging-chelating ligand (Fig.5.3(b)) (Zr(1)-O(7) 2.124(3), Zr(1)-O(9) 2.190(3), Zr(2)-O(9) 2.146(2) Å). The C(5)-O(8) distance of 1.236(5) Å clearly shows that this is a non-coordinated C=O group. Because of the bridging situation of trigonal planar O(9), the C(6)-O(9) distance is relatively long (1.448(5) Å). This is a rather unusual coordination of the dianion of a 2-hydoxycarboxylic acid. The dianion of 2-hydroxy-1-naphthoic acid in $Zr_6O_2(O^nPr)_{16}(OOC{-}C_{10}H_6O)_2(^nPrOH)_2$ is also a bridging-chelating ligand, but both oxygen atoms of the carboxy group are coordinated to the same Zr atom [99].

The singly deprotonated hmpH acts as a tetradentate ligand, connecting Zr(1), Zr(3) and Zr(4). O(4) of the carboxy group bridges Zr(1) and Zr(4) (Zr(1)-O(4) 2.255(3), Zr(4)-O(4) 2.493(2) Å). The second oxygen atom of the carboxy group coordinates to Zr(3) (Zr(3)-O(5)

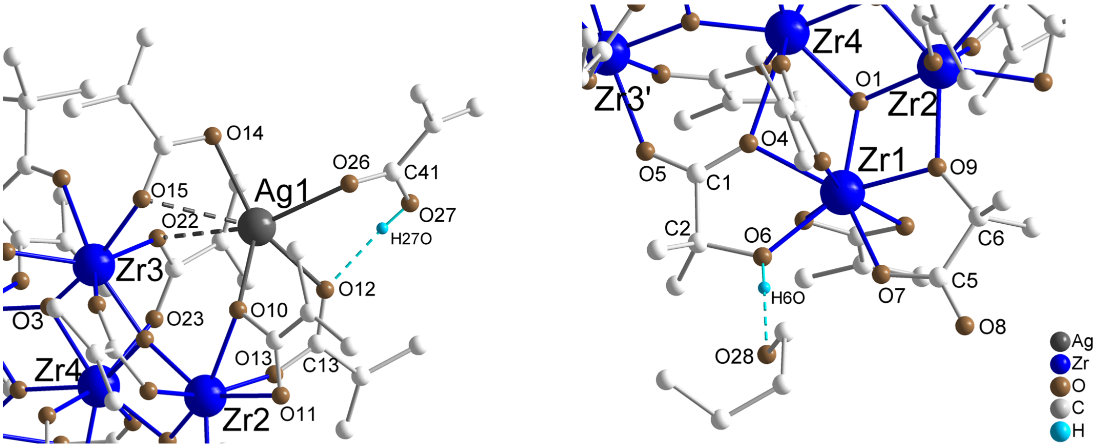

(a) Coordination sphere of Ag

(b) Coordination sphere of the hmp-H and hmp ligand

Figure 5.3: Details of the molecular structure of Ag2Zr8. Long Ag-O bonds are drawn with broken bonds.

2.257(3) Å). The oxygen atom of the hydroxo group O(6) is coordinated to Zr(1), with a bond distance of 2.231(3) Å, thus forming a five-membered metallacycle. The same bonding of a 2-hydroxy-carboxylate ligand (in its di-anionic form, however) was previously observed in $Zr_{10}O_6(OH)_4(OOC{-}C_6H_4OH)_8(OOC{-}C_6H_4O)_8$ which was prepared from $Zr(O^nPr)_4$and salicylic acid [99]. The hydrogen atom H(6o) was located in a difference Fourier map (O(6)-H(6o) 0.84(2) Å). It is hydrogen-bonded to the oxygen atom of the free butanol in the crystal (O(6)$\cdots$O(28) 2.591(4) Å). Both metallacycles, formed by the 2-(hydr)oxo-2-methylpropionate ligands with Zr(1), are almost coplanar. In the hmp and hmp-H ligand the C-C distances of the CH_3 groups are lengthened compared to the bonding situation in the methacrylic acid (C(2)-C(3) 1.524(6), C(2)-C(4) 1.517(6); C(6)-C(7) 1.512(6), C(6)-C(8) 1.527(6) Å).

To shed light on how the 2-hydroxy-2-methylpropionate ligands might be formed, the mother liquid was studied separately by NMR. The main signals were from unreacted methacrylic acid and butanol. In addition, small signals of butylmethacrylate and butylacetate were also identified. Formation of esters is a necessary requirement for the *in situ* generation of water. There was no indication of 2-hydroxy-2-methylpropionic acid or their anions, however, within the resolution of the NMR. This indicates that 2-hydroxy-2-methylpropionic acid is not formed in solution by addition of water to the double bond of methacrylic acid. Such reactions are catalysed by acids and give the Markownikov product. Alternatively, the 2-hydroxy-2-methylpropionate ligands might be formed in the coordination sphere of one of the involved metals, i.e. by the addition of Zr-OH groups to methacrylic acid or methacrylate ligands.

The formation of 2-hydroxy-2-methylpropionate ligands in this system is a unique observation. Although many methacrylate-substituted clusters of various metals have been prepared - for the reasons mentioned above - addition of an OH group to the methacrylate double bound was never observed before, even if the clusters contained OH groups, prominent examples being $Zr_6O_4(OH)_4(OOCR)_{12}$ clusters or their dimers [79]. This indicated that the silver ions play a crucial role, which is not understood yet.

Chapter 6

Structures of Monometalic Clusters

6.1 Monometallic Titanium Clusters

Not all reactions of metal alkoxides or metal acetates resulted in mixed-metal oxo cluster, also numerous monometalic clusters were identified in the samples. The structures of newly synthesised clusters is discussed in this chapter.

6.1.1 Ti6prop

A Ti6 cluster was obtained when 1 mmol of $Cr(acac)_3$ and 2 mmol of $Ti(O^iPr)_4$ were reacted with 12 mmol (0.898 g) of propionic acid. A Ti8prop ring was formed with higher proportion of $Cr(acac)_3$.

The cluster $Ti_6(\mu_3\text{-}O)_2(\mu_2\text{-}O)_4(O^iPr)_2(\mu_2\text{-}O^iPr)_{10}$ represents a new structure motif. Although several clusters with six Ti atoms are known in literature, this cluster is not isostructural to any of these. Two different structure types for Ti6 cluster are known (Sec. 1.7.3.2). In the first there are four core oxygen atoms and the cluster core is flat. The second type with six core oxygen atoms has a prismatic cluster core. Ti6prop has also six core oxygen atoms, but the cluster core is flat (Fig. 6.1).

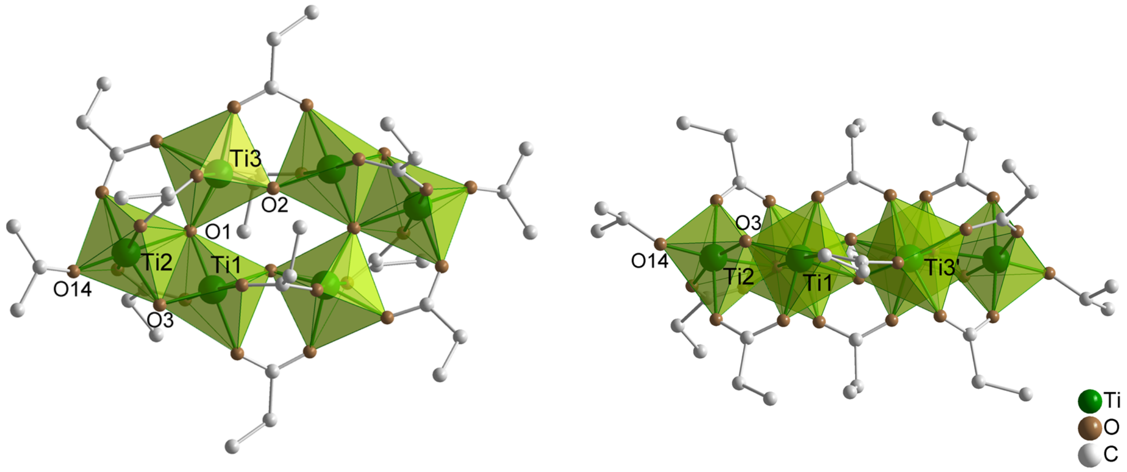

Figure 6.1: Molecular structure of $Ti_6(\mu_3\text{-}O)_2(\mu_2\text{-}O)_4(O^iPr)_2(\mu_2\text{-}O^iPr)_{10}$. Hydrogen atoms are omitted for clarity.

Compared to the flat $Ti_6O_4(OR)_8(OOCR,)_8$ cluster from literature, there is one core oxygen atom bridging these two Ti atoms, instead of one alkoxo group, which bridges the inner Ti(2) and the outer Ti(3) atom. The additional charge is compensated by the substitution of two terminal alkoxy groups on Ti(1) and Ti(2) with a propionate, bridging these two atoms. Hence there are now only two terminal alkoxy groups, which are coordinated to Ti(2).

The changes in the ligand sphere also affect some of the atom distances is the cluster. Tab. A.37-A.38 compares the bond lengths and angles of Ti6prop with $Ti_6O_4(O^nPr)_8(OMc)_8$ [78].

6.1.2 Ti6pivPB

This Ti cluster was identified as a side product in a sample containing 2 mmol $Ti(O^nPr)_4$, 2 mmol $Zr(O^nBu)_4$ and 18 mmol pivalic acid. The main product was the mixed-metal cluster Zr4Ti2pivnPr. When reproducing the experiment only Zr4Ti2pivnPr was identified.

The cluster $Ti_6(\mu_3\text{-}O)_2(\mu_2\text{-}O)_2(\mu_2\text{-}O^nBu)_2(O^nBu)_4(O^nPr)_2(\mu_2\text{-}OPiv)_8$ is isostructural to other Ti6O4 clusters with flat cluster core described in Sec. 1.7.3.2. There are two different OR ligands. One terminal alkoxy group on Ti(2) is a O^nPr group, all others are O^nBu groups (Fig.6.2). Some of the alkoxy and pivalate ligands showed positional disorder.

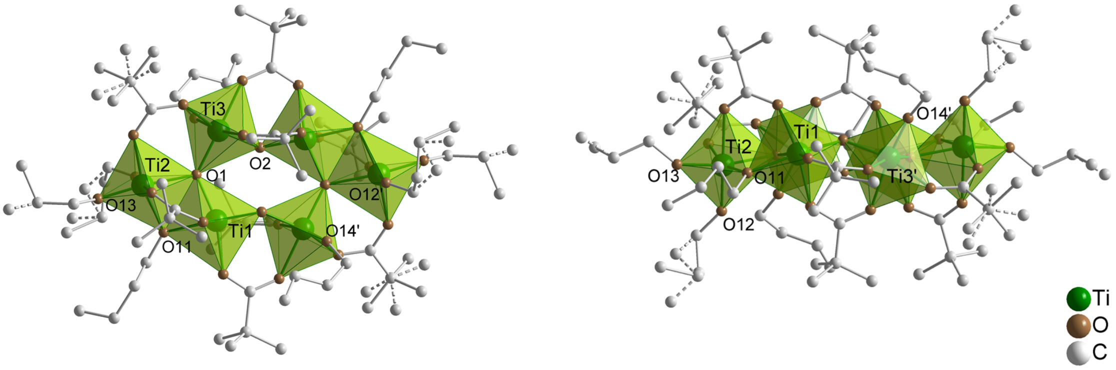

Figure 6.2: Molecular structure of $Ti_6(\mu_3\text{-}O)_2(\mu_2\text{-}O)_2(\mu_2\text{-}O^nBu)_2(O^nBu)_4(O^nPr)_2(\mu_2\text{-}OPiv)_8$. Disordered parts are drawn with dashed bonds. Hydrogen atoms are omitted for clarity.

6.1.3 Ti6pivBB

This Ti cluster was found in two samples containing 2 mmol $Ti(O^nBu)_4$, 1 mmol $Zr(O^nBu)_4$ and 13.5 mmol pivalic acid. It was also identified in one sample with a Ti:Zr:acid molar ratio 1:2:13.5, but Zr3Ti2piv was found when this experiment was repeated, which rearanged to Zr3Ti3piv after several months. A molar ratio of Ti:Zr:acid of 1:3:18 resulted in Zr6Ti8piv.

The cluster $Ti_6(\mu_3\text{-}O)_2(\mu_2\text{-}O)_2(\mu_2\text{-}O^nBu)_2(O^nBu)_6(\mu_2\text{-}OPiv)_8$ is isostructural to Ti6pivPB, with the exception that all OR ligands are replaced by O^nBu groups (Fig.6.3).

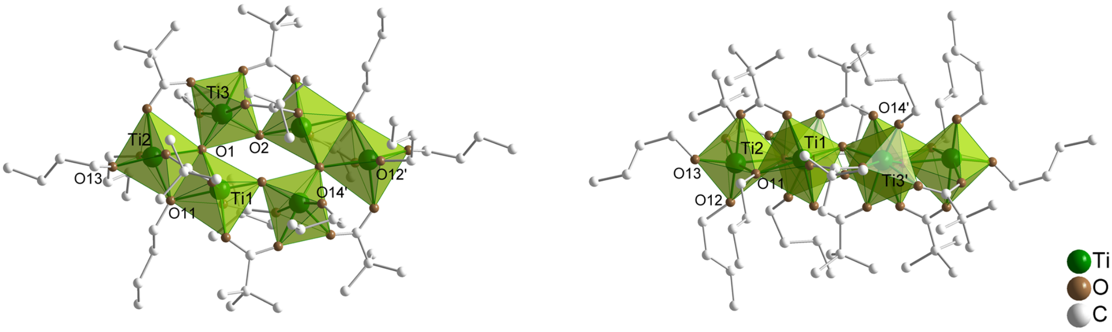

Figure 6.3: Molecular structure of $\mathrm{Ti_6(\mu_3\text{-}O)_2(\mu_2\text{-}O)_2(\mu_2\text{-}O^nBu)_2(O^nBu)_6(\mu_2\text{-}OPiv)_8}$. Disordered parts are drawn with dashed bonds. Hydrogen atoms are omitted for clarity.

6.1.4 Ti8prop

This cyclic Ti8 cluster was obtained from a sample of 1 mmol of Cr(acac)$_3$, 2 mmol of Ti(O^{i}Pr)$_4$ and 12 mmol (0.898 g). It was also found in a sample in which Zn(OAc)$_2$ or Cd(OAc)$_2$ was reacted with Ti(O^{i}Pr)$_4$ and propionic acid. In $\mathrm{Ti_8(\mu_2\text{-}O)_8(\mu_2\text{-}OProp)_{16}}$ the [TiO$_6$] octahedra are joined to a sixteen membered Ti-O ring (Fig. 6.4), as it was described for other Ti8O8 cluster (Sec. 1.7.4).

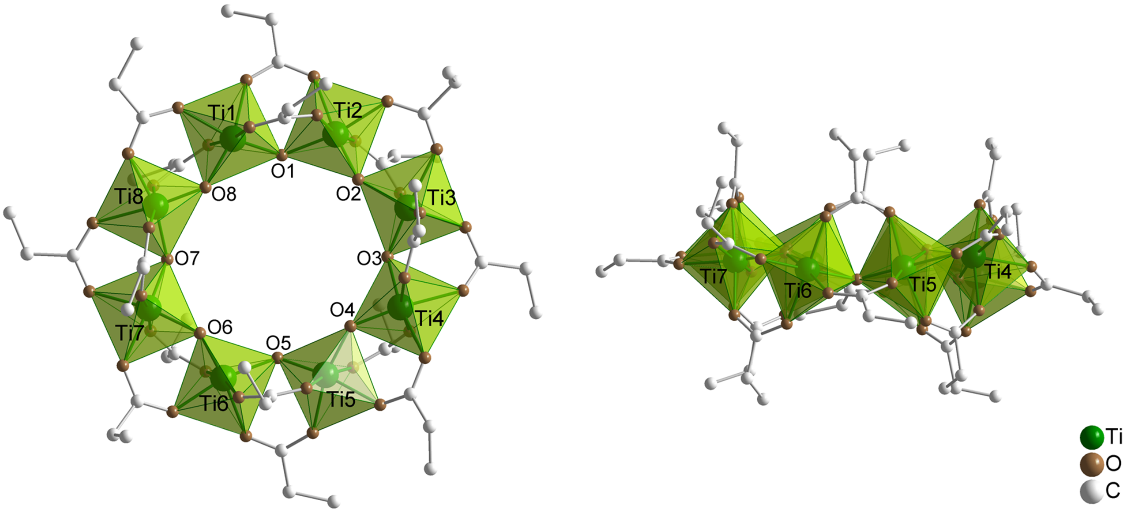

Figure 6.4: Molecular structure of $\mathrm{Ti_8(\mu_2\text{-}O)_8(\mu_2\text{-}OProp)_{16}}$. Hydrogen atoms are omitted for clarity.

6.2 Monometallic Zirconium Clusters

6.2.1 Zr4benz

Reaction of anhydrous FeCl$_2$ with Zr(O^{n}Bu)$_4$ and benzoic acid resulted in the formation of $\mathrm{Zr_4(\mu_3\text{-}O)_2(\mu_2\text{-}OBenz)_{10}(OBenz)_2}$ (Fig. 6.5). This cluster is isostructural to Zr$_4$O$_2$(OMc)$_{12}$ described by Trimmel et al. before [96].

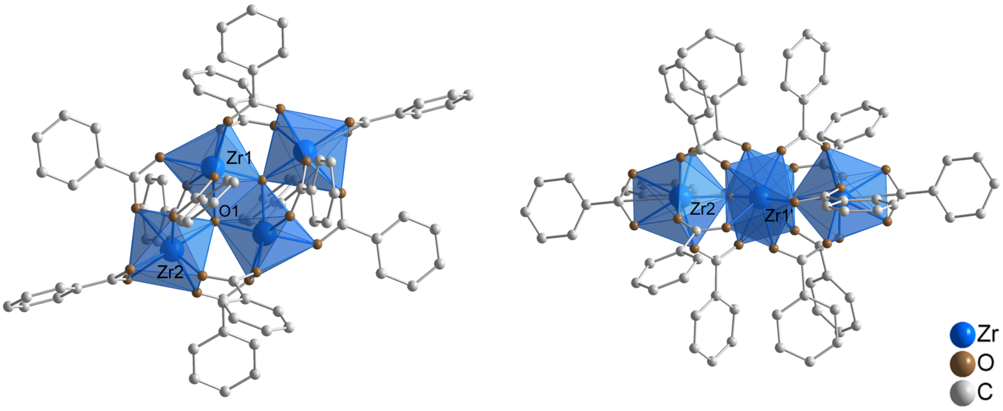

Figure 6.5: Molecular structure of $Zr_4(\mu_3\text{-}O)_2(\mu_2\text{-}OBenz)_{10}(OBenz)_2$. Hydrogen atoms are omitted for clarity.

6.2.2 Zr4piv

This monometallic cluster was obtained from a sample containing 1 mmol $Ti(O^iPr)_4$, 2 mmol $Zr(O^iPr)_4$ and 13.5 mmol pivalic acid. When repeating this experiment only the mixed-metal cluster ZrTi2piv was identified.

$Zr_4(\mu_3\text{-}O)_2(\mu_3\text{-}Piv)_2(\mu_2\text{-}OPiv)_8(OPiv)_2$ (Fig. 6.6) is isostructural to $Zr_4O_2(OMc)_{12}$ described by Kickelbick et. al. before [79].

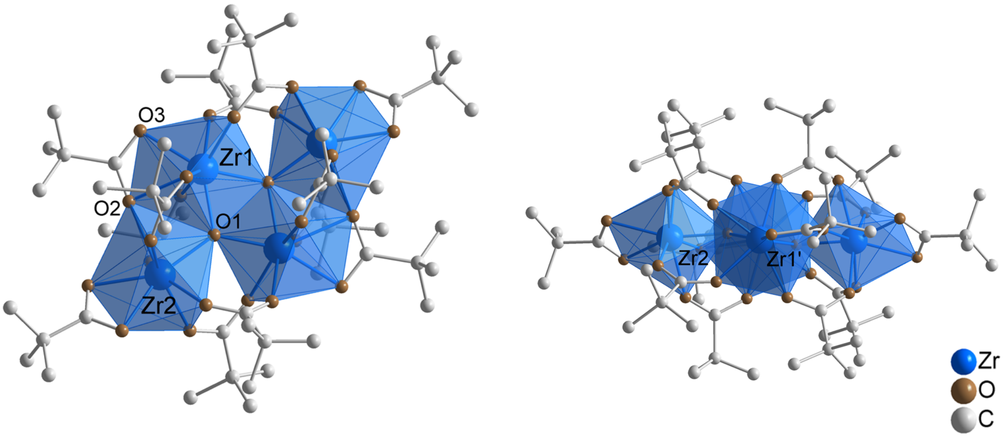

Figure 6.6: Molecular structure of $Zr_4(\mu_3\text{-}O)_2(\mu_3\text{-}OPiv)_2(\mu_2\text{-}OPiv)_8(OPiv)_2$. Hydrogen atoms are omitted for clarity.

6.2.3 Zr6piv

This cluster was the result of a reaction of 1 mmol $Ti(O^nPr)_4$, 2 mmol $Zr(O^nPr)_4$ with 13.5 mmol pivalic acid. It was the only cluster obtained from the combination of $Ti(O^nPr)_4$and $Zr(O^nPr)_4$.

$Zr_6(\mu_3\text{-}O)_4(\mu_2\text{-}O^nBu)_2(\mu_2\text{-}OPiv)_8(OPiv)_6$ represents a new structural motif (Fig. 6.7). A cluster core of Zr_6O_4 was not described in literature before. The structure of Zr6piv is actually closely related to the mixed Zr4Ti2met cluster (Sec.1.8), with has also four core oxygen atoms.

The cluster is a zig-zag chain of corner-sharing [ZrO_7] and [ZrO_8] polyhedra. The distance of adjacent Zr atoms are almost equal, between 3.2774(13) and 3.3921(14)Å. The core is slightly buckled, but the [$Zr_3(\mu_3\text{-O})$] units are almost flat, the sum of M-O-M angles is 355.6(9)° for O(1) and 354.7(9)° for O(2).

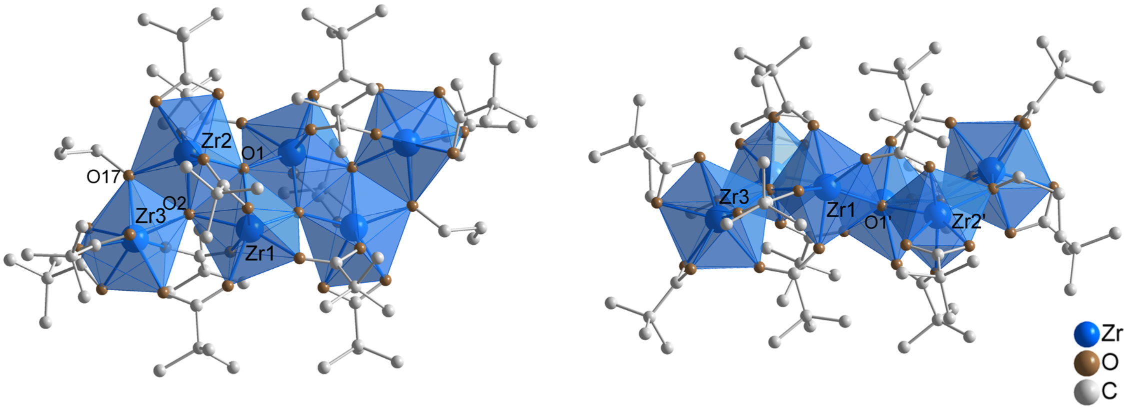

Figure 6.7: Molecular structure of $Zr_6(\mu_3\text{-O})_4(\mu_2\text{-O}^n\text{Bu})_2(\mu_2\text{-OPiv})_8(\text{OPiv})_6$. Hydrogen atoms are omitted for clarity.

One O^nPr group is bridging Zr(2) and Zr(3), all other ligands are pivalates. One pivalate is chelating Zr(2) and two are chelating Zr(3). The bond lengths of Zr-core oxygen atoms vary between 2.022(6) and 2.103(6) Å. The M-O distance of all bridging ligands are in the same range (Zr-OR 2.14; Zr-OPiv 2.126(7) - 2.218(6) Å). M-O bonds of chelating pivalates are typically longer, between 2.216(7) and 2.295(7) Å. All other bond lengths and angles are listed in Tabs. A.39 and A.40.

Chapter 7

Conclusions

Two main strategies were employed in order to synthesise new mixed-metal oxo clusters. The first are mixed Ti/Zr clusters, obtained by reacting Ti and Zr alkoxides with different carboxylic acids. The acid was always added in an excess (4 to 5 molar equivalents of acid per mol metal alkoxide). The kind of alkoxide was slightly varied (R = ^{i}Pr, ^{n}Pr and ^{n}Bu) as well as the metal/metal ratio.

The second task was to synthesise mixed-metal oxo cluster containing either Ti or Zr. Here the Ti or Zr alkoxide was mixed with metal acetates and few carboxylic acids, mainly methacrylic acid. The metal/acid ratio was again between 4 and 5 molar equivalents of acid per mol metal, whereas the kind of alkoxide and the metal/metal ratio were varied (up to 4 molar equivalents). The sources of the second metal were mainly their metal acetates. Few experiments were performed with other metal salts, i.e. $FeCl_2$ and $Cr(acac)_3$.

Synthesis was carried out mainly at room temperature, solvents were rarely used. The conclusions made here can only be applied for the given range of parameters.

A summary of all new mixed-metal oxo clusters obtained during the study is given in Tabs. 7.1 and 7.2.

The periodic table in Fig. 7.1 gives an overview on all tested element combinations. All elements marked green in combination with Ti resulted in mixed-metal oxo clusters, except for Ag which was the only element to give a cluster with Zr. The metals marked yellow were tested, but failed to give mixed-metal oxo clusters.

The clusters were mainly studied with regard to their molecular structure by single crystal X-ray diffraction. Some samples did not crystallise, but this does not necessarily mean that no clusters were obtained. This was, for example, the case for Ni and Co. For both metals clear solutions were obtained, i.e. the metal acetates dissolved completely, but no crystals were obtained. Their ionic size is close to that of Fe^{2+} and they usually have octahedral coordination sphere with oxygen atoms, hence it is likely that they react similar to Fe.

The metal acetates usually dissolved in the Ti alkoxide/acid solution. This worked for most metals, but not for Ba and Sc. Their acetates dissolved only poorly and even after several days of stirring the reaction mixture was a thick suspension. This is probably the major reason why those two metals failed to form mixed-metal oxo clusters.

Many mixed Mn/Ti alkoxides are known in the literature, hence it is likely that Mn and Ti are also able to form mixed oxo clusters. In this study only crystals of bad quality were obtained.

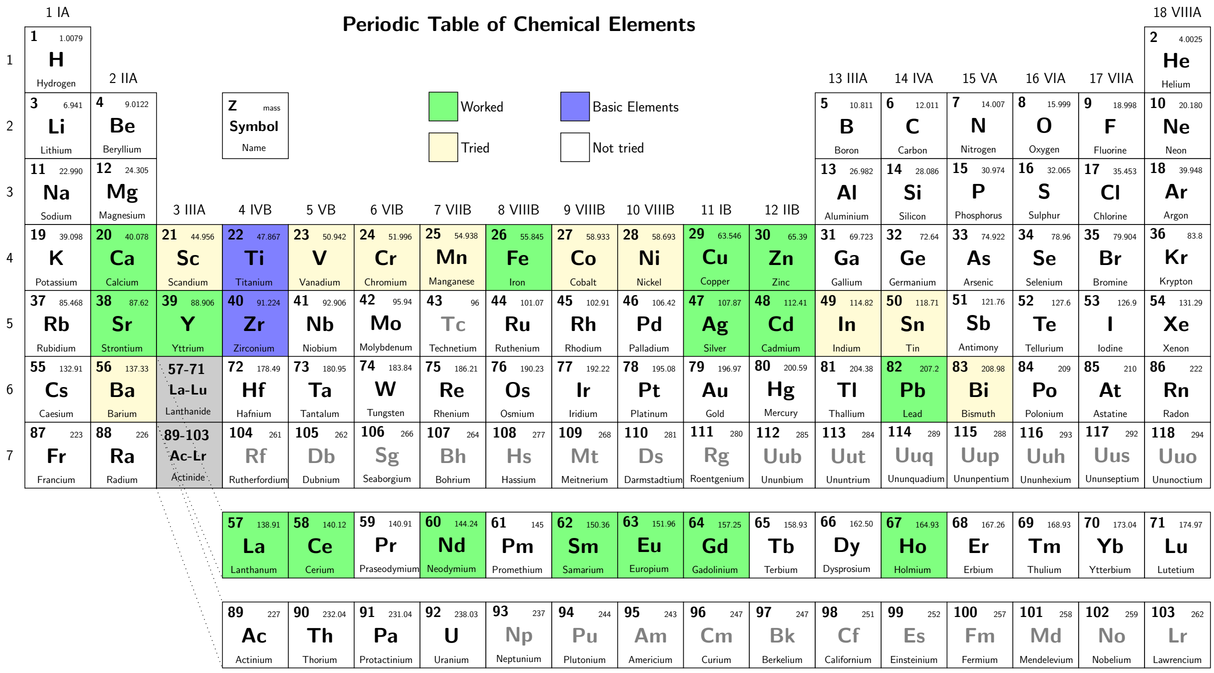

Figure 7.1: Green: Elements which gave mixed-metal oxo cluster with Ti or Zr. Yellow: Elements which gave no mixed metal oxo clusters. Blue: Basic elements Ti and Zr.

7.1 Metal Acetates

Metal acetates are an excellent source for mixed metal oxo clusters containing Ti. A large variety of new clusters was feasible. The advantages of metal acetates over other metal sources are undoubted. They exist for a large number of metals and are readily available. They are cheap in respect to the price of the pure metal. No precautions have to be taken when handling metal acetates, especially compared to metal alkoxides.

When synthesising new clusters from metal acetates no elevated temperatures are needed. Titanium alkoxides can be added without further modification. It is not necessary to use titanium alkoxide salts, or potassium salts, as for metal halides. There is no need to add solvents, because metal acetates usually dissolve in carboxylic acids. An excess of acetate is easily removed by filtration or through centrifugation. Hence, the number of compounds interfering with cluster formation or crystallisation is limited. Nevertheless adding solvents can improve crystal quality.

Most metal acetates contain crystal water or adsorbed water. The removal of this excess water is necessary because it would lead to too high condensation rates during the cluster synthesis and might hydrolyse the Ti alkoxides in advance, before they can react with the metal acetates or carboxylic acids in an uncontrolled manner.

7.2 Structure of the Obtained Clusters

7.2.1 Mixed Ti/Zr clusters

The structure of the cluster cores obtained with benzoic acid or derivatives thereof are isostructural to clusters with methacrylic acid. They all have a flat cluster core, in contrast to pivalate clusters with the same number of metal atoms. In pivalate clusters the six metal atoms are

Table 7.1: Summary of all mixed Zr/Ti oxo clusters obtained in this work. O/M = oxygen/metal ratio (degree of condensation), L/M = ligand/metal ratio.

O/M ((O+OH)/M)	L/M	compound
0.67	2.67	$\mathrm{Zr_4Ti_2O_4(O^nBu)_2(OBenz)_{14}}$
0.67	2.83	$\mathrm{Zr_4Ti_2O_4(OR)_{0.8}(OOCC_6H_4{-}^tBu)_{15.2}(HOOCC_6H_4{-}^tBu)}$
0.67	2.67	$\mathrm{Zr_2Ti_4O_4(O^nBu)_6(OOC{-}C_6H_4{-}CH_2Cl)_{10}}$
0.33	3.33	$\mathrm{ZrTi_2O(O^iPr)_4(OMc)_6}$
0.6	2.8	$\mathrm{Zr_3Ti_2O_3(O^nBu)_3(OPiv)_{11}}$
0.6	2.8	$\mathrm{Zr_2Ti_3O_3(O^nPr)_4(O^iPr)(OPiv)_9}$
0.83 (1.15)	2	$\mathrm{Zr_4Ti_2O_5(OH)_2(O^iPr)(OPiv)_{11}}$
0.83 (1.15)	2	$\mathrm{Zr_4Ti_2O_5(OH)_2(O^nPr)(OPiv)_{11}}$
0.83 (1.15)	2.13	$\mathrm{Zr_4Ti_2O_5(OH)_2(O^iPr)(OPiv)_{11}(HOPiv)}$
0.67 (1.15)	2.13	$\mathrm{Zr_3Ti_3O_4(OH)_3(O^nBu)_3(OPiv)_{10}}$
1.21 (1.36)	1.57	$\mathrm{Zr_6Ti_8O_{15}(OH)_4(O^nBu)_2(OPiv)_{20}(HOPiv)_2}$
1	2	$\mathrm{Zr_4Ti_3O_7(O^nBu)_2(OOCAda)_{12}}$

arranged in an octahedron. Flat cluster cores were also observed for pivalate clusters, but Zr2Ti3piv and Zr3Ti2piv are very unstable.

Pivalate clusters can be seen as a structural combination of monometallic Zr and Ti clusters. The characteristics of both, Ti and Zr clusters, can be identified in the mixed Ti/Zr pivalate clusters. The same is observed in the Ti/Zr cluster with adamantanecarboxylic acid.

7.2.2 Mixed metal oxo clusters containing Ti

The [$\mathrm{TiO_6}$] coordination polyhedron is retained in all obtained clusters. Although rational predictions on the formed cluster cores cannot be made, there was a tendency for cores containing six metal atoms. In clusters formed by Ti and divalent metals, the shape of the cluster cores can be derived from flat Ti6 cluster cores.

In most clusters the number of Ti atoms is higher than that of the second metal. Exceptions are only the Cd/Ti cluster, which contains more Cd atoms than Ti atoms, and Pb6Ti6 where the number of Pb and Ti atoms is equal.

All obtained cluster cores were centrosymmetric. Except for the large Pb/Ti clusters all cluster cores were flat. The lowest degree of condensation (oxygen to metal ratio) was obtained for Cd4Ti2 with 0.3, and the highest for the large Pb/Ti clusters Pb4Ti8Ac and Pb6Ti6 with 1.66 and 1.5, respectively. All other O/M ratios were between 0.6 and 0.8, which shows as well the relation to the Ti6 cluster with a flat cluster core, where the O/M ratio is 0.67.

The Ti8 ring was another recurring structural motive, as in Pb2Ti8, Pb2Ti6 or Sr2Ti8, or as an isolated cluster. The Ti8met ring was identified in samples of $\mathrm{Cu(OAc)_2}$, $\mathrm{Co(OAc)_2}$, $\mathrm{Bi(OAc)_3}$, $\mathrm{Sc(OAc)_3}$ and $\mathrm{Cr(acac)_3}$. The Ti8prop ring was obtained in $\mathrm{Zn(OAc)_2}$- and $\mathrm{Cr(acac)_3}$-containing samples.

Table 7.2: Summary of all mixed-metal oxo cluster containing Ti. CN = Coordination number, O/M = oxygen/metal ratio, L/M = Ligand/number of metal atoms.

Ion	CN	Ionic radius	O/M	L/M	compound
Ti^{4+}	6	0.605			
Zr^{4+}	7	0.78			
	8	0.84			
Zn^{2+}	4	0.6	0.67	1.67	$Zn_2Ti_4O_4(O^iPr)_2(OMc)_{10}$
Cd^{2+}	6	0.95	0.33	2.33	$Cd_4Ti_2O_2(OAc)_2(OMc)_{10}(HO^iPr)_2$
Ca^{2+}	7	1.06	0.67	2.00	$[Ca_2Ti_4O_4(OAc)_2(OMc)_{10}]_n$
	8	1.12	0.67	2.17	$[Ca_2Ti_4O_4(OAc)(OMc)_{11}(HOMc)]_n \cdot {}^nBuOH]_n$
Sr^{2+}	10	1.36	0.67	2.33	$[Sr_2Ti_4O_4(OMc)_{12}(HOMc)_2]_n$
	8	1.26	0.80	2.00	
	9	1.31			$Sr_2Ti_8O_8(O^iPr)_{1.73}(OAc)_{2.27}(OMc)_{16}$
Pb^{2+}	6+3	1.19 (1.35)	0.80	2.20	$Pb_2Ti_8O_8(O^nBu)_2(OAc)_{0.656}(OMc)_{17.354}({}^nBuOH)_2$
	6+3	1.19 (1.35)	0.80	2.20	$Pb_2Ti_8O_8(O^nBu)_2(OMc)_{18}(AllylOH)_2$
	6+4	1.19 (1.4)	0.80	2.20	$Pb_2Ti_8O_8(O^nPr)_2(OAc)_{0.484}(OMc)_{17.516}({}^nPrOH)_2$
	6+1	1.19 (1.23)			
	7+1	1.23 (1.29)	0.67	2.25	$Pb_2Ti_6O_5(O^iPr)_{2.76}(OMc)_{15.24}$
	6+1	1.19 (1.23)			
	7+1	1.23 (1.29)	0.67	2.25	$Pb_2Ti_6O_5(O^nPr)_3(OMc)_{15}$
	5		0.83	1.66	$Pb_4Ti_8O_{10}(O^iPr)_{18}(OAc)_2$
	6	1.19	0.75	1.50	$Pb_6Ti_6O_9(OAc)(OMc)_{17}$
Cu^{2+}	5	0.65	0.67	1.78	$Cu_4Ti_5O_6(OMc)_{16}$
			0.67	1.78	$Cu_4Ti_5O_6(OMc)_{16} \cdot 2\,CH_2Cl_2$
			0.67	1.78	$Cu_4Ti_5O_6(OProp)_{16}$
Fe^{2+}	6	0.61	0.67	2.23	$FeTi_5O_4(O^iPr)_4(OMc)_{10}$
La^{3+}	9	1.216	0.60	2.60	$LaTi_4O_3(O^iPr)_2(OMc)_{11}$
	8	1.16	0.75	2.50	$La_2Ti_6O_6(OMc)_{18}(HO^iPr)_2$
Ce^{3+}	9	1.196	0.60	2.60	$CeTi_4O_3(O^iPr)_2(OMc)_{11}$
	8	1.143	0.75	2.50	$Ce_2Ti_6O_6(OMc)_{18}(HO^iPr)_2$
Nd^{3+}	8	1.109	0.75	2.50	$Nd_2Ti_6O_6(HO^iPr)_2(OMc)_{18}$
Sm^{3+}	8	1.079	0.66	2.67	$Sm_2Ti_4O_4(OAc)_2(OMc)_{12}(HOMc)_2$
Eu^{3+}	8	1.066	0.66	2.67	$Eu_2Ti_4O_4(OAc)_2(OMc)_{12}(HOMc)_2$
Gd^{3+}	8	1.053	0.66	2.67	$Gd_2Ti_4O_4(OAc)_2(OMc)_{12}(HOMc)_2$
Ho^{3+}	8	1.015	0.66	2.67	$Ho_2Ti_4O_4(OAc)_2(OMc)_{12}(HOMc)_2$

7.3 Dependency of the Formed Cluster on Several Parameters

7.3.1 Kind of alkoxide

A dependency on the employed metal alkoxide was generally observed, but only for clusters containing OR groups. The kind of obtained Cu/Ti clusters is independent from the parent Ti alkoxide, because the clusters are pure carboxylate clusters and all alkoxo groups are substituted during the synthesis. The cluster core of Ca/Ti was the same, regardless of the used titanium alkoxide. For all other reactions different structures were obtained, when the Ti alkoxide was varied.

The greatest variety in the cluster core was observed for Sr. $Ti(O^iPr)_4$ and $Sr(OAc)_2$ lead to Sr_2Ti_8 based on the Ti8 cluster, whereas $Ti(O^nBu)_4$ resulted in the chain-like Sr_2Ti_4 cluster. The yield of reactions with $Ti(O^nBu)_4$ was very low and reactions with $Ti(O^nPr)_4$ did not lead to any crystals. The outcome of reactions with $Ti(O^nPr)_4$ is probably related to those of $Ti(O^nBu)_4$. Similarities of the shape of the two clusters, Sr2Ti8 and Sr2Ti4, are very hard to determine. It is interesting that $Sr(OAc)_2$ reacted like $Pb(OAc)_2$ with $Ti(O^iPr)_4$, but with $Ti(O^nBu)_4$ clusters like those obtained with $Ca(OAc)_2$ were formed.

$Ti(O^nBu)_4$ and $Pb(OAc)_2$ always resulted in Pb2Ti8, with a ring of eight Ti atoms, whereas with $Ti(O^iPr)_4$ two Ti atoms of the cluster core were missing in Pb2Ti6. With $Ti(O^nPr)_4$ both cluster types were obtained. This shows that the reactivity as well as the sterical hindrance of the O^nPr groups lies in between that of the O^iPr group and that of the O^nBu group.

For clusters with pivalate ligands a correlation of the used alkoxide was also generally observed. $M(O^iPr)_4$ resulted in smaller cluster cores than $M(O^nBu)_4$. ZrTi2piv was only obtained when $Ti(O^iPr)_4$ and $Zr(O^iPr)_4$ were used, but the large Zr6Ti8piv cluster resulted from a mixture of $Ti(O^nBu)_4$ and $Zr(O^nBu)_4$. Mixtures of different alkoxides gave clusters with 5 to 6 metal atoms. Although clusters with an octahedral Zr/Ti core were the most stable pivalate clusters, the alkoxide group was either O^iPr or O^nPr, but never O^nBu.

7.3.2 Kind of carboxylic acid

Most reactions were carried out with methacrylic acid, because it has a polymerisable group. The dependency on the acid was mainly studied for Ti and Zr.

Reactions with benzoic acid and benzoic acid derivatives resulted in the same cluster cores as with methacrylic acid. The sterical hindrance of the aryl groups is similar to that of methacrylate. Even ^tBu groups or Cl atoms on the phenyl ring had no influence.

Reactions with propionic acid always resulted in the monometallic Zr12 cluster [85], but with different crystal structures.

With pivalic acid mixed Ti/Zr clusters were also obtained. The structures of these can be seen as a combination of the monometallic clusters. For example, a M3 cluster or octahedral M6 clusters are known for Ti and Zr. The sterical hindrance of pivalate is very high, due to the structurally demanding ^tBu group. Reactions with adamantanecarboxylic acid also resulted in a mixed Ti/Zr clusters, with the main structural motive being a Zr3Ti3 octahedron. The degree of condensation is generaly higher for pivalate clusters and the adamantanecarboxylate cluster (Tab. 7.1).

The differences between propionic acid and methacrylic acid were also studied on Cu/Ti, Zn/Ti and Cd/Ti. Where for Cu/Ti and proponic acid the same cluster core was formed as with methacrylic acid, only the Ti cluster Ti8prop was identified for Zn and Cd.

7.3.3 Metal/metal ratio

All experiments were carried out with different metal ratios. Only for La and Ce a dependency on the formed cluster was observed. High Ti proportions resulted in LnTi4, whereas lower Ti proportions gave Ln2Ti6. In all other experiments only one cluster type was obtained. In general higher Ti proportions promoted crystal formation and quality. High metal acetate proportions often resulted in the formation of precipitate.

Only in the pivalic acid experiments different cluster types were observed for different Ti:Zr ratios. A real tendency depending on the Ti:Zr ratio cannot be seen, due to the complexity of the Ti/Zr/pivalic acid system.

7.3.4 Metal alkoxide/acid ratio

The metal/acid ratio was always kept between 4 and 5 molar equivalents acid per metal. Due to the variation in the metal acetate/metal alkoxide ratio the metal alkoxide/acid ratio also changed. Hence, conclusions for the metal/metal ratio can also be applied to the alkoxide/acid ratio, except for the Ti/Zr clusters, where the alkoxide/acid ratio was kept constant.

7.3.5 Conditions

Higher temperatures promote the substitution of alkoxo groups and acetate ligands. As the Cu-Ti clusters do not have any alkoxides of acetate ligands, the outcome of reactions at elevated temperatures was the same.

Heating $Pb(OAc)_2$ containing samples led to a completely new cluster core. Where the structure of clusters synthesised at room temperature could be derived from the Ti8 ring, it is a Pb/Ti sandwich structure for Pb6Ti6 which was made by heating the Ti alkoxide/ Pb acetate mixture. Nevertheless, the Ti atoms are again arranged in a ring, but a cyclic Ti6 ring is only known with N-methyl-2-oxy-2-methylproplamino-phenolat [169] and methyldiethoxoamine [170] as ligands. With carboxylic acids such a Ti6 ring can only be stabilised by additional metal atoms.

One of the two clusters which co-crystallised in Pb2Ti8 contains acetate ligands. Heating such a reaction micture one might expect that only the cluster Pb_2Ti_8 would be formed, but methacrylic acid was only added after heating, so the intermediate product of Pb6Ti6 is probably much different to Pb2Ti8 or Pb2Ti6.

7.3.6 Solvents

Reactions were mostly carried out without the addition of solvents. Only in the Zn and Cd samples CH_2Cl_2 was added, but both reactions where also carried out without solvents. For both metals, reactions with and without solvent lead to Zr_2Ti_4 and Cd_4Ti_2, respectively, but the presence of CH_2Cl_2 improved the crystal quality.

CH_2Cl_2 did not interfere with the formation of Cu/Ti clusters. When Cu_4Ti_5met was synthesised from $Cu(OMc)_2$, CH_2Cl_2 was present from the previous synthesis of copper methacrylate. The formed cluster was the same, only solvent molecules were incorporated into the crystal.

Most clusters are soluble in CH_2Cl_2. This is probably the reason why it has no effect on the cluster formation. Only the crystal structure can change due to the incorporation of solvent molecules.

Part III

Experimental

Chapter 8

Experimental Section

All experiments and measurements were carried out at Vienna University of Technology, Institute for Materials Chemistry, Group for Applied Inorganic Chemistry from November 2010 to Dezember 2013.

8.1 Synthesis

8.1.1 Procedure

All reactions were carried out under Ar atmosphere using standard Schlenk technique. Few syntheses were performed in an Ar glove box.

Liquid starting materials were weighted in by measuring their volume. First all solid starting materials (f.e. metal acetates) were weighted in and transfered to a dry Schlenk tube. The tube was then evacuated on the Schlenk line. Metals alkoxides were added with a syringe with Ar counter current flow. Then the carboxylic acid was added with a syringe and the reaction mixture was stirred for 1h up to 3 days.

Turbid solutions were either filtered with a syringe filter, or were centrifuged, to remove precipitates disrupting the crystalisation. The clear solutions were then kept undisturbed for crystallisation.

8.1.2 Starting materials

A list of all used chemicals, their purity and supplier are is given in Tab. 8.1.

Table 8.1: List of used Chemicals, their quality and supplier.

Chemical	**quality**	**supplier**
$Ti(O^iPr)_4$	97%	abcr
	≥97%	Aldrich
$Ti(O^nPr)_4$	≥97%	Aldrich
$Ti(O^nBu)_4$	98%	Aldrich
$Zr(O^iPr)_4 \cdot {}^iPrOH$	99.9% trace metal basis	Aldrich
$Zr(O^nPr)_4$	70 wt. % in 1-propanol	Aldrich
$Zr(O^nBu)_4$	80 wt. % in n-butanol	abcr, Aldrich
propionic acid	purum	Fluka
acrylic acid	99%, contains 180-200 ppm MEHQ*	Aldrich
methacrylic acid	99%, contains 250 ppm MEHQ*	Aldrich

Continued on next page

Chemical	**quality**	**supplier**
benzoic acid	99%	Sigma-Aldrich
4-(Cloromethyl)benzoic acid	95%	Aldrich
4-tBu-benzoic acid	99%	Aldrich
pivalic acid	99%	Sigma-Aldrich
adamantanecarboxylic acid	99%	Aldrich
$Ca(OAc)_2 \cdot H_2O$	99%	Fluka
$Sr(OAc)_2$	99.9%	Aldrich
$Ba(OAc)_2$	p.a.	Merck
$Sc(OAc) \cdot xH_2O$	99.9% trace metals basis	Strem
$Y(OAc) \cdot xH_2O$	99.9% metals basis	Aldrich
$La(OAc) \cdot xH_2O$	99.9% trace rare earth metals basis	Aldrich
$Ce(OAc) \cdot xH_2O$	99.9% trace metals basis	Aldrich
$Nd(OAc) \cdot xH_2O$	99.9%	Aldrich
$Sm(OAc) \cdot xH_2O$	99.9%	Aldrich
$Eu(OAc) \cdot xH_2O$	99.9%	Aldrich
$Gd(OAc) \cdot xH_2O$	99.9%	abcr
$Ho(OAc) \cdot xH_2O$	99.9%	abcr
$(OAc)_7Cr_3(OH)_2$	unknown	Strem
$Cr(acac)_2$	97%	Aldrich
$Mn(OAc)_2 \cdot 4\,H_2O$	99+%	Aldrich
$Fe(OAc)_2$	99.99%	Aldrich
$FeCl_2$	98%	Strem
$Co(OAc)_2 \cdot 4\,H_2O$	98+%	Aldrich
$Ni(OAc)_2 \cdot 4\,H_2O$	98%	Aldrich
$Cu(OAc)_2 \cdot H_2O$	$\geq$ 99.0 %	Fluka
Ag(OAc)	98%	Aldrich
$Zn(OAc)_2 \cdot H_2O$	p.a.	Fluka
$Cd(OAc)_2 \cdot H_2O$	99%	Merck
$In(OAc)_3 \cdot xH_2O$	99.9% trace metals basis	Aldrich
$SnCl_2$	98%	Aldrich
$Pb(Oac)_2 \cdot 2\,H_2O$	99.5%	Merck
$Bi(Oac)_3$	99.99% trace metals basis	Aldrich
$LiNMe_2$ preparation	5 wt% in hexane	Aldrich
KO^tBu	97%	Alfa Aesar

* MEHQ = 4 – Methoxyphenol

8.2 Instruments, Data Collection Strategies and Analysis Software

8.2.1 Single crystal X-ray diffraction

Single crystals were selected under a polarizing microscope and fixed on a glass or silica fibre with a cyanoacrylate based glue.

All measurements were performed at room temperature (RT) using MoKα (λ=0.71073 Å) radiation. Data were collected on a Bruker AXS SMART APEX II four- circle diffractometer with κ- geometry. To determine the orientation of the unit cell, a preliminary measurement was performed using the ω- scan technique. The data was collected in 3 runs with 20 images over 6°. With this information, the data collection strategy was then optimised to obtain full completeness and high redundancy. All data were measured with ϕ and ω- scans. The frame width was adapted and were between 0.3° and 1.2°, as well as the detector distance, which differed between 36 mm and 60 mm.

SAINT PLUS software (Bruker Analytical X-ray Instruments Inc. Madison, WI, USA 2007) was used to integrate the frames. The data were corrected for polarization and Lorentz effects, and an empirical absorption correction (SADABS) [171] was employed. The crystal structure was solved either by charge flipping (JANA2006) [172] or using the SHELX software package [173]. Refinement was performed by the full-matrix least-squares method based on F^2 (SHELXL97) using SHELXLE as a graphical interface [174].

All non-hydrogen atoms were treated anisotropically. Hydrogen atoms binding to carbon atoms were inserted in calculated positions and refined riding with the corresponding atom using the HFIX command in SHELX. For most OH groups it was possible to locate the hydrogen atom in the difference electron density map. If this approach was not suitable, an ideal possition for the hydrogen atom was calculated, consindering potential hydrogen bonds.

Symmetry was then checked with the program PLATON [175], and sometimes it was necessary to apply SQUEEZE of the same program. Structures were drawn using the software DIAMOND [176].

Crystal data, data collection parameters and refinement details are listed in the Appendix.

8.2.2 NMR

^{1}H and ^{13}C solution NMR spectra were recorded on a Bruker AVANCE 250 (250.13 MHz [1H], 62.86 MHz [13C]) equipped with a 5-mm inverse-broadband probe head and a z-gradient unit.

8.2.3 IR

Infrared spectra were recorded on a Bruker Tensor 27 spectrometer under ambient conditions performing 32 scans at a resolution of 4 cm^{-1} on a diamond ATR unit.

8.2.4 EDX

Energy-dispersive X-ray spectroscopy was performed on an FEI Quanta 200 with a tungsten filament and 20 kV accelerating voltage. Data were evaluated with the software program GENESIS spectrum (EDAX Inc.).

8.3 Structure Solution and Refinement

Structure solution and refinement was for many clusters straightforward and was carried out as described in Sec. 8.2.1. But not all crystals were of the best quality and therefore diffracted weakly.

Problems occurred especially with easily rotating groups, for example ^{t}butyl groups, or adamantane, although all crystals were measured at 100K. An increase of the number of atoms often comes with a decrease in diffraction, as X-rays are absorbed. The effect of heavy elements was no problem and also for the Pb containing samples good data was obtained.

8.3.1 ^{t}Bu benzoic acid

The crystal was very small and therefore diffraction was very weak. Nevertheless a disorder of the ligand sphere was observed. One of the bridging carboxylates is substituted by an alkoxo group by 40%. But the exact nature of this alkoxo group could not be resolved. Due to charge balance this oxygen cannot be a core oxygen. It is also possible that this group is an OH group. The substitution of the bridging carboxylate by an alkoxo group affected also a neighbouring chelating carboxylate, which was shifted towards the alkoxide.

8.3.2 Zr6Ti8piv

The crystal showed rhombohedral metric, but weak diffraction. The structure could be solved in space group $R\bar{3}$, except for the Zr5 cluster. Therefore the symmetry needed to be reduced to $P\bar{1}$. The Zr5 cluster shows only occupancy of about 50%; hence it was not possible to solve the full structure of the Zr5 cluster.

8.3.3 Adamantane carboxylic acid

The diffraction of the crystals was very weak. The adamantane groups were almost all disordered. The metric of the crystal is orthorhombic, but also refinement in space groups of lower symmetry did not resolve this problem. Hence the structure was solved in the orthorhombic space group *Pnma*. Due to the weak diffraction it was not possible to refine the disorder properly. A lot of the carbons still show large displacement factors.

8.3.4 Pb4Ti8Ac

This cluster is most probably non-merohedrally twinned. Reflexions were very close together and therefore could not be separated for twin refinement. In such a case, structure solution should be tried with untwinned treated data. Structure solution for the untwinned data was straightforward, but refinement resulted in some difficulties. Nevertheless the structure of the cluster could be refined to reasonable values.

8.3.5 Pb6Ti6

Some electron density remained around the non-coordinated allylic alcohol. This is most probably caused by a disorder of this solvent. As the exact elucidation of this electron density failed, SQUEEZE by PLATON was applied.

8.3.6 LnTi4

Structure solution and refinement was straightforward, but there were some features which were suspicious. Two clusters of equal composition and structure crystallised in the unit cell. Furthermore, the second cluster showed positional disorder. Due to these facts the crystal was checked for twinning. The metric of the crystal was clearly triclinic, so only non-merohedral twinning is possible. Examination of the diffraction patters showed only separated and well defined reflexions. As it was observed for both La and Ce, this is most probably a feature of this structure.

8.3.7 Ln2Ti4

Although all structures of this cluster type could be refined to satisfying values, there were still some unresolved electron density residues. The highest residual difference electron density was observed close to a methacrylic acid. The distances of this peak to any of the atoms, or other unresolved electron density maxima, does not fit to any known molecule or residue. If the data were cut off at lower degrees, the electron density of this maximum decreases. Nevertheless it was observed in all X-ray experiments, even though crystals were taken from multiple samples and of different composition. These clusters are isostructural to Y2Ti4 described in literature. Such an electron density is not mentioned there, therefore the cluster was reproduced, using $Y(OAc)_3$ as a source. The structure was redetermined and no such electron density was observed. Hence the unresolved electron density in the Ln2Ti4 clusters is most probably a feature of these structures and not caused by any disorder or partial substitution of ligands.

Chapter 9

Reactions

A short overview of all tested element combinations is given in Fig 9.1. A detailed description of all experiments is given below. They are listed within the section in ascending order of their atomic number, exept for experiments with titanium and zirconium, which are listed first.

9.1 Titanium and Zirconium

9.1.1 Propionic acid

Reactions of $Ti(O^nBu)_4$ and $Zr(O^nBu)_4$ with propionic acid in molar ratios Ti:Zr:acid of 2:1:13.5, 1:1:9 and 1:3:18 resulted in colourless crystals after one to two weeks. The cluster was identified as $[Zr_6O_4(OH)_4(OOCR)_{12}]_2$, the molecular structure is isostructural to the cluster reported by Puchberger et.al. [85], allthough the crystal structure is different. The same cluster was found

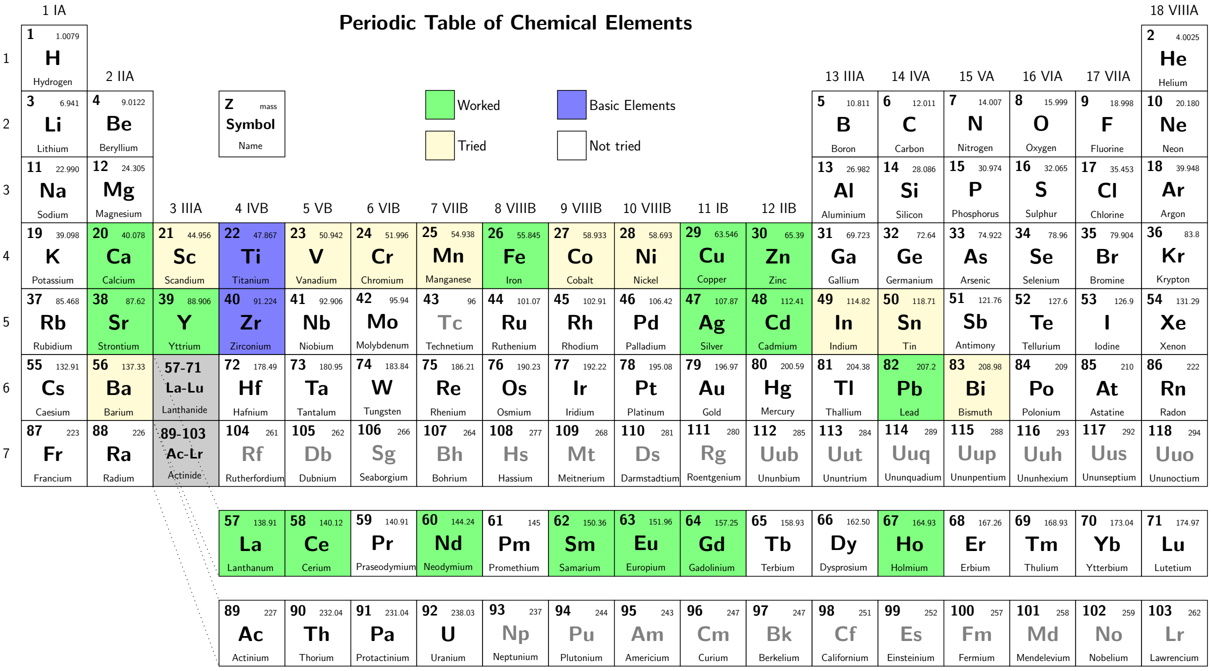

Figure 9.1: Green: Elements which gave mixed-metal oxo cluster with Ti or Zr. Yellow: Elements which gave no mixed metal oxo clusters. Blue: Basic elements Ti and Zr.

in samples containing $Ti(O^iPr)_4$, $Zr(O^nPr)_4$ and propionic acid in a molar ratio of 1:2:13.5 and 1:3:18.

9.1.2 Benzoic acid and derivatives

9.1.2.1 Benzoic acid

First 13.5 mmol (1.649 g) of benzoic acid (HOBenz) were dissolved in 3 ml of dry THF and then 2 mmol (0.680 g) of $Ti(O^nBu)_4$ and 1 mmol (0.384 g) of $Zr(O^nBu)_4$ were added. Colourless crystals of $Z_4Ti_2O_4(O\,^nBu)_2(OBenz)_{14}$ were obtained (Sec. 3.1.1) after 1 month, besides aggregates of a white amorphous powder. Higher proportions of Zr lead to immediate gelation of the reaction mixture.

9.1.2.2 4-^{t}Butyl benzoic acid

8 mmol (1.42 g) of 4-^{t}butyl benzoic acid were dissolved in 3 ml of dry THF. Then 1 mmol (0.284 g) of $Ti(O^iPr)_4$ and 1 mmol (0.384 g) of $Zr(O^nBu)_4$ were added, where a clear solution was obtained. After one week approximately 0.5 ml solvent was evaporated. Three days later very small colourless crystals of $Zr_4Ti_2O_4(OR)_{0.8}(^tBu{-}C_6H_4COO)_{15.2}$ were obtained (Sec. 3.1.2), besides much aggregated amorphous residue.

9.1.2.3 4-(Chloro-methyl)benzoic acid

1 mmol (0.340 g) of $Ti(O^nBu)_4$ and 1 mmol (0.384 g) of $Zr(O^nBu)_4$ were mixed with 9 mmol (1.627 g) of 4-(Cl-methyl)benzoic acid and then 1.5 ml of dry THF was added. Needles of $Zr_2Ti_4O_4(O\,^nBu)_6(OOC{-}C_6H_4{-}CH_2Cl)_{10}$ were obtained (Sec. 3.1.3) after six weeks. Yield: 0.08 g (17 % rel. to Zr).

The same structure was obtained from a sample containing 2 mmol of $Ti(O^nBu)_4$, 1 mmol of $Zr(O^nBu)_4$ and 13.5 mmol of 4-(Cl-methyl)benzoic acid in 1 ml dry THF.

9.1.3 Pivalic acid

All possible combinations of the three Ti alkoxides $Ti(O^iPr)_4$, $Ti(O^nPr)_4$, $Ti(O^nBu)_4$ and the three Zr alkoxides $Zr(O^iPr)_4$, $Zr(O^nPr)_4$, $Zr(O^nBu)_4$ were tested. The Ti:Zr ratio was varied, but the proportion of pivalic acid was always 4.5 mmol per mol metal alkoxide, if not otherwise reported. To reproduce the results, some syntheses were repeated. All these 27 experiments (Ti:Zr = 2:1, 1:1, 1:2) were performed on one day with alkoxides and pivalic acid from the same batch, to get a maximum of reproducibility.

9.1.3.1 Summary of all obtained cluster

Many clusters were obtained from multiple samples. A list of all cluster and the reactions in which they were identified is given in the following. All crystals were colourless and often of poor quality.

ZrTi2piv The crystal used for single crystal X-ray diffraction was taken from a sample containing 2 mmol (0.568 g) of $Ti(O^iPr)_4$, 2 mmol (0.568 g) of $Zr(O^iPr)_4$ and 18 mmol (1.84 g) of pivalic acid after 1 month crystallisation period. The same cluster was obtained from sample containing $Ti(O^iPr)_4$, $Zr(O^iPr)_4$ and HOPiv in the molar ratio 2:1:13.5 and 1:2:13.5. The crystals were of very good quality.

Zr3Ti2piv For single crystal X-ray diffraction the crystal was taken from a sample containing 1 mmol (0.351 g) of $Ti(O^nBu)_4$, 2 mmol (0.568 g) of $Zr(O^nBu)_4$ and 13.5 mmol (1.38 g) of pivalic acid one months after combining the precursors.

Zr2Ti3piv This cluster could only be identified in a sample containing 2 mmol (0.568 g) of $Ti(O^iPr)_4$, 2 mmol (0.568 g) of $Zr(O^nPr)_4$ and 18 mmol (1.84 g) of pivalic acid, after three weeks crystallisation period.

Zr4Ti2piviPr The crystal used for single crystal X-ray diffraction was taken from a sample containing 2 mmol (0.568 g) of $Ti(O^nPr)_4$, 2 mmol (0.568 g) of $Zr(O^iPr)_4$ and 18 mmol (1.84 g) of pivalic acid after 6 weeks crystallisation period. The cluster was also obtained from a mixture of 2 mmol (0.568 g) of $Ti(O^iPr)_4$, 1 mmol (0.568 g) of $Zr(O^nPr)_4$ and 13.5 mmol (1.38 g) of pivalic acid.

Zr4Ti2pivnPr Crystals for single crystal X-ray diffraction were taken from two different samples.

$Zr_4Ti_2O_5(OH)_2(O\,^nPr)(OPiv)_{11}\cdot 2.5HOPiv\cdot 0.5^nPrOH$ The crystal for X-ray diffraction was taken from a sample containing 2 mmol (0.568 g) of $Ti(O^iPr)_4$, 2 mmol (0.568 g) of $Zr(O^nPr)_4$ and 18 mmol (1.84 g) of pivalic acid after 10 months crystallisation period.

$Zr_4Ti_2O_5(OH)_2(O\,^nPr)(OPiv)_{11}\cdot 2\,HOPiv\cdot {}^nBuOH$ The crystal for X-ray diffraction was taken from a sample containing 2 mmol (0.702 g) of $Ti(O^nBu)_4$, 2 mmol (0.568 g) of $Zr(O^nPr)_4$ and 18 mmol (1.84 g) of pivalic acid. The same cluster was identified in samples containing 2 mmol (0.568 g) of $Ti(O^nPr)_4$, 1 mmol (0.568 g) of $Zr(O^nBu)_4$, 13.5 mmol (1.38 g) of pivalic acidand 2 mmol (0.568 g) of $Ti(O^nPr)_4$, 2 mmol (0.568 g) of $Zr(O^nBu)_4$, 18 mmol (1.84 g) of pivalic acid.

Zr4Ti2pivAc The crystal for single crystal X-ray diffraction was taken from a sample containing 1 mmol (0.284 g) of $Ti(O^iPr)_4$, 2 mmol (0.568 g) of $Zr(O^nPr)_4$ and 13.5 mmol (1.38 g) of pivalic acid 4 months after synthesis.

Zr6Ti8piv This cluster was only obtained from a sample containing 1 mmol (0.351 g) of $Ti(O^nBu)_4$, 3 mmol (1.153 g) $Zr(O^nBu)_4$ and 18 mmol (1.84 g) of pivalic acid four months after synthesis.

Ti6pivPB This cluster was found in a sample containing 2 mmol (0.568 g) of $Ti(O^nPr)_4$, 2 mmol (0.568 g) of $Zr(O^nBu)_4$ and 18 mmol (1.84 g) of pivalic acid after 4 weeks, besides Zr4Ti2pivnPr.

Ti6pivBB The crystal for single crystal X-ray diffraction was found in a sample containing 2 mmol (0.702 g) of $Ti(O^nBu)_4$, 1 mmol (0.568 g) of $Zr(O^nBu)_4$ and 13.5 mmol (1.38 g) of pivalic acid after 4 weeks and was also found when repeating the same experiment.

Zr4piv The crystal for single crystal X-ray diffraction was taken from a sample containing 1 mmol (0.284 g) of $Ti(O^iPr)_4$, 2 mmol (0.568 g) of $Zr(O^iPr)_4$ and 13.5 mmol (1.38 g) of pivalic acid 6 weeks after synthesis.

Zr6piv The crystal for single crystal X-ray diffraction was taken from a sample containing 1 mmol (0.284 g) of $Ti(O^nPr)_4$, 2 mmol (0.568 g) of $Zr(O^nPr)_4$ and 13.5 mmol (1.38 g) of pivalic acid 6 after 1 month.

9.1.3.2 Summary of all Ti and Zr alkoxide combinations

$Ti(O^iPr)_4$ and $Zr(O^iPr)_4$ The combination of $Ti(O^iPr)_4$ and $Zr(O^iPr)_4$ in ratios 2:1 and 1:1 resulted in big colourless crystals of fine quality after 2 weeks. Structure determination resulted in $ZrTi_2O(O^iPr)_4(OMc)_6$. The cluster is described in detail in Sec. 3.2.1.

Reaction of 1 mmol of $Ti(O^iPr)_4$ with 2 mmol of $Zr(O^iPr)_4$ gave colourless crystals of $Zr_4O_2(OPiv)_{12}$ (Sec. 6.2.2) after 6 weeks. When repeating the experiment, the crystals were identified as ZrTi2piv, but the crystal quality was poorer than before.

$Ti(O^iPr)_4$ and $Zr(O^nPr)_4$ Reacting 1 mmol of $Ti(O^iPr)_4$ and 1 mmol of $Zr(O^nPr)_4$ resulted in colourless crystals of Ti3Zr2piv (Sec.3.2.2.2) after 3 weeks. They rearranged after several months to $Zr_4Ti_2O_5(OH)_2(O^nPr)(OPiv)_{11}$ (Sec.3.2.3.1). Ti:Zr ratios of 2:1 resulted in $Zr_4Ti_2O_5(OH)_2(O^iPr)(OPiv)_{11}$ and a ratio of 1:2 in $Zr_4Ti_2O_5(OH)_2(O^iPr)(OPiv)_{11}(HOPiv)_1$ after 3 months. When repeating these experiments only dendritic crystals were obtained. Due to their small size and their poor quality it was not possible to determine their composition.

$Ti(O^iPr)_4$ and $Zr(O^nBu)_4$ The combination of $Ti(O^iPr)_4$ and $Zr(O^nBu)_4$ resulted after in colourless crystals of poor quality six weeks. The resolution and the number of reflexions were very low. A unit cell could be determined, which is equivalent to that of $Ti_6O_4(O^nBu)_8(OPiv)_8$ (Sec. 6.1).

$Ti(O^nPr)_4$ and $Zr(O^iPr)_4$ Reaction of 1 mmol of $Ti(O^nPr)_4$ and 1 mmol of $Zr(O^iPr)_4$ resulted in colourless crystals with the same unit cell as Zr4Ti2nPr after 6 weeks. Molar ratios of Ti:Zr of 2:1 and 1:2 resulted only in small dendritic crystals.

$Ti(O^nPr)_4$ and $Zr(O^nPr)_4$ All samples showed partial gelation and dendritic crystals. When equimolar amounts of Ti and Zr were used, prismatic colourless crystals were also found, which could be identified as $Zr_6O_4(O^nBu)_2(OPiv)_{14}$ (Sec. 6.2.3).

$Ti(O^nPr)_4$ and $Zr(O^nBu)_4$ In all samples dendritic crystals were found. Where a ratio of Ti:Zr 1:1 was applied prismatic crystals of Zr4Ti2pivnPr were identified after 6 weeks, as well as crystals of Ti6pivPB. When reproducing the experiment, only crystals of Zr4Ti2pivnPr were found. When first reacting 2 mmol of $Ti(O^nPr)_4$ and 1 mmol of $Zr(O^nBu)_4$ with 13.5 mmol pivalic acid, crystals of Zr4Ti2pivnPr were formed, but the second experiment failed to produce suitable crystals.

$Ti(O^nBu)_4$ and $Zr(O^iPr)_4$ The equimolar reaction of $Ti(O^nBu)_4$ and $Zr(O^iPr)_4$ resulted after in colourless crystals of Zr4Ti2iPr 2 months. All other ratios resulted only in dendritic crystals.

$Ti(O^nBu)_4$ and $Zr(O^nPr)_4$ Only dendritic crystals were found in all the samples six weeks after the synthesis, crystals of $Zr_4Ti_2O_5(OH)_2(O^nPr)(OPiv)_{11} \cdot 2\,HOPiv \cdot {}^nBuOH$ were found in the sample of 1 mmol of $Ti(O^nBu)_4$ and 1 mmol of $Zr(O^nPr)_4$ three months later. A detailed structure description of this cluster is given in Sec. 3.2.3.1. Later, the cluster was also identified in the Ti:Zr= 2:1 sample. Reaction of 1 mmol $Ti(O^nBu)_4$ and 1 mmol $Zr(O^nPr)_4$ resulted after 6 weeks in crystals with the same unit cell as Zr4Ti2nPr. Molar ratios of Ti:Zr of 2:1 and 1:2 resulted only in small dendritic crystals.

$Ti(O^nBu)_4$ and $Zr(O^nBu)_4$ When reacting 2 mmol of $Ti(O^nBu)_4$ and 1 mmol of $Zr(O^nBu)_4$ crystals were formed after 3 weeks. The structure of $Ti_6O_4(O^nBu)_8(OPiv)_8$ is decriped in detail in Sec. 6.1. The first experiment with a molar ratio Ti:Zr = 1:2 resulted also in Ti6pivBB, but the second experiment resulted after 1 month in $Zr_3Ti_2O_3(O^nBu)_3(OPiv)_{11}$ (Sec. 3.2.2). This cluster rearranged, and only $Zr_3Ti_3O_4(OH)_3(O^nBu)_3(OPiv)_{10}$ (Sec. 3.2.3.5) was found 7 months later. A reaction of 1 mmol of $Ti(O^nBu)_4$ and 3 mmol of $Zr(O^nBu)_4$ resulted after 4 months in crystals of $Zr_6Ti_8O_{15}(OH)_4(O^nBu)_2(OPiv)_{20}(HOPiv)_2$ (Sec. 3.2.4). The equimolar mixture resulted only in dendritic crystals, as well as with Ti:Zr ratios of 3:1 and 1:4.

9.1.4 Adamantane carboxylic acid

8 mmol (1.457 g) of adamantane carboxylic acid was dissolved in 3ml dry of THF. 1 mmol (0.284 g) of $Ti(O^iPr)_4$ and 1 mmol (0.384) of $Zr(O^nBu)_4$ were added to this solution. After 9 months crystals of $Zr_4Ti_3O_7(O^nBu)_2(OOCAda)_{12}$ (HOOCAda = 1-Adamantanecarboxylic acid) were obtained (Sec.3.3). Yield: 0.15 g (21% rel. to Zr).

9.2 Titanium and other Metals

9.2.1 Calcium

$[Ca_2Ti_4O_4(OAc)_2(OMc)_{10}]_n$ 2 mmol (0.363g) of dry $Ca(OAc)_2$ and 2 mmol (0.568 g) of $Ti(O^iPr)_4$ were reacted with 18 mmol (1.55 g) of methacrylic acid. A clear solution was obtained after 1 hour of stirring. After two weeks colourless crystals formed, beside much white precipitate. The resulting cluster $[Ca_2Ti_4O_4(OAc)_2(OMc)_{10}]_n$ is described in detail in Sec. 4.2.1.

The same structure was obtained when 2 mmol (0.363 g) of dry $Ca(OAc)_2$ and 2 mmol (0.702 g) of $Ti(O^nBu)_4$ were reacted with 18 mmol (1.55 g) of methacrylic acid. A clear solution was not obtained, therefore it was filtered before crystallisation.

$[Ca_2Ti_4O_4(OAc)(OMc)_{11}(HOMc) \cdot BuOH]_n$ When a Cu:$Ti(O^nBu)_4$ ratio of 1:2 was applied, a different structure of the Ca2Ti4 cluster was obtained. The structure is described in Sec. 4.2.1.2.

9.2.2 Strontium

$Sr_2Ti_8O_8(O^iPr)_{1.73}(OAc)_{2.27}(OMc)_{16}$ 2 mmol (0.411 g) $Sr(OAc)_2$ and 2 mmol (0.568 g) of $Ti(O^iPr)_4$ were reacted with 18 mmol (1.55 g) of methacrylic acid. The mixture turned yellow. After stirring for three days, the solution remained blurred, why it was filtered with a syringe filter. After 2 weeks pale-yellow crystals of $Sr_2Ti_8O_8(O^iPr)_{1.73}(OAc)_{2.27}(OMc)_{16}$ were obtained. A detailed structure description is given in Sec. 4.3.1. Yield: 0.23 g (40 % rel. Ti). The same cluster was obtained with a Sr:Ti:acid ration of 1:2:13.5.

^{1}H-NMR ($CDCl_3$, 250 MHz) $\delta = 1.22$ (d, 10.38H, CH_3, O^iPr), 1.82-1.99 (m, 48H, CH_3, OMc), 2.08 (s, 6.81H, CH_3, OAc), 4.03 (sep, 1.73H, CH, O^iPr), 5.32-5.64 (m, 16H, CH_2, OMc), 5.91-6.21 (m, 16H, CH_2, OMc).

IR (cm^{-1}): 2976 (w), 2360 (w), 1698 (s), 1644 (w), 1571 (m), 1523(m), 1414 (s), 1357 (s), 1220 (s), 1006(m), 937 (m), 828 (m).

$[Sr_2Ti_4O_4(OMc)_{12}(HOMc)_2]_n$ 1 mmol (0.411 g) of $Sr(OAc)_2$ and 1 mmol (0.351 g) of $Ti(O^nBu)_4$ were reacted with 12 mmol (1.03 g) of methacrylic acid. Small amounts of precipitate were formed after three days in the originally clear solution. Nevertheless, after 6 weeks one 1mm big colourless crystal was formed. It was identified as $[Sr_2Ti_4O_4(OMc)_{12}(HOMc)_2]_n$. A detailed structure description is given in Sec. 4.2.2.

When $Ti(O^nPr)_4$was reacted with $Sr(OAc)_2$ and methacrylic acid in Ti:Sr:acid molar ratios of 2:1:13.5, 1:1:9 and 1:2:13.5 no crystallisation occurred. Also reaction with propionic acid did not result in crystals.

9.2.3 Barium

When $Ba(OAc)_2$ and $Ti(O^iPr)_4$ were reacted with methacrylic acid in different proportions, the mixtures turned immediately yellow. Even after 16 h of stirring, much precipitate was still present. This was filtered off, but no crystals were obtained even after 1 year. Also reactions with acrylic acid failed to produce crystals.

9.2.4 Scandium

1 mmol (0.222g) of dry $Sc(OAc)_3$ and 0.95 mmol (0.270 g) of $Ti(O^iPr)_4$ were mixed with 9 mmol (0.919 g) of methacrylic acid. The $Sc(OAc)_3$ was only poorly soluble. A clear solution could not be obtained even after one week. The mixture was filtered and another 18 mmol (1.838 g) methacrylic acid were added to the solid residue and stirred for another 5 days. After 2 weeks colourless crystals were formed in the second solution, which were identified as $Ti_8O_8(OMc)_{16}$ [67].

9.2.5 Yttrium

$Y(OAc)_3$ and $Ti(O^iPr)_4$ were reacted in different ratios with methacrylic acid. All applied ratios (Y:Ti:acid 2:1:13.5, 2:2:18, 1:4:22.5) resulted in colourless crystals of $Y_2Ti_4O_4(OMc)_{14}(HOMc)_2$ [116] beside some white precipitate.

IR (cm^{-1}): 2979 (w), 2961 (w), 2928 (w), 1697 (w), 1643 (w), 1563 (s), 1454 (m), 1385 (s), 1368 (s), 1232 (s), 1007 (m), 938 (m), 852 (w), 826 (s), 760 (s), 654 (m).

9.2.6 Lanthanides

$LaTi_4O_3(O^iPr)_2(OMc)_{11}$ 1 mmol (0.316 g) of $La(OAc)_3$ was mixed with 2 mmol (0.568 g) of $Ti(O^iPr)_4$ and 13.5 mmol (1.162 g) of methacrylic acid. The solution was stirred for 1 day. Dark yellow crystals of $LaTi_4O_3(O^iPr)_2(OMc)_{11}$ were isolated after two weeks (Sec. 4.7.1). Yield: 0.567g (79% rel. La).

^{1}H-NMR (CD_2Cl_2, 250 MHz) $\delta = 1.19$-1.28 (m, 12H, CH_3, O^iPr), 1.62 - 2.08 (m, 33H, CH_3, OMc), 4.02 (sep, 2H, CH, O^iPr), 5.29 - 5.68 (m, 11H, $=CH_2$, OMc), 5.90 - 6.13 (m, 11H, $=CH_2$, OMc).

IR (cm^{-1}): 2978 (w), 2928 (w), 1680 (w), 1640 (w), 1542 (s), 1453 (m), 1403 (s), 1385 (s), 1366 (m), 1326 (m), 1231 (m), 1208 (w), 1053 (w), 1006 (w), 936 (m), 863 (w), 829 (m), 759 (w), 675 (m), 656 (m).

$La_2Ti_6O_6(HO^iPr)_2(OMc)_{18}$ 2 mmol (0.632 g) of $La(OAc)_3$ were mixed with 2 mmol (0.568 g) of $Ti(O^iPr)_4$ and 18 mmol (1.550 g) of methacrylic acid. The solution was stirred for 1 day. Dark yellow crystals were isolated after two weeks (Sec. 4.7.2). Yield: 0.324 g (84% rel. Ti). The same cluster was obtained with a molar ratio La:Ti:acid of 2:1:13.5.

^{1}**H-NMR** (CD_2Cl_2, 250 MHz) $\delta = 1.17$-1.28 (m, 12H, CH_3, $HO^{i}Pr$), 1.62 - 2.09 (m, 54H, CH_3, OMc), 4.02 (sep, 2H, CH, $HO^{i}Pr$), 5.29 - 5.67 (m, 18H, $=CH_2$, OMc), 5.89 - 6.23 (m, 18H, $=CH_2$, OMc).

^{13}**C-NMR** (CD_2Cl_2, 250 MHz) $\delta = 17.6$-18.0 (CH_3, HOMc), 21.7 (), 25.0 (CH_3, $HO^{i}Pr$), 64.3 - 64.6 (CH, $HO^{i}Pr$), 127.4 (CH_2, HOMc), 138.4 (C, HOMc), 172.8 (COO, HOMc).

IR (cm^{-1}): 3098 (w), 2976 (w), 2957 (w), 2927 (w), 1697 (w), 1643 (w), 1563 (s), 1543 (s), 1503 (w), 1453 (m), 1385 (s), 1363 (vs), 1327 (m), 1232 (s), 1121 (w), 1045 (w), 1007 (m), 940 (m), 849 (w), 827 (m), 807 (m), 745 (s), 656 (m), 612 (s).

$CeTi_4O_3(O^{i}Pr)_2(OMc)_{11}$ 1 mmol (0.317 g) of $Ce(OAc)_3$ was mixed with 6 mmol (1.705 g) of $Ti(O^{i}Pr)_4$ and 28 mmol (2.712 g) of methacrylic acid. The solution was stirred for 1 day. Brown crystals of $CeTi_4O_3(O^{i}Pr)_2(OMc)_{11}$ were isolated after two weeks (Sec. 4.7.1). Yield: 1.06 g (74% rel. Ce).

IR (cm^{-1}): 2975 (w), 2927 (w), 1698 (w), 1645 (m), 1601 (s), 1578 (s), 1516 (m), 1454 (m), 1415 (s), 1365 (s), 1235 (s), 1162 (w), 1123 (m), 1005 (m), 937 (m), 857 (w), 825 (s), 740 (m).

$Ce_2Ti_6O_6(HO^{i}Pr)_2(OMc)_{18}$ 1 mmol (0.317 g) of $Ce(OAc)_3$ was mixed with 2 mmol (0.568 g) of $Ti(O^{i}Pr)_4$ and 13.5 mmol (1.162 g)of methacrylic acid. The solution was stirred for 1 day. Orange crystals were isolated after two weeks. Yield: 0.305 g (79% rel. Ti). The same cluster was also obtained from samples with a molar ratio Ce:Ti:acid of 2:1:13.5 and 1:1:9 (Sec. 4.7.2).

^{1}**H-NMR** (CD_2Cl_2, 250 MHz) $\delta = 1.17$-1.28 (m, 12H, CH_3, $HO^{i}Pr$), 1.62 - 2.08 (m, 54H, CH_3, OMc), 4.01 (sep, 2H, CH, $HO^{i}Pr$), 5.33 - 5.68 (m, 18H, $=CH_2$, OMc), 6.05 - 6.22 (m, 18H, $=CH_2$, OMc).

^{13}**C-NMR** (CD_2Cl_2, 250 MHz) $\delta = 17.6$ (CH_3, HOMc), 21.7 (), 25.0 (CH_3, $HO^{i}Pr$), 64.4 - 67.8 (CH, $HO^{i}Pr$), 124.4 - 127.3 (CH_2, HOMc), 136.0 - 138.9 (C, HOMc), 172.5 (COO, HOMc).

IR (cm^{-1}): 2975 (w), 2927 (w), 1698 (w), 1645 (m), 1601 (m), 1577 (s), 1516 (m), 1454 (m), 1414 (s), 1385 (s), 1365 (s), 1235 (m), 1162 (w), 1123 (m), 1104 (m), 936 (m), 857 (s), 825 (m), 741 (m), 659 (m).

$Nd_2Ti_6O_6(HO^{i}Pr)_2(OMc)_{18}$ 1 mmol (0.321 g) of $Nd(OAc)_3$ was mixed with 2 mmol (0.568 g) of $Ti(O^{i}Pr)_4$ and 13.5 mmol (1.162 g) of methacrylic acid. The solution was stirred for 1 day and filtered with a syringe filter. Pale pink crystals were isolated after one week (Sec. 4.7.2). Yield: 0.293 g (76% rel. Ti).

IR (cm^{-1}): 2976 (w), 2927 (w), 1697 (w), 1643 (w), 1532 (s), 1541 (s), 1454 (m), 1363 (s), 1329 (s), 1230 (s), 1122 (w), 1007 (w), 939 (m), 849 (w), 828 (m), 808 (m), 739 (s), 657 (m).

$Sm_2Ti_4O_4(OAc)_2(OMc)_{12}(McOH)_2$ 2 mmol (0.955 g) of $Sm(OAc)_3$ was mixed with 2 mmol (0.568 g) of $Ti(O^{i}Pr)_4$ and 18 mmol (1.55 g) of methacrylic acid. The solution was stirred for 1 day. Colourless crystals were isolated after two weeks (Sec. 4.7.3). Yield: 0.352 g (37% rel. Sm). The same cluster was obtained from samples of Sm:Ti:acid molar ratio of 2:1:13.5 and 1:2:13.5.

$Eu_2Ti_4O_4(OAc)_2(OMc)_{12}(McOH)_2$ 1 mmol (0.329 g) of $Eu(OAc)_3$ was mixed with 2 mmol (0.568 g) of $Ti(O^{i}Pr)_4$ and 13.5 mmol (1.162 g) of methacrylic acid. The solution was stirred for 1 day. Colourless crystals were isolated after one week (Sec. 4.7.3). Yield: 0.779 g (81% rel. Eu).

IR (cm^{-1}): 2979 (w), 2927 (w), 1697 (w), 1643 (w), 1560 (s), 1454 (m), 1384 (s), 1367 (s), 1232 (s), 1006 (m), 937 (m), 851 (w), 826 (s), 754 (s), 653 (w), 601 (s).

$Gd_2Ti_4O_4(OAc)_2(OMc)_{12}(McOH)_2$ 1 mmol (0.334 g) of $Gd(OAc)_3$ was mixed with 2 mmol (0.568 g) of $Ti(O^iPr)_4$ and 13.5 mmol (1.162 g) of methacrylic acid. The solution was stirred for 1 day. Pale orange crystals were isolated after one week. Yield: 0.686g (71% rel. Gd). This cluster was also obtained with an educts ratio Gd:Ti of 1:1 and 2:1.

IR (cm^{-1}): 2979 (w), 2927 (w), 1698 (w), 1664 (w), 1644 (w), 1561 (s), 1454 (m), 1384 (s), 1367 (s), 1232 (s), 1129 (w), 1006 (m), 937 (m), 852 (w), 825 (s), 758 (s), 653 (m), 601 (s).

$Ho_2Ti_4O_4(OAc)_2(OMc)_{12}(McOH)_2$ 1 mmol (0.342 g) of $Ho(OAc)_3$ was mixed with 2 mmol (0.568 g) of $Ti(O^iPr)_4$ and 13.5 mmol (1.162 g) of methacrylic acid. The solution was stirred for 1 day. Orange crystals were isolated after one week. Yield: 0.756g (78% rel. Ho). This cluster was also obtained with an educts Ho:Ti ratio of 1:1 and 2:1.

IR (cm^{-1}): 2979 (w), 2961 (w), 2929 (w), 1697 (w), 1643 (w), 1561 (,), 1530 (s), 1455 (m), 1388 (s), 1371 (s), 1231 (s), 1006 (m), 942 (m), 868 (m), 851 (w), 829 (s), 761 (m), 658 (m), 601 (s).

9.2.7 Chromium

2 mmol (0.699 g) of $Cr(acac)_3$ and 1 mmol (0.284 g) of $Ti(O^iPr)_4$ were combined first with 28 mmol (2.39 g) of methacrylic acid. After one day stirring and adding another 11 mmol (0.91 g) methacrylic acid, a clear violet solution was obtained. Crystals of $Ti_8O_8(OMc)_{16}$ [67] were obtained after one week.

$Ti_6O_6(O^iPr)_2(OProp)_{10}$ 1 mmol (0.345 g) of $Cr(acac)_3$ and 2 mmol (0.568 g) of $Ti(O^iPr)_4$ were reacted with 12 mmol (0.898 g) of propionic acid. After one day 0.5 ml of ^iPrOH were added. Colourless crystals of $Ti_6O_6(O^iPr)_2(OMc)_{10}$ (Sec. 6.1.1) were obtained after 4 days. Yield: 0.102 g (25% rel. Ti)

^{1}H-NMR ($CDCl_3$, 250 MHz) $\delta = 1.27$ (m, 30H, CH_3, HOProp; 12H, CH_3, O^iPr), 2.32 - 2.49 (m, 20H, CH_2, HOProp), 4.00 (m, 2H, CH, O^iPr).

$Ti_8O_8(OProp)_{16}$ An equimolar ratio of 2 mmol (0.699 g) $Cr(acac)_3$, 2 mmol (0.568 g) $Ti(O^iPr)_4$ and 12 mmol (0.898 g) of propionic acid resulted after 5 days in $Ti_8O_8(OProp)_{16}$ (Sec. 6.1.4). Yield: 0.241 g (51% rel. Ti).

^{1}H-NMR ($CDCl_3$, 250 MHz) $\delta = 1.12$ (t, 48H, CH_3, HOProp), 2.37 - 2.45 (m, 32H, CH_2, HOProp).

9.2.8 Manganese

$Mn(OAc)_2$ and $Ti(O^iPr)_4$ were reacted with methacrylic acid in the molar ratios Mn:Ti:acid 1:2:13.5, 1:1:9, 2:1:13.5. A clear solution was obtained after one day, and after two weeks crystals were obtained. But their size and quality was not suitable for single crystal X-ray diffraction.

9.2.9 Iron

Reactions of dry $FeCl_2$ and $Ti(O^nBu)_4$ with propionic acid resulted in the recrystallization of $FeCl_2 \cdot 4\,H_2O$. With methacrylic acid and additional KO^tBu only dark precipitate was formed.

$FeTi_5O_4(O^iPr)_2(OMc)_{12}$ The red brown solution of 1 mmol (0.174 g) of $Fe(OAc)_2$, 2 mmol (0.568 g) of $Ti(O^iPr)_4$ and 17 mmol (1.44 g) of methacrylic acid was stirred for one week and then filtered. Redish-brown crystals of $FeTi_5O_4(O^iPr)_2(OMc)_{12}$ (Sec. 4.6) were obtained after two weeks. Yield: 0.120 g (41 % rel. Ti).

9.2.10 Cobalt

Reacting $Co(OAc)_2$ and $Ti(O^iPr)_4$with methacrylic acid in molar ratios Co:Ti:acid 1:1:10 and 5:1:22 gave a clear violet solution, but crystals were not obtained. Using acrylic acid in the same ratio instead, was also not successful.

9.2.11 Nickel

$Ni(OAc)_2$ was reacted with either $Ti(O^iPr)_4$ or $Ti(O^nBu)_4$ and methacrylic acid. For all applied ratios (Ni:Ti:acid 1:2:13.5, 1:1:9, 2:1:13.5) a very fine white precipitate was formed after few weeks. A ratio of Ni:Ti:acid 1:2:13.5 resulted also in tiny crystals, which showed very weak scattering.

9.2.12 Copper

$Cu(OMc)_2$ $Cu(OMc)_2$ was synthesised according to literature [177]. 40.5 mmol (5.00 g) of $Cu(CO_3)$ and 25.9 mmol (2.23 g) of methacrylic acid were stirred in 50 ml of CH_2Cl_2 for 4 days. The solution was filtered and the solvent was removed on a rotary evaporator. The blue precipitate was dried in vacuum.

$Cu_4Ti_5O_6(OMc)_{16}$ 2 mmol (0.363 g) of dry $(CuOAc)_2$ and 4 mmol (1.137 g) of $Ti(O^iPr)_4$ were reacted with 27 mmol (2.32 g) of methacrylic acid. The mixture was stirred for a day. The supernatant solution was transferred to another Schlenk tube. Dark green crystals could be isolated from the mother liquid after a week. They were identified as $Cu_4Ti_5O_6(OMc)_{16}$. The structure is described in detail in Sec.4.5.1. Crystals of the same cluster were also identified in the suspension, left after removing the solution. Yield: 0.28 g (21% rel. to Cu). After another week white crystals were observed in the reaction mixture. They were identified as $Ti_8O_8(OMc)_{16}$.

Cu4Ti5met can also be obtained using $Ti(O^nBu)_4$ and $Ti(O^nPr)_4$ as starting material. The Cu:Ti ratio as well as the metal:acid do not influence the formation of Cu4Ti5met, but solid $Cu(OAc)_2$ always remains in the mixture. Even when applying a Cu:Ti ratio of 4:5 it is not possible to get all the acetate in solution, even with a huge excess of 265 mmol methacrylic acid (for 4 mmol Cu and 5 mmol Ti). It is possible to avoid the formation of $Ti_8O_8(OMc)_{16}$ [67] by using a greater excess of methacrylic acid.

The reaction of 4 mmol (0.935g) of $Cu(OMc)_2$ with 5 mmol of (1.42 g) of $Ti(O^iPr)_4$ and 36 mmol (3.10 g) of methacrylic acid resulted in the same cluster of $Cu_4Ti_5O_6(OMc)_{16}$, but with a different crystal structure due to the incorporation of CH_2Cl_2 (see Sec.4.5.1).

$Cu_4Ti_5O_6(OProp)_{16}$ 1 mmol (0.182 g) of dry $Cu(OAc)_2$ and 1 mmol (0.284 g) of $Ti(O^iPr)_4$ were reacted with 24 mmol (1.44 g) of propionic acid. After two days stirring the solution was clear and blue. The solution was cooled to -18° and after two week green crystals of $Cu_4Ti_5O_6(OProp)_{16}$ (OProp= Propionate) were isolated. For a detailed structure description see Sec. 4.5.2. Yield: 0.29 g (25% rel. to Cu)

9.2.13 Silver

The reaction of 1 mmol (0.168 g) of Ag(OAc) and 1 mmol (0.284 g) of $Ti(O^iPr)_4$ with either 12 mmol (1.02 g) of methacrylic acid or 5 mmol (0.37 g) of propionic acid resulted in a clear solution. After several weeks a dark grey precipitate was formed.

9.2.14 Zinc

$Zn_2Ti_4O_4(O^iPr)_2(OMc)_{10}$ In a first experiment 1 mmol (0.284 g) of $Ti(O^iPr)_4$, 1 mmol (0.183 g) of dry $Zn(OAc)_2$ and 10 mmol (0.861 g) of methacrylic acid were mixed together at room temperature. After adding methacrylic acid the mixture immediately became orange. The colourless crystals, obtained after a week, were very small and of poor quality. Nevertheless cell dimensions could be determined. In a second attempt additionally 1.5 ml of dry CH_2Cl_2 was added to the mixture. After 1 week orange crystals could be isolated from the mother liquid. Single crystal X-ray diffraction gave the same unit cell dimensions as in the first experiment and the crystal quality was sufficient to be measured. Yield (after washing with dry n-heptane): 0.256g (77% rel. to Ti) The obtained molecular structure of $Zn_2Ti_4O_4(O^iPr)_2(OMc)_{10}$ is described in detail in section 4.1.1 on page 47. The same clusters were obtained with a Zn:Ti:acid molar ratio of 2:1:13.5 and 1:2:13.5. A greater excess of methacrylic acid while keeping the Zn:Ti ratio also resulted in Zn2Ti4met.

Only a ratio of Zn:Ti:met of 1:5:15 did not lead to crystallisation and the solution remained clear.

^{1}**H-NMR** ($CDCl_3$, 250 MHz) $\delta = 1.22$ (m, 12H, CH_3, O^iPr), 1.81-2.11 (m, 30H, CH_3, OMc), 4.52 (sep, 2H, CH, O^iPr), 5.35-5.68 (m, 10H, $=CH_2$, OMc), 5.98-6.43 (m, 10H, $=CH_2$, OMc).

IR (cm^{-1}): 611 (s), 686 (w), 790 (m), 825 (m), 859 (w), 942 (m), 988 (w), 1005 (w), 1113 (w), 1162 (w), 1241 (m), 1372 (m), 1411 (s), 1552 (s), 1644 (w), 2975 (w).

Mother liquid: ^{1}**H-NMR** ($CDCl_3$, 250 MHz) $\delta = 1.21$ (d, 6H, CH_3, HO^iPr), 1.25 (d, 6H, CH_3, McO^iPr, AcO^iPr), 1.93 (s, 3H, CH_3, OMc), 2.01 (s, 1H, OH, HO^iPr), 2.09 (s, 3H, CH_3, OAc), 4.04 (sep, 1H, CH, HO^iPr, 5.04 (m, 1H, CH, McO^iPr, AcO^iPr), 5.28 (s, 2H, CH_2Cl_2), 5.51 (s, 1H, CH_2, McO^iPr, 5.65 (s, 1H, CH_2, HOMc), 6.06 (s, 1H, CH_2, McO^iPr, 6.22 (s, 1H, CH_2, HOMc), 9.30 (b, 1H, HOAc, HOMc).

^{13}**C-NMR** ($CDCl_3$, 250 MHz) $\delta = 17.9$ (CH_3, HOMc), 21.7 (CH_3, McO^iPr, AcO^iPr), 25.1 (CH_3, HO^iPr), 53.4 (CH_2Cl_2), 64.6 (CH, HO^iPr), 127.5 (CH_2, HOMc), 135.9 (C, HOMc), 172.77 (COO, HOMc).

When $Zn(OAc)_2$ and $Ti(O^iPr)_4$were reacted with propionic acid in the ratio 1:1:25.6 the cluster $Ti_8O_8(OProp)_{16}$ was obtained. A detailed description of this cluster is given in Sec. 6.1.4.

9.2.15 Cadmium

$Cd_4Ti_2O_2(OAc)_2(OMc)_{10}(HO^iPr)_2$ 1 mmol (0.231 g) of $Cd(OAc)_2$ were mixed with 1 mmol (0.284 g) of $Ti(O^iPr)_4$ and 10 mmol (0.861 g) of methacrylic acid in 2 ml of dry CH_2Cl_2. The sample was stirred for 3 h and then filtered through a syringe filter. After 2 weeks colourless crystals could be isolated from the mother liquid. Yield (after washing with dry n-heptane): 0.198g (48% rel. Cd) The resulted molecular structure of $Cd_4Ti_2O_2(OAc)_2(OMc)_{10}(HO^iPr)_2$ is described in detail in section 4.1.2.

The cluster could also be obtained without solvent in molar ratios Cd:Ti:acid of 2:1:13.5, 1:1:10 and 1:2:13.5, but crystallisation took much longer and the crystal quality was poorer.

Experiments with propionic acid resulted after six months in crystals of Ti8prop.

9.2.16 Indium

Reacting $In(OAc)_3$ and $Ti(O^iPr)_4$ with methacrylic acid in molar ratios In:Ti:acid of 2:1:13.5, 1:1:9, 1:2:13.5 and stirring the mixture over night resulted in a clear solution, but crystals were not obtained.

9.2.17 Tin

$Sn(O^iBu)_2$ $LiNMe_2$ (30 ml of a 5% suspension in hexane; 0.02 mol; 2.0 eq) was added drop wise to a solution of $SnCl_2$ (1.935 g; 0.01 mol; 1.0 eq) in hexane at -10°. The mixture was stirred overnight and then filtered. The solvent was removed and then ^iBuOH was added (1.83 ml; 0.02 mol; 2 eq). The resulting yellow product was dried under vacuum.

0.25 mmol (0.066 g) of $Sn(O^iBu)_2$ in 5 ml of THF was reacted with 0.5 mmol (0.170 g) of $Ti(O^nBu)_4$and 4.5 mmol (0.387 g) of methacrylic acid, resulting in a clear solution. Crystallisation did not occur, even after evaporating solvent three times. Molar ratios of Sn:Ti:acid 1:4:27 and 1:1:13.5 also failed to crystallise.

9.2.18 Lead

$Pb_2Ti_8O_8(O^nBu)_2(OAc)_{0.65}(OMc)_{17.35}(^nBuOH)_2$ 1 mmol (0.328 g) of $Pb(OAc)_2$ and 1 mmol (0.340 g) of $Ti(O^nBu)_4$ were combined and then 4 mol (0.409 g) of methacrylic acid was added. After one day all $Pb(OAc)_2$ was solved and a clear solution was obtained. Colourless crystals of $Pb_2Ti_8O_8(O^nBu)_2(OAc)_{0.65}(OMc)_{17.35}(^nBuOH)_2$ could be isolated from the mother liquid (Sec. 4.3.2) after 3 weeks. Yield: 0.11 g (32 % rel. Ti).

^{1}H-NMR ($CDCl_3$, 250 MHz) δ = 0.80-0.96(m, 12H, CH_3, OBu), 1.27-1.42 (m, 8H, CH_2, OBu), 1.50-1.56 (m, 8H,CH_2, OBu), 1.69-2.01 (m, 48H, CH_3, OMc), 2.08 (s, 6.81H, CH_3, OAc), 4.30-4.37 (sep, 1.73, CH, O^iPr), 5.34-5.65 (m, 16H, CH_2, OMc), 5.91-6.35 (m, 16H, CH_2, OMc);

IR (cm^{-1}): 2957 (w), 2360 (w), 1696 (s),1642 (w), 1579 (m), 1503 (m), 1418 (s), 1220 (s), 1068(m), 1005 (m), 935(m), 824 (m), 666(s).

The same cluster could be synthesised with a Pb:Ti:acid molar ratio of 1:2:13.5. An excess of methacrylic acid in the molar ratio Pb:Ti:acid 1:1:9 and 1:1:18 resulted in the same cluster.

$Pb_2Ti_8O_8(OAllyl)_2(OMc)_{18}(AllylOH)_2$ 2 mmol (0.651 g) of $Pb(OAc)_2$ was mixed with 2 mmol (0.568 g) of $Ti(O^iPr)_4$ and 32 mmol (2.224 g) of dry allylic alcohol ($CH_2{=}CH{-}CH_2OH$) and 18.9 mmol (1.62 g) of methacrylic acid. Colourless crystals were isolated after 10 weeks (Sec. 4.3.2.1). Yield: 0.15 g (44 % rel. Ti).

$Pb_2Ti_8O_8(O^nPr)_2(OAc)_{0.48}(OMc)_{17.52}(nPrOH)_2$ 2 mmol (0.651 g) of $Pb(OAc)_2$ was mixed with 1 mmol (0.284 g) of $Ti(O^nPr)_4$ and 13.5 mmol (1.38 g) of methacrylic acid. After one month colourless crystals of $Pb_2Ti_8O_8(O^nPr)_2(OAc)_{0.48}(OMc)_{17.52}(^nPrOH)_2$ were obtained (Sec. 4.3.2). Yield: 0.11 g (33 % rel. Ti).

$Pb_2Ti_6O_5(O^iPr)_{2.76}(OMc)_{15.24}$ 2 mmol (0.651 g) of $Pb(OAc)_2$ was mixed with 4 mmol (1.137 g) of $Ti(O^iPr)_4$and 27 mmol (2.324 g) of methacrylic acid. Colourless crystals of $Pb_2Ti_6O_5(O^iPr)_{2.76}(OMc)_{15.24}$ were isolated after 2 weeks (Sec. 4.3.3). Yield: 0.39 g (26 % rel. Ti).

^{1}H-NMR ($CDCl_3$, 250 MHz) δ = 1.22-1.36 (m, 19.44H, CH_3, O^iPr), 1.63-1.95(m, 44.28H, CH_3, OMc), 4.92 (sep, 3.24H, CH, O^iPr), 5.23-5.52 (m, 14.76H, CH_2, OMc), 5.85-6.28 (m, 14.76H, CH_2, OMc);

IR (cm^{-1}): 2957 (w), 2360 (w), 1696 (s),1642 (w), 1579 (m), 1503 (m), 1418 (s), 1220 (s), 1068(m), 1005 (m), 935(m), 824 (m), 666(s).

This cluster can also be synthesised with a Pb:Ti:acid molar ratio of 1:1:4 and 1:1:8.

$Pb_2Ti_6O_5(O^nPr)_3(OMc)_{15}$ 1 mmol (0.325 g) of $Pb(OAc)_2$ was mixed with 2 mmol (0.568 g) of $Ti(O^nPr)_4$and 13.5 mmol (1.38 g) of methacrylic acid. Crystals of $Pb_2Ti_6O_5(O^nPr)_3(OMc)_{15}$ (Sec. 4.3.3 were isolated from the mother liquid after one week. Besides this cluster also crystals of $Pb_2Ti_8O_8(O^nPr)_2(OAc)_{0.48}(OMc)_{17.52}(^nPrOH)_2$ were identified.

$Pb_4Ti_8O_{10}(OAc)_2(O^iPr)_{18}$ It was attempted to synthesise $Pb_2Ti_2O(O^iPr)_8(OAc)_2$ according to literature [117]. 4 mmol (1.306 g) of dry $Pb(OAc)_2$ and 12 mmol (3.41 g) of $Ti(O^iPr)_4$ were stirred in 20 ml of dry n-hexane. The lead acetate was only poorly soluble, that is why the mixture was stirred for 3 days, where a clear solution was obtained. After two weeks no crystallisation occurred. 5 ml of the solvent was evaporated. Colourless crystals were obtained after 1 year, beside much white precipitate. The structure of $Pb_4Ti_8O_{10}(O^iPr)_{18}(OAc)_2$ is described in Sec. 4.4.1.

$Pb_6Ti_6O_9(OAc)(OMc)_{17}$ 2 mmol (0.651 g) of $Pb(OAc)_2$, 2 mmol (0.568 g) of $Ti(O^iPr)_4$ and 4 mmol (0.278 g) of dry allylic alcohol were heated for 2h at 70°C oil bath, where a clear solution was obtained. It was allowed to cool down and then 18.9 mmol (1.62 g) of methacrylic acid were added. A white precipitate was build, which disappeared after 1 h. After four months colourless crystals of $Pb_6Ti_6O_9(OAc)(OMc)_{17}$ (Sec 4.4.2) were obtained. Yield: 0.39 g (34 % rel. Ti).

9.2.19 Bismuth

When 1 mmol (0.386 g) $Bi(OAc)_3$ was reacted with either 1 mmol (0.284 g) or 2 mmol (0.568 g) of $Ti(O^iPr)_4$ and 9 mmol (0.763 g), 13.5 mmol (1.145 g) respectively of methacrylic acid, colourless crystals of $Ti_8O_8(OMc)_{16}$ were obtained after 6 weeks. They were identified as $Ti_8O_8(OMc)_{16}$ [67].

9.3 Zirconium and other Metals

9.3.1 Copper

Reaction of $Cu(OAc)_2$ with any of the three Zr alkoxides $Zr(O^iPr)_4$, $Zr(O^nPr)_4$ and $Zr(O^nBu)_4$, in molar ratios Cu:Zr:acid of 2:1:13.5, 1:1:9 and 1:2:13.5 always led to the formation of much precipitate. Using solvent also led to mixtures which could not be filtrated.

Reaction of $Cu(OMc)_2$ with $Zr(O^nBu)_4$ and methacrylic acid showed immediate gelation. When only 1 mmol (0.470 g) $Cu(OMc)_2$ and 1 mmol (0.384 g) $Zr(O^nBu)_4$were mixed together, a clear and very viscous solution was obtained.

$Cu(OMc)_2$ and $Zr(O^nPr)_4$ in the presence of CH_2Cl_2 also gave viscous solutions, but only amorphous solids were obtained.

9.3.2 Iron

$Zr_4O_2(OBenz)_{12}$ 1 mmol (0.126 g) of anhydrous $FeCl_2$, 1 mmol (0.384 g) of $Zr(O^nBu)_4$ and 9 mmol (1.099 g) of benzoic acid were reacted in 10 ml of dry THF. Crystals were obtained after two weeks. The structure of $Zr_4O_2(OBenz)_{12}$ is described in Sec. 6.2.1.

Reaction of 2 mmol (0.286 g) of anhydrous $FeCl_2$, 2 mmol (0.768 g) of $Zr(O^nBu)_4$ and 18 mmol (1.55 g) of methacrylic acid in the presence of 1 mmol (0.113 g) KO^tBu in 2.5 ml of dry toluene lead to an immediate formation of a white precipitate. It was not possible to filter the solution. When performing the reaction in more solvent, filtration was possible, but crystals were not obtained.

9.3.3 Silver

$Ag_2Zr_8O_6(hmp-H)_2(hmp)_2(OMc)_{16}(HOMc)_2$

(hmpH2 = 2-hydroxy-2-methylpropionic acid)

1 mmol (0.384 g) of $Zr(O^nBu)_4$ and 1 mmol (0.167g) of Ag(OAc) were reacted with 12 mmol (1.033 g) of methacrylic acid. A white precipitate was filtered off and after one week colourless crystals could be isolated from the filtrate. The structure is described in detail in Sec. 5.1. Yield: 0.11 g (35 % rel. Zr).

To exclude any influence of light, the experiment was repeated in the dark, with the same outcome. The cluster was only poorly soluble in $CDCl_3$, CD_2Cl_2 and C_6D_6.

^{1}**H-NMR** ($CDCl_3$, 250 MHz) δ = 1.66-3.05 (m, 78H, CH3), 5.35-5.67, 5.86-6.35 (m, 36H, $C{=}CH_2$).

9.3.4 Lead

Reaction of 2 mmol (0.568 g) of $Zr(O^nBu)_4$ with 2 mmol (0.651 g) of $Pb(OAc)_2$ and 18 mmol (1.55 g) of methacrylic acid resulted in colourless crystals of $Zr_6O_4(OH)_4(OMc)_{12}$ which is the same cluster as described by Kickelbick et.al. [99], but the crystal structure is different. No crystalisation occured when a molar ratio of Zr:Pb:acid of 1:2:13.5 was applied.

$Zr_6O_4(O^nBu)_4(OPiv)_{14}$ Reaction of 1 mmol (0.568 g) of $Zr(O^nBu)_4$ with 1 mmol (0.325 g) of $Pb(OAc)_2$ and 9 mmol (0.78 g) methacrylic acid resulted in colourless crystals after 2 weeks, besides a colourless gel.

Part IV

Appendix

Appendix A

Tables of Bond Lenghts and Angles

Table A.1: Bond lengths and atom distances for Zr4Ti2benz and Zr4Ti2tBubenz compared with those for Zr4Ti2met [78] in [Å]

	Zr4Ti2benz		**Zr4Ti2tBubenz**		**Zr4Ti2met**
		Disorder		**Disorder**	
Metal - metal distance					
Zr(1)-Zr(1)'	3.5532(5)		3.5464(14)		3.5684(6)
Zr(1)-Zr(2)	3.4935(13)	3.432(19)	3.7276(14)		3.4855(6)
Zr(1)-Ti(1)	3.1114(5)		3.0933(19)		3.1085(10)
Zr(1)-Ti(1)'	3.6966(5)		3.6988(18)		3.6938(9)
Zr(2)-Zr(2A)	0.214(18)				
Zr(2)-Ti(1)	3.7515(14)	3.722(11)	3.6808(19)		3.7497(10)
Core oxygen					
Zr(1)-O(1)	2.1426(16)		2.129(5)		2.148(3)
Zr(1)-O(1)'	2.1408(17)		2.156(5)		2.142(3)
Zr(1)-O(2)	2.1835(16)		2.222(6)		2.170(3)
Zr(2)-O(2)	2.086(2)	2.051(6)	2.089(5)		2.079(3)
Ti(1)-O(1)	1.8236(16)		1.806(6)		1.815(3)
Ti(1)-O(2)	1.8136(17)		1.817(5)		1.824(3)
μ_2- Alkoxy ligands/μ_2- carboxylates					
Zr(1)-O(3)	2.1760(17)		2.213(11)	2.191(11)	2.188(3)
Zr(2)-O(3)	2.149(2)	2.056(10)	2.247(15)	2.064(11)	2.135(3)
μ_2- Carboxylates					
Zr(1)-O(4)	2.1861(18)		2.168(6)		2.187(3)
Zr(1)-O(6)	2.1884(17)		2.173(7)		2.210(3)
Zr(1)-O(8)	2.2479(17)		2.221(7)		2.252(4)
Zr(1)-O(10)	2.2923(18)		2.269(5)		2.268(3)
Zr(2)-O(5)	2.144(2)	2.327(18)	2.097(6)		2.167(3)
Zr(2)-O(12)	2.177(2)	2.229(9)	2.090(7)		2.181(4)
Ti(1)-O(7)	2.0212(18)		2.015(6)		2.013(3)
Ti(1)-O(9)	2.0056(17)		2.042(6)		2.011(4)
Ti(1)-O(11)	2.0029(18)		1.993(5)		1.987(3)
Ti(1)-O(13)	2.0303(17)		2.060(6)		2.030(4)
Chelating carboxylates					
Zr(2)-O(14)	2.219(2)	2.100(13)	2.269(7)		2.289(4)
Zr(2)-O(15)	2.333(3)	2.140(19)	2.264(7)		2.233(3)
Zr(2)-O(16)	2.301(4)	2.27(3)	2.360(11)	2.25(2)	2.278(4)
Zr(2)-O(17)	2.194(2)	2.336(14)	2.300(13)	2.222(17)	2.244(3)

Table A.2: Bond angles [°] for Zr4Ti2benz and Zr4Ti2tBubenz compared with those for Zr4Ti2met [78]

	Zr4Ti2benz		**Zr4Ti2tBubenz**		**Zr4Ti2met**
		Disorder		**Disorder**	
Core oxygen					
Zr(1)- O(1) -Ti(1)	103.05(8)		103.3(2)		103.21(12)
Zr(1)'- O(1) -Ti(1)	137.49(9)		137.9(3)		137.80(14)
Zr(1)- O(1) -Zr(1)'	112.10(7)		111.7(2)		112.56(11)
Zr(1)- O(2) -Zr(2)	109.81(8)	108.5(2)	119.7(3)		110.24(11)
Zr(1)- O(2) -Ti(1)	101.83(8)		99.5(2)		101.88(12)
Zr(2)- O(2) -Ti(1)	148.28(10)	148.6(2)	140.8(3)		147.76(15)
$\sum$M- O(1) -M	352.6(2)		352.9(7)		353.6(4)
$\sum$M- O(2) -M	359.9(3)	358.9(5)	360.0(8)		359.9(4)
Oxygen atoms in *trans* position of the Ti coordination octahedron					
O- Ti(1) -O	171.78(7)-175.50(7)		170.0(3)-176.9(2)		
Oxygen atoms in *cis* position of the Ti coordination octahedron					
O- Ti(1) -O	85.28(7)-95.90(8)		84.3(3)-98.2(3)		
μ_2**- Alkoxy ligands**					
Zr(1)- O(3) -Zr(2)	107.76(8)	108.6(2)		113.4(6)	
Chelating carboxylates					
O(14)-C(40)-O(15)	118.1(3)		117.5(8)		117.2(5)
O(16)-C(47)-O(17)	118.3(3)	113.8(16)	119.7(13)	114.0(18)	118.8(4)

Table A.3: Bond lengths and atom distances for ZrTi2piv in [Å]

Metal - metal distance			
Zr(1)-Ti(1)	3.2300(4)	Zr(1)-Ti(2)	3.2362(4)
Metal - Core oxygen			
Zr(1)-O(1)	2.0533(12)		
Ti(1)-O(1)	1.9365(12)	Ti(2)-O(1)	1.9381(12)
μ_2- Alkoxy ligands			
Zr(1)-O(14)	2.2471(12)	Zr(1)-O(15)	2.2227(12)
Ti(1)-O(14)	1.9252(13)	Ti(2)-O(15)	1.9365(12)
μ_2- Pivalate			
Zr(1)-O(2)	2.2524(12)	Zr(1)-O(4)	2.2312(12)
Ti(1)-O(3)	2.0040(13)	Ti(2)-O(5)	2.0358(13)
Ti(1)-O(6)	2.0224(13)	Ti(2)-O(7)	1.9823(13)
Ti(1)-O(8)	2.0550(14)	Ti(2)-O(9)	2.0436(13)
Chelating pivalate			
Zr(1)-O(12)	2.2602(13)		
Zr(1)-O(13)	2.2540(13)		
η_1- Pivalate			
Zr(1)-O(10)	2.0972(12)	O(10)-C(21)	1.300(2)
O(1)···O(11)	3.7505(18)	O(11)-C(21)	1.219(2)
Terminal alkoxy ligands			
Ti(1)-O(16)	1.7682(13)	Ti(2)-O(17)	1.7852(13)

Table A.4: Bond angles for ZrTi2piv in [°]

Core oxygen	
Zr(1)-O(1)-Ti(1)	108.07(6)
Zr(1)-O(1)-Ti(2)	108.31(5)
Ti(1)-O(1)-Ti(2)	132.76(7)
***trans* oxygen atoms in [TiO_6] octahedron**	
O-Ti(1)-O	163.76(5)-176.11(6)
O-Ti(2)-O	163.17(6)-173.28(6)
***cis* oxygen atoms in [TiO_6] octahedron**	
O(1)-Ti(1)-O(14)	79.48(5)
O(14)-Ti(1)-O(16)	104.41(6)
O(1)-Ti(2)-O(15)	78.50(5)
O(15)-Ti(2)-O(17)	102.05(6)
O-Ti(1)-O	84.48(5)-95.25(5)
O-Ti(2)-O	84.95(5)-95.96(6)

Table A.5: Bond lengths and atom distances for Zr3Ti2piv and Zr2Ti3piv in [Å]

	Zr3Ti2piv				**Zr2Ti3piv**	
Metal - metal distance						
Ti(1)-Ti(2)	3.405(5)	3.406(3)	3.404(4)	Ti(1)-Ti(2)	3.602(6)	3.597(6)
Ti(1)-Zr(1)	3.744(3)	3.740(3)	3.754(4)	Ti(1)-Zr(1)	3.314(4)	3.314(4)
Ti(2)-Zr(1)	3.207(3)	3.195(3)	3.193(3)	Ti(2)-Zr(1)	3.285(4)	3.283(4)
Ti(2)-Zr(2)	3.759(3)	3.749(3)	3.764(4)	Ti(2)-Zr(2)	3.708(4)	3.725(4)
Zr(1)-Zr(2)	3.372(2)	3.3677(16)	3.3633(19)	Zr(1)-Zr(2)	3.385(3)	3.414(3)
Zr(1)-Zr(3)	3.4085(16)	3.4070(18)	3.404(2)	Zr(1)-Ti(3)	3.677(4)	3.289(5)
Zr(2)-Zr(3)	3.8844(18)	3.8911(18)	3.889(2)	Zr(2)-Ti(3)	3.289(5)	3.289(5)
Metal - core oxygen bonds						
Ti(1)-O(3)	1.836(9)	1.852(8)	1.827(10)	Ti(1)-O(3)	1.781(14)	1.807(13)
Ti(2)-O(2)	1.861(7)	1.821(9)	1.817(9)	Ti(2)-O(2)	1.844(11)	1.863(11)
Ti(2)-O(3)	1.971(10)	1.983(8)	1.993(8)	Ti(2)-O(3)	1.993(15)	1.970(14)
Zr(1)-O(1)	2.046(8)	2.073(9)	2.016(9)	Zr(1)-O(1)	2.066(12)	2.036(12)
Zr(1)-O(2)	2.118(8)	2.155(8)	2.138(8)	Zr(1)-O(2)	2.200(13)	2.191(13)
Zr(1)-O(3)	2.238(8)	2.198(9)	2.224(9)	Zr(1)-O(3)	2.244(12)	2.218(11)
Zr(2)-O(1)	2.086(9)	2.103(8)	2.105(8)	Zr(2)-O(1)	2.069(15)	2.130(15)
Zr(2)-O(2)	2.075(8)	2.079(8)	2.103(9)	Zr(2)-O(2)	2.036(10)	2.044(11)
Zr(3)-O(1)	2.077(8)	2.050(8)	2.082(9)	Ti(3)-O(1)	1.922(12)	1.923(12)
μ_2- Alkoxy ligands						
Zr(1)-O(4)	2.123(8)	2.150(9)	2.134(9)	Zr(2)-O(22)	2.285(13)	2.291(13)
Zr(3)-O(4)	2.169(9)	2.118(9)	2.152(10)	Ti(3)-O(22)	1.954(16)	1.967(17)
				Ti(1)-O(23)	1.965(13)	2.162(14)
				Zr(1)-O(23)	2.116(13)	1.957(13)
Terminal alkoxy ligands						
Ti(1)-O(27)	1.723(9)	1.737(9)	1.727(10)	Ti(1)-O(26)	1.731(13)	1.749(13)
Ti(2)-O(28)	1.744(8)	1.779(9)	1.734(10)	Ti(2)-O(25)	1.798(14)	1.787(15)
				Ti(3)-O(24)	1.759(16)	1.759(16)
μ_2- Pivalates bridging Ti and Zr						
Ti(1)-O(12)	2.018(10)	1.999(8)	1.987(9)	Ti(2)-O(14)	2.115(12)	2.102(13)
Ti(2)-O(14)	2.167(9)	2.167(9)	2.172(9)	Ti(2)-O(12)	1.991(14)	2.043(14)
Ti(2)-O(16)	1.976(11)	1.986(8)	2.027(10)	Zr(1)-O(15)	2.142(11)	2.155(11)
Zr(1)-O(11)	2.221(10)	2.189(9)	2.192(11)			
Zr(1)-O(13)	2.119(9)	2.124(8)	2.108(9)	Zr(2)-O(13)	2.237(12)	2.246(13)
Zr(2)-O(15)	2.251(9)	2.241(10)	2.218(10)	Ti(3)-O(4)	2.027(14)	2.070(14)
				Ti(3)-O(6)	2.013(16)	2.052(16)
				Ti(3)-O(8)	1.993(15)	1.970(14)
				Zr(1)-O(7)	2.249(13)	2.280(12)
				Zr(1)-O(9)	2.260(13)	2.250(13)
				Zr(2)-O(5)	2.179(13)	2.186(13)
μ_2- Pivalates bridging Ti						
Ti(1)-O(17)	2.034(10)	2.018(9)	2.020(9)	Ti(1)-O(11)	2.008(16)	1.987(16)
Ti(2)-O(18)	2.035(9)	2.006(9)	2.007(10)	Ti(2)-O(10)	2.082(12)	2.085(13)
μ_2- Pivalates bridging Zr						
Zr(1)-O(5)	2.112(10)	2.124(8)	2.130(10)	Zr(1)-O(16)	2.200(12)	2.196(12)
Zr(2)-O(6)	2.190(11)	2.237(9)	2.236(10)	Zr(2)-O(17)	2.184(12)	2.164(12)
Zr(2)-O(7)	2.194(9)	2.171(10)	2.124(11)			
Zr(2)-O(9)	2.148(8)	2.122(10)	2.167(10)			
Zr(3)-O(8)	2.102(9)	2.122(8)	2.176(9)			
Zr(3)-O(10)	2.194(10)	2.234(9)	2.138(9)			
Chelating Pivalates						
Ti(1)-O(25)	2.141(8)	2.163(9)	2.071(10)	Ti(1)-O(20)	2.227(13)	2.241(13)

Continued on next page

	Zr3Ti2piv				**Zr2Ti3piv**	
Ti(1)-O(26)	2.045(10)	2.064(9)	2.189(9)	Ti(1)-O(21)	2.064(15)	2.104(15)
Zr(2)-O(19)	2.294(10)	2.275(9)	2.224(10)	Zr(2)-O(18)	2.382(16)	2.404(16)
Zr(2)-O(20)	2.272(9)	2.324(8)	2.330(10)	Zr(2)-O(19)	2.174(14)	2.221(15)
Zr(3)-O(21)	2.328(9)	2.250(8)	2.235(8)			
Zr(3)-O(22)	2.263(9)	2.339(8)	2.313(10)			
Zr(3)-O(23)	2.299(9)	2.243(8)	2.212(9)			
Zr(3)-O(24)	2.203(9)	2.278(10)	2.285(10)			

Table A.6: Bond angles for Zr3Ti2piv in [°], the multiple values refer to the multiple clusters crystalised in the unit cell.

	Cluster 1	**Cluster 2**	**Cluster 3**
Core oxygen			
Zr(1)-O(1)-Zr(2)	109.4(3)	107.5(4)	109.4(4)
Zr(1)-O(1)-Zr(3)	111.5(4)	111.5(4)	112.3(4)
Zr(2)-O(1)-Zr(3)	137.9(4)	139.1(4)	136.5(5)
Ti(2)-O(2)-Zr(1)	107.2(4)	106.6(4)	107.4(4)
Ti(2)-O(2)-Zr(2)	145.5(4)	147.9(4)	147.4(4)
Zr(1)-O(2)-Zr(2)	107.1(3)	105.4(4)	105.0(4)
Ti(1)-O(3)-Ti(2)	126.8(5)	125.3(4)	126.0(5)
Ti(1)-O(3)-Zr(1)	133.3(5)	134.7(4)	135.6(4)
Ti(2)-O(3)-Zr(1)	99.0(4)	99.5(3)	98.3(4)
$\sum$M-O(1)-M	358.8(11)	358.1(12)	358.2(13)
$\sum$M-O(2)-M	359.8(11)	359.9(12)	359.8(12)
$\sum$M-O(3)-M	359.1(13)	359.5(11)	359.9(13)
Oxygen atoms in *trans* position of the Ti coordination octahedron			
O-Ti(1)-O	155.3(4)-166.0(4)	153.8(4)-164.7(4)	152.2(5)-166.6(4)
O-Ti(2)-O	164.1(4)-169.0(4)	164.2(4)-169.0(4)	162.5(4)-168.8(4)
Oxygen atoms in *cis* position of the Ti coordination octahedron			
O-Ti(1)-O	60.8(4)-104.0(4)	61.1(4)-108.0(4)	60.6(4)-106.4(4)
O-Ti(2)-O	78.5(3)-102.2(4)	79.6(3)-103.3(4)	78.0(4)-104.5(4)
μ_2- Alkoxo ligand			
Zr(1)-O(4)-Zr(3)	105.1(4)	106.0(4)	105.1(4)

Table A.7: Bond angles for Zr2Ti3piv in [°], the multiple values refer to the multiple clusters crystalised in the unit cell.

	Cluster 1	**Cluster 2**
Core oxygen		
Ti(3)-O(1)-Zr(1)	134.5(8)	137.4(8)
Ti(3)-O(1)-Zr(2)	110.9(6)	108.4(6)
Zr(1)-O(1)-Zr(2)	109.9(6)	110.1(6)
Ti(2)-O(2)-Zr(2)	145.6(7)	144.8(7)
Ti(2)-O(2)-Zr(1)	108.3(5)	107.8(5)
Zr(2)-O(2)-Zr(1)	106.0(5)	107.4(5)
Ti(1)-O(3)-Ti(2)	145.3(7)	144.5(7)
Ti(1)-O(3)-Zr(1)	110.3(7)	110.4(7)
Ti(2)-O(3)-Zr(1)	101.5(5)	103.1(5)
$\sum$M-O(1)-M	355.3(20)	355.9(20)
$\sum$M-O(2)-M	359.9(17)	360.0(17)
$\sum$M-O(3)-M	357.1(19)	358.0(19)
***trans* oxygen in [TiO$_6$] octahedron**		
O-Ti(1)-O	155.3(6)-159.7(6)	154.5(6)-161.1(6)
O-Ti(2)-O	161.2(6)-163.1(5)	160.2(6)-161.1(5)
O-Ti(3)-O	166.3(6)-174.7(8)	166.7(6)-178.1(8)
***cis* oxygen in [TiO$_6$] octahedron**		
O-Ti(1)-O	60.4(5)-105.8(6)	60.8(5)-107.6(6)
O-Ti(2)-O	78.6(5)-106.9(5)	77.7(6)-108.2(6)
O-Ti(3)-O	78.1(6)-97.7(7)	85.8(6)-98.1(7)
μ_2- Alkoxy ligands		
Ti(3)-O(4)-Zr(2)	101.5(6)	100.9(6)
Ti(1)-O(5)-Zr(1)	108.4(5)	107.1(5)

Table A.8: Bond lengths and atom distances for clusters with Zr$_4$Ti$_2$ core [Å]

	Zr4Ti2piviPr	**Zr4Ti2pivnPr**	**Zr4Ti2pivAc**
Metal - metal distance			
Ti(1)-Ti(2)	3.603(2)	3.6056(12)	3.546(3)
Ti(1)-Zr(1)	3.3340(18)	3.2734(8)	3.354(2)
Ti(1)-Zr(2)	3.282(2)	3.2790(8)	3.257(2)
Ti(1)-Zr(4)	3.631(2)	3.6849(9)	3.607(2)
Ti(2)-Zr(1)	3.099(2)	3.0796(8)	3.116(2)
Ti(2)-Zr(3)	3.089(2)	3.0423(8)	3.063(2)
Ti(2)-Zr(4)	3.665(2)	3.7714(10)	3.756(2)
Zr(1)-Zr(2)	3.5076(12)	3.5228(6)	3.5184(14)
Zr(1)-Zr(3)	3.4253(12)	3.4516(5)	3.4477(15)
Zr(2)-Zr(3)	3.5044(12)	3.4885(5)	3.5179(15)
Zr(2)-Zr(4)	3.4479(14)	3.4692(5)	3.4347(15)
Zr(3)-Zr(4)	3.4652(14)	3.5632(7)	3.5696(14)
Metal - core oxygen (OH) bonds			
Ti(1)-O(1)	1.924(6)	1.907(3)	1.900(6)
Ti(1)-O(2)	2.168(6)	2.155(3)	2.150(7)
Ti(1)-O(3)	1.923(7)	1.911(3)	1.935(7)
Ti(2)-O(1)	1.929(6)	1.940(3)	1.911(7)
Ti(2)-O(4)	1.887(7)	1.818(3)	1.806(6)
Ti(2)-O(5)	1.925(7)	1.872(3)	1.882(6)
Zr(1)-O(1)	2.129(6)	2.119(3)	2.161(6)

Continued on next page

	Zr4Ti2piviPr	**Zr4Ti2pivnPr**	**Zr4Ti2pivAc**
Zr(1)-O(2)	2.237(6)	2.238(3)	2.291(6)
Zr(1)-O(4)	2.140(6)	2.144(3)	2.165(7)
Zr(1)-O(6)	2.098(6)	2.098(3)	2.082(6)
Zr(2)-O(2)	2.205(6)	2.206(3)	2.185(6)
Zr(2)-O(3)	2.095(6)	2.111(3)	2.071(7)
Zr(2)-O(6)	2.085(6)	2.082(3)	2.085(6)
Zr(2)-O(7)	2.210(6)	2.227(3)	2.222(7)
Zr(3)-O(4)	2.147(6)	2.184(3)	2.157(6)
Zr(3)-O(5)	2.106(6)	2.114(3)	2.110(6)
Zr(3)-O(6)	2.102(6)	2.091(3)	2.126(7)
Zr(3)-O(7)	2.245(5)	2.231(3)	2.240(6)
Zr(4)-O(3)	2.048(6)	2.081(3)	2.082(6)
Zr(4)-O(5)	2.023(6)	2.166(3)	2.160(6)
Zr(4)-O(7)	2.294(6)	2.290(3)	2.255(6)
Terminal alkoxy ligand			
Ti(1)-O(8)-O(8)	1.731(7)	1.747(3)	1.738(7)
μ_2- pivalates bridging Zr and Ti			
Ti(1)-O(9)	2.039(7)	2.041(3)	2.017(7)
Ti(1)-O(11)	1.998(8)	2.014(3)	2.009(7)
Ti(2)-O(13)	2.011(7)	2.041(3)	2.054(7)
Ti(2)-O(15)	2.050(7)	2.048(3)	2.049(7)
Ti(2)-O(17)	1.940(9)	2.024(3)	2.015(7)
Zr(1)-O(10)	2.224(6)	2.206(3)	2.231(7)
Zr(1)-O(14)	2.227(6)	2.229(3)	2.209(7)
Zr(2)-O(12)	2.241(7)	2.230(3)	2.252(7)
Zr(3)-O(16)	2.215(6)	2.212(3)	2.235(7)
Zr(4)-O(18)	2.294(9)	2.178(3)	2.153(7)
μ_2- pivalates bridging Zr and Zr			
Zr(1)-O(19)			2.263(7)
Zr(2)-O(19)	2.197(6)	2.171(3)	
Zr(2)-O(21)			2.159(7)
Zr(3)-O(20)			2.226(7)
Zr(3)-O(21)	2.217(6)	2.234(3)	
Zr(3)-O(23)			2.211(7)
Zr(4)-O(20)	2.137(6)	2.207(3)	
Zr(4)-O(22)	2.118(7)	2.136(3)	2.230(8)
Zr(4)-O(24)			2.133(7)
Chelating Zr			
Zr(1)-O(23)	2.243(6)	2.291(3)	
Zr(1)-O(24)	2.247(6)	2.233(3)	
Zr(2)-O(25)	2.241(6)	2.220(3)	2.257(8)
Zr(2)-O(26)	2.276(7)	2.301(3)	2.406(7)
Zr(3)-O(27)	2.289(6)	2.254(3)	
Zr(3)-O(28)	2.249(6)	2.240(3)	
Zr(4)-O(29)	2.317(11)	2.280(3)	2.283(7)
Zr(4)-O(30)	2.266(13)	2.263(3)	2.245(7)
η_1- pivalic acid (pivalate)			
Zr(1)-O(29)			2.111(7)
Zr(3)-O(31)			2.200(7)

Table A.9: Bond lengths and atom distances for Zr3Ti3piv compared to those for $Zr_6O_4(OH)_4(OMc)_{12}$ [79] and $Ti_6O_6(O^iPr)_6(OPiv)_6$ [46] in [Å].

	Zr3Ti3	**Zr6met**	**Ti6piv**		**Zr3Ti3**	**Zr6met**	**Ti6piv**
Metal - metal distance							
Ti1(1)-Ti(2)	3.5694(8)	3.480(3)	3.0978(9)	Ti(2)-Ti(3)	3.5630(8)		
Ti(1)-Zr(1)	3.3271(7)	3.506(3)	3.4689(9)	Zr(1)-Zr(2)	3.5220(5)		
Ti(1)-Zr(2)	3.2593(7)	3.548(3)	4.6508(10)	Zr(1)-Zr(3)	3.5088(4)		
Ti(1)-Ti(3)	3.5747(8)			Zr(2)-Zr(3)	3.5128(4)		
Ti(2)-Zr(1)	3.2806(7)			Ti(3)-Zr(2)	3.2735(7)		
Ti(2)-Zr(3)	3.2449(7)			Ti(3)-Zr(3)	3.2776(7)		
μ_3- Oxygen (OH)				**Terminal alkoxy ligand**			
Ti(1)-O(1)	1.930(2)	2.172(18)	1.877(3)	Ti(1)-O(8)	1.751(2)		1.750(4)
Ti(1)-O(2)	2.089(2)	2.050(13)	1.891(3)	Ti(2)-O(9)	1.765(2)		
Ti(1)-O(3)	1.937(2)	2.063(15)	2.143(3)	Ti(3)-O(10)	1.756(2)		
Ti(2)-O(1)	1.908(2)	2.411(16)		**μ_2- Pivalates bridging Zr and Ti**			
Ti(2)-O(4)	2.038(2)			Ti(1)-O(11)	2.021(2)	2.100(18)	2.046(3)
Ti(2)-O(5)	1.947(2)			Ti(1)-O(13)	2.034(2)	2.13(2)	2.051(3)
Zr(1)-O(1)	2.181(2)			Ti(2)-O(15)	2.005(2)	2.193(19)	
Zr(1)-O(2)	2.246(2)			Ti(2)-O(17)	2.060(2)		
Zr(1)-O(4)	2.233(2)			Ti(3)-O(19)	2.025(2)		
Zr(1)-O(6)	2.113(2)			Ti(3)-O(21)	2.021(2)		
Zr(2)-O(2)	2.184(2)			Zr(1)-O(12)	2.235(2)		
Zr(2)-O(3)	2.107(2)			Zr(1)-O(16)	2.237(2)		
Zr(2)-O(6)	2.094(2)			Zr(2)-O(14)	2.212(2)		
Zr(2)-O(7)	2.216(2)			Zr(2)-O(20)	2.219(2)		
Zr(3)-O(4)	2.178(2)			Zr(3)-O(18)	2.203(2)		
Zr(3)-O(5)	2.123(2)			Zr(3)-O(22)	2.215(2)		
Zr(3)-O(6)	2.093(2)			**Chelating Zr**			
Zr(3)-O(7)	2.227(2)			Zr(2)-O(23)	2.254(2)	2.330(18)	
Ti(3)-O(3)	1.925(2)			Zr(2)-O(24)	2.246(2)		
Ti(3)-O(5)	1.898(2)			Zr(3)-O(25)	2.237(2)		
Ti(3)-O(7)	2.136(2)			Zr(3)-O(26)	2.228(2)		
η_1- Pivalic acids coordinated to Zr							
Zr(1)-O(27)	2.138(2)						
Zr(1)-O(29)	2.168(2)						

Table A.10: Bond angles for clusters with Zr_4Ti_2 core in [°]

	Zr4Ti2piviPr	**Zr4Ti2pivnPr**	**Zr4Ti2pivAc**
μ_3 – **Oxygen(OH)**			
$\sum$M-O(1)-M	346.3(4)	346.4(4)	347.9(9)
$\sum$M-O(2)-M	298.6(3)	298.7(3)	299.1(7)
$\sum$M-O(3)-M	355.5(4)	355.5(4)	354.9(10)
$\sum$M-O(4)-M	306.0(4)	306.01(4)	306.7(9)
$\sum$M-O(5)-M	349.9(4)	350.0(4)	350.0(9)
$\sum$M-O(6)-M	339.3(4)	339.3(4)	338.5(9)
$\sum$M-O(7)-M	307.5(4)	307.4(3)	309.4(9)
Oxygen in trans position of the Ti coordination octahedron			
O-Ti(1)-O	159.5(3)-176.2(3)	159.39(13)-176.51(14)	160.6(3)-178.8(3)
O-Ti(2)-O	171.4(3)-178.1(4)	171.79(12)-177.31(14)	171.8(3)-174.8(3)
Oxygen in cis position of the Ti coordination octahedron			
O-Ti(1)-O	78.0(2)-105.4(3)	78.86(12)-102.78(14)	78.4(3)-102.8(3)
O-Ti(2)-O	84.9(3)-97.0(3)	85.52(12)-91.80(13)	85.3(3)-95.2(3)

Table A.11: Bond angles for Zr3Ti3piv compared to those for $Zr_6O_4(OH)_4(OMc)_{12}$ [79] and $Ti_6O_6(O^iPr)_6(OPiv)_6$ [46] in [°].

	Zr3Ti3piv	**Zr6met**	**Ti6piv**
Core oxygen (OH)			
$\sum$M-O(1)-M	351.30(31)	321.9(18)	334.8(4)
$\sum$M-O(2)-M	304.89(26)	349.0(17)	
$\sum$M-O(3)-M	351.42(31)		
$\sum$M-O(4)-M	304.21(27)		
$\sum$M-O(5)-M	350.56(31)		
$\sum$M-O(6)-M	340.83(28)		
$\sum$M-O(7)-M	299.40(25)		
Oxygen atoms in *trans* position of the Ti coordination octahedron			
O-Ti(1)-O	162.34(10)-179.34(10)		159.55(14)-176.90(13)
O-Ti(2)-O	162.83(10)-171.04(10)		
O-Ti(3)-O	161.87(10)-175.13(10)		
Oxygen atoms in *cis* position of the Ti coordination octahedron			
O-Ti(1)-O	78.92(9)-101.55(10)		77.44(11)-101.20(15)
O-Ti(2)-O	79.88(9)-107.60(10)		
O-Ti(3)-O	79.34(9)-104.95(10)		

Table A.12: Bond lengths and atom distances for Zr6Ti8piv in [Å].

1^{st} Fragment		2^{nd} Fragment	
Metal - metal distance			
Ti(1)-Ti(2)	3.525(4)	Ti(5)-Ti(6)	3.567(4)
Ti(1)-Ti(3)	3.533(4)	Ti(5)-Ti(7)	3.570(5)
Ti(1)-Ti(4)	3.372(7)	Ti(5)-Ti(8)	4.534(4)
Ti(1)-Zr(1)	3.295(5)	Ti(5)-Zr(4)	3.142(5)
Ti(1)-Zr(2)	3.304(5)	Ti(5)-Zr(5)	3.138(5)
Ti(2)-Ti(3)	3.516(4)	Ti(6)-Ti(7)	3.527(4)
Ti(2)-Ti(4)	3.395(7)	Ti(6)-Ti(8)	3.399(6)
Ti(2)-Zr(1)	3.315(5)	Ti(6)-Zr(4)	3.312(5)
Ti(2)-Zr(3)	3.307(5)	Ti(6)-Zr(6)	3.255(5)
Ti(3)-Ti(4)	3.380(6)	Ti(7)-Ti(8)	3.385(7)
Ti(3)-Zr(2)	3.308(5)	Ti(7)-Zr(5)	3.326(5)
Ti(3)-Zr(3)	3.296(5)	Ti(7)-Zr(6)	3.280(5)
Ti(4)-Ti(8)	3.150(7)		
Zr(1)-Zr(2)	3.513(3)	Zr(4)-Zr(5)	3.462(3)
Zr(1)-Zr(3)	3.521(3)	Zr(4)-Zr(6)	3.524(3)
Zr(2)-Zr(3)	3.510(2)	Zr(5)-Zr(6)	3.516(3)
μ_3- Oxygen (OH)			
Ti(1)-O(1)	1.967(14)	Ti(5)-O(29)	1.872(14)
Ti(1)-O(2)	2.195(15)	Ti(5)-O(30)	1.777(16)
Ti(1)-O(3)	1.952(13)	Ti(5)-O(31)	1.936(14)
Ti(2)-O(1)	1.924(14)	Ti(6)-O(29)	1.905(14)
Ti(2)-O(4)	2.248(15)	Ti(6)-O(32)	2.134(16)
Ti(2)-O(5)	1.925(13)	Ti(6)-O(33)	1.920(13)
Ti(3)-O(3)	1.959(14)	Ti(7)-O(31)	1.894(14)
Ti(3)-O(5)	1.909(13)	Ti(7)-O(33)	1.910(13)
Ti(3)-O(7)	2.172(15)	Ti(7)-O(35)	2.121(15)
Zr(1)-O(1)	2.064(15)	Zr(4)-O(29)	2.198(15)
Zr(1)-O(2)	2.233(14)	Zr(4)-O(30)	2.206(15)
Zr(1)-O(4)	2.239(13)	Zr(4)-O(32)	2.237(14)
Zr(1)-O(6)	2.077(13)	Zr(4)-O(34)	2.121(14)
Zr(2)-O(2)	2.211(13)	Zr(5)-O(30)	2.218(15)
Zr(2)-O(3)	2.053(14)	Zr(5)-O(31)	2.152(15)
Zr(2)-O(6)	2.089(14)	Zr(5)-O(34)	2.046(14)
Zr(2)-O(7)	2.216(14)	Zr(5)-O(35)	2.214(13)
Zr(3)-O(4)	2.234(13)	Zr(6)-O(32)	2.233(14)
Zr(3)-O(5)	2.110(14)	Zr(6)-O(33)	2.103(14)
Zr(3)-O(6)	2.157(14)	Zr(6)-O(34)	2.092(14)
Zr(3)-O(7)	2.210(14)	Zr(6)-O(35)	2.235(13)

1^{st} Fragment		2^{nd} Fragment	
μ_2- Oxygen			
Ti(1)-O(8)	1.672(15)	Ti(6)-O(36)	1.825(15)
Ti(2)-O(9)	1.710(15)	Ti(7)-O(37)	1.799(15)
Ti(3)-O(10)	1.700(15)		
Ti(4)-O(8)	1.959(15)	Ti(8)-O(36)	1.799(15)
Ti(4)-O(9)	1.951(15)	Ti(8)-O(37)	1.810(15)
Ti(4)-O(10)	1.936(15)		
μ_2- O^nBu			
Ti(4)-O(62)	1.985(16)	Ti(8)-O(62)	2.057(16)
Ti(4)-O(63)	1.943(16)	Ti(8)-O(63)	2.106(17)
μ_2- Pivalates bridging Ti and Ti			
Ti(4)-O(60)	1.994(17)	Ti(8)-O(61)	1.989(16)
Ti(5)-O(38)	2.015(19)	Ti(8)-O(39)	2.006(17)
μ_2- Pivalates bridging Ti and Zr			
Ti(1)-O(11)	2.017(15)	Ti(5)-O(40)	2.031(16)
Ti(1)-O(13)	1.981(15)	Ti(5)-O(42)	2.052(17)
Ti(2)-O(15)	2.020(15)	Ti(6)-O(44)	2.013(16)
Ti(2)-O(18)	1.993(14)	Ti(6)-O(46)	2.030(15)
Ti(3)-O(19)	2.016(15)	Ti(7)-O(48)	1.964(15)
Ti(3)-O(21)	2.042(16)	Ti(7)-O(50)	2.024(15)
Zr(1)-O(12)	2.202(15)	Zr(4)-O(41)	2.206(16)
Zr(1)-O(16)	2.192(14)	Zr(4)-O(45)	2.282(17)
Zr(2)-O(14)	2.199(15)	Zr(5)-O(43)	2.188(17)
Zr(2)-O(20)	2.205(16)	Zr(5)-O(49)	2.284(15)
Zr(3)-O(17)	2.203(14)	Zr(6)-O(47)	2.197(15)
Zr(3)-O(22)	2.196(16)	Zr(6)-O(51)	2.219(15)
μ_2- Pivalates bridging Zr			
		Zr(4)-O(52)	2.247(17)
		Zr(5)-O(53)	2.215(17)
Chelating Pivalates			
Zr(1)-O(23)	2.251(16)	Zr(6)-O(54)	2.225(17)
Zr(1)-O(24)	2.270(15)	Zr(6)-O(55)	2.256(16)
Zr(2)-O(25)	2.268(16)		
Zr(2)-O(26)	2.225(15)		
Zr(3)-O(27)	2.245(15)		
Zr(3)-O(28)	2.294(16)		
η_1- Pivalic acids			
		Zr(4)-O(56)	2.155(16)
		Zr(5)-O(58)	2.088(16)

Table A.13: Bond angles in Zr6Ti8piv for [°]

1 st Fragment		**2 nd Fragment**	
μ_3- **Oxygen (OH)**			
$\sum$M- O(1) -M	352.1(22)	$\sum$M-O(29)-M	349.5(22)
$\sum$M- O(2) -M	297.6(17)	$\sum$M-O(30)-M	309.6(20)
$\sum$M- O(3) -M	351.8(20)	$\sum$M-O(31)-M	347.5(21)
$\sum$M- O(4) -M	294.3(15)	$\sum$M-O(32)-M	299.0(18)
$\sum$M- O(5) -M	352.5(19)	$\sum$M-O(33)-M	350.8(19)
$\sum$M- O(6) -M	326.1(18)	$\sum$M-O(34)-M	342.3(19)
$\sum$M- O(7) -M	300.6(17)	$\sum$M-O(35)-M	302.4(17)
μ_2- **Oxygen**			
Ti(1)- O(8) -Ti(4)	136.3(9)	Ti(6)-O(36)-Ti(8)	139.4(9)
Ti(2)- O(9) -Ti(4)	135.9(8)	Ti(7)-O(37)-Ti(8)	139.4(8)
Ti(3)-O(10)-Ti(4)	136.6(9)		
Oxygen atoms in *trans* position of the Ti coordination octahedron			
O- Ti(1) -O	159.9(7)-174.0(7)	O- Ti(5) -O	172.8(7)-177.0(7)
O- Ti(2) -O	158.2(7)-173.9(6)	O- Ti(6) -O	162.5(7)-174.5(6)
O- Ti(3) -O	158.4(7)-172.4(6)	O- Ti(7) -O	159.3(7)-174.1(6)
O- Ti(4) -O	168.7(7)-176.6(7)	O- Ti(8) -O	165.8(7)-166.5(7)
Oxygen atoms in *cis* position of the Ti coordination octahedron			
O- Ti(1) -O	76.7(6)-102.9(7)	O- Ti(5) -O	85.6(7)-96.9(6)
O- Ti(2) -O	77.1(6)-103.2(7)	O- Ti(6) -O	80.5(6)-100.7(6)
O- Ti(3) -O	76.5(6)-103.7(7)	O- Ti(7) -O	78.0(6)-102.6(7)
O- Ti(4) -O	78.9(7)-96.9(6)	O- Ti(8) -O	73.6(6)-101.6(7)
μ_2- **O^nBu**			
Ti(4)-O(62)-Ti(8)	102.4(7)	Ti(4)-O(63)-Ti(8)	102.1(7)

Table A.14: Bond lengths and atom distances for Zr4Ti3ada in [Å]

Metal- metal distance			
Zr(1)-Zr(1)’	3.333(2)	Zr(1)-Ti(1)	3.089(3)
Zr(1)-Zr(2)	3.601(2)	Ti(1)-Ti(2)	3.568(3)
Metal - core oxygen			
Zr(1)-O(1)	2.141(7)	Ti(1)-O(1)	1.915(8)
Zr(1)-O(2)	2.138(6)	Ti(1)-O(2)	1.847(9)
Zr(1)-O(4)	2.038(6)	Ti(2)-O(1)	1.928(7)
Zr(2)-O(4)	2.117(11)	Ti(2)-O(3)	1.900(4)
Zr(2)-O(5)	2.029(8)	Ti(2)-O(5)	1.791(8)
Zr(3)-O(3)	2.130(9)		
μ_3- **Carboxylates**			
Zr(1)-O(8)	2.205(8)	Ti(1)-O(7)	2.067(9)
Zr(1)-O(12)	2.175(8)	Ti(1)-O(9)	1.945(11)
Zr(1)-O(15)	2.182(7)	Ti(2)-O(11)	2.036(8)
Zr(1)-O(16)	2.154(7)	Ti(2)-O(13)	2.021(8)
Zr(2)-O(17)	2.142(8)		
Zr(3)-O(10)	2.258(11)		
Zr(3)-O(14)	2.225(8)		
μ_2- **Alkoxy ligands**			
Zr(3)-O(6)	2.113(8)	Ti(2)-O(6)	2.103(7)
Chelating carboxylates			
Zr(2)-O(18)	2.282(16)	Zr(3)-O(20)	2.258(8)
Zr(2)-O(19)	2.196(16)		

Table A.15: Bond angles for Zr4Ti3ada in [°]

Core oxygen	
$\sum$M-O(1)-M	347.2(10)
$\sum$M-O(2)-M	315.2(10)
$\sum$M-O(3)-M	350.9(11)
$\sum$M-O(4)-M	349.9(11)
$\sum$M-O(5)-M	326.8(11)
***trans* oxygen atoms of the $[TiO_6]$ octahedron**	
O-Ti(1)-O	171.5(4)-173.8(5)
O-Ti(2)-O	164.2(3)-174.0(4)
***cis* oxygen atoms of the $[TiO_6]$ octahedron**	
O-Ti(1)-O	85.6(3)-98.6(3)
O-Ti(2)-O	76.1(3)-98.9(4)

Table A.16: Bond lengths and atom distances [Å] for Zn/Cd-Ti clusters compared to $Ti_6(O^nPr)_8(OMc)_8$ [78] [Ti6flat]

	Zn2Ti4	**Ti6flat**		**Cd4Ti2**
Metal - metal distance				
Zn(1)-Ti(1)	3.1470(4)	3.1054(8)	Ti(1)-Cd(1)	3.4499(9)
Zn(1)-Ti(2)	3.2701(4)	3.5680(9)	Ti(1)-Cd(2)	3.4521(9)
Zn(1)-Ti(1)'	6.2194(5)	6.4879(1)	Ti(1)-Cd(1)'	5.9410(12)
Zn(1)-Ti(2)'	6.3108(5)	6.348(1)	Ti(1)-Cd(2)'	7.2545(13)
Zn(1)-Zn(1)'	8.6834(5)	9.0219(10)	Ti(1)-Ti(1)'	8.9992(16)
Ti(1)-Ti(2)	3.3652(5)	3.4587(8)	Cd(1)-Cd(2)	3.8904(8)
Ti(1)-Ti(1)'	4.6657(6)	4.6966(8)	Cd(1)-Cd(1)'	3.6618(8)
Ti(1)-Ti(2)'	3.3652(1)	3.3758(8)	Cd(1)-Cd(2)'	3.9525(8)
Ti(2)-Ti(2)'	5.0633(6)	4.9659(8)	Cd(2)-Cd(2)'	6.9358(14)
Metal - core oxygen bonds				
Zn(1)-O(1)	1.9747(13)	2.070(2)	Ti(1)-O(1)	1.698(2)
Ti(1)-O(1)	1.8712(13)	1.910(2)	Cd(1)-O(1)	2.262(2)
Ti(1)-O(2)	1.7550(13)	1.766(2)		
Ti(2)-O(1)	1.9231(14)	1.911(2)	Cd(2)-O(1)	2.267(2)
Ti(2)-O(2)	1.8784(13)	1.885(2)		
Terminal alkoxy ligands			**Terminal alkohol ligand**	
Ti(2)-O(13)	1.7821(14)	1.768(3)		
Ti(3)-O(8)		1.794(3)		
Ti(3)-O(9)		1.806(3)	Ti(1)-O(14)	2.227(2)
μ_2- Alkoxy ligands			**μ_3- Methacrylate**	
Ti(2)-O(7)		2.084(2)	Cd(1)-O(2)	2.260(2)
Ti(3)-O(7)		1.966(2)	Cd(1)'-O(2)	2.355(2)
			Cd(2)-O(3)	2.267(3)
			Chelating/μ_2- bridging acetate	
			Cd(1)-O(4)	2.232(2)
			Cd(2)-O(4)	2.336(2)
			Cd(2)-O(5)	2.368(2)
μ_2- Methacrylates bridging Zn(Cd) and Ti				
Zn(1)-O(3)	1.9462(17)		Ti(1)-O(7)	2.012(2)
Zn(1)-O(5)	1.9568(16)	2.064(2)	Ti(1)-O(9)	1.997(2)
Zn(1)-O(7)	1.9399(16)	2.152(3)	Ti(1)-O(11)	1.977(2)
			Ti(1)-O(13)	1.986(2)
Ti(1)-O(4)	2.1057(15)		Cd(1)-O(6)	2.256(2)
Ti(1)-O(6)	2.0123(14)	2.011(2)	Cd(1)-O(8)	2.260(2)
Ti(2)-O(8)	2.0435(14)	2.052(3)	Cd(2)-O(10)	2.279(3)
			Cd(2)-O(12)	2.228(3)
μ_2- Methacrylates bridging Ti				
Ti(1)-O(9)	2.0752(14)	2.049(2)		
Ti(1)-O(11)	1.9994(14)	2.010(2)		
Ti(2)-O(10)	2.0383(15)	2.090(2)		
Ti(2)-O(12)	2.0936(14)	2.091(2)		

Table A.17: Bond angles [°] for Zn/Cd-Ti clusters compared to $\mathrm{Ti_6(O^nPr)_8(OMc)_8}$ [78] [Ti6flat]

	Zn2Ti4	**Ti6flat**		**Cd4Ti2**
Core oxygen				
Zn(1)-O(1)-Ti(1)	109.80(7)	102.49(10)	Cd(1)-O(1)-Cd(2)	118.40(9)
Zn(1)-O(1)-Ti(2)	114.05(6)	127.38(10)	Cd(1)-O(1)-Ti(1)	120.55(11)
Ti(1)-O(1)-Ti(2)	136.01(7)	129.72(11)	Cd(2)-O(1)-Ti(1)	120.36(11)
$\sum$M-O(1)-M	359.86(20)	354.61(31)	$\sum$M-O(1)-M	359.31(31)
Ti(1)-O(2)-Ti(2)	135.67(8)	135.24(12)		
O-Zn(1)-O	103.24(6)-116.79(6)			
Oxygen atoms in *trans* position of the Cd(Ti) coordination octahedron				
O-Ti(1)-O	166.70(6)-168.43(6)	162.88(10)-175.98(9)	O-Ti(1)-O	164.38(10)-178.06(10)
O-Ti(2)-O	165.23(6)-174.36(6)	164.09(10)-169.88(10)	O-Cd(1)-O	160.91(9)-179.40(9)
O-Ti(3)-O		163.15(11)-174.53(11)	O-Cd(2)-O	155.42(9)-174.23(10)
Oxygen atoms in *cis* position of the Cd(Ti) coordination octahedron				
O-Ti(1)-O	78.71(6)-101.52(6)	79.89(9)-99.76(10)	O-Ti(1)-O	81.19(9)-98.31(10)
O-Ti(2)-O	80.89(6)-97.83(6)	77.29(9)-99.33(11)	O-Cd(1)-O	75.00(10)-105.58(9)
O-Ti(3)-O		78.15(9)-104.47(9)	O-Cd(2)-O	55.50(8)-109.49(9)
			Chelating/μ_2- Bridging methacrylate	
			Cd(1)-O(2)-Cd(2)	105.00(10)
			Cd(1)-O(4)-Cd(2)	119.85(10)

Table A.18: Bond lengths and atom distances for chain like Ca/Sr-Ti clusters [Å]. The two values for Ca2Ti4a and Sr2Ti4 are due to the doubling of the assymetric unit compared to Ca2T4

	Ca2Ti4	**Ca2Ti4a**			**Sr2Ti4met**	
Metal - metal distance						
Ca(1)-Ca(1)'	4.0045(9)	3.7089(8)		Sr(1)-Sr(2)	3.9228(3)	
Ca(1)-Ti(1)	3.5083(6)	3.5606(7)	3.5653(8)	Sr(1)-Ti(1)	3.6312(4)	3.6707(4)
Ca(1)-Ti(2)'	3.6524(6)	3.6737(7)	3.7374(7)	Sr(1)-Ti(2)'	3.7280(4)	3.7421(4)
Ti(1)-Ti(1)'	4.6141(5)	4.7162(7)	3.7224(7)	Ti(1)-Ti(1)'	4.7773(5)	4.6768(5)
Ti(1)-Ti(2)	3.3719(5)	3.3713(7)	3.3968(7)	Ti(1)-Ti(2)	3.3691(5)	3.3695(5)
Ti(1)-Ti(2)'	3.4498(6)	3.4366(6)	3.4406(7)	Ti(1)-Ti(2)'	3.4312(5)	3.4185(5)
Ti(2)-Ti(2)'	5.0253(6)	4.9102(6)	4.9450(7)	Ti(2)-Ti(2)'	4.8400(5)	4.9200(5)
Metal - core oxygen bonds						
Ca(1)-O(1)	2.4549(16)	2.5004(18)	2.5336(18)	Sr(1)-O(1)	2.5808(15)	2.6114(15)
Ti(1)-O(1)	1.9645(16)	1.9307(19)	1.9681(19)	Ti(1)-O(1)	1.8033(16)	1.8104(16)
Ti(1)-O(2)	1.7297(16)	1.7445(18)	1.7273(19)	Ti(1)-O(2)	1.8361(15)	1.8341(15)
Ti(2)-O(1)	1.7600(16)	1.7736(19)	1.7487(18)	Ti(2)-O(1)	1.8840(16)	1.8777(16)
Ti(2)-O(2)	1.9124(16)	1.8745(18)	1.9304(19)	Ti(2)-O(2)	1.7775(15)	1.7849(15)
Linking carboxylate						
Ca(1)-O(3)	2.4276(17)	2.560(2)	2.432(2)	Sr(1)-O(3)	2.8769(17)	2.8622(16)
Ca(1)-O(4)	2.6594(19)	2.5101(19)	2.546(2)	Ti(1)-O(3)	2.0165(16)	2.0329(15)
Ca(1)'-O(4)	2.2916(18)	2.3604(19)	2.389(2)	Sr(2)-O(4)	2.598(4)	2.469(2)
Ti(1)-O(3)	2.1116(18)	2.1011(19)	2.106(2)	Sr(2)-O(4A)	2.438(13)	
				Sr(1)-O(5)	2.5947(16)	2.5720(15)
				Sr(2)-O(5)	2.7048(16)	2.6320(15)
				Ti(1)-O(6)	1.9623(16)	1.9622(16)
μ_2- methacrylic acid bridging Ca				**Terminal methacrylic acid on Sr**		
Ca(1)-O(15)		2.489(2)		Sr(1)-O(15)	2.5577(17)	2.5559(17)
Ca(2)-O(15)		2.812(2)				
μ_2- methacrylates bridging Ca(Sr) and Ti						
Ca(1)-O(5)	2.361(2)	2.362(2)	2.413(2)	Sr(1)-O(7)	2.6322(16)	2.5704(17)
Ca(1)-O(7)	2.317(2)	2.417(2)	2.385(2)	Ti(2)-O(8)	1.9534(16)	1.9385(16)
Ca(1)-O(9)	2.342(2)	2.358(2)	2.300(2)	**Chelating Sr, bridging Sr and Ti**		
Ti(1)-O(6)	1.9633(18)	1.935(2)	1.956(2)	Sr(1)-O(13)	2.9464(17)	2.9930(16)
Ti(2)-O(8)	1.950(2)	1.9667(19)	1.942(2)	Sr(1)-O(14)	2.5585(18)	2.5792(17)
Ti(2)-O(10)	1.9575(19)	1.957(2)	1.9821(19)	Ti(2)-O(13)	2.0263(16)	2.0248(16)
μ_2- methacrylates bridging Ti						
Ti(1)-O(11)	2.0205(18)	2.025(2)	2.026(2)	Ti(1)-O(9)	2.0479(16)	2.0192(16)
Ti(1)-O(13)	2.0044(17)	2.034(2)	2.002(2)	Ti(1)-O(11)	2.0874(17)	2.0822(16)
Ti(2)-O(12)	2.0256(18)	2.045(2)	2.0321(19)	Ti(2)-O(10)	2.0128(16)	2.0434(16)
Ti(2)-O(14)	2.1585(18)	2.127(2)	2.1424(19)	Ti(2)-O(12)	2.0707(17)	2.0728(16)

Table A.19: Bond angles for the chain like Ca/Ti clusters in [°]

	Ca2Ti4	**Ca2Ti4a**	
Core oxygen			
Ca(1)-O(1)-Ti(1)	104.55(7)	106.22(8)	104.04(7)
Ca(1)-O(1)-Ti(2)	119.20(8)	117.52(9)	120.46(9)
Ti(1)-O(1)-Ti(2)	135.64(9)	136.12(10)	135.47(10)
Ti(1)-O(2)-Ti(2)	135.53(10)	137.33(11)	136.39(11)
$\sum$M-O(1)-M	359.39(24)	359.86(27)	359.97(26)
Oxygen atoms in *trans* position of the Ti coordination octahedron			
O-Ti(1)-O	165.67(7)-172.97(8)	169.19(8)-172.95(8)	166.62(9)-171.86(9)
O-Ti(2)-O	164.03(8)-178.40(9)	165.02(9)-177.17(8)	160.91(8)-177.20(8)
Oxygen atoms in *cis* position of the Ti coordination octahedron			
O-Ti(1)-O	81.11(7)-98.70(8)	81.93(8)-99.66(8)	80.67(8)-101.00(8)
O-Ti(2)-O	81.14(8)-98.36(8)	81.72(8)-98.23(8)	81.15(8)-98.91(8)
Chelating/μ_3-Bridging (linking) carboxylates			
Ca(1)-O(3)-Ti(1)	101.00(7)	99.15(8)	103.34(8)
Ca(1)-O(4)-Ca(1)'	107.73(7)	99.15(7)	97.38(7)

Table A.20: Bond angles for the chain like Sr/Ti clusters in [°]

	Sr2Ti4met	
Core oxygen		
Sr(1)- O(1) -Ti(1)	110.59(7)	110.93(7)
Sr(1)- O(1) -Ti(2)	112.29(7)	111.90(7)
Ti(1)- O(1) -Ti(2)	137.04(9)	135.91(9)
Ti(1)- O(2) -Ti(2)	137.60(9)	137.19(9)
$\sum$M- O(1) -M	359.92(23)	358.74(23)
***trans* oxygen atoms in the [TiO_6] octahedron**		
O- Ti(1) -O	171.01(7)-173.90(7)	169.02(7)-174.05(7)
O- Ti(2) -O	170.19(7)-174.39(7)	169.71(7)-174.26(7)
***cis* oxygen atoms in the [TiO_6] octahedron**		
O- Ti(1) -O	85.37(7)-98.49(7)	83.60(7)-99.10(7)
O- Ti(2) -O	83.03(7)-97.94(7)	82.06(6)-97.97(7)
μ_3- Methacrylates (linking)		
Sr(1)- O(3) -Ti(1)	94.17(6)	95.67(6)
Sr(1)- O(5) -Sr(2)	95.48(5)	97.83(5)
Chelating/μ_2-Bridging Methacrylates		
Sr(1)-O(13)-Ti(2)	95.34(6)	94.47(6)

Table A.21: Comparison of the bond lengths [Å] and atom distances for Sr2Ti8, Pb2Ti8 and Pb2Ti6

Sr2Ti8		**Pb2Ti8**		**Pb2Ti6**	
Metal- metal distance					
Sr(1)-Sr(1)'	3.791(3)	Pb(1)-Pb(1)'	4.515(4)	Pb(1)-Pb(2)	3.8448(3)
Sr(1)-Ti(1)	3.5096(17)	Pb(1)-Ti(1)	3.630(3)	Pb(1)-Ti(1)	3.5681(6)
Sr(1)-Ti(1)'	5.9326(17)	Pb(1)-Ti(1)'	4.297(3)		
Sr(1)-Ti(2)	3.563(4)	Pb(1)-Ti(2)	3.593(3)	Pb(1)-Ti(2)	3.3438(6)
Sr(1)-Ti(3)	3.4821(16)	Pb(1)-Ti(3)	3.580(3)	Pb(1)-Ti(3)	3.8087(6)
Sr(1)-Ti(4)	4.0161(16)	Pb(1)-Ti(4)	3.809(3)	Pb(1)-Ti(4)	4.7070(6)
Sr(1)-Ti(4)'	4.186(2)	Pb(1)-Ti(4)'	4.088(3)	Pb(2)-Ti(3)	4.6086(7)
Sr(1)-Sr(1A)	0.520(11)	Pb(1)-Pb(1A)	0.2372(79)	Pb(2)-Ti(4)	3.7613(6)
				Pb(2)-Ti(5)	3.3263(6)
				Pb(2)-Ti(6)	3.6811(7)
Ti(1)-Ti(2)	3.405(3)	Ti(1)-Ti(2)	3.4894(18)	Ti(1)-Ti(2)	3.4686(10)
Ti(1)-Ti(4)'	3.4347(12)	Ti(1)-Ti(4)'	3.3732(18)	Ti(1)-Ti(4)'	
Ti(2)-Ti(3)	3.520(3)	Ti(2)-Ti(3)	3.428(2)	Ti(2)-Ti(3)	3.4747(9)
Ti(3)-Ti(4)	3.3745(13)	Ti(3)-Ti(4)	3.4613(18)	Ti(3)-Ti(4)	3.3598(8)
				Ti(4)-Ti(5)	3.4892(8)
				Ti(5)-Ti(6)	3.4722(9)
Ti(1)-Ti(1)'	8.9806(14)	Ti(1)-Ti(1)'	6.5494(18)	Ti(1)-Ti(5)	9.9191(9)
				Ti(1)-Ti(6)	9.8278(9)
Ti(2)-Ti(2)'	9.9830(44)	Ti(2)-Ti(2)'	9.7419(17)	Ti(2)-Ti(6)	9.9631(9)
Ti(3)-Ti(3)'	7.8787(14)	Ti(3)-Ti(3)'	9.5930(18)		
Ti(4)-Ti(4)'	7.2755(13)	Ti(4)-Ti(4)'	6.4845(23)		
Metal - core oxygen					
Sr(1)-O(1)	2.535(3)	Pb(1)-O(1)	2.572(5)	Pb(1)-O(1)	2.344(2)
Sr(1)-O(2)	2.554(3)	Pb(1)-O(2)	2.654(5)	Pb(1)-O(2)	2.558(2)
Sr(1)-O(3)	2.699(3)	Pb(1)-O(3)	2.9325(51)	Pb(1)-O(5)	3.3747(21)
Sr(1)-O(4)	2.863(3)	Pb(1)-O(4)	3.1706(57)	Pb(2)-O(3)	2.543(2)
		Pb(1)-O(4)'	2.9306(44)	Pb(2)-O(4)	2.393(2)
Ti(1)-O(1)	1.791(3)	Ti(1)-O(1)	1.859(4)	Pb(2)-O(5)	3.2502(22)
Ti(1)-O(4)	1.849(3)	Ti(1)-O(4)	1.855(5)		
Ti(2)-O(1)	1.886(4)	Ti(2)-O(1)	1.831(4)	Ti(1)-O(1)	1.978(2)
Ti(2)-O(2)	1.904(4)	Ti(2)-O(2)	1.843(4)	Ti(2)-O(1)	1.780(2)
Ti(3)-O(2)	1.776(3)	Ti(3)-O(2)	1.796(4)	Ti(2)-O(2)	1.881(2)
Ti(3)-O(3)	1.840(3)	Ti(3)-O(3)	1.815(4)	Ti(3)-O(2)	1.794(2)
Ti(4)-O(3)	1.816(3)	Ti(4)-O(3)	1.863(4)	Ti(3)-O(5)	1.823(2)
Ti(4)-O(4)	1.808(3)	Ti(4)-O(4)	1.824(5)	Ti(4)-O(3)	1.817(2)
				Ti(4)-O(5)	1.812(2)
				Ti(5)-O(3)	1.848(2)
				Ti(5)-O(4)	1.780(2)
				Ti(6)-O(4)	1.972(2)
μ_3- Acetates				**μ_3- Methacrylates**	
Sr(1)'-O(5)	2.601(3)			Pb(1)-O(13)	2.995(3)
Sr(1)-O(5)	2.491(3)			Pb(1)-O(15)	2.884(2)
Ti(3)-O(6)	1.998(3)			Pb(2)-O(13)	2.699(2)
				Pb(2)-O(15)	2.870(3)
				Ti(3)-O(14)	1.966(3)
				Ti(4)-O(16)	1.954(2)
				μ_2- Alkoxy ligands	
				Pb(1)-O(6)	2.798(2)
				Ti(1)-O(6)	1.842(2)

Continued on next page

Sr2Ti8		Pb2Ti8		Pb2Ti6	
μ_2- Methacrylates bridging Sr(Pb) and Ti					
Sr(1)-O(7)	2.527(3)	Pb(1)-O(5)	2.391(7)	Pb(1)-O(9)	2.443(2)
Sr(1)-O(9)	2.582(4)	Pb(1)-O(7)	2.388(6)	Pb(1)-O(11)	2.415(2)
Ti(1)-O(8)	1.948(3)	Ti(2)-O(6)	1.940(6)	Pb(2)-O(17)	2.459(2)
Ti(4)-O(10)	1.931(3)	Ti(3)-O(8)	1.955(5)	Pb(2)-O(19)	2.491(3)
				Ti(1)-O(10)	1.979(2)
				Ti(2)-O(12)	1.955(3)
				Ti(5)-O(18)	1.969(2)
				Ti(6)-O(20)	1.943(3)
μ_2- Methacrylates bridging Ti					
Ti(1)-O(11)	2.071(3)	Ti(1)-O(11)	2.055(5)	Ti(1)-O(23)	2.052(2)
Ti(1)-O(13)	2.030(3)	Ti(1)-O(13)	2.067(5)	Ti(1)-O(25)	2.120(3)
Ti(1)-O(15)	2.062(3)	Ti(1)-O(15)	2.072(5)	Ti(2)-O(24)	2.038(2)
Ti(2)-O(12)	2.039(5)	Ti(2)-O(12)	2.044(5)	Ti(2)-O(26)	2.004(2)
Ti(2)-O(14)	2.125(5)	Ti(2)-O(17)	2.033(5)	Ti(2)-O(27)	2.074(3)
Ti(2)-O(17)	2.047(5)	Ti(3)-O(18)	2.033(5)	Ti(3)-O(28)	2.061(2)
Ti(3)-O(18)	2.064(3)	Ti(3)-O(19)	2.073(5)	Ti(3)-O(29)	2.082(2)
Ti(3)-O(19)	2.099(3)	Ti(4)-O(14)	2.056(5)	Ti(3)-O(31)	2.039(2)
Ti(3)-O(21)	1.988(3)	Ti(4)-O(16)	2.044(5)	Ti(4)-O(30)	2.049(2)
Ti(4)-O(16)	2.063(3)	Ti(4)-O(20)	2.069(5)	Ti(4)-O(32)	2.061(2)
Ti(4)-O(20)	2.003(3)			Ti(4)-O(33)	2.071(2)
Ti(4)-O(22)	2.153(3)			Ti(5)-O(34)	2.090(2)
				Ti(5)-O(35)	2.019(2)
				Ti(5)-O(37)	2.027(2)
				Ti(6)-O(36)	2.070(2)
				Ti(6)-O(38)	2.045(2)
Carboxylate/alkoxy ligand in disordered part					
Sr(1)-O(23B)	3.04(2)	Pb(1)-O(9)	2.482(9)	Pb(2)-O(21)	2.761(4)
Ti(2)-O(23)	1.723(5)	Ti(4)-O(10)	1.863(5)	Pb(2)-O(22)	3.027(3)
Ti(2A)-O(23)	2.195(17)	Pb(1A)-O(25A)	2.73(3)	Ti(6)-O(22)	1.891(3)
		Ti(1)-O(23)	1.833(6)		
Terminal alkoxy ligands					
		Ti(2)-O(21)	1.999(5)	Ti(1)-O(7)	1.765(2)
				Ti(6)-O(8)	1.766(3)
Terminal carboxylic acid					
		Ti(3)-O(24)	2.078(5)		

Table A.22: Comparison of the bond angles for Sr2Ti8, Pb2Ti8 and Pb2Ti6 [°]

	Sr2Ti8		**Pb2Ti8**		**Pb2Ti6**
		Disorder		**Disorder**	
Core oxygen					
∑M-O(1)-M	349.3(5)	343.6(2)	359.1(7)	359.4(7)	353.2(3)
∑M-O(2)-M	357.0(5)	353.8(2)	359.0(8)	359.3(7)	359.7(3)
∑M-O(3)-M	357.7(4)	353.9(5)	331.0(7)	329.8(7)	359.9(3)
∑M-O(4)-M	359.4(6)	359.2(7)			354.7(3)
Oxygen atoms in *trans* position of the Ti coordination octahedron					
O-Ti(1)-O	169.84(15)-172.75(14)		169.2(2)-169.4(2)		169.35(10)-172.89(11)
O-Ti(2)-O	163.7(2)-168.6(2)	160.6(11)-167.8(10)	171.2(2)-174.1(2)		170.36(11)-176.99(11)
O-Ti(3)-O	166.07(13)-177.34(14)		167.9(2)-173.7(2)		168.28(10)-174.64(10)
O-Ti(4)-O	165.96(14)-173.03(14)		167.0(2)-170.2(2)		168.44(10)-173.29(9)
O-Ti(5)-O					169.94(10)-177.02(10)
O-Ti(6)-O					170.72(11)-174.38(11)
Oxygen atoms in *cis* position of the Ti coordination octahedron					
O-Ti(1)-O	82.17(13)-96.48(14)		81.8(2)-98.2(2)		82.81(9)-100.51(11)
O-Ti(2)-O	76.87(17)-104.5(2)	77.5(6)-107.4(10)	83.5(2)-95.2(2)		80.37(10)-96.85(11)
O-Ti(3)-O	82.28(13)-97.98(14)		83.58(19)-96.7(2)		81.35(10)-97.95(10)
O-Ti(4)-O	81.46(13)-99.80(14)		79.17(19)-99.4(2)		79.95(9)-94.65(10)
O-Ti(5)-O					83.12(9)-96.56(11)
O-Ti(6)-O					83.42(9)-100.85(12)

Table A.23: Bond lengths and atom distances for Pb4Ti8 given in [Å]

Metal - metal distances					
Pb(1)-Pb(2)	3.8287(4)	Pb(1)-Pb(4)	7.9325(6)	Pb(2)-Pb(4)	6.1687(4)
Pb(1)-Pb(3)	3.8332(4)	Pb(2)-Pb(3)	3.6733(11)	Pb(3)-Pb(4)	6.1601(4)
Pb(1)-Ti(1)	3.5111(11)	Pb(2)-Ti(1)	3.5056(10)	Pb(3)-Ti(2)	3.4987(10)
Pb(1)-Ti(2)	3.5336(10)	Pb(2)-Ti(3)	3.6733(11)	Pb(3)-Ti(3)	3.6743(11)
Pb(1)-Ti(3)	6.3052(12)	Pb(2)-Ti(2)	6.2925(11)	Pb(3)-Ti(1)	6.2870(12)
Pb(1)-Ti(4)	3.8849(10)	Pb(2)-Ti(4)	3.3989(10)	Pb(3)-Ti(5)	3.4078(10)
Pb(1)-Ti(5)	3.8640(9)	Pb(2)-Ti(6)	3.3778(9)	Pb(3)-Ti(6)	3.3670(10)
Pb(4)-Ti(6)	3.3295(9)	Pb(4)-Ti(7)	3.3100(10)	Pb(4)-Ti(8)	3.3268(10)
Ti(1)-Ti(4)	3.1887(13)	Ti(2)-Ti(5)	3.1862(13)	Ti(3)-Ti(6)	2.9684(13)
Ti(4)-Ti(5)	3.8219(14)	Ti(4)-Ti(6)	2.9113(13)	Ti(5)-Ti(6)	2.9095(13)
Ti(6)-Ti(7)	3.6679(13)	Ti(6)-Ti(8)	3.6409(13)		
Ti(7)-Ti(8)	3.0351(13)				
μ_4- **Oxygen**					
Pb(1)-O(1)	2.306(4)	Pb(2)-O(1)	2.398(4)	Pb(3)-O(2)	2.396(4)
Pb(1)-O(2)	2.299(4)	Pb(2)-O(3)	2.295(3)	Pb(3)-O(3)	2.293(3)
				Pb(4)-O(8)	2.237(3)
Ti(1)-O(1)	1.978(4)	Ti(4)-O(1)	2.050(4)	Ti(6)-O(8)	1.955(4)
Ti(2)-O(2)	1.986(4)	Ti(5)-O(2)	2.053(4)	Ti(7)-O(8)	2.118(4)
Ti(3)-O(3)	2.064(4)	Ti(6)-O(3)	1.950(4)	Ti(8)-O(8)	2.112(3)
μ_3- **Oxygen**					
Pb(2)-O(4)	2.388(3)	Pb(3)-O(5)	2.402(4)	Pb(4)-O(7)	2.387(4)
Ti(3)-O(7)	1.867(4)	Ti(5)-O(5)	1.866(4)	Ti(6)-O(5)	1.938(4)
Ti(4)-O(4)	1.862(4)	Ti(5)-O(6)	1.917(4)	Ti(6)-O(6)	2.027(4)
Ti(4)-O(6)	1.921(4)	Ti(6)-O(4)	1.949(3)	Ti(6)-O(7)	1.932(4)
μ_2- **Oxygen**					
Ti(4)-O(9)	1.852(4)	Ti(7)-O(9)	1.812(4)		
Ti(5)-O(10)	1.844(4)	Ti(8)-O(10)	1.814(4)		
μ_2- **OAc**					
Ti(1)-O(13)	2.165(5)	Ti(4)-O(14)	2.062(4)		
Ti(2)-O(15)	2.152(4)	Ti(5)-O(16)	2.081(4)		
μ_3- **O^{i}Pr**					
Pb(1)-O(11)	2.295(4)	Pb(2)-O(11)	2.622(4)	Pb(3)-O(11)	2.620(4)
Pb(4)-O(12)	2.508(4)	Ti(7)-O(12)	2.176(4)	Ti(8)-O(12)	2.175(4)
μ_2- **O^{i}Pr**					
Pb(1)-O(17)	2.7794(45)	Ti(1)-O(17)	1.872(5)	Ti(4)-O(23)	1.989(4)
Pb(1)-O(18)	2.8377(41)	Ti(1)-O(19)	1.863(4)	Ti(5)-O(24)	1.995(4)
Pb(2)-O(19)	2.689(4)	Ti(1)-O(23)	2.086(4)	Ti(7)-O(25)	1.946(4)
Pb(2)-O(21)	2.8352(40)	Ti(2)-O(18)	1.873(4)	Ti(7)-O(27)	2.045(4)
Pb(3)-O(22)	2.8702(40)	Ti(2)-O(20)	1.879(4)	Ti(8)-O(26)	1.944(4)
Pb(3)-O(20)	2.634(4)	Ti(2)-O(24)	2.084(4)	Ti(8)-O(27)	2.037(4)
Pb(4)-O(25)	2.402(4)	Ti(3)-O(21)	1.866(4)		
Pb(4)-O(26)	2.419(4)	Ti(3)-O(22)	1.860(4)		
Terminal O^{i}Pr					
Ti(1)-O(28)	1.804(4)	Ti(3)-O(30)	1.802(4)	Ti(8)-O(32)	1.798(4)
Ti(2)-O(29)	1.807(4)	Ti(7)-O(31)	1.788(4)		

Table A.24: Bond angles for Pb4Ti8 given in [°]

μ_4- **Oxygen**		μ_3-**O^{i}Pr**	
M- O(1) -M	99.36(15)-126.11(17)	Pb(1)-O(11)-Pb(2)	102.07(14)
M- O(2) -M	99.70(14)-125.14(17)	Pb(1)-O(11)-Pb(3)	102.29(14)
M- O(3) -M	95.34(15)-118.02(15)	Pb(2)-O(11)-Pb(3)	97.24(13)
M- O(8) -M	91.70(14)-128.43(18)	Pb(4)-O(12)-Ti(7)	89.66(13)
μ_3- **Oxygen**		Pb(4)-O(12)-Ti(8)	90.26(14)
Ti(4)- O(6) -Ti(5)	169.5(2)	Ti(7)-O(12)-Ti(8)	88.48(14)
Ti(4)- O(6) -Ti(6)	94.98(15)	μ_2-**O^{i}Pr**	
Ti(5)- O(6) -Ti(6)	95.04(15)	Pb(1)-O(17)-Ti(1)	96.06(18)
$\sum$ M- O(4) -M	304.0(5)	Pb(1)-O(18)-Ti(2)	94.88(16)
$\sum$ M- O(5) -M	306.3(5)	Pb(2)-O(19)-Ti(1)	99.12(15)
$\sum$ M- O(6) -M	356.5(5)	Pb(3)-O(20)-Ti(2)	100.30(15)
$\sum$ M- O(7) -M	360.0(5)	Pb(3)-O(21)-Ti(3)	100.74(16)
μ_2- **Oxygen**		Pb(3)-O(22)-Ti(3)	99.71(16)
Ti(4)- O(9) -Ti(7)	138.0(2)	Ti(1)-O(23)-Ti(4)	102.95(17)
Ti(5)-O(10)-Ti(8)	136.7(2)	Ti(2)-O(24)-Ti(5)	102.70(16)
		Pb(4)-O(25)-Ti(7)	98.61(15)
		Pb(4)-O(26)-Ti(8)	98.79(15)
		Ti(7)-O(27)-Ti(8)	96.09(16)

Table A.25: Bond lengths and atom distances for Pb6Ti6 in [Å]

Metal - metal distance					
Pb(1)-Pb(2)	3.9100(6)	Pb(4)-Pb(5)	3.9884(9)	Pb(4A)-Pb(5)	4.062(10)
Pb(1)-Pb(3)	7.0049(13)	Pb(4)-Pb(6)	7.011(2)	Pb(4A)-Pb(6A)	7.078(9)
Pb(1)-Pb(3A)	7.047(19)	Pb(4)-Pb(6A)	7.044(4)	Pb(4A)-Pb(6)	7.041(9)
Pb(2)-Pb(3)	4.0036(11)	Pb(5)-Pb(6)	3.932(2)		
Pb(2)-Pb(3A)	3.99(2)	Pb(5)-Pb(6A)	3.939(3)		
Pb(2)-Pb(5)	4.5535(7)	Pb(3)-Pb(6)	6.619(3)	Pb(3A)-Pb(6A)	6.88(2)
		Pb(3)-Pb(6A)	6.668(3)	Pb(3A)-Pb(6)	6.83(2)
Pb(3)-Pb(3A)	0.31(2)	Pb(4)-Pb(4A)	0.357(15)	Pb(6)-Pb(6A)	0.088(5)
Pb(1)-Pb(1)'	4.3999(7)	Pb(4)-Pb(4)'	4.7630(11)		
Pb(1)-Ti(1)	3.8443(8)	Pb(4)-Ti(3)	3.7615(14)	Pb(4A)-Ti(3)	3.630(14)
Pb(1)-Ti(2)	3.7851(8)	Pb(4)-Ti(4)	3.8407(14)	Pb(4A)-Ti(4)	3.566(16)
Pb(2)-Ti(3)	3.6048(8)	Pb(5)-Ti(1)	3.8578(8)		
Pb(2)-Ti(4)	3.7557(8)	Pb(5)-Ti(2)	3.5653(8)		
Pb(3)-Ti(5)	3.6784(16)	Pb(6)-Ti(5)	3.758(3)		
Pb(3)-Ti(6)	3.7454(16)	Pb(6)-Ti(6)	3.675(3)		
Pb(3A)-Ti(5)	3.77(2)	Pb(6A)-Ti(5)	3.939(3)		
Pb(3A)-Ti(6)	4.00(2)	Pb(6A)-Ti(6)	3.687(3)		
Ti(1)-Ti(6)	3.5041(9)	Ti(2)-Ti(3)	3.5914(10)	Ti(4)-Ti(5)	3.4930(10)
Ti(1)-Ti(2)	2.8522(8)	Ti(3)-Ti(4)	2.8398(8)	Ti(5)-Ti(6)	2.9370(9)
Metal - μ_3-core oxygen bonds					
Pb(1)-O(1)	2.284(2)	Pb(4)-O(4)	2.277(2)	Pb(4A)-O(4)	2.081(11)
Pb(2)-O(2)	2.509(2)	Pb(5)-O(5)	2.519(2)		
Pb(3)-O(3)	2.244(3)	Pb(3A)-O(3)	2.42(2)		
Pb(6)-O(6)	2.262(3)	Pb(6A)-O(6)	2.305(4)		
Ti(1)-O(1)	1.901(2)	Ti(3)-O(2)	1.873(2)	Ti(5)-O(3)	1.930(2)
Ti(1)-O(5)	1.831(2)	Ti(3)-O(4)	1.931(2)	Ti(5)-O(6)	1.902(2)
Ti(2)-O(1)	1.932(2)	Ti(4)-O(2)	1.850(2)	Ti(6)-O(3)	1.909(2)
Ti(2)-O(5)	1.900(2)	Ti(4)-O(4)	1.895(2)	Ti(6)-O(6)	1.936(2)
Metal - μ_2-core oxygen bonds					
Ti(1)-O(9)	1.868(2)	Ti(4)-O(8)	1.856(2)		
Ti(2)-O(7)	1.837(2)	Ti(5)-O(8)	1.810(2)		
Ti(3)-O(7)	1.841(2)	Ti(6)-O(9)	1.799(2)		
Carboxylates chelating Pb and μ_3-bridging Pb atoms					
Pb(1)-O(10)	2.426(2)	Pb(4)-O(12)	2.496(3)	Pb(4A)-O(12)	2.569(8)
Pb(2)-O(10)	2.512(2)	Pb(5)-O(12)	2.657(3)		
Pb(2)-O(11)	2.756(2)	Pb(5)-O(13)	2.674(3)		
Pb(3)-O(11)	2.549(3)	Pb(6)-O(13)	2.562(3)		
Pb(3A)-O(11)	2.603(13)	Pb(6A)-O(13)	2.587(4)		
Methacrylates chelating Pb and μ_2-bridging Pb atoms					
Pb(2)-O(16)	2.674(2)	Pb(5)-O(20)	2.659(3)		
Pb(2)-O(17)	2.370(2)	Pb(5)-O(21)	2.382(3)		
Pb(3)-O(16)	2.613(3)	Pb(6)-O(20)	2.610(4)		
Pb(3A)-O(16)	2.40(2)	Pb(6A)-O(20)	2.557(4)		
μ_3- Methacrylates bridging two Pb and one Ti					
Pb(1)-O(14)	2.664(2)	Pb(4)-O(18)	2.735(3)	Pb(4A)-O(18)	2.964(105)
Pb(2)-O(14)	2.639(2)	Pb(5)-O(18)	2.585(2)		
Ti(3)-O(15)	2.001(2)	Ti(2)-O(19)	2.008(2)		

Continued on next page

μ_2- Methacrylates bridging Pb and Ti					
Pb(1)-O(22)	2.422(2)	Pb(4)-O(30)	2.545(3)	Pb(4A)-O(30)	2.503(7)
Pb(1)-O(24)	2.515(3)	Pb(4)-O(32)	2.432(3)	Pb(4A)-O(32)	2.151(15)
Pb(3)-O(26)	2.430(3)	Pb(6)-O(34)	2.425(5)		
Pb(3)-O(28)	2.407(3)	Pb(6)-O(36)	2.427(3)		
Pb(3A)-O(26)	2.55(2)	Pb(6A)-O(34)	2.503(5)		
Pb(3A)-O(28)	2.67(2)	Pb(6A)-O(36)	2.435(4)		
Ti(1)-O(23)	2.052(2)	Ti(3)-O(31)	2.018(2)		
Ti(2)-O(25)	1.991(2)	Ti(4)-O(33)	2.015(3)		
Ti(5)-O(27)	2.059(2)	Ti(5)-O(35)	1.991(3)		
Ti(6)-O(29)	1.989(3)	Ti(6)-O(37)	2.086(2)		
μ_2- Methacrylates bridging Ti atoms					
Ti(1)-O(38)	2.081(2)	Ti(4)-O(41)	2.097(2)		
Ti(1)-O(45)	2.072(2)	Ti(4)-O(42)	2.051(2)		
Ti(2)-O(39)	2.080(2)	Ti(3)-O(40)	2.084(2)		
Ti(6)-O(44)	2.045(3)	Ti(5)-O(43)	2.059(3)		
Distance to solvent molecule					
Pb(6)-O(46)	3.1177(220)	Pb(6A)-O(46)	3.0836(220)		

Table A.26: Bond angles for Pb6Ti6 in [°]

μ_3- Core oxygen			
Ti(1)-O(1)-Ti(2)	96.15(10)	Ti(3)-O(4)-Ti(4)	95.85(10)
Pb(1)-O(1)-Ti(1)	133.22(11)	Pb(4)-O(4)-Ti(3)	126.56(11)
Pb(1)-O(1)-Ti(2)	127.53(11)	Pb(4)-O(4)-Ti(4)	133.84(11)
Ti(3)-O(2)-Ti(4)	99.42(11)	Ti(1)-O(5)-Ti(2)	99.70(10)
Pb(2)-O(2)-Ti(3)	109.81(10)	Pb(5)-O(5)-Ti(1)	124.18(11)
Pb(2)-O(2)-Ti(4)	118.20(10)	Pb(5)-O(5)-Ti(2)	106.73(9)
Ti(5)-O(3)-Ti(6)	99.79(11)	Ti(5)-O(6)-Ti(6)	99.84(11)
Pb(3)-O(3)-Ti(5)	123.39(12)	Pb(6)-O(6)-Ti(5)	128.74(15)
Pb(3)-O(3)-Ti(6)	128.60(13)	Pb(6)-O(6)-Ti(6)	121.98(14)
Pb(3A)-O(3)-Ti(5)	119.9(3)	Ti(4)-O(4)-Pb(4A)	127.5(4)
Pb(3A)-O(3)-Ti(6)	134.5(5)	Ti(3)-O(4)-Pb(4A)	129.5(2)
		Ti(5)-O(6)-Pb(6A)	130.66(15)
		Ti(6)-O(6)-Pb(6A)	120.57(14)
$\sum$ M-O(1)-M	356.90(32)		
$\sum$ M-O(2)-M	327.43(31)		
$\sum$ M-O(3)-M	351.78(36)	$\sum$ M-O(3)-M(A)	354.2(9)
$\sum$ M-O(4)-M	356.25(32)	$\sum$ M-O(4)-M(A)	352.9(7)
$\sum$ M-O(5)-M	330.61(30)		
$\sum$ M-O(6)-M	350.56(40)	$\sum$ M-O(6)-M(A)	351.07(40)
μ_2- Core oxygen			
Ti(2)-O(7)-Ti(3)	155.13(13)		
Ti(4)-O(8)-Ti(5)	144.63(14)		
Ti(1)-O(9)-Ti(6)	145.69(13)		
***trans* oxygen atoms in [TiO_6]**		***cis* oxygen atoms in [TiO_6]**	
O-Ti(1)-O	166.69(10)-171.92(10)	O-Ti(1)-O	79.95(9)-99.13(10)
O-Ti(2)-O	165.57(10)-172.70(10)	O-Ti(2)-O	80.10(9)-98.35(10)
O-Ti(3)-O	164.29(10)-172.90(10)	O-Ti(3)-O	81.13(10)-98.15(10)
O-Ti(4)-O	166.18(11)-172.28(10)	O-Ti(4)-O	81.47(10)-98.83(10)
O-Ti(5)-O	163.76(11)-168.02(11)	O-Ti(5)-O	80.15(10)-100.69(10)
O-Ti(6)-O	165.83(10)-167.49(10)	O-Ti(6)-O	79.09(10)-100.79(10)
Carboxylate chelating Pb and μ_3-bridging Pb			
Pb(1)-O(10)-Pb(2)	104.72(8)	Pb(4)-O(12)-Pb(5)	101.40(9)
Pb(2)-O(11)-Pb(3)	97.92(8)	Pb(5)-O(13)-Pb(6)	97.33(10)
O(10)-C(1)-O(11)	121.1(3)	O(12)-C(5)-O(13)	121.3(3)
Pb(3A)-O(11)-Pb(2)	96.3(3)	Pb(4A)-O(12)-Pb(5)	102.02(16)
		Pb(5)-O(13)-Pb(6A)	96.94(11)
Methacrylate chelating Pb and μ_2-bridging Pb			
Pb(1)-O(14)-Pb(2)	95.00(7)	Pb(4)-O(18)-Pb(5)	97.08(8)
Pb(2)-O(16)-Pb(3)	98.45(9)	Pb(5)-O(20)-Pb(6)	96.53(12)
O(14)-C(9)-O(15)	125.0(3)	O(18)-C(17)-O(19)	124.2(3)
O(16)-C(13)-O(17)	121.8(3)	O(20)-C(21)-O(21)	122.1(3)
Pb(2)-O(16)-Pb(3A)	103.5(5)	Pb(5)-O(20)-Pb(6A)	98.06(13)

Table A.27: Bond lengths and atom distances for Cu/Ti clusters in [Å], the two values of the Cu4Ti5metS cluster are due to the two clusters crystalising in the unit cell

	Cu4Ti5met	**Cu4Ti5metS**		**Cu4Ti5Prop**
Metal - metal distance				
Cu(1)-Ti(1)	3.00593(16)	3.0055(2)	3.0061(3)	3.0132(3)
Cu(1)-Ti(2)	3.2864(3)	3.2856(3)	3.3239(4)	3.3016(5)
Cu(1)-Ti(3)	3.6153(3)	3.6198(4)	3.5816(4)	3.6219(5)
Cu(2)-Ti(2)	3.3254(3)	3.3241(4)	3.3277(4)	3.3325(5)
Cu(2)-Ti(3)	3.4660(3)	3.4595(4)	3.4398(4)	3.4204(4)
Ti(1)-Ti(2)	3.5252(2)	3.5162(3)	3.5215(3)	3.5240(4)
Ti(1)-Ti(3)	3.5406(3)	3.5494(3)	3.5376(3)	3.5443(4)
Ti(2)-Ti(3)	3.3959(3)	3.4006(4)	3.3862(4)	3.3995(6)
Metal - core oxygen bonds				
Cu(1)-O(1)	1.9585(9)	1.9588(10)	1.9764(11)	1.9695(15)
Cu(1)-O(2)	2.3432(9)	2.3532(11)	2.3192(10)	2.3499(14)
Cu(2)-O(3)	2.1982(9)	2.1894(11)	2.2022(10)	2.1841(15)
Ti(1)-O(1)	1.9176(8)	1.9169(10)	1.9250(10)	1.9162(14)
Ti(1)-O(2)	1.9183(9)	1.9167(11)	1.9148(11)	1.9221(15)
Ti(2)-O(1)	1.8508(9)	1.8444(11)	1.8445(11)	1.8551(15)
Ti(2)-O(3)	1.7985(9)	1.7938(11)	1.8046(11)	1.7954(16)
Ti(3)-O(2)	1.7684(10)	1.7705(11)	1.7734(11)	1.7646(15)
Ti(3)-O(3)	1.9075(9)	1.9192(11)	1.8826(11)	1.9068(15)
μ_2- Carboxylates bridging Cu and Ti				
Cu(1)-O(4)	1.9680(10)	1.9637(12)	1.9445(12)	1.9600(17)
Cu(1)-O(6)	1.9419(10)	1.9313(12)	1.9306(12)	1.9297(18)
Cu(1)-O(8)	1.9279(10)	1.9330(12)	1.9474(12)	1.9342(16)
Cu(2)-O(10)	1.9388(11)	1.9387(13)	1.9496(13)	1.9517(17)
Cu(2)-O(12)	1.9736(11)	1.9708(13)	1.9740(12)	1.9632(17)
Cu(2)-O(14)	1.9596(11)	1.9622(12)	1.9685(13)	1.9688(19)
Cu(2)-O(16)	1.9322(11)	1.9280(12)	1.9206(13)	1.9286(18)
Ti(1)-O(5)	1.9942(9)	1.9948(11)	1.9906(11)	2.0066(16)
Ti(2)-O(7)	2.0625(10)	2.0655(11)	2.0490(12)	2.0646(17)
Ti(2)-O(11)	1.9970(9)	2.0152(12)	2.0085(12)	2.0212(17)
Ti(2)-O(13)	2.0263(10)	2.0382(11)	2.0262(11)	2.0196(16)
Ti(3)-O(9)	2.0009(10)	1.9884(12)	2.0114(11)	1.9985(16)
Ti(3)-O(15)	1.9381(10)	1.9532(12)	1.9452(12)	1.9631(18)
Ti(3)-O(17)	2.1077(11)	2.0920(12)	2.0725(12)	2.0917(16)
μ_2- Carboxylates bridging Ti and Ti				
Ti(2)-O(18)	2.0081(9)	2.0048(11)	2.0033(12)	2.0072(16)
Ti(3)-O(19)	2.0131(10)	2.0183(12)	2.0358(12)	2.0281(18)

Table A.28: Bond angles for Cu/Ti clusters in [°], the two values of the Cu4Ti5metS cluster are due to the two clusters crystalised in the unit cell

	Cu4Ti5met	**Cu4Ti5metS**		**Cu4Ti5Prop**
Core oxygen				
Cu(1)-O(1)-Ti(1)	101.70(4)	101.69(5)	100.79(5)	101.68(7)
Cu(1)-O(1)-Ti(2)	119.22(4)	119.48(5)	120.86(5)	119.34(7)
Ti(1)-O(1)-Ti(2)	138.60(5)	138.40(6)	138.19(6)	138.26(8)
Cu(1)-O(2)-Ti(1)	89.14(4)	88.87(4)	89.95(4)	89.13(5)
Cu(1)-O(2)-Ti(3)	122.50(4)	122.13(5)	121.55(5)	122.72(8)
Ti(1)-O(2)-Ti(3)	147.60(5)	148.55(6)	147.12(6)	148.02(9)
Cu(2)-O(3)-Ti(2)	112.23(4)	112.75(5)	111.92(5)	113.38(7)
Cu(2)-O(3)-Ti(3)	114.99(4)	114.55(5)	114.50(5)	113.29(7)
Ti(3)-O(3)-Ti(3)	132.76(5)	132.63(6)	133.36(6)	133.33(8)
$\sum$ M-O(1)-M	359.52(13)	359.57(16)	359.84(16)	359.28(22)
$\sum$ M-O(2)-M	359.24(13)	359.55(15)	358.62(15)	359.87(22)
$\sum$ M-O(3)-M	359.98(13)	359.93(16)	359.78(16)	360.00(22)
Oxygen in *trans* position of the Ti/Cu coordination polyhedron				
O(1)-Cu(1)-O(8)	173.68(4)	174.92(5)	175.82(5)	174.57(6)
O(4)-Cu(1)-O(6)	162.38(4)	163.64(5)	164.07(5)	159.15(7)
O(10)-Cu(2)-O(16)	163.77(5)	157.31(6)	155.91(5)	160.49(7)
O(12)-Cu(2)-O(14)	162.29(5)	168.93(5)	169.33(5)	163.54(7)
O-Ti(1)-O	180	180	180	180
O-Ti(2)-O	168.44(4)-172.92(4)	167.99(5)-173.42(5)	168.42(5)-174.05(5)	168.87(7)-174.44(7)
O-Ti(3)-O	169.73(4)-175.79(5)	169.93(5)-176.72(5)	169.57(5)-173.93(5)	170.72(7)-177.74(7)
Oxygen in *cis* position of the Ti/Cu coordination polyhedron				
O(1)-Cu(1)-O(2)	75.56(3)	75.62(4)	75.84(4)	75.48(6)
O(2)-Cu(1)-O(6)	104.27(4)	104.22(5)	103.33(5)	107.65(7)
O-Cu(1)-O	85.88(5)-99.35(4)	85.87(5)-100.15(4)	85.57(5)-93.52(5)	87.89(7)-99.37(6)
O-Cu(2)-O	86.28(5)-99.65(4)	86.27(6)-103.02(5)	86.36(6)-105.58(5)	87.48(8)-100.28(6)
O-Ti(1)-O	87.51(4)-92.48(4)	87.94(4)-92.06(4)	87.43(4)-92.57(4)	87.77(6)-92.23(6)
O-Ti(2)-O	82.06(4)-98.51(4)	82.58(5)-99.44(5)	82.87(5)-97.83(5)	83.63(7)-98.03(7)
O-Ti(3)-O	83.95(4)-96.78(5)	83.41(5)-93.84(5)	82.23(5)-96.86(5)	84.21(7)-95.86(8)

Table A.29: Bond lengths and atoms distances for FeTi5 in [Å] compared to that of $Ti_6O_4(O^nPr)(OMc)_8$ [39]

	FeTi5	**Ti6 Cluster**
Metal - metal distance		
Fe/Ti(1)-Fe/Ti(2)	3.4215(10)	3.4587(8)
Fe/Ti(1)-Ti(3)	3.4917(10)	3.5680(9)
Fe/Ti(1)-Fe/Ti(1)'	4.9351(9)	4.9659(8)
Fe/Ti(1)-Fe/Ti(2)'	3.3037(10)	3.3758(8)
Fe/Ti(2)-Ti(3)	3.0466(11)	3.1054(8)
Fe/Ti(2)-Fe/Ti(2)'	4.4507(10)	4.6966(8)
Ti(3)-Ti(3)	8.8357(13)	9.0219(10)
Metal - core oxygen bonds		
Fe/Ti(1)-O(1)	1.918(3)	1.910(2)
Fe/Ti(1)-O(2)	1.875(3)	1.885(2)
Fe/Ti(2)-O(1)	1.904(3)	1.911(2)
Fe/Ti(2)-O(2)	1.776(3)	1.766(2)
Ti(3)-O(1)	1.990(3)	2.070(2)
μ_2**- Alkoxy ligands**		
Fe/Ti(2)-O(13)	2.137(3)	2.084(2)
Ti(3)-O(13)	1.902(3)	1.966(2)
μ_2**- Methacrylates bridging Ti and Fe/Ti**		
Fe/Ti(1)-O(7)	2.044(3)	2.064(2)
Fe/Ti(1)-O(9)	2.040(3)	
Fe/Ti(2)-O(11)	2.030(3)	2.011(2)
Ti(3)-O(8)	2.025(4)	2.052(3)
Ti(3)-O(10)	1.974(4)	
Ti(3)-O(12)	2.031(4)	2.152(3)
μ_2**- Methacrylates bridging Fe/Ti and Fe/Ti**		
Fe/Ti(1)-O(3)	2.015(3)	2.091(2)
Fe/Ti(1)-O(5)	2.061(3)	2.090(2)
Fe/Ti(2)-O(4)	2.012(3)	2.010(2)
Fe/Ti(2)-O(6)	2.047(3)	2.049(2)
Terminal alkoxy ligands		
Ti(3)-O(14)	1.773(3)	1.768(3)
		1.794(3)
		1.806(3)

Table A.30: Bond angles for FeTi5 in [°] compared to that of $Ti_6O_4(O^nPr)(OMc)_8$ [39]

	FeTi5	**Ti6 Cluster**
Core oxygen		
Fe/Ti(1)- O(1) -Fe/Ti(2)	127.09(15)	129.72(11)
Fe/Ti(1)- O(1) -Ti(3)	126.61(14)	127.38(10)
Fe/Ti(2)- O(1) -Ti(3)	102.95(12)	102.49(10)
$\sum$M- O(1) -M	356.7(4)	354.61(31)
Fe/Ti(1)- O(2) -Fe/Ti(2)	129.57(15)	135.24(12)
Oxygen atoms in *trans* position of the Fe/Ti coordination octahedron		
O-Fe/Ti(1)-O	167.32(13)-173.56(13)	164.09(10)-169.88(10)
O-Fe/Ti(2)-O	164.04(12)-178.72(13)	162.88(10)-175.98(9)
O- Ti(3) -O	168.23(14)-179.55(17)	163.15(11)-174.53(11)
Oxygen atoms in *cis* position of the Fe/Ti coordination octahedron		
O-Fe/Ti(1)-O	85.30(15)-99.16(12)	77.29(9)-99.33(11)
O-Fe/Ti(2)-O	75.91(12)-103.05(12)	79.89(9)-99.76(10)
O- Ti(3) -O	79.61(12)-100.42(16)	78.15(9)-104.47(9)
μ_2- **O^iPr**		
Fe/Ti(2)- O(13) -Ti(3)	97.77(12)	100.09(10)

Table A.31: Bond lengths and atom distances for LaTi4 [Å].

	1st cluster	**2nd cluster**	**Disorder**
Metal- metal distance			
La(1)-Ti(1)	4.1282(6)	3.969(5)	
La(1)-Ti(2)	3.4489(5)	3.342(5)	3.481(3)
La(1)-Ti(3)	3.4571(5)	3.534(4)	3.406(3)
La(1)-Ti(4)	4.0530(6)	4.058(8)	4.104(5)
Ti(1)-Ti(2)	3.4350(7)	3.4293(9)	
Ti(1)-Ti(4)			
Ti(2)-Ti(3)	3.5336(7)	3.5278(11)	
Ti(3)-Ti(4)	3.4308(8)	3.368(6)	3.470(4)
La(2)-La(2A)		0.262(5)	
Ti(8)-Ti(8A)		0.412(8)	
Metal - core oxygen			
La(1)-O(1)	2.6410(18)	2.478(5)	2.695(4)
La(1)-O(2)	2.4793(17)	2.474(5)	2.480(3)
La(1)-O(3)	2.6228(18)	2.774(5)	2.561(4)
Ti(1)-O(1)	1.9688(18)	1.985(2)	
Ti(2)-O(1)	1.7904(18)	1.775(2)	
Ti(2)-O(2)	1.8249(18)	1.821(3)	
Ti(3)-O(2)	1.8409(18)	1.835(3)	
Ti(3)-O(3)	1.7786(18)	1.782(2)	
Ti(4)-O(3)	1.9702(19)	1.829(7)	2.045(5)
μ_2- Methacrylate bridging La and Ti			
La(1)-O(4)	2.5455(18)	2.472(4)	2.686(4)
La(1)-O(6)	2.447(2)	2.378(6)	2.457(4)
La(1)-O(8)	2.5447(19)	2.502(5)	2.584(4)
La(1)-O(10)	2.558(2)	2.595(5)	2.514(4)
La(1)-O(12)	2.533(2)	2.513(5)	2.422(4)
La(1)-O(14)	2.548(2)	2.62(2)	2.551(14)
Ti(1)-O(5)	1.927(2)	1.911(3)	
Ti(1)-O(7)	1.977(2)	2.000(3)	
Ti(2)-O(9)	1.981(2)	1.988(2)	
Ti(3)-O(11)	1.975(2)	1.972(3)	
Ti(4)-O(13)	1.925(2)	2.018(7)	1.959(5)
Ti(4)-O(15)	1.938(2)	1.900(18)	1.923(11)
μ_2- Methacrylate bridging Ti			
Ti(1)-O(16)	2.038(2)	2.042(3)	
Ti(1)-O(17)	2.051(2)	2.039(3)	
Ti(2)-O(18)	2.056(2)	2.046(3)	
Ti(2)-O(19)	2.019(2)	2.014(2)	
Ti(2)-O(20)	2.0826(19)	2.099(2)	
Ti(3)-O(21)	2.084(2)	2.070(3)	
Ti(3)-O(22)	2.041(2)	2.037(2)	
Ti(3)-O(24)	2.035(2)	2.038(3)	
Ti(4)-O(23)	2.029(2)	2.262(8)	1.930(5)
Ti(4)-O(25)	2.046(2)	2.064(7)	2.057(5)
Terminal alkoxy ligand			
Ti(1)-O(26)	1.782(2)	1.751(3)	
Ti(4)-O(27)	1.774(2)	1.755(15)	1.773(9)

Table A.32: Bond lengths and atom distances for La2Ti6 compared with those of Eu2Ti4 in [Å]

La2Ti6			**Eu2Ti4**		
		Disorder			**Disorder**
Metal- metal distance					
La(1)-La(1)'	4.243(2)	4.22(7)	Eu(1)-Eu(1)'	3.938(6)	3.961(8)
La(1)-Ti(1)	3.4567(15)	3.55(2)	Eu(1)-Ti(1)	3.302(2)	3.517(4)
La(1)-Ti(1)'	3.8973(18)	3.797(18)	Eu(1)-Ti(1)'	3.848(3)	3.665(5)
La(1)-Ti(2)	3.6557(18)	3.618(11)	Eu(1)-Ti(2)	3.780(3)	3.933(5)
La(1)-Ti(3)	4.3801(19)	4.33(2)			
Ti(1)-Ti(2)	3.5346(11)		Ti(1)-Ti(2)	3.5014(9)	
Ti(1)-Ti(1)'	6.023(1)		Ti(1)-Ti(1)'	5.9927(9)	
Ti(2)-Ti(3)	3.3811(12)				
Ti(2)-Ti(2)'	9.4754(13)		Ti(2)-Ti(2)'	9.6585(9)	
Ti(3)-Ti(3)'	12.6655(18)				
La(1)-La(1A)	0.27(3)		Eu(1)-Eu(1A)	0.247(7)	
Metal - core oxygen					
La(1)-O(1)	2.538(3)	2.62(2)	Eu(1)-O(1)	2.319(3)	2.327(6)
La(1)-O(1)'	2.552(3)	2.441(18)	Eu(1)-O(1)'	2.457(4)	2.468(5)
La(1)-O(2)	2.526(3)	2.563(15)	Eu(1)-O(2)	2.491(3)	2.699(5)
	3.0454(34)	2.972(15)	Ti(1)-O(1)	1.718(2)	
Ti(1)-O(1)	1.705(3)		Ti(1)-O(2)	2.022(2)	
Ti(1)-O(2)	1.987(3)		Ti(2)-O(2)	1.730(2)	
Ti(2)-O(2)	1.743(3)				
Ti(2)-O(3)	1.976(3)				
Ti(3)-O(3)	1.742(3)				
μ_2- Methacrylate bridging La and Ti					
La(1)-O(4)	2.447(4)	2.61(3)	Eu(1)-O(3)	2.368(3)	2.287(6)
La(1)-O(6)	2.482(4)	2.32(3)	Eu(1)-O(5)	2.464(3)	2.230(5)
La(1)-O(8)	2.496(4)	2.76(4)	Eu(1)-O(7)	2.330(4)	2.519(6)
La(1)-O(10)	2.545(4)	2.30(4)	Eu(1)-O(9)	2.341(4)	2.355(6)
La(1)-O(12)	2.458(4)	2.563(19)	Eu(1)-O(11)	2.382(4)	2.340(6)
Ti(1)-O(5)	2.004(3)		Ti(1)-O(4)	2.019(2)	
Ti(1)-O(7)	1.977(3)		Ti(1)-O(6)	1.958(2)	
Ti(1)-O(9)	1.990(3)		Ti(1)-O(8)	1.992(2)	
Ti(2)-O(11)	1.954(3)		Ti(2)-O(10)	1.987(3)	
Ti(3)-O(13)	1.944(4)		Ti(2)-O(12)	1.981(3)	
μ_2- Methacrylate bridging Ti					
Ti(1)-O(14)	2.185(3)		Ti(1)-O(13)	2.128(2)	
Ti(2)-O(15)	1.974(3)		Ti(2)-O(14)	1.991(3)	
Ti(2)-O(16)	2.023(3)				
Ti(2)-O(18)	2.101(3)				
Ti(3)-O(17)	2.010(4)				
Ti(3)-O(19)	2.011(4)				
Terminal alkoxy ligand					
Ti(3)-O(20)	1.924(4)				
η_1- Methacrylate (methacrylic acid)					
Ti(3)-O(22)	2.158(4)		Ti(2)-O(15)	2.140(2)	
			Ti(2)-O(17)	1.974(3)	

Table A.33: Bond angles for LaTi4 [°].

	1st cluster	**2nd cluster**	**Disorder**
Angles between La- core oxygen bonds			
O(1)-La(1)-O(2)	60.33(6)	58.22(12)	59.18(10)
O(2)-La(1)-O(3)	60.40(6)	62.33(13)	61.19(10)
Core oxygen			
La(1)-O(1)-Ti(1)	126.53(8)	125.22(15)	126.78(12)
La(1)-O(1)-Ti(2)	100.45(7)	102.34(15)	100.26(12)
Ti(1)-O(1)-Ti(2)	132.00(10)	131.53(13)	
La(1)-O(2)-Ti(2)	105.50(7)	101.08(13)	107.08(13)
La(1)-O(2)-Ti(3)	105.34(8)	109.26(13)	103.22(13)
Ti(2)-O(2)-Ti(3)	149.13(10)	149.53(13)	
La(1)-O(3)-Ti(3)	101.80(8)	99.42(15)	101.82(13)
La(1)-O(3)-Ti(4)	123.24(8)	122.3(2)	125.69(16)
Ti(3)-O(3)-Ti(4)	132.39(10)	137.6(2)	130.01(18)
$\sum$M-O(1)-M	358.98(25)	359.2(4)	358.6(4)
$\sum$M-O(2)-M	359.96(25)	359.9(4)	359.8(4)
$\sum$M-O(3)-M	357.43(10)	359.3(4)	357.5(5)
Oxygen in *trans* position of the Ti coordination octahedron			
O-Ti(1)-O	168.85(10)-175.18(10)	172.91(12)-174.45(14)	
O-Ti(2)-O	166.58(9)-171.61(9)	167.40(11)-171.77(12)	
O-Ti(3)-O	167.37(8)-173.38(9)	169.03(12)-174.22(12)	
O-Ti(4)-O	168.04(10)-175.37(9)	158.6(4)-174.4(5)	172.8(3)-174.8(4)
Oxygen in *cis* position of the Ti coordination octahedron			
O-Ti(1)-O	84.29(10)-97.74(10)	85.00(11)-95.22(12)	
O-Ti(2)-O	80.29(9)-99.98(8)	82.79(10)-99.38(11)	
O-Ti(3)-O	80.51(9)-98.63(9)	79.67(10)-98.82(11)	
O-Ti(4)-O	83.70(10)-96.29(11)	78.5(3)-101.4(7)	83.84(19)-96.0(4)
Torsion angle			
Ti(1)-Ti(2)-Ti(3)-Ti(4)	-60.253(32)	59.08(14)	66.98(9)

Table A.34: Bond angles for La2Ti6 compared with those of Eu2Ti4 in [°]

La2Ti6			**Eu2Ti4**		
		Disorder			**Disorder**
Core oxygen					
La(1)-O(1)-La(1)	112.93(12)	112.6(3)	Eu(1)-O(1)-Eu(1)'	111.06(11)	111.37(17)
La(1)-O(1)-Ti(1)	107.50(14)	131.8(3)	Eu(1)-O(1)-Ti(1)	108.87(12)	113.13(15)
La(1)-O(1)-Ti(1)'	131.54(15)	108.4(3)	Eu(1)-O(1)-Ti(1)'	133.59(12)	129.34(15)
La(1)-O(2)-Ti(1)	99.27(12)	101.8(5)	Eu(1)-O(2)-Ti(1)	93.46(10)	95.25(14)
La(1)-O(2)-Ti(2)	116.61(15)	112.9(7)	Eu(1)-O(2)-Ti(2)	126.19(12)	123.80(15)
Ti(1)-O(2)-Ti(2)	142.62(17)		Ti(1)-O(2)-Ti(2)	137.75(12)	
La(1)-O(3)-Ti(2)	90.89(11)	91.7(3)			
La(1)-O(3)-Ti(3)	130.38(16)	132.0(3)			
Ti(2)-O(3)-Ti(3)	130.7(2)				
$\sum$M-O(1)-M	352.0(4)	352.8(9)	$\sum$M-O(1)-M	353.5(4)	353.8(5)
$\sum$M-O(2)-M	358.5(4)	357.3(14)	$\sum$M-O(2)-M	357.4(3)	356.8(44)
$\sum$M-O(3)-M	351.0(10)	354.4(8)			
Oxygen atoms in *trans* position of the Ti coordination octahedron					
O-Ti(1)-O	162.60(14)-172.52(14)		O-Ti(1)-O	165.70(10)-173.11(10)	
O-Ti(2)-O	168.63(14)-175.71(15)		O-Ti(2)-O	162.28(11)-173.25(12)	
O-Ti(3)-O	162.80(17)-173.0(2)				
Oxygen atoms in *cis* position of the Ti coordination octahedron					
O-Ti(1)-O	77.84(13)-98.06(13)		O-Ti(1)-O	80.51(10)-97.77(10)	
O-Ti(2)-O	82.41(14)-96.64(14)		O-Ti(2)-O	80.10(11)-102.31(10)	
O-Ti(3)-O	80.4(2)-101.17(18)				

Table A.35: Bond lengths and atom distances for Ag2Zr8 [Å].

Metal -metal distance					
Ag(1)-Ag(1)'	12.1953(11)	Zr(1)-Zr(2)	3.3995(6)	Zr(2)-Zr(4)	3.4015(7)
Ag(1)-Zr(2)	3.9730(7)	Zr(1)-Zr(3)	6.0729(8)	Zr(3)-Zr(4)	3.3361(6)
Ag(1)-Zr(3)	3.7378(8)	Zr(1)-Zr(3)'	5.8689(9)	Zr(4)-Zr(4)'	3.4051(8)
		Zr(1)-Zr(4)	3.6020(6)		
Core oxygen					
Zr(1)-O(1)	2.013(2)	Zr(3)-O(2)	2.032(2)	Zr(4)-O(2)	2.210(3)
Zr(2)-O(1)	2.085(3)	Zr(3)-O(3)	2.012(3)	Zr(4)-O(3)	2.145(2)
Zr(2)-O(2)	2.009(3)	Zr(4)-O(1)	2.122(2)	Zr(4)-O(3)'	2.068(3)
hmp ligand		**hmp-H ligand**			
Zr(1)-O(4)	2.255(3)	Zr(1)-O(7)	2.124(3)		
Zr(1)-O(6)	2.231(3)	Zr(1)-O(9)	2.190(3)		
Zr(3)'-O(5)	2.257(3)	Zr(2)-O(9)	2.146(2)		
Zr(4)-O(4)	2.493(2)				
O(4)-C(1)	1.273(5)	O(7)-C(5)	1.280(5)		
O(5)-C(1)	1.233(5)	O(8)-C(5)	1.236(5)		
O(6)-C(2)	1.434(5)	O(9)-C(6)	1.448(5)		
C(1)-C(2)	1.524(5)	C(5)-C(6)	1.541(5)		
C(2)-C(3)	1.524(6)	C(6)-C(7)	1.512(6)		
C(2)-C(4)	1.517(6)	C(6)-C(8)	1.527(6)		
Chelating/bridging and μ_3- methacrylates					
Ag(1)-O(10)	2.440(3)	Ag(1)-O(14)	2.288(3)	Ag(1)-O(22)	2.759(3)
Zr(2)-O(10)	2.324(3)	Ag(1)-O(15)	2.839(3)	Zr(3)-O(22)	2.230(3)
Zr(2)-O(11)	2.254(3)	Zr(3)-O(15)	2.101(3)	Zr(4)-O(23)	2.187(3)
μ_2- Methacrylate					
Ag(1)-O(12)	2.347(3)	Zr(3)-O(19)	2.180(3)		
Zr(2)-O(13)	2.076(3)	Zr(3)-O(20)	2.151(3)		
Zr(1)-O(16)	2.190(3)	Zr(4)-O(17)	2.207(3)		
Zr(2)-O(18)	2.144(3)	Zr(4)-O(21)	2.189(3)		
Chelating methacrylate		**Terminal methacrylic acid**			
Zr(1)-O(24)	2.227(3)	Ag(1)-O(26)	2.457(4)		
Zr(1)-O(25)	2.274(3)	O(26)-C(41)	1.207(6)		
		O(27)-C(41)	1.329(6)		

Table A.36: Bond angles for Ag2Zr8 [°].

Core oxygen					
Zr(1)-O(1)-Zr(2)	112.10(12)	Zr(2)-O(2)-Zr(3)	146.81(14)	Zr(3)-O(3)-Zr(4)	106.70(11)
Zr(1)-O(1)-Zr(4)	121.16(12)	Zr(2)-O(2)-Zr(4)	107.38(10)	Zr(3)-O(3)-Zr(4)'	144.50(12)
Zr(2)-O(1)-Zr(4)	107.90(10)	Zr(3)-O(2)-Zr(4)	103.62(11)	Zr(4)-O(3)-Zr(4)'	107.82(11)
$\sum$Zr-O(1)-Zr	341.2(3)	$\sum$Zr-O(2)-Zr	357.8(3)	$\sum$Zr-O(3)-Zr	359.0(3)
Chelating/bridging methacrylate					
Ag(1)-O(10)-Zr(2)	113.00(12)	Ag(1)-O(15)-Zr(3)	97.22(11)	Ag(1)-O(22)-Zr(3)	96.47(11)
O(11)-C(9)-O(10)	116.9(4)	O(14)-C(17)-O(15)	122.5(4)	O(22)-C(33)-O(23)	124.9(4)
hmp ligand		**hmp-H ligand**			
O(4)-Zr(1)-O(6)	67.99(9)	O(7)-Zr(1)-O(9)	72.94(10)		
Zr(1)-O(4)-Zr(4)	98.57(10)	Zr(1)-O(9)-Zr(2)	103.23(11)		
O(5)-C(1)-O(4)	125.8(4)	O(8)-C(5)-O(7)	124.0(4)		

Table A.37: Bond lengths and atom distances in [Å] for Ti6prop compared to those for $\mathrm{Ti_6O_4(O^{n}Pr)_6(OMc)_6}$ [Ti6met] [39].

	Ti6prop	**Ti6met**		**Ti6prop**	**Ti6met**
Metal- metal distance			**μ_2- Core oxygen atoms (μ_2- Alkoxy ligands)**		
Ti(1)-Ti(2)	3.6219(9)	3.5680(9)	Ti(2)-O(3)	1.801(2)	2.084(2)
Ti(1)-Ti(3)	3.3884(11)	3.4587(8)	Ti(3)-O(3)	1.855(2)	1.966(2)
Ti(1)-Ti(1)'	4.6663(2)	4.9659(8)	**μ_2- Methacrylates**		
Ti(1)-Ti(2)'	3.3885(9)	3.3758(8)	Ti(1)-O(4)	2.021(2)	2.011(2)
Ti(1)-Ti(3)'	6.0933(12)	6.348(1)	Ti(1)-O(6)	2.047(2)	2.090(2)
Ti(2)-Ti(3)	2.8525(10)	3.1054(8)	Ti(1)-O(8)	2.132(3)	2.091(2)
Ti(2)-Ti(2)'	5.0230(11)	4.6966(8)	Ti(2)-O(5)	2.002(2)	2.152(3)
Ti(2)-Ti(3)'	6.6211(12)	6.4879(1)	Ti(2)-O(7)	2.043(2)	2.049(2)
Ti(3)-Ti(3)'	8.8725(14)	9.0219(10)	Ti(2)-O(10)	2.019(2)	2.052(3)
μ_3- Core oxygen atoms			Ti(2)-O(12)	2.035(2)	
Ti(1)-O(1)	1.922(2)	1.910(2)	Ti(3)-O(9)	2.012(2)	2.010(2)
Ti(2)-O(1)	1.870(2)	1.911(2)	Ti(3)-O(11)	2.022(2)	2.064(2)
Ti(3)-O(1)	2.043(2)	2.070(2)	Ti(3)-O(13)	2.023(2)	
μ_2- Core oxygen atoms			**Terminal alkoxy ligands**		
Ti(1)-O(2)	1.801(2)	1.766(2)	Ti(3)-O(14)	1.770(2)	1.806(3)
Ti(2)-O(2)	1.998(2)	1.885(2)			1.768(3)
					1.794(3)

Table A.38: Bond angles for Ti6prop compared to those for $\mathrm{Ti_6(OnPr)_8(OMc)_8}$ [39] [°].

	Ti6prop	**Ti6met**
Core oxygen		
Ti(1)-O(1)-Ti(2)	129.97(12)	102.49(10)
Ti(1)-O(1)-Ti(3)	132.17(13)	129.72(11)
Ti(2)-O(1)-Ti(3)	92.50(10)	127.38(10)
$\sum$Ti-O(1)-Ti	354.64(35)	359.59(31)
Ti(1)-O(2)-Ti(2)	132.20(12)	135.24(12)
Ti(2)-O(3)-Ti(3)	102.55(11)	100.09(10)
Oxygen atoms in *trans* position of the Ti coordination octahedron		
O-Ti(1)-O	166.90(10)-168.48(10)	164.09(10)-169.88(10)
O-Ti(2)-O	175.15(10)-178.05(10)	163.15(11)-174.53(11)
O-Ti(3)-O	164.67(10)-173.80(10)	162.88(10)-175.98(9)
Oxygen atoms in *cis* position of the Ti coordination octahedron		
O-Ti(1)-O	77.84(10)-102.65(11)	79.89(9)-99.76(10)
O-Ti(2)-O	84.92(10)-96.62(10)	77.29(9)-99.33(11)
O-Ti(3)-O	78.03(10)-100.21(11)	78.15(9)-104.47(9)

Table A.39: Bond lengths and atom distances for Zr6piv [Å].

Metal- metal distance		**μ_2- Methacrylates**	
Zr(1)-Zr(2)	3.2774(13)	Zr(1)-O(3)	2.181(7)
Zr(1)-Zr(3)	3.9075(14)	Zr(1)-O(5)	2.218(6)
Zr(1)-Zr(1)'	3.3887(18)	Zr(1)-O(7)	2.173(7)
Zr(2)-Zr(3)	3.3921(14)	Zr(1)-O(9)	2.126(7)
Zr(2)-Zr(2)'		Zr(2)-O(4)	2.154(7)
Zr(3)-Zr(3)'		Zr(2)-O(6)	2.115(7)
μ_3- Core oxygen		Zr(3)-O(8)	2.156(7)
Zr(1)-O(1)	2.091(6)	Zr(3)-O(10)	2.179(6)
Zr(1)-O(2)	2.103(6)	**Chelating methacrylates**	
Zr(1)-O(1)'	2.095(6)	Zr(2)-O(11)	2.286(7)
Zr(2)-O(1)	2.022(6)	Zr(2)-O(12)	2.219(7)
Zr(2)-O(2)	2.032(7)	Zr(3)-O(13)	2.283(7)
Zr(3)-O(2)	2.074(6)	Zr(3)-O(14)	2.234(7)
μ_2- Alkoxy ligands		Zr(3)-O(15)	2.295(7)
Zr(2)-O(17)	2.138(6)	Zr(3)-O(16)	2.216(7)
Zr(3)-O(17)	2.139(6)		

Table A.40: Bond angles for Zr6piv in [°]

Core oxygen	
Zr(1)- O(1) -Zr(2)	105.5(3)
Zr(1)- O(1) -Zr(1)'	108.1(3)
Zr(2)- O(1) -Zr(1)'	145.0(3)
Zr(1)- O(2) -Zr(2)	104.8(3)
Zr(1)- O(2) -Zr(3)	138.5(3)
Zr(2)- O(2) -Zr(3)	111.4(3)
$\sum$Zr- O(1) -Zr	355.6(9)
$\sum$Zr- O(1) -Zr	354.7(9)
μ_2- Alkoxy ligand	
Zr(2)-O(17)-Zr(3)	104.9(2)

Appendix B

Data and Parameters of Single Crystal X-ray Diffraction

Table B.1: Crystal data, data collection parameters and refinement details of Zr/Ti carboxylate clusters

Compound	**Zr4Ti2benz**	**Zr4Ti2tBu-benz**	**Zr4Ti2Cl-benz**
Crystal data			
Empirical formula	$C_{61}H_{60}O_{19}TiZr_2$	$C_{86.30}H_{103.20}O_{18.27}TiZr_2$	$C_{78}H_{82.67}Cl_{6.67}O_{22.50}Ti_{2.67}Zr_{1.33}$
M_r	1327.43	1663.23	1865.8
Cell setting	triclinic	triclinic	monoclinic
Space group	$P\bar{1}$	$P\bar{1}$	$P2_1/n$
Temperature (K)	100(2)	100(2)	100(2)
a Å	13.2781(6)	16.7501(5)	28.5684(9)
b Å	13.9784(7)	17.0751(5)	15.5558(5)
c Å	18.2662(9)	20.7999(6)	30.3692(10)
$\alpha(°)$	109.2160(10)	100.328(2)	90.00
$\beta(°)$	101.5140(10)	104.133(2)	100.964(2)
$\gamma(°)$	101.461(2)	115.839(2)	90.00
V (Å^3)	3006.2(3)	4906.1(2)	13249.9(7)
Z	2	2	6
$D_x(Mg \cdot m^{-3})$	1.466	1.126	1.403
$\mu(mm^{-1})$	0.543	0.345	0.654
Crystal form, colour	brick, colourless	fragment, colourless	brick, colourless
Crystal size (mm)	0.56 x 0.32 x 0.30	0.24 x 0.16 x 0.12	0.58 x 0.41 x 0.35
Data collection			
T_{min}, T_{max}	0.7509, 0.8541	0.9219, 0.9598	0.5946, 0.7461
No. of measured, independent and observed reflections	18055, 18055, 13178	43353, 19976, 11123	211935, 40176, 23162
Criterion for observed reflections	$I > 2\sigma(I)$	$I > 2\sigma(I)$	$I > 2\sigma(I)$
R_{int}	0.0501	0.0495	0.0788
$\Theta_{max}(°)$	30.71	26.46	30.53
Refinement			
Refinement on	F^2	F^2	F^2
$R[F^2 > 2\sigma(F)], \omega R(F^2), S$	0.0461, 0.1288, 1.088	0.1107, 0.3490, 1.101	0.0994, 0.2759, 1.490
No. of reflections	18055	19976	40176
No. of parameters	770	1072	1541
No. of restrains	0	32	0
Weighting scheme*	$x = 0.0659, y = 1.9858$	$x = 0.1614, y = 16.9673$	$x = 0.10, y = 0$
$(\Delta/\sigma)_{max}$	0.004	0	5.678
$\Delta\rho_{max}$,$\Delta\rho_{max}$ (e Å^{-3})	1.762, -0.736	1.203, -0.767	1.203, -0.767

*$\omega = 1/[\sigma^2(F_0^2) + (xP)^2 + yP]$, where $P = (F_0^2 + 2F_c^2)/3$

Table B.2: Crystal data, data collection parameters and refinement details for Zr/Ti pivalate clusters

Compound	**ZrTi2piv**	**Zr3Ti2piv**	**Zr2Ti3piv**
Crystal data			
Empirical formula	$C_{42}H_{82}O_{17}Ti_2Zr$	$C_{50.25}H_{94.50}O_{21}Ti_{1.50}Zr_{2.25}$	$C_{59.50}H_{115}O_{26}Ti_3Zr_2$
M_r	1046.1	1311.85	1572.66
Cell setting	monoclinic	triclinic	triclinic
Space group	$P2_1/n$	$P1$	$P1$
Temperature (K)	100(2)	100(2)	100(2)
a Å	12.5949(6)	14.9266(11)	14.495(2)
b Å	22.6786(11)	15.1407(11)	14.632(2)
c Å	18.8861(10)	33.451(2)	19.051(3)
$\alpha(°)$	90	79.130(2)	79.910(4)
$\beta(°)$	90.263(2)	85.300(2)	89.770(5)
$\gamma(°)$	90	60.9100(17)	89.860(5)
V (Å^3)	5394.5(5)	6487.4(8)	3978.0(10)
Z	4	4	2
$D_x(Mg \cdot m^{-3})$	1.288	1.343	1.313
$\mu(mm^{-1})$	0.54	0.596	0.609
Crystal form, colour	brick, colourless	fragment, colourless	fragment, colourless
Crystal size (mm)	0.36 x 0.22 x 0.19	0.25 x 0.18 x 0.15	0.24 x 0.14 x 0.12
Data collection			
T_{min}, T_{max}	0.6932, 0.7461	0.8653, 0.9159	0.5048, 0.7448
No. of measured, independent and observed reflections	233596, 16507, 13602	93963, 31679, 23785	47715, 18906, 13280
Criterion for observed reflections	$I > 2\sigma(I)$	$I > 2\sigma(I)$	$I > 2\sigma(I)$
R_{int}	0.0553	0.1219	0.1197
$\Theta_{max}(°)$	30.55	23.19	25.38
Refinement			
Refinement on	F^2	F^2	F^2
$R[F^2 > 2\sigma(F)], \omega R(F^2), S$	0.0384, 0.0865, 1.161	0.0736, 0.1800, 1.089	0.1180, 0.3064, 1.752
No. of reflections	16507	31679	18906
No. of parameters	665	2809	836
No. of restrains	6	3	10
Weighting scheme*	$x = 0.0224, y = 5.5860$	$x = 0.0958, y = 0.0658$	$x = 0.1, y = 0.0$
$(\Delta/\sigma)_{max}$	0.003	2.909	1.593
$\Delta\rho_{max}$,$\Delta\rho_{max}$ (e Å^{-3})	0.766, -0.845	1.345, -0.716	2.148, -2.014

*$\omega = 1/[\sigma^2(F_0^2) + (xP)^2 + yP]$, where $P = (F_0^2 + 2F_c^2)/3$

Table B.3: Crystal data, data collection parameters and refinement details for Zr/Ti pivalate clusters

Compound	**Zr4Ti2piviPr**	**Zr4Ti2pivnPr**	**Zr4Ti2pivnPr.BuOH**	**Zr4Ti2pivAc**
Crystal data				
Empirical formula	$C_{68}H_{128}O_{34}Ti_2Zr_4$	$C_{36.35}H_{67.75}O_{17.88}TiZr_2$	$C_{71.57}H_{136.95}O_{34.90}Ti_2Zr_4$	$C_{36.50}H_{69}O_{18.50}TiZr_2$
M_r	1950.38	2014.73	2016.74	1034.26
Cell setting	monoclinic	monoclinic	monoclinic	triclinic
Space group	$C2/c$	$P2_1$	$P2_1/n$	$P\bar{1}$
Temperature (K)	100(2)	100(2)	100(2)	100(2)
a Å	48.731(4)	14.6518(4)	21.5529(13)	15.4930(8)
b Å	16.3430(15)	25.8497(6)	15.4766(9)	15.8440(7)
c Å	24.034(2)	14.9056(4)	30.0414(18)	20.3727(10)
$\alpha(°)$	90	90	90	89.144(3)
$\beta(°)$	96.778(2)	118.5600(10)	93.435(2)	85.229(3)
$\gamma(°)$	90	90	90	89.331(3)
V (Å^3)	19007(3)	4958.5(2)	10002.8(10)	4982.8(4)
Z	8	4	4	4
$D_x(Mg \cdot m^{-3})$	1.363	1.368	1.339	1.379
$\mu(mm^{-1})$	0.655	0.633	0.626	0.631
Crystal form, colour	brick, colourless	fragment, colourless	fragment, colourless	brick, colourless
Crystal size (mm)	0.30 x 0.25 x 0.25	0.29 x 0.25 x 0.22	0.25, 0.20, 0.17	0.24 x 0.18 x 0.12
Data collection				
T_{min}, T_{max}	0.8277, 0.8533	0.6212, 0.7460	0.8593, 0.9011	0.8632, 0.9281
No. of measured, independent and observed reflections	205793, 15207, 12390	125978, 27223, 22273	17745, 17745, 14385	54104, 13144, 6448
Criterion for observed reflections	$I > 2\sigma(I)$	$I > 2\sigma(I)$	$I > 2\sigma(I)$	$I > 2\sigma(I)$
R_{int}	0.0313	0.039	0.0259	0.2065
$\Theta_{max}(°)$	24.22	30.12	25.09	22.66
Refinement				
Refinement on	F^2	F^2	F^2	F^2
$R[F^2 > 2\sigma(F)], \omega R(F^2), S$	0.0988, 0.2728, 1.046	0.0461, 0.1064, 1.048	0.0571, 0.1209, 1.169	0.0706, 0.1726, 1.002
No. of reflections	15207	27223	17745	13144
No. of parameters	1006	1161	1120	1049
No. of restrains	17	8	24	8
Weighting scheme*	$x = 0.1478, y = 431.3293$	$x = 0.0543, y = 8.8872$	$x = 0.0217, y = 53.5780$	$x = 0.069, y = 0.0$
$(\delta/\sigma)_{max}$	0.001	0.001	0.001	0
$\delta\rho_{max}$,$\delta\rho_{max}$ (e Å^{-3})	3.179, -2.123	1.075, -1.007	1.271, -0.796	1-139, -0.824

*$\omega = 1/[\sigma^2(F_0^2) + (xP)^2 + yP]$, where $P = (F_0^2 + 2F_c^2)/3$

Table B.4: Crystal data, data collection parameters and refinement details for Zr/Ti pivalate and adamantanecarboxylate clusters

Compound	**Zr3Ti3piv**	**Zr6Ti8piv**	**Zr4Ti3ada**
Crystal data			
Empirical formula	$C_{67}H_{129.50}O_{32.35}Ti_3Zr_3$	$C_{131.28}H_{222}O_{72.61}Ti_8Zr_{6.76}$**	$C_{70}H_{100.50}O_{16.50}Ti_{1.50}Zr_2$
M_r	1870.17	3961.64**	1460.29
Cell setting	monoclinic	triclinic	orthorhombic
Space group	$C2/c$	$P\overline{1}$	$Pnma$
Temperature (K)	100(2)	100(2)	100(2)
a Å	14.8095(9)	65.721(6)	36.368(2)
b Å	26.5262(16)	65.773(2)	20.5963(15)
c Å	46.039(3)	26.1129(15)	19.1335(13)
$\alpha(°)$	90	90.240(3)	90
$\beta(°)$	95.006(2)	90.010(5)	90
$\gamma(°)$	8	119.920(6)	90
V (Å^3)	18017.0(19)	97832(11)	14331.7(17)
Z	4	18	8
$D_x(Mg \cdot m^{-3})$	1.379	1.210**	1.354
$\mu(mm^{-1})$	0.661	0.655**	0.51
Crystal form, colour	brick, colourless	fragment, colourless	brick, colourless
Crystal size (mm)	0.25, 0.17, 0.13	0.22, 0.18, 0.12	0.30 x 0.23 x 0.20
Data collection			
T_{min}, T_{max}	0.8521, 0.9190	0.6212, 0.7460	0.6230, 0.7449
No. of measured, independent and observed reflections	187694, 18991, 13452	186783, 85671, 19980	282224, 10803, 8558
Criterion for observed reflections	$I > 2\sigma(I)$	$I > 2\sigma(I)$	$I > 2\sigma(I)$
R_{int}	0.0778	0.0797	0.1098
$\Theta_{max}(°)$	26.79	22.67	23.49
Refinement			
Refinement on	F^2	F^2	F^2
$R[F^2 > 2\sigma(F)], \omega R(F^2), S$	0.431, 0.0999, 1.022	0.1416, 0.3862, 1.109	0.1345, 0.3295, 1.094
No. of reflections	18991	85671	10803
No. of parameters	1209	3157	778
No. of restrains	14	210	210
Weighting scheme*	$x = 0.0324, y = 58.7179$	$x = 0.0386, y = 13.7774$	$x = 0.1357, y = 312.3555$
$(\Delta/\sigma)_{max}$	0.001	4.736	0.001
$\Delta\rho_{max}$,$\delta\rho_{max}$ (e Å^{-3})	0.723, -0.621	2.606, -1.902	1.864, -1.447

*$\omega = 1/[\sigma^2(F_0^2) + (xP)^2 + yP]$, where $P = (F_0^2 + 2F_c^2)/3$

** due to the incompleteness of the second cluster, these values are not correct

Table B.5: Crystal data, data collection parameters and refinement details for mixed Ti and mixed Ag/Zr clusters

Compound	**Zn2Ti4**	**Cd4Ti2**	**Ag2Zr8**	**FeTi5**
Crystal data				
Empirical formula	$C_{46}H_{64}O_{26}Ti_4Zn_2$	$C_{50}H_{70}Cd_4O_{28}Ti_2$	$C_{104}H_{148}Ag_2O_{60}Zr_8$	$C_{26}H_{39}Fe_{0.50}O_{14}Ti_{2.50}$
M_r	1327.43	1664.46	3305.72	723.25
Cell setting	triclinic	monoclinic	triclinic	monoclinic
Space group	$P\bar{1}$	$C2/c$	$P\bar{1}$	$P2_1/n$
Temperature (K)	100(2)	100(2)	100(2)	100(2)
a Å	10.0269(3)	22.290(4)	14.6881(15)	12.0904(10)
b Å	12.7249(4)	15.173(3)	16.1286(17)	11.1928(9)
c Å	13.1321(5)	21.026(4)	16.9996(17)	24.9189(19)
$\alpha(°)$	106.1700(19)	90.00	107.950(4)	90.00
$\beta(°)$	96.9500(19)	110.224(5)	109.560(4)	97.830(3)
$\gamma(°)$	111.9500(17)	90.00	105.640(4)	90.00
V (Å^3)	1444.16(8)	6673(2)	3283.1(6)	3340.7(5)
Z	1	4	1	4
$D_x(Mg \cdot m^{-3})$	1.558	1.379	1.672	1.438
$\mu(mm^{-1})$	1.425	0.661	0.99	0.859
Crystal form, colour	brick, colourless	fragment, colourless	brick, colourless	brick, redish-brown
Crystal size (mm)	0.19 x 0.18 x 0.15	0.22 x 0.20 x 0.14	0.21 x 0.12 x 0.1	0.46 x 0.39 x 0.19
Data collection				
T_{min}, T_{max}	0.6213, 0.7473	0.7258, 0.8115	0.6239, 0.7456	0.6934, 0.8538
No. of measured, independent and observed reflections	18055, 18055, 13178	122456, 10180, 8084	101362, 15281, 8972	95122, 8702, 6080
Criterion for observed reflections	$I > 2\sigma(I)$	$I > 2\sigma(I)$	$I > 2\sigma(I)$	$I > 2\sigma(I)$
R_{int}	0.0817	0.031	0.1397	0.0439
$\Theta_{max}(°)$	37.02	30.52	27.79	28.85
Refinement				
Refinement on	F^2	F^2	F^2	F^2
$R[F^2 > 2\sigma(F)], \omega R(F^2), S$	0.0476, 0.1160, 1.000	0.0367, 0.0839, 1.224	0.0493, 0.0804, 1.003	0.0721, 0.1880, 1.119
No. of reflections	13888	10180	15281	8702
No. of parameters	359	391	840	399
No. of restrains	0	1	10	0
Weighting scheme*	$x = 0.0464, y = 0.4048$	$x = 0.0111, y = 45.3277$	$x = 0.0257, y = 0.3104$	$x = 0.0580, y = 11.3336$
$(\Delta/\sigma)_{max}$	0.001	0.002	0.000	0.000
$\Delta\rho_{max}$,$\Delta\rho_{max}$ (e Å^{-3})	0.918, -0.671	1.534, -0.786	0.928, -1.027	1.065, -0.794

$^*\omega = 1/[\sigma^2(F_0^2) + (xP)^2 + yP]$, where $P = (F_0^2 + 2F_c^2)/3$

Table B.6: Crystal data, data collection parameters and refinement details for Ca/Ti and Sr/Ti chain-like clusters

Compound	**Ca2Ti4**	**Ca2Ti4a**	**Sr2Ti4**
Crystal data			
Empirical formula	$C_{22}H_{28}CaO_{14}Ti_2$	$C_{54}H_{74}Ca_2O_{31}Ti_4$	$C_{56}H_{72}O_{32}Sr_2Ti_4$
M_r	652.32	1490.89	1623.98
Cell setting	orthorhombic	triclinic	triclinic
Space group	$Pccn$	$P\bar{1}$	$P\bar{1}$
Temperature (K)	100(2)	100(2)	100(2)
a Å	20.4104(7)	13.9656(6)	12.7300(4)
b Å	23.1828(9)	15.3582(7)	13.4769(4)
c Å	12.5984(4)	16.7388(7)	22.8051(5)
$\alpha(°)$	90	81.340(2)	83.9400(11)
$\beta(°)$	90	83.406(2)	80.5600(11)
$\gamma(°)$	90	75.256(2)	63.5300(11)
V (Å^3)	5961.2(4)	3421.4(3)	3452.55(17)
Z	8	2	2
$D_x(Mg \cdot m^{-3})$	1.454	1.447	1.562
$\mu(mm^{-1})$	0.77	0.684	2.06
Crystal form, colour	brick, colourles	fragment, colourles	fragment, colourles
Crystal size (mm)	0.45 x 0.40 x 0.22	0.29 x 0.23 x 0.19	0.20 x 0.18 x 0.15
Data collection			
T_{min}, T_{max}	0.6321, 0.7472	0.6636, 0.7455	0.5171, 0.7465
No. of measured, independent and observed reflections	257146, 14564, 9971	101946, 15413, 10380	117417, 21081, 14895
Criterion for observed reflections	$I > 2\sigma(I)$	$I > 2\sigma(I)$	$I > 2\sigma(I)$
R_{int}	0.0692	0.071	0.0598
$\Theta_{max}(°)$	36.74	27.44	30.58
Refinement			
Refinement on	F^2	F^2	F^2
$R[F^2 > 2\sigma(F)], \omega R(F^2), S$	0.0645, 0.1799, 1.183	0.0420, 0.1208, 1.062	0.0388, 0.885, 1.020
No. of reflections	14564	15413	21081
No. of parameters	358	850	877
No. of restrains	0	4	2
Weighting scheme	$x = 0.0517, y = 13.5390$	$x = 0.0564, y = 1.8169$	$x = 0.0344, y = 2.5320$
$(\Delta/\sigma)_{max}$	0.005	0.001	0.002
$\Delta\rho_{max}$,$\Delta\rho_{max}$ (e Å^{-3})	1.724, -0.632	0.829, -0.547	0.844, -0.694

*$\omega = 1/[\sigma^2(F_0^2) + (xP)^2 + yP]$, where $P = (F_0^2 + 2F_c^2)/3$

Table B.7: Crystal data, data collection parameters and refinement details for Pb/Ti and Sr/Ti clusters

Compound	**Sr2Ti8**	**Pb2Ti8**	**Pb2Ti8Allyl**	**Pb2Ti8nPr**
Crystal data				
Empirical formula	$C_{73.73}H_{104.93}O_{46.27}Sr_2Ti_8$	$C_{86.61}H_{126.60}O_{48}Pb_2Ti_8$	$C_{84}H_{112}O_{48}Pb_2Ti_8$	$C_{83.03}H_{117}O_{48}Pb_2Ti_8$
M_r	2290.02	2733.38	2687.32	2680.71
Cell setting	monoclinic	triclinic	triclinic	triclinic
Space group	$P2_1/c$	$P\bar{1}$	$P\bar{1}$	$P\bar{1}$
Temperature (K)	100(2)	100(2)	100(2)	100(2)
a Å	13.2578(13)	14.0681(12)	14.1810(11)	14.2441(12)
b Å	24.965(2)	14.6846(13)	15.2581(12)	15.4061(15)
c Å	15.3483(15)	16.3755(15)	15.5176(13)	15.4465(15)
$\alpha(°)$	90	69.750(3)	101.441(4)	101.500(5)
$\beta(°)$	107.820(4)	67.220(2)	109.443(4)	109.516(4)
$\gamma(°)$	90	69.320(2)	114.474(4)	114.056(4)
V (Å^3)	4836.2(8)	2776.5(4)	2651.3(4)	2686.6(4)
Z	2	1	1	1
$D_x(Mg \cdot m^{-3})$	1.573	1.635	1.683	1.657
$\mu(mm^{-1})$	1.807	3.649	3.82	3.769
Crystal form, colour	fragment, colourless	brick, colourless	brick, colourless	brick, colourless
Crystal size (mm)	0.21 x 0.18 x 0.15	0.38 x 0.18 x 0.15	0.39 x 0.20 x 0.16	0.36 x 0.20 x 0.14
Data collection				
T_{min}, T_{max}	0.6283, 0.7455	0.5123, 0.7449	0.5175, 0.7459	0.5356, 0.7458
No. of measured, independent and observed reflections	124406, 11041, 7087	76085, 8017, 6083	106565, 15058, 11482	87645, 14608, 9947
Criterion for observed reflections	$I > 2\sigma(I)$	$I > 2\sigma(I)$	$I > 2\sigma(I)$	$I > 2\sigma(I)$
R_{int}	0.092	0.0756	0.0438	0.0696
$\Theta_{max}(°)$	27.53	23.34	29.76	29.32
Refinement				
Refinement on	F^2	F^2	F^2	F^2
$R[F^2 > 2\sigma(F)], \omega R(F^2), S$	0.0590, 0.1296, 1.171	0.0430, 0.1151, 1.109	0.0398, 0.1030, 1.087	0.0533, 0.1281, 1.096
No. of reflections	11041	8017	15058	14608
No. of parameters	633	667	692	674
No. of restrains	6	11	1	6
Weighting scheme*	$x = 0.0229, y = 15.7086$	$x = 0.0525, y = 7.6879$	$x = 0.0447, y = 4.2832$	$x = 0.0386, y = 13.7774$
$(\Delta/\sigma)_{max}$	0.001	0.002	0.008	0.002
$\Delta\rho_{max}$,$\Delta\rho_{max}$ (e Å^{-3})	0.667, -0.696	1.128, -1.205	1.657, -1.041	4.526, -2.795

*$\omega = 1/[\sigma^2(F_0^2) + (xP)^2 + yP]$, where $P = (F_0^2 + 2F_c^2)/3$

Table B.8: Crystal data, data collection parameters and refinement details for Pb/Ti clusters

Compound	**Pb2Ti6**	**Pb2Ti6nPr**	**Pb6Ti6met**	**Pb4Ti8Ac**
Crystal data				
Empirical formula	$C_{68}\cdot75\,H_{94}\cdot47\,O_{37}\cdot75\,Pb_2Ti_6$	$C_{67}\cdot78\,H_{94}\cdot97\,O_{37}\cdot78\,Pb_2Ti_6$	$C_{73}H_{93}O_{46}Pb_6Ti_6$	$C_{58}H_{132}O_{32}Pb_4Ti_8$
M_r	2226.7	2215.89	3237.01	2553.6
Cell setting	monoclinic	triclinic	monoclinic	monoclinic
Space group	$P2_1/n$	$P\bar{1}$	$P2_1/n$	$P2_1/n$
Temperature (K)	100(2)	100(2)	100(2)	100(2)
a Å	13.7364(8)	16.1532(6)	14.1702(18)	14.4586(12)
b Å	24.3488(13)	21.6793(7)	19.755(3)	26.347(2)
c Å	27.4983(15)	28.2095(9)	35.927(5)	23.7350(19)
$\alpha(°)$	90	112.330(2)	90.00	90.00
$\beta(°)$	100.253(3)	101.644(2)	90.010(2)	90.086(4)
$\gamma(°)$	90	94.160(2)	90.00	90.00
V (Å^3)	9050.3(9)	8827.6(5)	10057(2)	9041.5(12)
Z	4	4	4	4
$D_x(Mg\cdot m^{-3})$	1.634	1.667	2.138	1.876
$\mu(mm^{-1})$	4.289	4.397	10.538	8.152
Crystal form, colour	brick, colourless	fragment, colourless	fragment, colourless	brick, colourless
Crystal size (mm)	0.18 x 0.15 x 0.11	0.19 x 0.16 x 0.13	0.32 x 0.24 x 0.12	0.41 x 0.32 x 0.28
Data collection				
T_{min}, T_{max}	0.5616, 0.7459	0.4888, 0.5987	0.5345, 0.7461	0.4793, 0.7458
No. of measured, independent and observed reflections	139559, 25476, 18468	204391, 30311, 16537	31237, 31237, 28038	203814, 24486, 19725
Criterion for observed reflections	$I > 2\sigma(I)$	$I > 2\sigma(I)$	$I > 2\sigma(I)$	$I > 2\sigma(I)$
R_{int}	0.0641	0.1118	0.0212	0.036
$\Theta_{max}(°)$	29.66	24.81	30.77	29.28
Refinement				
Refinement on	F^2	F^2	F^2	F^2
$R[F^2 > 2\sigma(F)], \omega R(F^2), S$	0.0346, 0.0720, 0.976	0.0477, 0.1339, 1.064	0.0266, 0.525, 1.197	0.0391, 0.788, 1.072
No. of reflections	25476	30311	31237	24486
No. of parameters	1114	2113	1209	939
No. of restrains	0	97	4	0
Weighting scheme *	$x = 0.0296, y = 8.3837$	$x = 0.0431, y = 32.6485$	$x = 0.0064, y = 37.3328$	$x = 0.000, y = 113.9125$
$(\Delta/\sigma)_{max}$	0.006	0.011	0.028	0.004
$\Delta\rho_{max}$,$\Delta\rho_{max}$ (e Å^{-3})	1.751, -0.882	2.442, -0.966	1.512, -1.536	3.546, -2.289

*$\omega = 1/[\sigma^2(F_0^2) + (xP)^2 + yP]$, where $P = (F_0^2 + 2F_c^2)/3$

Table B.9: Crystal data, data collection parameters and refinement details for Cu/Ti clusters

Compound	**Cu4Ti5met**	**Cu4Ti5metS**	**Cu4Ti5prop**
Crystal data			
Empirical formula	$C_{64}H_{80}Cu_4O_{38}Ti_5$	$C_{66}H_{84}Cl_4Cu_4O_{38}Ti_5$	$C_{48}H_{80}Cu_4O_{38}Ti_5$
M_r	1950.94	2120.79	1758.78
Cell setting	triclinic	triclinic	monoclinic
Space group	$P\bar{1}$	$P\bar{1}$	$P2_1/n$
Temperature (K)	100(2)	100(2)	100(2)
a Å	12.6920(3)	13.8581(9)	15.7865(9)
b Å	12.7556(3)	17.5769(12)	13.6433(9)
c Å	13.5790(4)	18.4259(13)	16.5323(10)
$\alpha(°)$	91.5890(10)	92.384(2)	90
$\beta(°)$	69.9670(10)	101.658(2)	108.080(4)
$\gamma(°)$	84.0630(10)	91.658(2)	90
V (Å^3)	2034.97(9)	4395.4(5)	3384.9(4)
Z	1	2	2
$D_x(Mg \cdot m^{-3})$	1.592	1.608	1.726
$\mu(mm^{-1})$	1.575	1.583	1.882
Crystal form, colour	fragment, dark-green	brick, dark-green	brick, dark-green
Crystal size (mm)	0.38 x 0.33 x 0.30	0.50 x 0.32 x 0.14	0.29 x 0.25 x 0.22
Data collection			
T_{min}, T_{max}	0.5860, 0.6495	0.6155, 0.7468	0.5171, 0.7465
No. of measured, independent and observed reflections	80190, 25086, 16843	307807, 36953, 28749	134762, 12959, 9150
Criterion for observed reflections	$I > 2\sigma(I)$	$I > 2\sigma(I)$	$I > 2\sigma(I)$
R_{int}	0.0291	0.0318	0.0502
$\Theta_{max}(°)$	40.31	34.42	33.25
Refinement			
Refinement on	F^2	F^2	F^2
$R[F^2 > 2\sigma(F)], \omega R(F^2), S$	0.0413, 0.1090, 1.028	0.0342, 0.0868, 1.090	0.0486, 0.0943, 1.114
No. of reflections	25086	36953	12959
No. of parameters	510	1100	466
No. of restrains	0	0	0
Weighting scheme*	$x = 0.0499, y = 0.6248$	$x = 0.0275, y = 4.6424$	$x = 0.0298, y = 3.7190$
$(\Delta/\sigma)_{max}$	0.002	0.002	0.001
$\Delta\rho_{max}$,$\Delta\rho_{max}$ (e Å^{-3})	1.089, -0.703	1.044, -0.997	0.932, -1.034

*$\omega = 1/[\sigma^2(F_0^2) + (xP)^2 + yP]$, where $P = (F_0^2 + 2F_c^2)/3$

Table B.10: Crystal data, data collection parameters and refinement details for Ti/Lanthanide clusters

Compound	**LaTi4**	**CeTi4**	**La2Ti6**
Crystal data			
Empirical formula	$C_{50}H_{69}LaO_{27}Ti_4$	$C_{50}H_{69}CeO_{27}Ti_4$	$C_{39}H_{53}LaO_{22}Ti_3$
M_r	1432.56	1433.66	1156.42
Cell setting	triclinic	triclinic	monoclinic
Space group	$P\overline{1}$	$P\overline{1}$	$P2_1/n$
Temperature (K)	100(2)	100(2)	100(2)
a Å	11.8330(6)	11.7983(10)	13.2380(10)
b Å	12.8405(7)	12.9135(12)	25.401(2)
c Å	41.567(2)	41.763(4)	16.1311(13)
$\alpha(°)$	84.8600(10)	84.820(2)	90
$\beta(°)$	85.8980(10)	86.530(2)	113.483(4)
$\gamma(°)$	89.2520(10)	89.790(2)	90
V (Å^3)	6274.0(6)	6325.2(10)	4975.0(7)
Z	2	2	4
$D_x(Mg \cdot m^{-3})$	1.517	1.506	1.544
$\mu(mm^{-1})$	1.233	1.267	1.381
Crystal form, colour	brick, dark-yellow	brick, orange	brick, orange
Crystal size (mm)	0.36 x 0.34 x 0.30	0.35 x 0.28 x 0.21	0.30 x 0.27 x 0.22
Data collection			
T_{min}, T_{max}	0.6841, .7464	0.6773, 0.7459	0.6821, 0.7509
No. of measured, independent and observed reflections	217332, 36907, 30664	210874, 34198, 28928	235033, 15865, 12066
Criterion for observed reflections	$I > 2\sigma(I)$	$I > 2\sigma(I)$	$I > 2\sigma(I)$
R_{int}	0.0340	0.0507	0.0354
$\Theta_{max}(°)$	30.15	29.68	31.14
Refinement			
Refinement on	F^2	F^2	F^2
$R[F^2 > 2\sigma(F)], \omega R(F^2), S$	0.0482, .01093, 1.159	0.0390, 0.0874, 1.100	0.0622, 0.1398, 1.353
No. of reflections	36907	34198	15865
No. of parameters	1656	1525	623
No. of restrains	9	0	3
Weighting scheme*	$x = 0.0308, y = 10.2792$	$x = 0.0258, y = 7.7332$	$x = 0.0134, y = 19.2502$
$(\Delta/\sigma)_{max}$	0.005	0.044	0.036
$\Delta\rho_{max}$,$\Delta\rho_{max}$ (e Å^{-3})	0.972, -1.086	1.164, -0.916	1.752, -1.350

*$\omega = 1/[\sigma^2(F_0^2) + (xP)^2 + yP]$, where $P = (F_0^2 + 2F_c^2)/3$

Table B.11: Crystal data, data collection parameters and refinement details for Ti/Lanthanide clusters

Compound	**Ce2Ti6**	**Nd2Ti6**	**Sm2Ti4**
Crystal data	$C_{39}H_{53}CeO_{22}Ti_3$	$C_{39}H_{52}NdO_{22}Ti_3$	$C_{64}H_{82}Sm_2O_{36}Ti_4$
Empirical formula			
M_r	1157.63	1160.75	1919.6
Cell setting	monoclinic	monoclinic	triclinic
Space group	$P2_1/n$	$P2_1/n$	$P\bar{1}$
Temperature (K)	100(2)	100(2)	100(2)
a Å	13.2605(4)	13.2948(8)	11.380(2)
b Å	25.3631(8)	25.2726(16)	12.408(2)
c Å	16.1410(5)	16.1438(10)	14.525(3)
$\alpha(°)$	90.00	90.00	84.321(5)
$\beta(°)$	113.5940(10)	113.833(2)	82.172(5)
$\gamma(°)$	90.00	90.00	77.799(5)
V (Å^3)	4974.8(3)	4961.7(5)	1980.9(6)
Z	4	4	1
$D_x(Mg \cdot m^{-3})$	1.546	1.554	1.609
$\mu(mm^{-1})$	1.437	1.570	1.928
Crystal form, colour	brick, orange	brick, orange	brick, yellow
Crystal size (mm)	0.35 x 0.22 x 0.20	0.38 x 0.28 x 0.23	0.25 x 0.24 x 0.14
Data collection			
T_{min}, T_{max}	0.6331, 0.7620	0.5868, 0.7141	0.6442, 0.7740
No. of measured, independent and observed reflections	253922, 17295, 13604	254702, 14637, 11393	101878, 15288, 11271
Criterion for observed reflections	$I > 2\sigma(I)$	$I > 2\sigma(I)$	$I > 2\sigma(I)$
R_{int}	0.0639	0.0720	0.0413
$\Theta_{max}(°)$	32.32	30.15	33.41
Refinement			
Refinement on	F^2	F^2	F^2
$R[F^2 > 2\sigma(F)], \omega R(F^2), S$	0.0448, 0.1144, 1.213	0.060, 0.1487, 1.313	0.0450, 0.1280, 1.186
No. of reflections	17295	14637	15288
No. of parameters	646	610	525
No. of restrains	5	5	0
Weighting scheme*	$x = 0.0331, y = 8.4502$	$x = 0.0295, y = 21.1794$	$x = 0.0352, y = 6.6674$
$(\Delta/\sigma)_{max}$	0.000	0.006	0.005
$\Delta\rho_{max}$,$\Delta\rho_{max}$ (e Å^{-3})	1.374, -1.352	1.700, -1.626	5.639, -1.522

*$\omega = 1/[\sigma^2(F_0^2) + (xP)^2 + yP]$, where $P = (F_0^2 + 2F_c^2)/3$

Table B.12: Crystal data, data collection parameters and refinement details for Ti/Lanthanide clusters

Compound	**Eu2Ti4**	**Gd2Ti4**	**Ho2Ti4**
Crystal data			
Empirical formula	$C_{64}H_{82}Eu_2O_{36}Ti_4$	$C_{64}H_{82}Gd_2O_{36}Ti_4$	$C_{64}H_{82}Ho_2O_{36}Ti_4$
M_r	1922.82	1933.4	1948.76
Cell setting	triclinic	triclinic	triclinic
Space group	$P\bar{1}$	$P\bar{1}$	$P\bar{1}$
Temperature (K)	100(2)	99(2)	99(2)
a Å	11.3836(8)	11.396(3)	11.3885(14)
b Å	12.3936(8)	12.404(3)	12.3637(14)
c Å	14.5215(10)	14.432(4)	14.4795(18)
$\alpha(°)$	84.291(2)	84.769(6)	84.293(3)
$\beta(°)$	82.203(2)	81.551(6)	82.365(3)
$\gamma(°)$	77.637(2)	77.581(4)	77.237(2)
V (Å^3)	1977.5(2)	1966.8(10)	1965.6(4)
Z	1	1	1
$D_x(Mg \cdot m^{-3})$	1.615	1.632	1.646
$\mu(mm^{-1})$	2.033	2.135	2.462
Crystal form, colour	cube, colourless	fragment, orange	fragment, orange
Crystal size (mm)	0.33 x 0.30 x 0.29	0.34 x 0.29 x 0.20	0.22 x 0.19 x 0.18
Data collection			
T_{min}, T_{max}	0.5535, 0.5902	0.5305, 0.6747	0.6134, 0.6656
No. of measured, independent and observed reflections	87054, 12723, 9772	126245, 17528, 14698 14698	109256, 15143, 11798
Criterion for observed reflections	$I > 2\sigma(I)$	$I > 2\sigma(I)$	$I > 2\sigma(I)$
R_{int}	0.0495	0.0365	0.0414
$\Theta_{max}(°)$	31.18	35.19	33.31
Refinement			
Refinement on	F^2	F^2	F^2
$R[F^2 > 2\sigma(F)], \omega R(F^2), S$	0.036, 0.0958, 1.100	0.0611, 0.1460, 1.100	0.0378, 0.1056, 1.180
No. of reflections	12723	17528	15143
No. of parameters	525	524	525
No. of restrains	0	0	0
Weighting scheme*	$x = 0.0334, y = 2.9260$	$x = 0.0349, y = 10.5736$	$x = 0.0283, y = 5.3174$
$(\Delta/\sigma)_{max}$	0.005	0.003	0.006
$\Delta\rho_{max}$,$\Delta\rho_{max}$ (e Å^{-3})	2.573, -1.077	6.219, -1.949	5.029, -1.621

*$\omega = 1/[\sigma^2(F_0^2) + (xP)^2 + yP]$, where $P = (F_0^2 + 2F_c^2)/3$

Table B.13: Crystal data, data collection parameters and refinement details for monometallic Ti clusters

Compound	**Ti6prop**	**Ti6pivPB**	**Ti6pivBB**	**Ti8ring prop**
Crystal data				
Empirical formula	$C_{36}H_{64}O_{28}Ti_6$	$C_{34}H_{67}O_{14}Ti_3$	$C_{72}H_{144}O_{28}Ti_6$	$C_{57}H_{96}O_{46}Ti_8$
M_r	1232.27	843.58	1745.27	1900.54
Cell setting	triclinic	triclinic	triclinic	orthorhombic
Space group	$P\bar{1}$	$P\bar{1}$	$P\bar{1}$	$P2_12_12_1$
Temperature (K)	100(2)	100(2)	100(2)	100(2)
a Å	9.3628(14)	12.9459(12)	13.7251(17)	12.5558(5)
b Å	11.467(2)	13.7887(12)	13.893(2)	23.7348(9)
c Å	12.838(2)	13.9853(14)	14.654(2)	27.6245(12)
$\alpha(^\circ)$	73.427(8)	72.890(4)	95.722(5)	90.00
$\beta(^\circ)$	89.342(7)	68.050(3)	111.837(4)	90.00
$\gamma(^\circ)$	75.625(7)	74.700(3)	111.654(4)	90.00
V (Å^3)	1277.0(4)	2179.4(4)	2317.9(6)	8232.4(6)
Z	1	2	1	4
$D_x(Mg \cdot m^{-3})$	1.602	1.285	1.250	1.53
$\mu(mm^{-1})$	0.987	0.594	0.560	0.83
Crystal form, colour	brick, colourless	fragment, colourless	plate, colourless	brick, colourless
Crystal size (mm)	0.33 x 0.31 x 0.29	0.32x 0.24 x 0.14	0.44, 0.17, 0.10	0.60 x 0.37 x 0.28
Data collection				
T_{min}, T_{max}	0.5699, 0.7456	0.6183, 0.7451	0.6335, 0.7448	0.5586, 0.7463
No. of measured, independent and observed reflections	27774, 6202, 3413	49328, 7506, 5319	40063, 6064, 3647	295453, 28667, 23879
Criterion for observed reflections	$I > 2\sigma(I)$	$I > 2\sigma(I)$	$I > 2\sigma(I)$	$I > 2\sigma(I)$
R_{int}	0.1313	0.0457	0.1013	0.054
$\Theta_{max}(^\circ)$	28.15	24.81	22.6	32.08
Refinement				
Refinement on	F^2	F^2	F^2	F^2
$R[F^2 > 2\sigma(F)], \omega R(F^2), S$	0.0529, 0.0994, 0.952	0.0527, 0.1616, 1.035	0.0665, 0.2030, 1.029	0.571, 0.1291, 1.137
No. of reflections	6202	7506	6064	28667
No. of parameters	323	511	494	1054
No. of restrains	0	11	0	1
Weighting scheme*	$x = 0.0352, y = 0$	$x = 0.0838, y = 3.4542$	$x = 0.0991, y = 5.9464$	$x = 0.0452, y = 13.4208$
$(\Delta/\sigma)_{max}$	0.000	0.000	0.000	0.002
$\Delta\rho_{max}$,$\Delta\rho_{max}$ (e Å^{-3})	0.904, -0.914	0.802, -0.672	0.967, -0.654	1.324, -0.638

$^*\omega = 1/[\sigma^2(F_0^2) + (xP)^2 + yP]$, where $P = (F_0^2 + 2F_c^2)/3$

Table B.14: Crystal data, data collection parameters and refinement details for monometallic Zr clusters

Compound	**Zr4benz**	**Zr4piv**	**Zr6piv**
Crystal data			
Empirical formula	$C_{92}H_{76}O_{28}Zr_4$	$C_{60}H_{108}O_{26}Zr_4$	$C_{38}H_{70}O_{17}Zr_3$
M_r	1994.41	1610.34	1072.6
Cell setting	triclinic	monoclinic	triclinic
Space group	$P\bar{1}$	$P2_1/c$	$P\bar{1}$
Temperature (K)	100(2)	100(2)	100(2)
a Å	12.8511(5)	18.7166(13)	14.9627(15)
b Å	13.5791(3)	20.8039(14)	16.7023(16)
c Å	14.0135(2)	19.3094(13)	21.019(2)
$\alpha(°)$	118.9600(10)	90.00	109.509(2)
$\beta(°)$	95.2700(10)	91.278(3)	90.427(3)
$\gamma(°)$	98.0600(10)	90.00	90.086(3)
V (Å^3)	2082.20(10)	7516.8(9)	4951.2(8)
Z	1	4	4
$D_x(Mg \cdot m^{-3})$	1.591	1.42	1.439
$\mu(mm^{-1})$	0.571	0.61	0.682
Crystal form, colour	fragment, colourless	brick, colourless	fragment, colourless
Crystal size (mm)	0.20 x 0.17 x 0.12	0.37 x 0.28 x 0.26	0.20 x 0.15 x 0.11
Data collection			
T_{min}, T_{max}	0.6443, 0.7454	0.8055, 0.8573	0.8756, 0.9287
No. of measured, independent and observed reflections	48489, 8466, 6257	133890, 9992, 8479	178665, 25760, 12122
Criterion for observed reflections	$I > 2\sigma(I)$	$I > 2\sigma(I)$	$I > 2\sigma(I)$
R_{int}	0.0602	0.0328	0.2245
$\Theta_{max}(°)$	26.36	22.83	28.84
Refinement			
Refinement on	F^2	F^2	F^2
$R[F^2 > 2\sigma(F)], \omega R(F^2), S$	0.0367, 0.0820, 1.015	0.1069, 0.3090. 1.175	0.1101, 0.2335, 1.062
No. of reflections	8466	9992	25760
No. of parameters	559	845	1088
No. of restrains	0	0	0
Weighting scheme*	$x = 0.0341, y = 1.3815$	$x = 0.0928, y = 377.8724$	$x = 0.0528, y = 55.2331$
$(\Delta/\sigma)_{max}$	0.002	0.000	0.002
$\Delta\rho_{max}$,$\Delta\rho_{max}$ (e Å^{-3})	0.877, -0.641	3.139, -1.857	2.734, -1.856

*$\omega = 1/[\sigma^2(F_0^2) + (xP)^2 + yP]$, where $P = (F_0^2 + 2F_c^2)/3$

References

[1] Cotton, F. A. *Acc. Chem. Res.* **1968**, *2*, 240–247.

[2] Sanchez, C.; Belleville, P.; Popall, M.; Nicole, L. *Chem. Soc. Rev.* **2011**, *40*, 696–753.

[3] Gross, S. *J. Mater. Chem.* **2011**, 15853–15861.

[4] Rozes, L.; Sanchez, C. *Chem. Soc. Rev.* **2011**, *40*, 1006–1030.

[5] Schubert, U. *J. Mater. Chem.* **2005**, *15*, 3701–3715.

[6] Schubert, U. *Chem. Soc. Rev.* **2011**, 575–582.

[7] Walther, P.; Puchberger, M.; Kogler, F. R.; Schwarz, K.; Schubert, U. *Phys. Chem. Chem. Phys.* **2009**, *11*, 3640–3647.

[8] Rozes, L.; Steunou, N.; Fornasieri, G.; Sanchez, C. *Monatshefte für Chemie - Chem. Mon.* **2006**, *137*, 501–528.

[9] Schubert, U.; Husing, N. *Synthesis of Inorganic Materials*; WILEY-VCH Verlag GmbH, 2012.

[10] Sanchez, C.; In, M.; Toledano, P.; Griesmar, P. *Mater. Res. Soc. Symp. Proc.* **1992**, *271*, 669–680.

[11] Brinker, C.; G.W.Scherer *Sol-Gel Science: The Physics and Chemistry of Sol-Gel Processing*; Academic Press: Boston, 1990.

[12] Sanchez, C.; Livage, J.; Henry, M.; Babonneau, F. *J. Non. Cryst. Solids* **1988**, *100*, 65–76.

[13] Ibers, J. A. *Nature* **1963**, *197*, 686–687.

[14] Wright, D. A.; Williams, D. A. *Acta Crystallogr., Sect. B: Struct. Sci.* **1968**, *24*, 1107–1114.

[15] Boyle, T. J.; Alam, T. M.; Mechenbier, E. R.; Scott, B. L.; Ziller, J. W. *Inorg. Chem.* **1997**, *3*, 3293–3300.

[16] Caughlan, C. N.; Smith, H. S.; Katz, W.; Hodgson, W.; Crowe, R. W. *J. Am. Chem. Soc.* **1951**, *73*, 5652–5654.

[17] Babonneau, F.; Doeuff, S.; Leaustic, A.; Sanchez, C.; Cartier, C.; Verdaguer, M. *Inorg. Chem.* **1988**, *27*, 3166–3172.

[18] Bradley, D.; Mehrotra, R.; Rothwell, I.; Singh, A. *Alkoxo and Aryloxo Derivatives of Metals*; Academic Press, 2001.

[19] Turova, N. Y.; Turevskaya, E. P.; Kessler, V. G.; Yanovskaya, M. I. *The Chemistry of Metal Alkoxides*; Springer, 2002.

[20] Schubert, U. *Macromol. Symp.* **2008**, *267*, 1–8.

[21] Schubert, U. *Chem. Mater.* **2001**, *13*, 3487–3494.

[22] Boyle, T. J.; Tyner, R. P.; Alam, T. M.; Scott, B. L.; Ziller, J. W.; Potter, B. G. *J. Am. Chem. Soc.* **1999**, *121*, 12104–12112.

[23] Doeuff, S.; Dromzee, Y.; Taulelle, F.; Sanchez, C. *Inorg. Chem.* **1989**, *28*, 4439–4445.

[24] Steunou, N.; Robin, F.; Boubekeur, K.; Sanchez, C. *Inorg. Chim. Acta* **1998**, *279*, 144–151.

[25] Papiernik, R.; Hubert-Pfalzgraf, L. G.; Vaissermann, J.; Gonvalves, M. *Dalt. Trans.* **1998**, *14*, 2285–2288.

[26] Boyle, T. J.; Alam, T. M.; Tafoya, C. J.; Scott, B. L. *Inorg. Chem.* **1998**, *4*, 5588–5594.

[27] Pandey, A.; Gupta, V. D.; Nöth, H. *Eur. J. Inorg. Chem.* **2000**, 1351–1357.

[28] Senouci, A.; Yaakoub, M.; Huguenard, C.; Henry, M. *J. Mater. Chem.* **2004**, *14*, 3215–3237.

[29] Day, V. *Inorg. Chim. Acta* **1995**, *229*, 391–405.

[30] Mijatovic, I.; Kickelbick, G.; Puchberger, M.; Schubert, U. *New J. Chem.* **2003**, *27*, 3–5.

[31] Reis, D. M.; Nunes, G. G.; Sa, E. L.; Friedermann, G. R.; Mangrich, A. S.; Evans, D. J.; Hitchcock, P. B.; Leigh, G. J.; Soares, J. F. *New J. Chem.* **2004**, *28*, 1168–1176.

[32] Mehner, A.; Rüffer, T.; Lang, H.; Pohlers, A.; Hoyer, W.; Spange, S. *Adv. Mater.* **2008**, *20*, 4113–4117.

[33] Mehner, A.; Rüffer, T.; Lang, H.; Schlesinger, M.; Mehring, M.; Spange, S. *New J. Chem.* **2013**, *37*, 1290–1293.

[34] Lv, Y.; Willkomm, J.; Leskes, M.; Steiner, A.; King, T. C.; Gan, L.; Reisner, E.; Wood, P. T.; Wright, D. S. *Chem. Eur. J.* **2012**, *18*, 11867–11870.

[35] Ghosh, R.; Nethaji, M.; Samuelson, A. G. *Chem. Commun.* **2003**, *1586*, 2556–2557.

[36] Benedict, J. B.; Coppens, P. *J. Am. Chem. Soc.* **2010**, *132*, 2938–2944.

[37] Lei, X.; Shang, M.; Fehlner, T. P. *Organometallics* **1996**, *15*, 3779–3781.

[38] Lei, X.; Shang, M.; Fehlner, T. P. *Organometallics* **1997**, *16*, 5289–5301.

[39] Moraru, B.; Hüsing, N.; Kickelbick, G.; Schubert, U.; Fratzl, P.; Peterlik, H. *Chem. Mater.* **2002**, *14*, 2732–2740.

[40] Cadra, S.; Velasquez, E.; Moreau, L.; Giorgi, M.; Balland-Longeau, a.; Thibonnet, J. *Tetrahedron Lett.* **2011**, *52*, 3982–3986.

[41] Moran, P. D.; Rickard, C. E. F.; Bowmaker, G. A.; Cooney, R. P.; Bartlett, J. R.; Woolfrey, J. L. *Inorg. Chem.* **1998**, *37*, 1417–1419.

[42] Fric, H.; Schubert, U. *J. Sol-Gel Sci. Technol.* **2008**, *48*, 2–5.

[43] Yanovskii, A. I.; Dolgushin, F. M.; Yanovskaya, M. I.; Kotova, N. M.; Struchkov, Y. T.; Turova, N. Y. *Russ. J. Inorg. Chem.* **1997**, *42*, 450–453.

[44] Rabe, S.; Mueller, U. *Zeitschrift für Naturforsch. B, Chem. Sci.* **1997**, *55*, 1291–1295.

[45] Sui, R.; Charpentier, P. a.; Rizkalla, a. S.; Jennings, M. C. *Acta Crystallogr. Sect. E: Struct. Rep. Online* **2006**, *62*, m373–m375.

[46] Piszczek, P.; Grodzicki, A.; Richert, M.; Wojtczak, A. *Inorg. Chim. Acta* **2004**, *357*, 2769–2775.

[47] Rammal, A.; Brisach, F.; Henry, M. *C. R. Chim.* **2002**, *5*, 59–66.

[48] Czakler, M.; Artner, C.; Schubert, U. *Eur. J. Inorg. Chem.* **2012**, *2012*, 3485–3489.

[49] Ammala, P. S.; Batten, S. R.; Kepert, C. M.; Spiccia, L.; van den Bergen, A. M.; West, B. O. *Inorg. Chim. Acta* **2003**, *353*, 75–81.

[50] Seisenbaeva, G. A.; Mallah, T.; Kessler, V. G. *Dalton Trans.* **2010**, *39*, 7774–7779.

[51] Piszczek, P.; Radtke, A.; Muziol, T.; Richert, M.; Chojnacki, J. *Dalton Trans.* **2012**, *41*, 8261–8269.

[52] Piszczek, P.; Richert, M.; Radtke, A.; Muziol, T.; Wojtczak, A. *Polyhedron* **2009**, *28*, 3872–3880.

[53] Piszczek, P.; Richert, M.; Wojtczak, A. *Polyhedron* **2008**, *27*, 602–608.

[54] Gautier-Luneau, I.; Mosset, A.; Galy, J. *Zeitschrift für Krist.* **1987**, *180*, 83–95.

[55] Schubert, U.; Arpac, J. E.; Glaubitt, W.; Helmerich, A.; Chau, C. *Chem. Mater.* **1992**, *4*, 291–295.

[56] Laaziz, I.; Larbot, A.; Guizard, C.; Durand, J.; Cot, L.; Joffre, J. *Acta Crystallogr., Sect. C: Cryst. Struct. Commun.* **1990**, *46*, 2332–2334.

[57] Gao, Y.; Kogler, F. R.; Peterlik, H.; Schubert, U. *J. Mater. Chem.* **2006**, *16*, 3268.

[58] Heinz, P.; Puchberger, M.; Bendova, M.; Baumann, S. O.; Schubert, U. *Dalt. Trans.* **2010**, *39*, 7640–7644.

[59] Biechel, F.; Dubuc, J.; Henry, M. *New J. Chem.* **2004**, *28*, 764–769.

[60] Schmid, R.; Mosset, A.; Galy, J. *J. Chem. Soc. Dalt. Trans.* **1991**, 1999.

[61] Frot, T.; Marrot, J.; Sanchez, C.; Rozes, L.; Sassoye, C. *Zeitschrift für Anorg. und Allg. Chemie* **2013**, *639*, 2181–2185.

[62] Belli Dell'Amico, D.; Calderazzo, F.; Costa, L.; Franchi, E.; Gini, L.; Labella, L.; Marchetti, F. *J. Mol. Struct.* **2008**, *890*, 295–297.

[63] Piszczek, P.; Richert, M.; Grodzicki, A.; Glowiak, T.; Wojtczak, A. *Polyhedron* **2005**, *24*, 663–670.

[64] Barrow, H.; Brown, D. A.; Alcock, N. W.; Clase, H. J.; Wallbridge, M. G. H. *Chem. Commun.* **1995**, 1231–1232.

[65] Frot, T.; Cochet, S.; Laurent, G.; Sassoye, C.; Popall, M.; Sanchez, C.; Rozes, L. *Eur. J. Inorg. Chem.* **2010**, *2010*, 5650–5659.

[66] Chaumont, C.; Huen, E.; Huguenard, C.; Mobian, P.; Henry, M. *Polyhedron* **2013**, *57*, 70–76.

[67] Artner, C.; Czakler, M.; Schubert, U. *Chem. Eur. J.* **2014**, *20*, 493–498.

[68] Day, V. W.; Eberspacher, T. A.; Klemperer, W. G.; Park, C. W.; Rosenberg, F. S. *J. Am. Chem. Soc.* **1991**, *113*, 8190–8192.

[69] Kickelbick, G.; Schubert, U. *Eur. J. Inorg. Chem.* **1998**, 159–161.

[70] Steunou, N.; Ribot, F.; Boubekeur, K.; Maquet, J.; Sanchez, C. *New J. Chem.* **1999**, *23*, 1079–1086.

[71] Day, V. W.; Eberspacher, T. a.; Klemperer, W. G.; Park, C. W. *J. Am. Chem. Soc.* **1993**, *115*, 8469–8470.

[72] Boyle, T. J.; Ottley, L. A. M.; Hoppe, S. M.; Campana, C. F. *Inorg. Chem.* **2010**, *49*, 10798–10808.

[73] Benedict, J. B.; Freindorf, R.; Trzop, E.; Cogswell, J.; Coppens, P. *J. Am. Chem. Soc.* **2010**, *132*, 13669–13671.

[74] Fornasieri, G.; Rozes, L.; Le Calvé, S.; Alonso, B.; Massiot, D.; Rager, M. N.; Evain, M.; Boubekeur, K.; Sanchez, C. *J. Am. Chem. Soc.* **2005**, *127*, 4869–4878.

[75] Périneau, F.; Pensec, S.; Sassoye, C.; Ribot, F.; van Lokeren, L.; Willem, R.; Bouteiller, L.; Sanchez, C.; Rozes, L. *J. Mater. Chem.* **2011**, *21*, 4470–4475.

[76] Sokolow, J. D.; Trzop, E.; Chen, Y.; Tang, J.; Allen, L. J.; Crabtree, R. H.; Benedict, J. B.; Coppens, P. *J. Am. Chem. Soc.* **2012**, *134*, 11695–11700.

[77] Campana, C. F.; Chen, Y.; Day, V. W.; Klemperer, W. G.; Sparks, R. A. *J. Chem. Soc. Dalt. Trans.* **1996**, 691.

[78] Moraru, B.; Kickelbick, G.; Schubert, U. *Eur. J. Inorg. Chem.* **2001**, *2001*, 1295–1301.

[79] Kickelbick, G.; Schubert, U. *Chem. Ber.* **1997**, *130*, 473–477.

[80] Demsar, A.; Kosmrlj, J.; Petricek, S. *J. Am. Chem. Soc.* **2002**, *124*, 3951–3958.

[81] Trabelsi, S.; Janke, A.; Haessler, R.; Zafeiropoulos, N. E.; Fornasieri, G.; Bocchini, S.; Rozes, L.; Stamm, M.; Gerard, J.-F.; Sanchez, C. *Macromolecules* **2005**, *38*, 6068–6078.

[82] Rozes, L.; Fornasieri, G.; Trabelsi, S.; Creton, C.; Zafeiropoulos, N.; Stamm, M.; Sanchez, C. *Prog. Solid State Chem.* **2005**, *33*, 127–135.

[83] Mijatovic, I.; Kickelbick, G.; Schubert, U. *Eur. J. Inorg. Chem.* **2001**, *2001*, 1933–1935.

[84] Kogler, F. R.; Jupa, M.; Puchberger, M.; Schubert, U. *J. Mater. Chem.* **2004**, *14*, 3133–3138.

[85] Puchberger, M.; Kogler, F. R.; Jupa, M.; Gross, S.; Fric, H.; Kickelbick, G.; Schubert, U. *Eur. J. Inorg. Chem.* **2006**, 3283–3293.

[86] In, M.; Sanchez, C. *J. Phys. Chem. B* **2005**, *109*, 23870–8.

[87] Starikova, Z. *Polyhedron* **1999**, *18*, 941–947.

[88] Boyle, T. J.; Ottley, L. A. M.; Rodriguez, M. a. *Polyhedron* **2005**, *24*, 1727–1738.

[89] Evans, W. J.; Ansari, M. A.; Ziller, J. W. *Polyhedron* **1998**, *17*, 869–877.

[90] Lorber, C.; Choukroun, R.; Vendier, L. *Organometallics* **2008**, *27*, 5017–5024.

[91] Pandey, A.; Pandey, A.; Parak, W.; Mayer, P. *Inorg. Chim. Acta* **2006**, *359*, 4511–4518.

[92] Ammala, P. S.; Cashion, J. D.; Kepert, C. M.; Murray, K. S.; Moubaraki, B.; Spiccia, L.; West, B. O. *J. Chem. Soc. Dalt. Trans.* **2001**, *3*, 2032–2041.

[93] Day, V. W.; Klemperer, W. G.; Pafford, M. M. *Inorg. Chem.* **2001**, *40*, 5738–5746.

[94] Saruhashi, K.; Kobayashi, S. *J. Am. Chem. Soc.* **2006**, *128*, 11232–11235.

[95] Sobota, P.; Przybylak, S.; Jerzykiewcz, L. B. *Organometallics* **2002**, *21*, 22–24.

[96] Trimmel, G.; Gross, S.; Kickelbick, G.; Schubert, U. *Appl. Organomet. Chem.* **2001**, *15*, 401–406.

[97] Kickelbick, G.; Holzinger, D.; Brick, C.; Trimmel, G.; Moons, E. *Chem. Mater.* **2002**, 4382–4389.

[98] Piszczek, P.; Radtke, a.; Grodzicki, a.; Wojtczak, a.; Chojnacki, J. *Polyhedron* **2007**, *26*, 679–685.

[99] Kickelbick, G.; Wiede, P.; Schubert, U. *Inorg. Chim. Acta* **1999**, *284*, 1–7.

[100] Pappas, I.; Fitzgerald, M.; Huang, X.-Y.; Li, J.; Pan, L. *Cryst. Growth Des.* **2009**, *9*, 5213–5219.

[101] Otero, A.; Fernandez-Baeza, J.; Antinolo, A.; Tejeda, J.; Lara-Sanchez, A.; Sanchez-Barba, L.; Fernandez-Lopez, M.; Lopez-Solera, I. *Inorg. Chem.* **2004**, *43*, 1350–1358.

[102] Pan, L.; Heddy, R.; Li, J.; Zheng, C.; Huang, X.-Y.; Tang, X.; Kilpatrick, L. *Inorg. Chem.* **2008**, *47*, 5537–5539.

[103] Reza, M. Y.; Matsushima, H.; Koikawa, M.; Nakashima, M.; Tokii, T. *Bull. Chem. Soc. Jpn.* **1998**, *71*, 155–160.

[104] Reza, M. Y.; Matsushima, H.; Koikawa, M.; Nakashima, M.; Tokii, T. *Polyhedron* **1999**, *18*, 787–792.

[105] Faccini, F.; Fric, H.; Schubert, U.; Wendel, E.; Tsetsgee, O.; Müller, K.; Bertagnolli, H.; Venzo, A.; Gross, S. *J. Mater. Chem.* **2007**, *17*, 3297–3307.

[106] Piszczek, P.; Radtke, A.; Wojtczak, A.; Muziol, T.; Chojnacki, J. *Polyhedron* **2009**, *28*, 279–285.

[107] Petit, S.; Morlens, S.; Yu, Z.; Luneau, D.; Pilet, G.; Soubeyroux, J.-L.; Odier, P. *Solid State Sci.* **2011**, *13*, 665–670.

[108] Kickelbick, G.; Schubert, U. *J. Chem. Soc. Dalt. Trans.* **1999**, 1301–1306.

[109] Moraru, B.; Gross, S.; Kickelbick, G.; Trimmel, G.; Schubert, U. *Monatshefte für Chemie* **2001**, *132*, 993–999.

[110] Morosin, B. *Acta Crystallogr., Sect. B: Struct. Sci.* **1977**, *B33*, 303–305.

[111] Day, V. W.; Klemperer, W. G.; Pafford, M. M. *Inorg. Chem.* **2005**, *44*, 5397–5404.

[112] V. G. Kessler; G. I. Spijksma; G. A. Seisenbaeva; S. Hakansson; D. H .A. Blank; H. J. M. Bouwmeester *J. Sol-Gel Sci. Technol.* **2006**, *40*, 163.

[113] Hubert-Pfalzgraf, L. G. *Coord. Chem. Rev.* **1998**, *178-180*, 967–997.

[114] Lucky, R. A.; Sui, R.; Charpentier, P. A.; Jennings, M. C. *Acta Crystallogr. Sect. E: Struct. Rep. Online* **2007**, *63*, m2429–m2430.

[115] Gross, S.; Kickelbick, G.; Puchberger, M.; Schubert, U. *Monatshefte f?r Chemie / Chem. Mon.* **2003**, *134*, 1053–1063.

[116] Jupa, M.; Kickelbick, G.; Schubert, U. *Eur. J. Inorg. Chem.* **2004**, *2004*, 1835–1839.

[117] Hubert-Pfalzgraf, L. G.; Daniele, S.; Papiernik, R.; Massiani, M.-C.; Septe, B.; Vaissermann, J.; Daran, J.-C. *J. Mater. Chem.* **1997**, *7*, 753–762.

[118] Chae, H. K.; Payne, D. A.; Zhengkui, X.; Ma, L. *Chem. Mater.* **1994**, *6*, 1589–1592.

[119] Hamid, M.; Tahir, A. A.; Mazhar, M.; Zeller, M.; Hunter, A. D. *Inorg. Chem.* **2007**, *46*, 4120–4127.

[120] Abu Bakar, S.; Tajammul Hussain, S.; Mazhar, M. *New J. Chem.* **2012**, *36*, 1844–1851.

[121] Tudyka, S.; Pflanz, K.; Aldinger, F.; Borrmann, H.; Fischer, P. *Zeitschrift für Anorg. und Allg. Chemie* **1997**, *623*, 1163–1167.

[122] Seisenbaeva, G. A.; Baranov, A. I.; Shcheglov, P. A.; Kessler, V. G. *Inorg. Chim. Acta* **2004**, *357*, 468–474.

[123] Malpezzi, L.; Zucchini, U.; Dall'Occo, T. *Inorg. Chim. Acta* **1991**, *180*, 245–249.

[124] Hernandez-Sanchez, B. A.; Boyle, T. J.; Baros, C. M.; Brewer, L. N.; Headley, T. J.; Tallant, D. R.; Rodriguez, M. A.; Tuttle, B. A. *Chem. Mater.* **2007**, *19*, 1459–1471.

[125] Turevskaya, E. P.; Kessler, V. G.; Turova, N. Y.; Pisarevsky, A. P.; Yanovsky, A. I.; Struchkov, Y. T. *J. Chem. Soc. Chem. Commun.* **1994**, 2303–2304.

[126] Yanovskii, A. I.; Turevskaya, E. P.; Yanovskaya, M. I.; Kessler, V. G.; Turova, N. Y.; Pisarevskii, A. P.; Stuchkov, Y. T. *Russ. J. Inorg. Chem.* **1995**, *40*, 355–373.

[127] Seisenbaeva, G. A.; Gohil, S.; Kessler, V. G.; Andrieux, M.; Legros, C.; Ribot, P.; Brunet, M.; Scheid, E. *Appl. Surf. Sci.* **2011**, *257*, 2281–2290.

[128] Seisenbaeva, G. A.; Kessler, V. G.; Pazik, R.; Strek, W. *Dalton Trans.* **2008**, 3412–3421.

[129] Sobota, P.; Drag-Jarzabek, A.; John, L.; Utko, J.; Jerzykiewicz, L. B.; Duczmal, M. *Inorg. Chem.* **2009**, *48*, 6584–6593.

[130] Baxter, I.; Drake, S. R.; Hursthouse, M. B.; Malik, K. A.; Mingos, D. M. P.; Plakatouras, J. C.; Otway, D. J. *Polyhedron* **1998**, *17*, 625–639.

[131] Petrella, A. J.; Roberts, N. K.; Raston, C. L.; Craig, D. C.; Thornton-Pett, M.; Lamb, R. N. *Eur. J. Inorg. Chem.* **2003**, *2003*, 4153–4158.

[132] Yanovskii, A.; Starikova, Z.; Yanovskaya, M. I.; Kotova, N. M.; Turova, N. Y. *Russ. J. Inorg. Chem.* **2003**, *48*, 1456.

[133] Pettinari, C.; Marchetti, F.; Pettinari, R.; Vertlib, V.; Drozdov, A.; Timokhin, I.; Troyanov, S.; Min, Y.-S.; Kim, D. *Inorg. Chim. Acta* **2003**, *355*, 157–167.

[134] Yanovsky, A. I.; Yanovskaya, M. I.; Limar, V. K.; Kessler, V. G.; Turova, N. Y.; Struchkov, Y. T. *J. Chem. Soc. Chem. Commun.* **1991**, 1605–1606.

[135] Gaskins, B.; Lannutti, J. J.; Finnen, D. C.; Pinkerton, A. A. *Acta Crystallogr., Sect. C: Cryst. Struct. Commun.* **1994**, *50*, 1387–1390.

[136] Kessler, V. G.; Hubert-Pfalzgraf, L. G.; Daniele, S.; Gleizes, A. *Chem. Mater.* **1994**, 2336–2342.

[137] Pazik, R.; Hreniak, D.; Strek, W.; Kessler, V.; Seisenbaeva, G. *J. Alloys Compd.* **2008**, *451*, 557–562.

[138] Starikova, Z. A.; Yanovsky, A. I.; Kotova, N. M.; Yanovskaya, M. I.; Turova, N. Y.; Benlian, D. *Polyhedron* **1997**, *16*, 4347–4351.

[139] Campion, J.-F.; Payne, D. A.; Chae, H. K.; Maurin, J. K.; Wilson, S. R. *Inorg. Chem.* **1991**, *30*, 3244–3245.

[140] Veith, M.; Mathur, S.; Huch, V. *Inorg. Chem.* **1997**, *36*, 2391–2399.

[141] Albinati, A.; Faccini, F.; Gross, S.; Kickelbick, G.; Rizzato, S.; Venzo, A.; Strutturale, C.; Venezian, V.; Molecolari, T.; Chimiche, S.; Marzolo, V. *Inorg. Chem.* **2007**, *46*, 3459–3466.

[142] Hubert-Pfalzgraf, L. G.; Abada, V.; Vaissermann, J. *Polyhedron* **1999**, *18*, 3497–3504.

[143] Daniele, S.; Hubert-Pfalzgraf, L. G. *Polyhedron* **1994**, *13*, 927–932.

[144] Moustiakimov, M.; Kritikos, M.; Westin, G. *Acta Crystallogr., Sect. C: Cryst. Struct. Commun.* **1998**, *54*, 29–31.

[145] Westin, G.; Norrestam, R.; Nygren, M.; Wijk, M. *J. Solid State Chem.* **1998**, *158*, 149–158.

[146] Berger, E.; Westin, G. *J. Sol-Gel Sci. Technol.* **2010**, *53*, 681–688.

[147] Villiers, C.; Thuéry, P.; Ephritikhine, M. *Acta Crystallogr., Sect. C: Cryst. Struct. Commun.* **2005**, *61*, m64–m66.

[148] Eslava, S.; Goodwill, B. P. R.; McPartlin, M.; Wright, D. S. *Inorg. Chem.* **2011**, *50*, 5655–5662.

[149] Eslava, S.; Hengesbach, F.; McPartlin, M.; Wright, D. S. *Chem. Commun.* **2010**, *46*, 4701–4703.

[150] Nunes, G. G.; Reis, D. M.; Amorim, P. T.; Sá, E. L.; Mangrich, A. S.; Evans, D. J.; Hitchcock, P. B.; Jeffery Leigh, G.; Nunes, F. S.; Soares, J. F. *New J. Chem.* **2002**, *26*, 519–522.

[151] Seisenbaeva, G. A.; Gohil, S.; Kessler, V. G. *Inorg. Chem. Commun.* **2004**, *7*, 18–20.

[152] Kessler, V. G.; Gohil, S.; Parola, S. *Dalt. Trans.* **2003**, 544–550.

[153] Lai, Y.-H.; Lin, C.-Y.; Lv, Y.; King, T. C.; Steiner, A.; Muresan, N. M.; Gan, L.; Wright, D. S.; Reisner, E. *Chem. Commun.* **2013**, *49*, 4331–4333.

[154] Lv, Y.; Willkomm, J.; Steiner, A.; Gan, L.; Reisner, E.; Wright, D. S. *Chem. Sci.* **2012**, *3*, 2470–2473.

[155] Tahir, A. A.; Hamid, M.; Mazhar, M.; Zeller, M.; Hunter, A. D.; Nadeem, M.; Akhtar, M. J. *Dalton Trans.* **2008**, 1224–1232.

[156] Veith, M.; Mathur, S.; Huch, V. *Inorg. Chem.* **1996**, *35*, 7295–7303.

[157] Rodriguez-Delgado, A.; Chen, E. Y.-X. *Inorg. Chim. Acta* **2004**, *357*, 3911–3919.

[158] Mishra, S.; Jeanneau, E.; Berger, M.-H.; Hochepied, J.-F.; Daniele, S. *Inorg. Chem.* **2010**, *49*, 11184–11189.

[159] Veith, M.; Mathur, S.; Huch, V. *Chem. Commun.* **1997**, 2197–2198.

[160] Veith, M.; Mathur, S.; Mathur, C.; Huch, V. *Organometallics* **1998**, *17*, 1044–1051.

[161] Boyle, T. J.; Segall, J. M.; Alam, T. M.; Rodriguez, M. A.; Santana, J. M. *J. Am. Chem. Soc.* **2002**, *124*, 6904–6913.

[162] Brethon, A.; Hubert-Pfalzgraf, L. G.; Daran, J.-C. *Dalt. Trans.* **2006**, *2*, 250–257.

[163] Brethon, A.; Hubert-Pfalzgraf, L. G. *J. Sol-Gel Sci. Technol.* **2006**, *39*, 159–167.

[164] Papiernik, R.; Hubert-Pfalzgraf, L. G.; Veith, M.; Huch, V. *Chem. Ber.* **1997**, *130*, 1361–1363.

[165] Daniele, S.; Papiernik, R.; Hubert-Pfalzgraph, L. G.; Jagner, S.; Hikansson, M. *Inorg. Chem.* **1995**, *34*, 628–632.

[166] Parola, S.; Papiernik, R.; Hubert-Pfalzgraf, L. G.; Jagner, S.; H\aa kansson, M. *J. Chem. Soc. Dalt. Trans.* **1997**, *2*, 4631–4636.

[167] Shannon, R. D. *Acta Crystallogr., Sect. A: Found. Crystallogr.* **1976**, *32*, 751–767.

[168] Hartshorn, R. M.; Hey-Hawkins, E.; Kalio, R.; Leigh, G. J. *Pure Appl. Chem.* **2007**, *79*, 1779–1799.

[169] Zaitsev, K. V.; Oprunenko, Y. F.; Churakov, A. V.; Howard, J. A.; Karlov, S. S.; Zaitseva, G. S. *J. Organomet. Chem.* **2008**, *693*, 173–179.

[170] Kemmitt, T.; Al-Salim, N. I.; Gainsford, G. J. *Eur. J. Inorg. Chem.* **1999**, *1999*, 1847–1849.

[171] Bruker; *SADABS*; 2001.

[172] Petricek, V.; Dusek, M.; Palatinus, L.; *Jana2006*; 2006. jana.fzu.cz.

[173] Sheldrick, G. M. *Acta Crystallogr., Sect. A: Found. Crystallogr.* **2008**, *64*, 112–122.

[174] Hübschle, C. B.; Sheldrick, G. M.; Dittrich, B. *J. Appl. Crystallogr.* **2011**, *44*, 1281–1284.

[175] Spek, A. *Acta Crystallogr. Sect. D: Biol. Crystallogr.* **2009**, *65*, 148–155.

[176] Brandenburg, K.; *Diamond - Crystal and Molecular Structure Visualization*; 2012. www.crystalimpact.com/diamond.

[177] Dam, H. A.; Kim, D. *Ind. Eng. Chem. Res.* **2009**, *48*, 5679–5685.